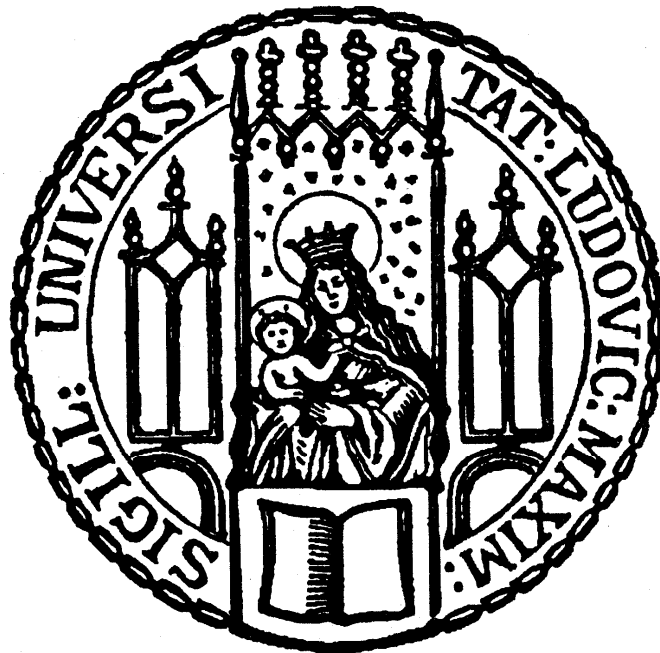


Einzelzell-Analyse unkultivierter magnetotaktischer Bakterien

Dissertation der Fakultät für Biologie der
Ludwig-Maximilians-Universität München



vorgelegt von
Sebastian Kolinko
aus München

München
09.10.2014

Die vorliegende Doktorarbeit wurde im Zeitraum von März 2010 bis September 2014 an der Ludwig-Maximilians-Universität München in Martinsried durchgeführt.

Gutachter:

1. Gutachter: Prof. Dr. Dirk Schüler (Universität Bayreuth)
2. Gutachter: Prof. Dr. Anton Hartmann (Ludwig-Maximilians-Universität München)

Vorgelegt am 09.10.2014

Tag des Promotionskolloquiums: 15.12.2014

Publikationen und Manuskripte

Manuskript 1:

Kolinko S., Wanner G., Katzmann, E., Kiemer F., Fuchs B. M., und Schüler D.

Clone libraries and single cell genome amplification reveal extended diversity of uncultivated magnetotactic bacteria from marine and freshwater environments. *Environmental Microbiology* (2013), 15(5):1290-301.

Manuskript 2:

Kolinko S., Jogler C., Katzmann E., Wanner G., Peplies J., und Schüler D.

Single-cell analysis reveals a novel uncultivated magnetotactic bacterium within the candidate division OP3. *Environmental Microbiology* (2012), 14(7):1709-21.

Manuskript 3:

Kolinko S., Richter M., Glöckner, F.-O., Brachmann A., und Schüler D.

Single-cell genomics reveals potential for magnetite and greigite biomineralization in an uncultivated multicellular magnetotactic prokaryote. *Environmental Microbiology Reports* (2014), doi: 10.1111/1758-2229.12198, im Erscheinen.

Manuskript 4:

Kolinko S., Richter M., Glöckner, F.-O., Brachmann A., und Schüler D.

Single-cell analysis of phylogenetic deep-branching MTB reveal a conserved set of proteobacterial magnetosome genes. Manuskript in Vorbereitung.

Manuskript 5:

Jogler C., Wanner G., Kolinko, S., Niebler M., Amann R., Petersen N., Kube M., Reinhardt R., und Schüler D. Conservation of proteobacterial magnetosome genes and structures in an uncultivated member of the deep-branching *Nitrospirae* phylum. *Proceedings of the National Academy of Sciences* (2011), 108(3) 1134-39.

Manuskript 6:

Lefèvre C. T., Trubitsyn D., Abreu F., Kolinko S., de Almeida L. G. P., de Vasconcelos A. T. R., Lins U., Schüler D., Ginet N., Pignol D., und Bazylinski, D. A. Monophyletic origin of magnetotaxis and the first magnetosomes. *Environmental Microbiology* (2013) 15(8) 2267-74.

Manuskript 7:

Lefèvre C. T., Trubitsyn D., Abreu F., Kolinko S., Jogler C., de Almeida L. G. P., de Vasconcelos A. T. R., Kube M., Reinhardt R., Lins U., Pignol D., Schüler, D., Bazylinski D. A., und Ginet N. Comparative genomic analysis of magnetotactic bacteria from the *Deltaproteobacteria* provides new insights into magnetite and greigite magnetosome genes required for magnetotaxis. *Environmental Microbiology* (2013), 15(10):2712-35.

Beiträge zu Publikationen und Manuskripten

Manuskript 1:

S.K. und D.S. entwickelten die Studie. S.K. charakterisierte durch Einzelzell- und Metagenom-Analysen die phylogenetische Diversität verschiedener magnetotaktischer Populationen. W.G. und E.K. führten elektronenmikroskopische Analysen durch. F.K. konstruierte eine Genombank aus Einzelzell-DNA. B.F. berechnete die phylogenetischen Dendogramme. Das Manuskript wurde von S.K. und D.S. verfasst.

Manuskript 2:

S.K., C.J. und D.S. entwickelten die Studie. S.K. verwendete Einzelzell-Techniken um ein unkultiviertes MTB phylogenetisch, morphologisch und ultrastrukturell zu analysieren. W.G. und E.K. führten elektronenmikroskopische Analysen durch. J.P. berechnete die phylogenetischen Dendogramme. Das Manuskript wurde von S.K. und D.S. verfasst.

Manuskript 3:

S.K. und D.S. entwickelten die Studie. S.K. vereinzelte einen unkultivierten multizellulären Prokaryoten mittels Einzelzell-Techniken, amplifizierte sein Genom und analysierte dieses hinsichtlich seiner Magnetosomengene. A.B. sequenzierte die Einzelzell-DNA. M.R. und F-O.G. führten die Genom Assemblierung und Annotation durch. Das Manuskript wurde von S.K. und D.S. verfasst.

Manuskript 4:

S.K. und D.S. entwickelten die Studie. S.K. analysierte die Genome unkultivierter MTB durch Einzelzell-Techniken und führte funktionelle Genomanalysen und phylogenetische Analysen durch. A.B. sequenzierte die Einzelzell-DNA. M.R. und F-O.G. führten die Genom Assemblierung und Annotation durch. Das Manuskript wurde von S.K. und D.S. verfasst.

Manuskript 5:

S.K. analysierte vereinzelte Zellen des unkultivierten MTB *Candidatus Magnetobacterium bavaricum* und identifizierte konservierte Magnetosomengene durch PCR.

Manuskript 6:

S.K. analysierte vereinzelte Zellen des unkultivierten MTB *Candidatus Magnetobacterium bavaricum*, assemblierte und analysierte dessen Genom und identifizierte das konservierte Magnetosomengen *mamK*.

Manuskript 7:

S.K. analysierte vereinzelte Zellen des unkultivierten MTB *Candidatus Magnetobacterium bavaricum*, assemblierte und analysierte dessen Genom und identifizierte konservierte Magnetosomengene.

Hiermit bestätige ich diese Angaben,

Sebastian Kolinko

Prof. Dr. Dirk Schüler

Index

Publikationen und Manuskripte	II
Beiträge zu Publikationen und Manuskripten	IV
Index	VI
Abkürzungen	VIII
Zusammenfassung	1
Summary	3
<u>Kapitel I</u>	5
1. Einleitung	5
1.1. Magnetotaktische Bakterien	5
1.2. Struktur und Eigenschaften der Magnetosomen	5
1.3. Mechanismus und Genetik der Magnetosomenbiosynthese	7
1.4. Isolierung magnetotaktischer Reinkulturen	11
1.5. Kultivierungsunabhängige Analyse magnetotaktischer Bakterien	13
1.5.1. Analyse natürlicher MTB Populationen	13
1.5.2. Diversität und Phylogenie unkultivierter MTB	14
1.5.3. Genomische Untersuchung unkultivierter MTB	16
1.6. Genomische Analyse unkultivierter Bakterien durch Einzelzell-Techniken	17
1.7. Zielsetzung	19
2. Ergebnisse und Diskussion	20
2.1. Abundanzunabhängige Analyse der Diversität magnetotaktischer Populationen	20
2.1.1. Entwicklung einer Einzelzell-Strategie für die abundanzunabhängige Analyse unkultivierter MTB	20
2.1.2. Systematischer Vergleich von Einzelzell-Strategie mit Metagenomischen Diversitäts-Analysen	22
2.2. Etablierung genomischer Analysen einzelner unkultivierter MTB	23
2.2.1. Funktionelle Genomanalyse und Kultivierungsversuche unkultivierter magnetotaktischer <i>Nitrospirae</i>	25
2.2.2. Erstmalige Identifikation und phylogenetische, ultrastrukturelle und genomische Analyse eines MTB des <i>Omnitrophica</i> Phylums	27
2.2.3. Greigit- und Magnetit-magnetosomengene in einem multizellulären magnetotaktischen Prokaryoten	30
2.2.4. Genetische Diversität der Magnetosomenbiosynthese unkultivierter <i>Nitrospirae</i>	32

2.3. Ausblick	36
3. Referenzen	38
4. Zusätzliche Informationen	53
<u>Kapitel II</u>	54
Publikationen und Manuskripte	54
1. Clone libraries and single cell genome amplification reveal extended diversity of uncultivated magnetotactic bacteria from marine and freshwater environments.	54
2. Single-cell analysis reveals a novel uncultivated magnetotactic bacterium within the candidate division OP3.	68
3. Single-cell genomics reveals potential for magnetite and greigite biomineralization in an uncultivated multicellular magnetotactic prokaryote.	85
4. Single-cell analysis of phylogenetic deep-branching MTB reveal a conserved set of proteobacterial magnetosome genes.	95
5. Conservation of proteobacterial magnetosome genes and structures in an uncultivated member of the deep-branching <i>Nitrospirae</i> phylum.	128
6. Monophyletic origin of magnetotaxis and the first magnetosomes.	148
7. Comparative genomic analysis of magnetotactic bacteria from the <i>Deltaproteobacteria</i> provides new insights into magnetite and greigite magnetosome genes required for magnetotaxis.	158
Curriculum vitae	197
Danksagung	198
Eidesstattliche Erklärung	199

Abkürzungen

Bp	<u>B</u> asen <u>p</u> aare
CDF	<u>c</u> ation <u>d</u> iffusion <u>f</u> acilitator
CDS	<u>c</u> oding <u>s</u> equence
CM	<u>c</u> ytoplasmatic <u>m</u> embrane
EDX	<u>e</u> nergy- <u>d</u> ispersive <u>X</u> -ray spectroscopy
FISH	<u>F</u> luoreszenz <u>i</u> n <u>s</u> itu <u>H</u> ybridisierung
MAI	<u>M</u> agnetsomen <u>i</u> n <u>s</u> el
Mad	<u>m</u> agnetosome <u>a</u> ssociated <u>d</u> eltaproteobacteria
Mam	<u>m</u> agnetosome <u>m</u> embrane associated
Man	<u>m</u> agnetosome <u>a</u> ssociated <u>n</u> itrospirae
MDA	<u>m</u> ultiple <u>d</u> isplacement <u>a</u> mplification
MM	<u>M</u> agnetosomen <u>m</u> embran
MMP	<u>M</u> agnetotaktischer <u>m</u> ultizellulärer <u>P</u> rokaryot
Mms	<u>m</u> agnetosome <u>m</u> embrane <u>s</u> pecific
MTB	<u>M</u> agnetotaktische <u>B</u> akterien
NGS	<u>n</u> ext <u>g</u> eneration <u>s</u> equencing
OATZ	<u>o</u> xic- <u>a</u> noxic <u>t</u> ransition <u>z</u> one
ORF	<u>o</u> pen <u>r</u> eading <u>f</u> rame
PCR	<u>p</u> olymerase <u>c</u> hain <u>r</u> eaction
SAG	<u>s</u> ingle <u>a</u> mplified <u>g</u> enome
TEM	<u>T</u> ransmissions <u>e</u> lektronen <u>m</u> ikroskopie
WGA	<u>w</u> hole <u>g</u> enome <u>a</u> mplification
WT	<u>W</u> ildtyp

Zusammenfassung

Magnetotaktische Bakterien (MTB) sind Mikroorganismen, die die einzigartige Fähigkeit besitzen sich am Erdmagnetfeld auszurichten. Dies wird durch die Synthese intrazellulärer Nanometer großer, von einer Membran umschlossenen magnetische Eisenkristalle, sogenannte Magnetosomen, ermöglicht. Der Prozess der Magnetosomenbiosynthese und seine Genetik wurden anhand von wenigen Modellorganismen analysiert. Trotz einer hohen morphologischen und phylogenetischen Diversität, mit Vertretern in den Phyla *Proteobacteria* und *Nitrospirae*, befindet sich jedoch nur ein Bruchteil der MTB in Reinkultur, wodurch kultivierungsunabhängige Methoden benötigt werden um die große Mehrheit der MTB und ihrer Genetik zu analysieren. Durch metagenomische Studien gelang es die phylogenetische Diversität und die Genetik unkultivierter MTB zu analysieren, wobei diese Studien auf hoch abundante Spezies limitiert sind und niedrig abundante Spezies nicht erfasst werden.

Im Rahmen dieser Doktorarbeit sollte durch die Verwendung von Einzelzell-Techniken die Charakterisierung unkultivierter MTB von ihrer Abundanz entkoppelt werden. Nach der magnetischen Anreicherung wurden individuelle MTB unter mikroskopischer Kontrolle durch Mikromanipulation sortiert. Vereinzelte Zellen wurden ultrastrukturell analysiert oder deren genomische DNA für weiterführende Analysen amplifiziert. Der Ansatz wurde verwendet um die phylogenetische, morphologische und ultrastrukturelle Diversität mariner und limnischer MTB Populationen systematisch zu identifizieren, und wurde durch parallel durchgeführte metagenomische Analysen validiert. Hierdurch konnte die maximale Diversität der magnetotaktischen Populationen erfasst und neben bereits charakterisierten MTB zahlreiche neue unkultivierte magnetotaktische Bakterien der *Proteobacteria* und *Nitrospirae* analysiert werden. Die Identifikation dieser unerwarteten Diversität deutet auf eine größere Diversität niedrig abundanter MTB hin als ursprünglich angenommen. Die Erstellung einer genomischen Klonbank aus der Einzelzell-DNA eines magnetotaktischen Alphaproteobakteriums gab erste Hinweise über dessen Metabolismus, reichte allerdings nicht für eine funktionelle Genomanalyse aus.

Im zweiten Teil dieser Arbeit wurde ein niedrig abundantes und morphologisch auffälliges MTB durch Einzelzell-Techniken analysiert, welches durch metagenomische Ansätze nicht zu identifizieren war. Ultrastrukturelle Analysen dieses ovoiden MTB identifizierten neben bis zu 200 projektilförmige Magnetitmagnetosomen, schwefelhaltige intrazelluläre Granula. Dies deutete auf einen Schwefel oxidierenden Metabolismus hin, der durch genomische Analysen tatsächlich bestätigt wurde. Des Weiteren wird dieses MTB phylogenetisch dem tiefabzweigendem Kandidatenphylum *Omnitrophica* zugeschrieben, welches zusammen mit den *Planctomycetes*, *Verrucomicrobia*, *Chlamydiae*, *Lentisphaerae* und *Poribacteria* ein monophyletisches Superphylum, das sogenannte „PVC Superphylum“ bildet. Zudem gelang

es uns die ersten Magnetosomengene des Kandidatenphylums *Omnitrophica* zu identifizieren und zu analysieren. Hierdurch repräsentiert dieses MTB den ersten morphologisch beschriebenen Vertreter innerhalb dieser phylogenetischen Gruppe und deutet weiterhin auf eine größere Verbreitung der Magnetotaxis hin.

Im dritten Teil wurde das Genom eines multizellulären magnetotaktischen Prokaryoten aus der Nordsee, das durch Einzelzell-Techniken erhalten wurde, sequenziert und hinsichtlich seiner Magnetosomengene analysiert. Einige der identifizierten Magnetosomengene lagen in zwei homologen Kopien vor und bildeten zwei unabhängige Operons. Während die Gene des ersten Operons hohe Ähnlichkeiten zu Magnetosomengenen, die putativ an der Greigitbiomineralisierung beteiligt sind, aufwiesen, zeigten die Gene des zweiten Operons eine hohe Ähnlichkeit zu Magnetitmagnetosomengenen. Dies führte zu der These, dass diese MTB potentiell in der Lage sind sowohl Magnetit- als auch Greigitmagnetosomen zu synthetisieren, was durch die Identifikation beider Mineralien in einem phylogenetisch sehr ähnlichen MTB unterstützt wird. Die geringe Ähnlichkeit beider Operons zueinander und höhere Ähnlichkeit zu Operons in anderen MTB führte zu der Hypothese, dass eine Duplikation der Gene in einem gemeinsamen Vorfahren erfolgte und dann durch späteren horizontalen Gentransfer auf weitere MTB übertragen wurden.

Abschließend wurden die Einzelzell-Genome verschiedener magnetotaktischer *Nitrospirae* sequenziert, assembliert und funktionell analysiert, wodurch in allen untersuchten MTB ein putativ chemolithoautotropher sowie diazotropher Metabolismus festgestellt und für Kultivierungsversuche verwendet wurde. Durch die Identifikation weiterer Magnetosomengene konnte das Verständnis für die genetische Kontrolle projektilförmiger Magnetosomen vertieft werden. Im Rahmen dieser Doktorarbeit konnten wir neben der Identifikation einer unerwarteten phylogenetischen Diversität der MTB, die genetische Diversität der Magnetosomenbiosynthese stark erweitern und signifikant zu dem Verständnis der Biomineralisation in phylogenetisch tiefzweigenden MTB beitragen.

Summary

Magnetotactic bacteria (MTB) are microorganisms, which possess the unique ability to align along geomagnetic field lines. This is possible due to the synthesis of intracellular nanometer sized membrane enveloped magnetic iron crystals, so called magnetosomes. The process of magnetosome biosynthesis and its genetics was analyzed only for a few model organisms. Despite a high morphological and phylogenetical diversity, with representatives in the phyla *Proteobacteria* and *Nitrospirae*, only a small proportion of MTB are in axenic culture, making culture independent techniques necessary to analyze the majority of uncultivated MTB. Metagenomic studies enabled to analyze the phylogenetic diversity and genetics of uncultivated MTB, but being limited to high-abundant species and missing low-abundant species.

In this thesis we applied single-cell techniques to characterize uncultivated MTB independently from their abundance. After magnetic enrichment, individual MTBs were sorted under microscopic control via micromanipulation. The ultrastructures of single cells were analyzed or their genome was amplified for downstream analysis. This approach was used to systematically address the phylogenetical, morphological and ultrastructural diversity of marine and limnic MTB populations, and was validated by simultaneous metagenomic analysis. Thereby, the maximal diversity of magnetotactic populations was recovered and besides already characterized MTB, numerous new uncultivated magnetotactic bacteria of the *Proteobacteria* and *Nitrospirae* were analyzed. The identification of this unexpected diversity indicates a higher diversity of low-abundant MTB than originally expected. The construction of a genomic insertion library from single-cell DNA of a magnetotactic alphaproteobacterium gave first metabolic informations, but was not sufficient for functional genomics analysis.

In the second part of this thesis we were able to analyze a low-abundant and morphologically conspicuous MTB by single-cell analysis that escaped detection by metagenomic approaches. Ultrastructural analysis of this ovoid shaped MTB identified up to 200 bullet-shaped magnetosomes per cell and sulfur-rich intracellular inclusions. This indicates a sulfur oxidizing metabolism, which was confirmed by genomic analysis. This MTB is phylogenetically affiliated with the deep-branching candidate phylum *Omnitrophica*, which forms with the *Planctomycetes*, *Verrucomicrobia*, *Chlamydiae*, *Lentisphaerae* und *Poribacteria* a monophyletic superphylum, the so called "PVC superphylum". Furthermore, we were able to identify and analyze the first magnetosome genes of the candidate phylum *Omnitrophica*. Therefore, this MTB represents the first magnetotactic representative within this phylogenetic group and indicates a higher phylogenetic distribution of the magnetic trait.

In the third part, we sequenced and assembled the genome of a multicellular magnetotactic prokaryote from the North Sea that was obtained by single-cell techniques. Several

magnetosome genes were present in two homologous copies and formed two separate operons. While genes of the first operon were most similar to those putatively involved in greigite biomineralization, gene of the second operon were most similar to magnetite magnetosome genes. This led to the hypothesis, that these MTB are potentially able to synthesize magnetite and greigite magnetosomes, which is supported by the identification of both iron minerals in a phylogenetic close MTB. The minor similarity between both operons and the higher similarity to homologous operons in other MTB indicate ancient gene duplication followed by subsequent mutation in a common ancestor and an acquirement via horizontal gene transfer.

Finally, single amplified genomes of different magnetotactic *Nitrospirae* were sequenced, assembled and functionally analyzed, identifying a putative chemolithoautotrophic metabolism, which was utilized for preliminary cultivation approaches. The identification of further magnetosome genes increased the understanding of the biosynthesis of bullet-shaped magnetosomes.

Besides the identification of an unexpected phylogenetic diversity of MTB in this thesis, we were able to increase the genetic diversity of magnetosome biosynthesis and therefore significantly contribute to the comprehension of the biomineralization of magnetosomes in deep-branching MTB

Kapitel I

Einleitung

1.1. Magnetotaktische Bakterien

Bereits 1963 berichtete der italienische Mikrobiologe Salvatore Bellini (Bellini, 1963) erstmals von Bakterien, die sich augenscheinlich entlang eines Magnetfeldes ausrichteten. Da die Ursache des zellulären Magnetsinns nicht aufgeklärt werden konnte und die Beobachtung auf große Skepsis stieß, gerieten diese Bakterien bis zu ihrer Wiederentdeckung durch Richard Blakemore (Blakemore, 1975) in Vergessenheit. Aufgrund ihrer gerichteten Schwimmbewegung in magnetischen Feldern wurden diese Organismen als magnetotaktische Bakterien (MTB) bezeichnet. MTB sind ubiquitär vorkommende aquatische Mikroorganismen und sind in marinen und limnischen Sedimenten beheimatet (Flies *et al.*, 2005a; Flies *et al.*, 2005b; Simmons *et al.*, 2004; Spring *et al.*, 1992; Spring *et al.*, 1993; Spring *et al.*, 1995; Wenter *et al.*, 2009). MTB bevorzugen als Gradientenorganismen mikroaerobe oder anoxische Bedingungen und befinden sich typischerweise in ihrem Habitat an der oxisch-anoxischen Übergangszone (OATZ, engl.: „oxic anoxic transition zone“) (Flies *et al.*, 2005a; Frankel *et al.*, 1997; Lefèvre *et al.*, 2011a; Spring *et al.*, 1993). Die Analyse kultivierter und unkultivierter MTB identifizierte neben einer enormen morphologischen Diversität mit Kokken, Spirillen, Stäbchen und multizellulären Aggregaten (Abbildung 1) eine bemerkenswerte phylogenetische Diversität mit Vertretern in den Klassen der *Alpha*-, *Gamma*- und *Deltaproteobacteria* sowie dem Phylum *Nitrospirae*. Trotz dieser Unterschiede biosynthetisieren alle MTB intrazelluläre membranumhüllte magnetische Nanokristalle, sogenannte Magnetosomen, welche es der Zelle erlauben sich magnetisch auszurichten (Bazylinski & Frankel, 2004; Frankel *et al.*, 1997; Jogler & Schüler, 2009).

1.2. Struktur und Eigenschaften der Magnetosomen

Magnetosomen sind komplexe prokaryotische Organellen und bestehen aus einem anorganischen Nanokristall aus dem Eisenoxid Magnetit (Fe_3O_4) und/oder dem Eisensulfid Greigit (Fe_3S_4), welcher von einer proteinhaltigen Lipidmembran umhüllt ist (Bazylinski & Frankel, 2004; Frankel *et al.*, 1997; Jogler & Schüler, 2009). Im Gegensatz zu anorganisch hergestellten Nanokristallen weisen Magnetosomenpartikel eine nahezu perfekte monokristalline Struktur und Reinheit auf und lassen sich unterschiedlichsten speziesspezifischen Morphologien zuordnen (Faivre & Schüler, 2008). Neben kubo-oktaedrischen Magnetosomen wie sie durch die Alphaproteobakterien *Magnetospirillum gryphiswaldense* und *Magnetospirillum magneticum* produziert werden, wurden weitere Morphologien wie elongiert kubo-oktaedrisch, hexagonal prismatisch und projektilförmig in

anderen MTB gefunden (Abbildung 1) (Lefèvre & Bazylinski, 2013). Magnetosomen aus Greigit wurden bisher nur in marinen MTB der Klasse der *Deltaproteobacteria* gefunden und sind im Gegensatz zu solchen aus Magnetit unregelmäßiger und polydispers (Bazylinski *et al.*, 1995; Lefèvre *et al.*, 2011c). Trotz dieser starken morphologischen Variabilität liegt die Partikelgröße der meisten Magnetosomen mit 35 bis 120 nm im „single-domain“-Bereich (Faivre & Zuddas, 2007; Faivre & Schüler, 2008). Innerhalb dieses Größenbereichs sind bei Raumtemperatur alle magnetischen Dipolmomente innerhalb des Magnetosomenkristalls parallel ausgerichtet, was zu einer maximalen und stabilen Eigenmagnetisierung des Kristalls führt (Faivre & Schüler, 2008). Außerhalb dieses Größenbereichs verringert sich das magnetische Dipolmoment. Während größere (>120 nm) Partikel mehrere Domänen mit antiparalleler Orientierung ausbilden, ist die Magnetisierungsrichtung in kleinen Kristallen (<35 nm) thermisch fluktuierend und weisen kein richtungsstabiles Dipolmoment auf.

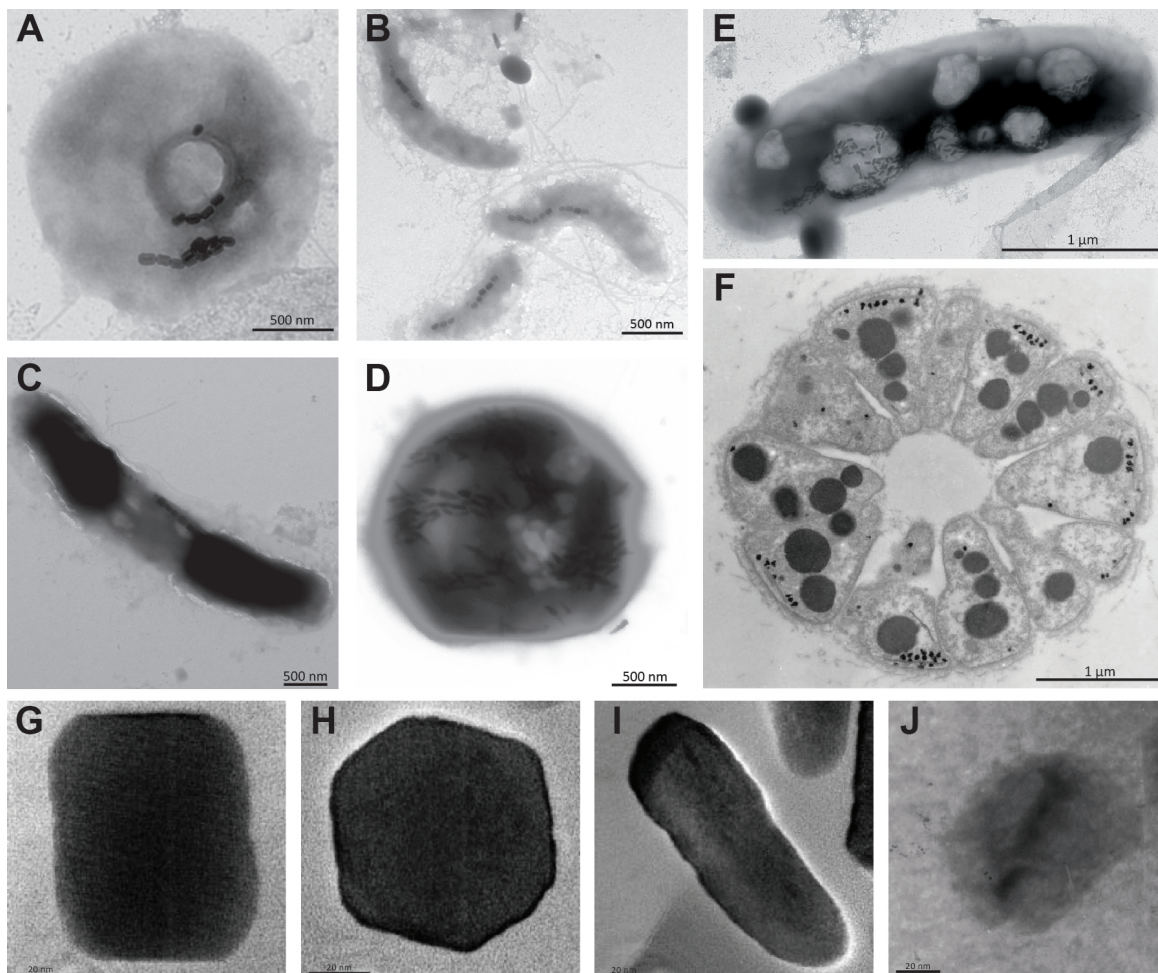


Abbildung 1: Elektronenmikroskopische Aufnahmen verschiedener MTB und Magnetosomen Morphologien. MTB weisen eine heterogene Zellmorphologie mit Kokken (A), Spirillen (B), Vibrionen (C), Ovoiden (D), Stäbchen (E) und multizellulären Aggregaten (F). Während Magnetitmagnetosomen diverse definierte Morphologien wie hexagonal prismatisch (G), kubo-oktaedrisch (H) und projektilförmig (I) aufweisen, sind Greigitmagnetosomen (J) in ihrer Morphologie weniger definiert und unregelmäßiger (Übernommen und modifiziert aus Keim *et al.*, 2003, Faivre & Zuddas, 2007 und Bazylinski *et al.*, 1995)

Durch die lineare Anordnung von ca. 20 Magnetosomen in Ketten entlang der Zellachse wird das Dipolmoment der einzelnen Magnetosomen summiert und ermöglicht der Zelle sich im schwachen Erdmagnetfeld (ca. 50 μT) auszurichten (Blakemore, 1982). Hierdurch können MTB im Gegensatz zu nicht-magnetotaktischen Bakterien die Dimensionalität der chemo-aerotaktischen Orientierung in chemischen Gradienten ihres stratifizierten Mikrohabitats reduzieren und hierdurch ihr bevorzugtes Habitat effizienter finden. Anhand von *M. gryphiswaldense* konnte gezeigt werden, dass ein komplexes Zusammenspiel von magnetischer Ausrichtung mit Aerotaxis, Zellpolarität, chemotaktischen Signaltransduktionskaskaden und gerichteter Schwimmbewegung für die Magnetotaxis von Nöten sind (Popp *et al.*, 2014). Neben der Funktion als magnetischer Sensor, werden weitere mögliche Funktionen der Magnetosomenbiomineralisation diskutiert. So wird den Magnetosomen eine Funktion als Eisenspeicher zugesprochen (Junge, 2008). Des Weiteren könnte die Sequestrierung löslichen zytosolischen Eisens in Form von Magnetosomen der Bildung schädlicher Sauerstoffspezies durch die Fenton-Reaktion entgegenwirken (Blakemore, 1982; Guo *et al.*, 2012; Schübbe *et al.*, 2003).

1.3. Mechanismus und Genetik der Magnetosomenbiosynthese

Die Biosynthese von Magnetosomen in funktionelle Ketten erfolgt in mehreren räumlich und zeitlich aufeinander abgestimmten Schritten, wie die i) Vesikelbildung, ii) Eisenakkumulation, iii) Nukleation und Wachstum von Kristallen, sowie iv) die Anordnung in linearen Ketten. Die Kompartimentalisierung in vom Zytosol getrennten Magnetosomenvesikeln (Gorby *et al.*, 1988; Komeili *et al.*, 2004) erlaubt die Bildung und Aufrechterhaltung der physikochemischen Bedingungen, die für die Magnetosomenbiomineralisierung nötig sind (Baumgartner *et al.*, 2013; Faivre *et al.*, 2004; Faivre & Schüler, 2008) und ermöglicht die gezielte Eisenakkumulation, wodurch die für die Nukleation benötigte Eisenkonzentration räumlich getrennt vom Zytosol erreicht wird und keine reaktiven Sauerstoffspezies durch die Fenton-Reaktion im Zytosol entstehen. Die Vesikelbiogenese ist eine Voraussetzung für die Magnetosomenbildung, da Mutanten von *M. gryphiswaldense* denen die Fähigkeit zur Vesikelbildung fehlt, nicht mehr in der Lage sind Magnetosomen zu synthetisieren (Lohsse *et al.*, 2011; Murat *et al.*, 2010). In Magnetospirillen wurde gezeigt, dass die Vesikel durch Einstülpung der Zytoplasmamembran (CM, engl.: „cytoplasmamembrane“) entstehen (Katzmann *et al.*, 2010; Komeili *et al.*, 2006). Während die Lipidzusammensetzung von Magnetosomenmembran (MM) und CM identisch ist, unterscheidet sich die Proteinzusammensetzung beider Membranen grundlegend voneinander (Gorby *et al.*, 1988; Grünberg *et al.*, 2001; Grünberg *et al.*, 2004). Proteomische Analysen der MM und CM von *M. gryphiswaldense* identifizierten >20 magnetosomenspezifische Proteine (Grünberg *et al.*,

2001; Grünberg *et al.*, 2004). Durch reverse Genetik wurden die verantwortlichen Magnetsomengene erstmals in *M. gryphiswaldense* identifiziert, wo sie in vier Operons innerhalb einer 115 kb großen genomischen Region gruppiert sind (Grünberg *et al.*, 2001; Grünberg *et al.*, 2004; Lohsse *et al.*, 2011). Diese Region weist Ähnlichkeiten zu anderen sogenannten Genominseln, wie zum Beispiel Pathogenitätsinseln, auf und wurde daher als „Magnetosomeninsel (MAI)“ bezeichnet (Grünberg *et al.*, 2001; Lohsse *et al.*, 2011; Ullrich *et al.*, 2005). Diese ist für die Magnetosomenbiosynthese verantwortlich, zumal der spontane partielle Verlust der MAI in *M. gryphiswaldense* zu einem unmagnetischen Phänotyp führte (Ullrich *et al.*, 2005). Zudem führte die heterologe Expression der Magnetsomengene aller 4 Operons der MAI aus *M. gryphiswaldense* in dem nichtmagnetischen Bakterium *Rhodospirillum rubrum* zur Bildung von Magnetitpartikeln und einer magnetischen Ausrichtung von *R. rubrum* (Kolinko *et al.*, 2014).

Die Funktionen der einzelnen Magnetosomenoperons und der Gene wurden bisher durch genetische Analysen in den Referenzbakterien *M. gryphiswaldense* und *M. magneticum* untersucht (Lohsse *et al.*, 2011; Murat *et al.*, 2010; Scheffel *et al.*, 2008). So wird dem *mamGFDC* Operon (2,4 kb) in *M. gryphiswaldense* eine Kontrolle der Magnetosomengröße zugeschrieben, da die *mamGFDC*-Deletionsmutante eine um 25% verringerte Kristallgröße aufwies (Scheffel *et al.*, 2008). Neben der Synthese kleinerer Magnetosomenkristalle mit zum Teil abweichenden und unregelmäßigen Kristallmorphologien führte die Deletion des *mms6* Operons (3,7 kb) in *M. gryphiswaldense* zu einer dispersen Anordnung einzelner Magnetosomen bzw. kürzerer Magnetosomenketten innerhalb der Zelle (Lohsse *et al.*, 2011). Die Deletion des *mamXY*-Operons (5,1 kb) führte zu 50% kleineren und unregelmäßigen Magnetosomen sowie einer Dislokation der Magnetosomenkette (Lohsse *et al.*, 2011; Raschdorf *et al.*, 2014). Im Gegensatz zu *mamGFDC*, *mamXY* und dem *mms6* Operon ist lediglich das 16,4 kb große *mamAB* Operon absolut essentiell für die Bildung von Magnetosomen-ähnlichen Kristallen, da dessen Deletion zu einem völlig unmagnetischen Phänotyp sowie der Abwesenheit der Magnetosomen in *M. gryphiswaldense* und *M. magneticum* führt (Lohsse *et al.*, 2011; Murat *et al.*, 2010; Ullrich & Schüler, 2010).

Ähnliche Gencluster mit zum Teil homologen Genen konnten mittlerweile in allen Genomen kultivierter MTB wie *Magnetococcus marinus*, *Magnetovibrio blakemorei*, dem Stamm SS-5, *Desulfovibrio magneticus* und *Candidatus Desulfamplus magnetomortis* BW-1 identifiziert werden (Jogler *et al.*, 2009a; Lefèvre & Bazylinski, 2013; Lefèvre *et al.*, 2013).

Trotz der enormen Diversität dieser MTB, enthalten die Gencluster neben homologen Magnetsomengenen weitere homologe Gene mit unbekanntem Funktionen und sind trotz keiner strikten Syntenie in ähnlichen Operonstrukturen arrangiert (Abreu *et al.*, 2011; Jogler *et al.*, 2009a; Jogler *et al.*, 2009b; Jogler *et al.*, 2011; Lefèvre & Bazylinski, 2013).

Im Gegensatz zu dem *mms6*, *mamGFDC* und *mamXY* Operons die schwach konserviert sind, wurden *mamAB*-ähnliche Operons bisher in allen untersuchten MTB gefunden und enthalten einen universell konservierten Satz von lediglich 10 Magnetosomengenen (*mamABEIKLMOPQ*) (Abbildung 2), welche ein breites Spektrum für die Magnetosombiosynthese wichtigen Funktionen wie Vesikelbildung, Proteinsortierung, Eisentransport, Kristallnukleation, Größenkontrolle und Kettenbildung kodieren (Lefèvre & Bazylinski, 2013; Lefèvre *et al.*, 2013; Lohsse *et al.*, 2011). Die möglichen Funktionen dieser konservierten Gene wurden *in silico* sowie *in vivo* mit Deletionsmutagenese analysiert und werden im Folgenden kurz beschrieben.

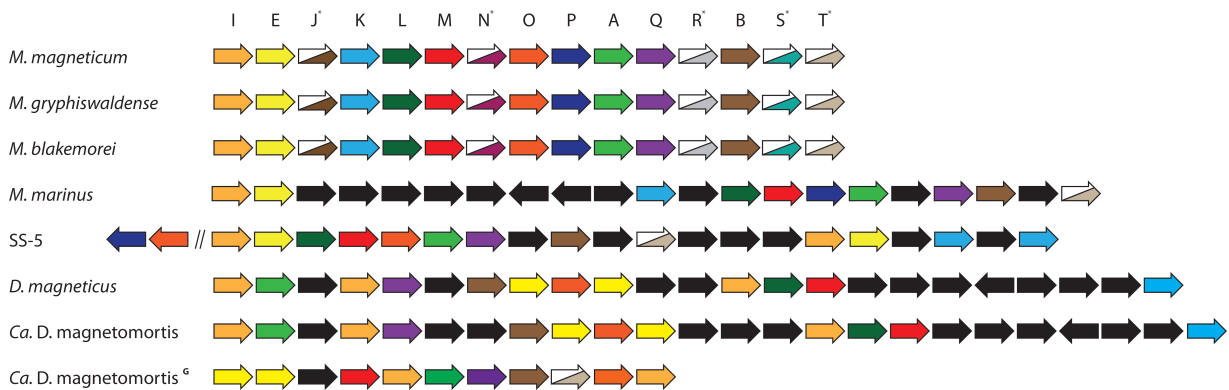


Abbildung 2: Genanordnung der konservierten Magnetosomengene (*mamABEIKLMOPQ*) und nicht konservierten Gene (*mamJNRST**) der kultivierten MTB *M. magneticum*, *M. gryphiswaldense*, *M. blakemorei*, *M. marinus*, Stamm *SS-5*, *D. magneticus* und *Ca. D. magnetomortis* BW-1 (^G = zweites *mamAB*-ähnliches Operon; volle Pfeile signalisieren konservierte Gene; halbe Pfeile deuten nicht konservierte Gene an; gleiche Farbe deuten homologe Gene an).

An der Vesikelbiogenese sind vermutlich die Magnetosomenproteine **MamB**, **MamL** und **MamQ** beteiligt (Lohsse *et al.*, 2014; Uebe *et al.*, 2011). Während für MamL keine Funktion prognostiziert werden kann, gehört MamB und **MamM** zu der CDF-Proteinsuperfamilie (engl.: „cation diffusion facilitator“) (Uebe *et al.*, 2011). Zusammen bilden diese ein Heterodimer, welches am Eisentransport in die Magnetosomenvesikel sowie an Protein-Protein-Interaktionen beteiligt ist (Uebe *et al.*, 2011). Das Magnetosomenprotein MamQ gehört zur konservierten LemA-Proteinfamilie, die zwar in Bakterien weitverbreitet ist, für die jedoch bisher noch keine Funktion prognostiziert wurde (Lohsse *et al.*, 2014). An der Proteinsortierung vor und während der Vesikelgenese sind vermutlich das TPR-Protein (engl.: „tetratricopeptide repeat“) **MamA** und die Serinprotease der HtrA-Familie **MamE** beteiligt (Komelli *et al.*, 2004; Murat *et al.*, 2010). MamE besitzt eine einzigartige und MTB-spezifische Cytochrome C-ähnliche Domäne, die sogenannte „Magnetochrome“-Domäne, welche vermutlich an der Redox-Kontrolle für die Magnetitkristallisation beteiligt ist (Raschdorf *et al.*, 2013; Siponen *et al.*, 2012). Ebenso sind **MamO** und **MamI** am Kristallisationsprozess beteiligt. So führte die Deletion von *mamI* zu kleinen und schwach kristallinen Partikeln aus dem unmagnetischen Eisenoxid Hämatit (Fe₂O₃) (Lohsse *et al.*,

2014). An der Größenkontrolle der Magnetosomenkristalle scheint weiterhin **MamP** beteiligt zu sein, da die *M. gryphiswaldense* Δ *mamP* Mutante nur maximal 6, allerdings sehr große Magnetitkristalle (ca. 60 nm) und viele sehr kleine (ca. 15 nm) unregelmäßige Hämatitkristalle bildet. Das Aktin-ähnliche Protein **MamK** bildet ein dynamisches Proteinfilament innerhalb der Zelle, das zu einer Kettenanordnung der Magnetosomen beiträgt und wichtig für die dynamische Lokalisierung sowie Segregation der Magnetosomenketten ist (Katzmann *et al.*, 2010; Komeili *et al.*, 2006).

Im Gegensatz zu MTB der Alphaproteobakterien synthetisieren MTB der Deltaproteobakterien und des *Nitrospirae* Phylums projektilförmige Magnetosomen und besitzen neben dem *mamAB* Operon keine Homologe zu den *mms6*, *mamGFDC* oder *mamXY* Operons. Allerdings wurde kürzlich zusätzlich zu einer Reihe von *mam*-Genen in diesen MTB ein spezifisches Set von 30 *mad* Genen (engl.: „magnetosome associated deltaproteobacteria“) identifiziert (Lefèvre *et al.*, 2013). Die Abwesenheit der Gene der zuvor in Alphaproteobakterien beschriebenen *mamGFDC*, *mamXY* und *mms6* Operons deutet daraufhin, dass die *mad*-Gene deren Funktionen zum Teil in Deltaproteobakterien substituieren. Aufgrund fehlender experimenteller Daten können Vorhersagen für die Funktionen von nur wenigen Mad Proteinen lediglich anhand von Proteinhomologien und Analysen konservierter Domänen getroffen werden. Die Proteine Mad17 und Mad30 haben eine signifikante Ähnlichkeit zu dem Fe(II)-Transporter FeoB bzw. FeoA, aufgrund dessen eine Funktion in der Eisenaufnahme postuliert wurde (Lefèvre *et al.*, 2013). Das Protein Mad28 enthält wie MamK eine konservierte Aktin-ähnliche Domäne und könnte daher ebenso wie MamK vermutlich an der Positionierung und Segregation der Magnetosomenkette beteiligt sein (Lefèvre *et al.*, 2013). Das Vorkommen bestimmter homologer Magnetosomengene in allen MTB widerlegte die ursprüngliche Hypothese einer polyphyletischen Evolution der Magnetotaxis (DeLong *et al.*, 1993) und könnte durch zwei Hypothesen erklärt werden, i) eine Hypothese würde einen gemeinsamen magnetotaktischen Vorfahren aller magnetischer und unmagnetischer der *Nitrospirae* und *Proteobacteria* annehmen. Dies würde den mehrmaligen Verlust der Magnetosomengene in nicht-magnetotaktischen Bakterien bedeuten. Dies wird gestützt durch den spontanen Verlust der MAI, wie er bei kultivierten MTB häufiger beobachtet wurde (Ullrich *et al.*, 2005). Wahrscheinlicher erscheint jedoch ii) die Übertragung der Magnetosomengene durch horizontalen Gentransfer (HGT) auf unterschiedliche phylogenetische Gruppen (Abreu *et al.*, 2011; Jogler *et al.*, 2009a; Jogler *et al.*, 2011).

Neben der in der MAI organisierten essentiellen Magnetosomengenen wurden kürzlich eine Reihe von weiteren Faktoren außerhalb der MAI entdeckt, die einen Effekt auf die Magnetosomenbiosynthese haben. So resultiert die Deletion von Genen der Denitrifikation (Nitratreduktase Nap und Nitritreduktase Nir) und aeroben Atmung (Cytochrom C Oxidase

cbb₃) in *M. gryphiswaldense* in der Biomineralisation kleinerer und unregelmäßig geformter Magnetosomen (Li *et al.*, 2012; Li *et al.*, 2013; Li *et al.*, 2014a). Zusätzlich zu ihren allgemeinen metabolischen Funktionen sind diese Proteine somit vermutlich an der Kontrolle der Redoxbedingungen während der Magnetitbiomineralisation beteiligt (Li *et al.*, 2014b). Des Weiteren führte die Deletion des Eisen(II)-Transporter-Systems FeoAB, des Eisenaufnahmeregulators Fur (engl.: „ferric uptake regulator“) sowie zweier Eisenreduktasen (*fer5* und *fer6*) zu der Bildung weniger und kleinerer Kristalle pro Zelle bzw. keiner Magnetosomen in *M. gryphiswaldense* (Rong *et al.*, 2008; Rong *et al.*, 2012; Uebe *et al.*, 2010; Zhang *et al.*, 2013).

Zusammenfassend ist festzuhalten, dass Informationen zur genetischen Determination der Magnetosomenbiomineralisation nur auf wenige kultivierte Vertreter der *Alpha*- und *Deltaproteobacteria* sowie auf vereinzelte metagenomische Klone und Genfragmente unkultivierter MTB beschränkt sind (Abreu *et al.*, 2011; Jogler *et al.*, 2009a; Jogler *et al.*, 2009b; Jogler *et al.*, 2011). Dagegen waren zu Beginn der Arbeit keine Informationen für die genetische Diversität der Biomineralisation projektilförmiger Magnetosomen in phylogenetisch entfernten MTB mit abweichenden Kristallen, Größen und Anordnungen verfügbar.

1.4. Isolierung magnetotaktischer Reinkulturen

Bakterielle Reinkulturen waren bis vor kurzem die einzige Möglichkeit, Bakterien und ihre metabolischen Fähigkeiten zu charakterisieren. Bisher gelang allerdings nur ein geringer Anteil (0,1%) aller Mikroorganismen in Reinkultur (Amann *et al.*, 1995; Kogure *et al.*, 1980; Rappé & Giovannoni, 2003; Torsvik & Ovreas, 2002). Der komplexe Anspruch an Kultivierungsmedien, Bedingungen und komplexe Wechselwirkungen wie zum Beispiel Quorumsensing, Syntrophie und Zelladhäsion können im Labor nicht oder nur unzureichend imitiert werden (Bruns *et al.*, 2002; Bruns *et al.*, 2003; Caldwell *et al.*, 1997; Gich *et al.*, 2012). Zudem sind viele Mikroorganismen oligotroph, wodurch sie in nur geringen Zellzahlen wachsen und durch eine hohe Nährstoffkonzentration sogar im Wachstum gehemmt werden können.

Im Vergleich zur großen morphologischen und phylogenetischen Diversität der MTB in Umweltproben ist die Anzahl von Isolaten in Laborkultur sehr gering und auf das Phylum der *Proteobacteria* beschränkt (Tabelle 1). Erst zwanzig Jahre nach der ersten Isolierung magnetotaktischer Alphaproteobakterien (Bazyliński *et al.*, 1988; Blakemore *et al.*, 1979; Schüler, 1990) gelang es ein magnetotaktisches Deltaproteobakterium zu isolieren (Sakaguchi *et al.*, 2002).

Tabelle 1: Verschiedene magnetotaktische Isolate aus marinen und limnischen Habitaten in zeitlicher Reihenfolge ihrer Isolation.

Stamm	Phylogenetische Zuordnung	Morphotyp	Habitat	Referenz
<i>Magnetospirillum magnetotacticum</i> MS-1	<i>Alphaproteobacteria</i>	Spirillum	limnisch	Blakemore <i>et al.</i> , 1979
<i>Magnetovibrio blakemorei</i> MV-1	<i>Alphaproteobacteria</i>	Vibrio	marin	Bazylinski <i>et al.</i> , 1988
<i>Magnetospirillum gryphiswaldense</i> MSR-1	<i>Alphaproteobacteria</i>	Spirillum	limnisch	Schüler, 1990
<i>Magnetococcus marinus</i> MC-1	<i>Alphaproteobacteria</i>	Kokkus	marin	Meldrum <i>et al.</i> , 1993
<i>Magnetospirillum magneticum</i> AMB-1	<i>Alphaproteobacteria</i>	Spirillum	limnisch	Kawaguchi <i>et al.</i> , 1995
<i>Desulfovibrio magneticus</i> RS-1	<i>Deltaproteobacteria</i>	Vibrio	marin	Sakaguchi <i>et al.</i> , 2002
<i>Ca. Desulfamplus magnetomortis</i> BW-1	<i>Deltaproteobacteria</i>	Stäbchen	marin	Lefèvre <i>et al.</i> , 2011c
SS-5, BW-2	<i>Gammaproteobacteria</i>	Stäbchen	limnisch	Lefèvre <i>et al.</i> , 2012

Die erste Isolierung magnetischer Gammaproteobakterien in Reinkultur gelang erst kürzlich parallel zu dieser Doktorarbeit (Lefèvre *et al.*, 2012) (Tabelle 1). Jedoch gibt es keine universelle Isolationsstrategie, da MTB hinsichtlich ihrer Phylogenie und Physiologie eine heterogene Gruppe anspruchsvoller Gradientenorganismen mit sehr heterogenen Wachstumsansprüchen und langen Generationszeiten darstellen.

In jüngster Zeit gelangen bemerkenswerte Isolierungen magnetotaktischer Bakterien in Reinkultur wie zum Beispiel den alkaliphilen magnetischen Stämmen ML-1, ZZ-1 und AV-1. Diese konnten isoliert und kultiviert werden, indem das Medium für den nahverwandten nichtmagnetotaktischen Sulfat-reduzierer *Desulfonatronum thiodismutans* MLF-1 leicht modifiziert wurde (Lefèvre *et al.*, 2011b; Pikuta *et al.*, 2003). Das Bakterium *Ca. D. magnetomortis* BW-1 ist nahverwandt mit *Desulfobacterium vacuolatum* (Rees *et al.*, 1998), und konnte in einem leicht modifizierten *D. vacuolatum* Medium isoliert und kultiviert werden (Lefèvre *et al.*, 2011c). Funktionelle Genomanalysen unkultivierter MTB können Rückschlüsse auf den potentiellen Metabolismus geben und somit zur Isolation und Kultivierung beitragen. Dieser Ansatz führte kürzlich zu einer Anreicherungskultur des MMP *Ca. M. multicellularis* (Abreu *et al.*, 2014), nachdem durch bioinformatische Analysen ein Sulfat-reduzierender und organische Säuren-oxidierender Metabolismus postuliert wurde (Wenter *et al.*, 2009).

Trotz dieser Kultivierungsfortschritte sind nach wie vor Reinkulturen in der Minderheit und kultivierungsunabhängige Methoden sind somit eine wichtige Möglichkeit, um einen Einblick in die morphologische, phylogenetische und genomische Diversität der MTB zu erhalten.

1.5. Kultivierungsunabhängige Analyse magnetotaktischer Bakterien

1.5.1. Analyse natürlicher MTB Populationen

Für die Analyse unkultivierter MTB unter Laborbedingungen können Sedimente mit MTB bei Raumtemperatur in Flaschen oder kleinen Aquarien, in sogenannte Mikrokosmen, im Labor über Jahre gelagert werden. Hierbei kommt es jedoch oft zu einer selektiven Massenentwicklung bestimmter MTB Spezies unter einer gleichzeitigen Abnahme der Diversität (Flies *et al.*, 2005a; Flies *et al.*, 2005b; Vali *et al.*, 1987). Durch ihre gerichtete Bewegung in Magnetfeldern können MTB gezielt aus ihrem Habitat angereichert und von anderen Mikroorganismen und Sedimentpartikeln separiert werden (Flies *et al.*, 2005b). So bildet sich ein sichtbares MTB-Pellet am Fokuspunkt eines Magneten, welches für weitere Analyse abgenommen werden kann (Frankel *et al.*, 1997; Schüler & Bazylinski, 2007). Um annähernd kontaminationsfreie Anreicherungen magnetischer Bakterien zu erhalten, wurden Methoden wie die „Racetrack“-Methoden (Wolfe *et al.*, 1987) oder eine „magnetische Falle“ (Jogler *et al.*, 2009b; Lins *et al.*, 2003) entwickelt. Durch magnetische Felder werden MTB dazu veranlasst, sich von nicht-magnetischen Bakterien zu trennen und durch ein zusätzliches Hindernis zu schwimmen. Hierdurch werden magnetische Anreicherungen mit einer hohen Reinheit ermöglicht (<1% Kontamination) (Jogler *et al.*, 2009b).

Mit diesen Techniken konnte gezeigt werden, dass MTB ubiquitär in aquatischen Habitaten wie marinen und limnischen Sedimenten vorkommen (Flies *et al.*, 2005a; Flies *et al.*, 2005b; Simmons *et al.*, 2004; Spring *et al.*, 1992; Spring *et al.*, 1993; Spring *et al.*, 1995; Wenter *et al.*, 2009). Mehrere Analysen der Vertikalverteilung von MTB in Kombination der Messung chemischer Parameter zeigten eine heterogene Verteilung, was auf eine Anpassung als Gradientenorganismen hindeutet (Flies *et al.*, 2005a; Frankel *et al.*, 1997; Lefèvre *et al.*, 2011a; Spring *et al.*, 1993). MTB befinden sich typischer Weise an oder unterhalb der oxisch-anoxischen Übergangszone (OATZ, engl.: „oxic anoxic transition zone“) und besetzen speziesabhängig unterschiedliche Bereiche. So befanden sich innerhalb der oxischen Zone eines Brackwasserhabitats hauptsächlich Kokken, während im mikroaeroben leicht sulfidischen Bereich neben Kokken und Stäbchen hauptsächlich Vibrionen nachgewiesen wurden (Stolz, 1992). Der anaerobe sulfidische Bereich enthielt hingegen magnetotaktische Stäbchen, Vibrionen und sogar multizelluläre Aggregate. Zudem wurde die vertikale Verteilung von magnetit- und greigitbildenden MTB innerhalb eines marinen Sediments verglichen (Bazylinski *et al.*, 1995). Während sich magnetitbildende MTB innerhalb und

oberhalb der OATZ befanden, kamen MTB mit Greigitmagnetosomen innerhalb der anaeroben sulfidischen Bereiche vor, wobei die Anzahl der Greigitkristalle pro Zelle mit steigender Sedimenttiefe und Sulfidkonzentration zunahm.

Untersuchungen der Biogeographie weisen auf einen Zusammenhang zwischen der Populationszusammensetzung oder der Abundanz einiger MTB in Abhängigkeit bestimmter Umweltbedingungen wie Salinität, Temperatur und Substratkonzentration hin (Lin *et al.*, 2012; Lin *et al.*, 2013; Martins *et al.*, 2009; Martins *et al.*, 2012; Postec *et al.*, 2012).

Basierend auf den Eigenschaften kultivierter MTB und zahlreichen Analysen unkultivierter Vertreter sind die meisten MTB mesophile Mikroorganismen die in Habitaten mit einem nahezu neutralen pH beheimatet sind. Eine Ausnahme bildet ein moderat thermophiles MTB aus einer heißen Quelle in Nevada (USA), welches Temperaturen von bis zu 63°C tolerierte (Lefèvre *et al.*, 2010). Eine weitere Ausnahme bilden alkaliphile MTB aus dem Mono Lake in Kalifornien (USA) die ihr optimales Wachstum bei einem basischen pH-Wert von 9 aufwiesen (Lefèvre *et al.*, 2011b).

1.5.2. Diversität und Phylogenie unkultivierter MTB

Da magnetotaktische Bakterien selektiv aus Umweltproben angereichert werden können, dienten sie frühzeitig als Modellorganismen für die Anwendung kultivierungsunabhängiger Methoden, wie zum Beispiel der vergleichenden 16S rRNA Genanalyse. Hierdurch konnte festgestellt werden, dass die MTB eine phylogenetisch diverse Gruppe darstellen (Abbildung 3). Die Klasse der *Alphaproteobacteria* enthält die ersten und meisten kultivierten MTB (Kawaguchi *et al.*, 1995; Meldrum *et al.*, 1993; Schüler, 1990) und enthält zusammen mit unkultivierten magnetotaktischen Alphaproteobakterien ca. 60% aller bekannten 16S rRNA Gensequenzen der MTB (Bazylnski *et al.*, 2013a; Bazylnski *et al.*, 2013b; Lin *et al.*, 2011b; Schleifer *et al.*, 1991; Williams *et al.*, 2011). Die magnetischen Kokken und Spirillen der Alphaproteobakterien bilden mit den *Magnetococcales* und den *Rhodospirillales* zwei eigene phylogenetische Gruppen innerhalb der Alphaproteobakterien (DeLong *et al.*, 1993; Schüler, 1999; Spring *et al.*, 1992; Spring *et al.*, 1995). Magnetotaktische Alphaproteobakterien wurden sowohl in marinen als auch in limnischen Habitaten identifiziert und bilden typischerweise kubo-oktaedrische und elongiert prismatische Magnetitmagnetosomen.

Kürzlich gelang der eindeutige Nachweis von kultivierten und unkultivierten magnetotaktischen Gammaproteobakterien (Abbildung 3) (Lefèvre *et al.*, 2012; Wang *et al.*, 2013). Ebenso wie die magnetischen Alphaproteobakterien synthetisieren sie kubo-oktaedrische bzw. elongiert prismatische Magnetitmagnetosomen (Lefèvre *et al.*, 2012).

Die *Deltaproteobacteria* umfassen mit magnetotaktischen Vibrios, Stäbchen und multizellulären Aggregaten, die sowohl Magnetit- als auch Greigitmagnetosomen bilden, eine breite morphologische und ultrastrukturelle Diversität. Greigitmagnetosomen wurden ausschließlich oder gemeinsam mit projektilförmigen Magnetitmagnetosomen in einzelnen Zellen identifiziert (Bazylinski *et al.*, 1995; Farina *et al.*, 1990) und sind in ihrer Morphologie weniger definiert als solche aus Magnetit und haben eine equidimensionale bis projektilförmige Morphologie (Abreu *et al.*, 2007; Abreu *et al.*, 2008; Lefèvre *et al.*, 2011c; Sakaguchi *et al.*, 2002; Wenter *et al.*, 2009). Während Magnetit-bildende Deltaproteobakterien sowohl in limnischen als auch in marinen Sedimenten vorkommen, wurden Greigitbildner bisher nur in marinen oder Brackwasser-Sedimenten nachgewiesen (Abreu *et al.*, 2007; Lefèvre & Bazylinski, 2013; Sakaguchi *et al.*, 2002).

MTB sind phylogenetisch jedoch nicht auf das Phylum der *Proteobacteria* beschränkt. Das unkultivierte MTB *Candidatus Magnetobacterium bavaricum*, welches in bayrischen Süßwasserseen, wie dem Chiemsee gefunden wurde, wurde anhand seiner 16S rRNA Gensequenz dem tiefabzweigendem *Nitrospirae* Phylum zugeordnet (Abbildung 3) (Spring *et al.*, 1993). Hinsichtlich seiner ungewöhnlichen Größe von 8-10 µm Länge und 1,5-2 µm Durchmesser sowie der Mineralisation von bis 1.000 Magnetsomen pro Zelle unterscheidet sich die *Ca. M. bavaricum* Morphologie stark von anderen MTB. Die Identifikation morphologisch und phylogenetisch ähnlicher MTB deuten auf eine kosmopolitische Verbreitung hin (Isambert *et al.*, 2007; Lin & Pan, 2009; Lin & Pan, 2010; Lin *et al.*, 2011a; Lins *et al.*, 2000). Bemerkenswert ist der Nachweis von 16S rRNA Gensequenzen mit einer hohen Ähnlichkeit zu *Ca. M. bavaricum* in mit Petroleum und Benzen verunreinigten Habitaten (Kao *et al.*, 2008; Kleinsteuber *et al.*, 2008; Schwarz *et al.*, 2007; Suzuki *et al.*, 2004).

Die vertikale Verteilung von *Ca. M. bavaricum* wurde bereits in mehreren Studien untersucht (Jogler *et al.*, 2010; Spring *et al.*, 1993) und zeigte eine Häufung unter mikroaerophilen Bedingungen an der OATZ und ein weiteres Maximum in anoxischen Sedimentschichten. Eine eindeutige Korrelation zu anderen chemischen Gradienten wie der Nitrat-, Sulfid-, oder Ammoniumkonzentration konnte hingegen nicht nachgewiesen werden (Jogler *et al.*, 2010; Spring *et al.*, 1993). Zudem stellt *Ca. M. bavaricum* aufgrund seiner Abundanz ($0,64 \pm 0,17\%$) in einigen Zellschichten und seinem Zellvolumen ($25,8 \pm 4,1 \mu\text{m}^3$) einen großen Teil (ca. 30%) des Biovolumens dar, und nimmt wahrscheinlich eine wichtige Rolle in der mikrobiellen Ökologie ein. Aufgrund der durch biochemische und EDX-Analysen identifizierten intrazellulären Schwefelgranula in *Ca. M. bavaricum* und der Biomineralisation von bis zu 1.000 Magnetosomen pro Zellen, wurde eine eisenabhängige dissimilatorische Sulfidoxidation mit Sauerstoff als terminalen Elektronenakzeptor postuliert (Spring *et al.*, 1993). Hierbei entsteht Magnetit als Nebenprodukt und könnte neben der magnetischen

Ausrichtung im Habitat auch der Energiegewinnung dienen. Jedoch konnte ein solcher Metabolismus in keinem MTB nachgewiesen werden und erscheint aufgrund der geringen durchschnittlichen Partikelzahl pro Zelle eher unwahrscheinlich.

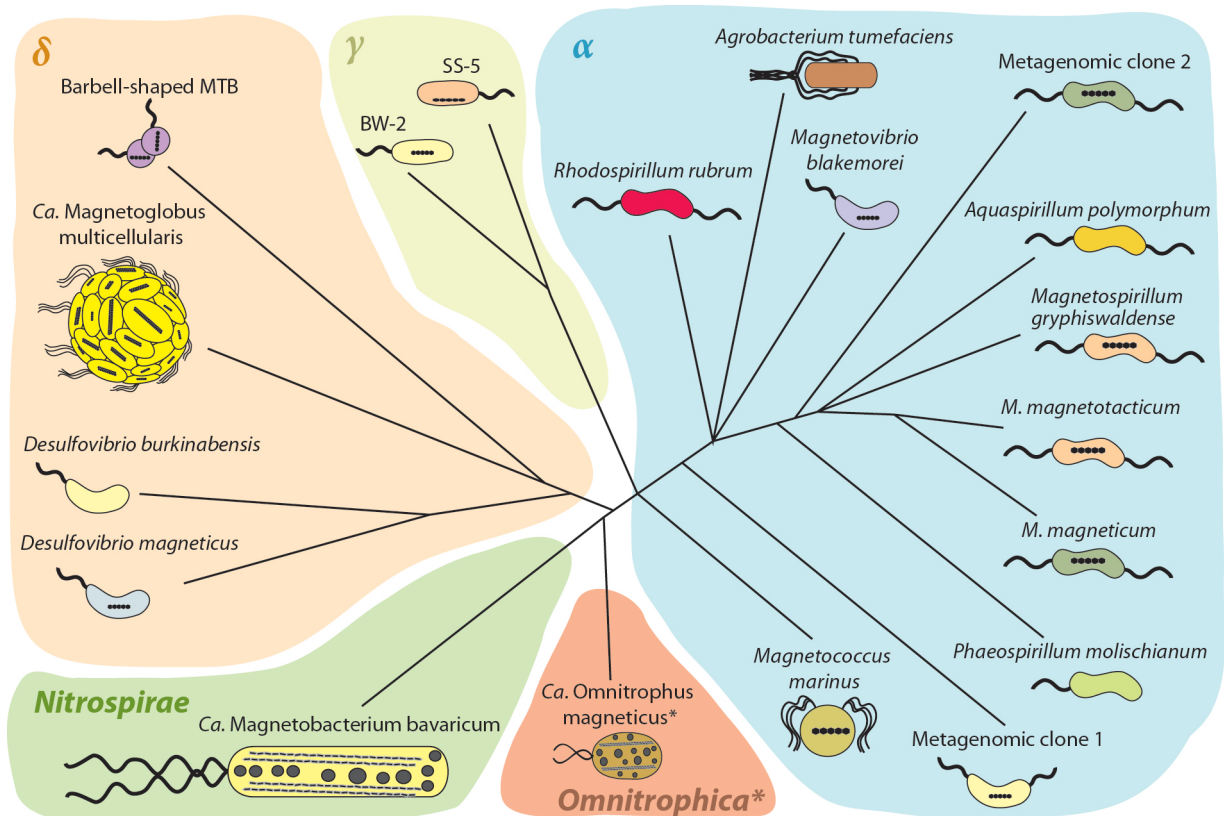


Abbildung 3: Schematischer phylogenetischer Baum magnetotaktischer Bakterien der Klassen der *Alpha*-, *Gamma*- und *Deltaproteobacteria* sowie des tiefzweigenden Phylums *Nitrospirae*. Verzweigungen sind nicht maßstabsgetreu. Repräsentative Morphotype einzelner phylogenetischer Gruppen sind schematisch dargestellt. Inklusive des erst im Rahmen dieser Arbeit identifizierten magnetotaktischen *Omnitrophica Candidatus Omnitrophus magneticus* (* = Ergebnis dieser Arbeit) (Abbildung modifiziert aus: Jogler & Schüler, 2009).

1.5.3. Genomische Untersuchungen unkultivierter MTB

Die genomische Analyse von Bakterien war lange Zeit auf kultivierte Reinkulturen beschränkt. Erst sogenannte metagenomische Techniken ermöglichten die Analyse unkultivierter Bakterien. Hierbei wird die DNA eines Habitats bzw. einer Anreicherung isoliert und in einen Vektor, wie zum Beispiel einem Fosmid kloniert und für weitere Analysen in leicht kultivierbare Mikroorganismen wie z.B. *Escherichia coli* transformiert oder transduziert (Handelsman *et al.*, 1998; Kim *et al.*, 1992; Park *et al.*, 2008; Shizuya *et al.*, 1992; Wahl *et al.*, 1987). Hierdurch können auch größere Genomfragmente, wie zum Beispiel ganze Operonstrukturen analysiert werden. Aufgrund der Komplexität metagenomischer Banken sind Klone niedrig abundanter Spezies stark unterrepräsentiert und schwer zu identifizieren,

was der sprichwörtlichen Suche nach der „Nadel im metagenomischen Heuhaufen“ gleicht. Durch magnetische Anreicherungen wird diese Komplexität stark reduziert und ist selektiv für MTB. Hierdurch gelang es erstmals eine metagenomische Klonbank herzustellen und zwei metagenomische Klone mit Magnetosomengen, die aufgrund der Sequenzähnlichkeit mutmaßlich alphaproteobakteriellen Ursprungs sind, zu identifizieren (Jogler *et al.*, 2009b). In weiteren metagenomischen Studien konnte durch die Identifikation des 16S rRNA Gens ein *Ca. M. bavaricum* spezifischer und mehrere *Ca. M. bavaricum*-ähnliche metagenomische Klone gefunden werden, welche jedoch keine Magnetosomengene enthielten (Jogler *et al.*, 2010; Lin *et al.*, 2011a). Zudem konnte durch eine strake Anreicherung eine partielle MAI mit den ersten Greigitmagnetosomengen eines Greigit-bildenden MTB, dem MMP *Ca. M. multicellularis*, identifiziert werden (Abreu *et al.*, 2011).

Diese Techniken sind jedoch abundanzabhängig, wodurch die Analyse seltener Bakterien erschwert wird, oft sogar unmöglich ist und identifizierte Klone meist anonym sind. Diese Limitationen können durch die genomische Analyse einzelner Zellen überwunden werden.

1.6. Genomische Analyse unkultivierter Bakterien durch Einzelzell-Techniken

Die genomische Analyse einzelner Zellen stellt eine elegante Methode zur Analyse unkultivierter Bakterien dar, da diese nicht mehr auf das Vorhandensein von Reinkulturen angewiesen ist. Durch die Verwendung von Durchflusszytometrie (FACS engl.: „fluorescence-activated cell sorting“) und Mikromanipulation ist es möglich einzelne Zellen für weiterführende Analyse zu erhalten. Jedoch enthalten einzelne Mikroorganismen nicht ausreichend genetisches Material für genomische Analysen. Durch die Amplifikation ganzer Genome (WGA, engl.: whole genome amplification“) ist es erstmals möglich aus wenigen Femtogramm chromosomaler DNA einzelner Zellen ausreichend DNA für eine Sequenzierung zu gewinnen (Dean *et al.*, 2002; Lasken, 2009; Raghunathan *et al.*, 2005; Woyke *et al.*, 2009; Woyke *et al.*, 2010). Hierdurch wurde es erstmals möglich, abundanzunabhängige genomische Analysen durchzuführen. Bei dieser isothermalen Genom-Amplifikation binden nach der DNA-Denaturierung randomisierte Hexamer-Primer an die einzelsträngige DNA, die dann als Polymerisationsstartpunkt dienen. Die phi29 DNA-Polymerase bildet mit der DNA einen sehr stabilen Komplex, der neben einer hohen Halbwertszeit von 1-13 Minuten die Fähigkeit besitzt, bereits synthetisierte Komplementärstränge zu verdrängen, wodurch weitere Primerbindestellen für eine erneute Amplifikationsrunde entstehen (MDA engl.: „multi displacement amplification“).

Trotz dieser Fortschritte enthält die WGA-DNA nicht ausreichend Material für klassische Sanger-Sequenzierungen. Durch die rasante Entwicklung neuer Sequenzierungstechniken der sogenannten nächsten Sequenzierergeneration (NGS, engl.: „next generation

sequencing“) sind Sequenzierungen signifikant billiger, schneller, genauer und zuverlässiger als klassische Sanger-Techniken und benötigen vor allem darüber hinaus weniger DNA-Material. Hierdurch ermöglichen NGS-Techniken die Sequenzierung von WGA-DNA aus einzelnen Zellen.

Im Prinzip basieren NGS Systeme auf der Kettenabbruchsynthese nach Sanger. Die Basenabfolge eines kleinen DNA-Fragmentes wird sukzessive während der Resynthesierung eines Einzelstranges identifiziert (Sanger & Coulson, 1975; Sanger *et al.*, 1977). Im Gegensatz zur klassischen Sangersequenzierung sind NGS Systeme nicht auf einzelne DNA-Fragmente limitiert, sondern führen mehrere Kettenabbruchreaktionen parallel durch und produzieren somit in einem einzigen Reaktionsverfahren enorme Sequenzierdaten. Die erzeugten Sequenzierfragmente sind zwar wesentlich kürzer (100-300 bp) im Vergleich zur klassischen Sangersequenzierung (500-750 bp) und weisen eine größere Fehlerrate auf, können aber durch Überlappungen mit anderen Fragmenten und der multiplen Abdeckung eines Bereiches relativ zuverlässig zu größeren Contigs *de novo* oder optimaler Weise anhand einer Referenzsequenz assembliert werden (Bankevich *et al.*, 2012; Gnerre *et al.*, 2011; Li *et al.*, 2010; Zerbino & Birney, 2008; Zerbino *et al.*, 2009).

Während die Sequenzassemblierung genomischer DNA aus Reinkulturen gut etabliert ist und in Contigs von mehreren 100 kb resultieren kann, stellen *de novo* Assemblierungen aus WGA-DNA erhaltenen Sequenzierdaten aufgrund mehrerer Besonderheiten eine große Herausforderung dar. So kommt es neben der Chimärenbildung zu einer ungleichmäßigen Amplifikation der chromosomalen DNA (Dean *et al.*, 2001; Raghunathan *et al.*, 2005). Hierdurch werden bestimmte Bereiche besonders gut abgedeckt während andere Bereiche unterrepräsentiert sind und während der *de novo* Assemblierung herausfallen (Rodrigue *et al.*, 2009; Swan *et al.*, 2011). Da die WGA unspezifisch ist und bereits kleinste DNA-Verunreinigungen amplifiziert werden, ist die Kontaminationsfreiheit des Templates von entscheidender Bedeutung für spätere Analysen. Trotz dieser Probleme stellt die Kombination von Einzelzell-Genomik in Kombination mit NGS-Techniken eine elegante Alternative zur klonierungsabhängigen Metagenomik dar und ermöglichte erstmals ebenso die *de novo* Genomassemblierung eines unkultivierten Bakteriums aus einer einzigen Zelle (Woyke *et al.*, 2010), wie die späte Überführung des Mörders „Jack the Ripper“ (Edwards, 2014).

1.7. Zielsetzung

Gemessen an der großen morphologischen und phylogenetischen Diversität der MTB ist die Anzahl der bisherigen isolierten MTB verschwindend gering und insbesondere die genetische Vielfalt der Magnetosomenbiosynthese kaum erforscht. Daher war das Ziel dieser Arbeit die Entwicklung kultivierungs- und abundanzunabhängiger Methoden zur phylogenetischen, ultrastrukturellen und genomischen Analyse unkultivierter MTB, um deren Verbreitung und Diversität zu erfassen und insbesondere die an der Magnetosomenbiosynthese beteiligten Gene zu identifizieren. Der im Zuge dieser Arbeit entwickelte Einzelzell-Ansatz sollte zunächst durch die Analyse und Beschreibung verschiedener mariner und limnischer Habitat validiert und für die Identifikation morphologisch und phylogenetisch auffälliger MTB verwendet werden. Schließlich wurden ausgewählte Einzelzell-Genome für die Identifikation ihrer Magnetosomengene und funktionellen Genomanalyse sequenziert und assembliert.

2. Ergebnisse und Diskussion

Die Diversität der MTB ist hinsichtlich ihrer Morphologie, Ultrastruktur und Phylogenie außerordentlich bemerkenswert. Trotz großer Fortschritte in der Kultivierung neuer MTB Spezies befindet sich die überwältigende Mehrheit magnetischer Bakterien nicht in Reinkultur. Bisherige Analysen unkultivierter MTB würden nur häufige Repräsentanten dieser Gruppe erfassen. In dieser Arbeit wurde durch die Etablierung und Verwendung von abundanzunabhängigen Einzelzell-Techniken die Voraussetzung für die Analyse der Phylogenie, der Genetik der Magnetosomenbiosynthese sowie des metabolischen Potentials neuartiger und seltener magnetotaktischer Vertreter ermöglicht.

2.1. Abundanzunabhängige Analyse der Diversität magnetotaktischer Populationen

2.1.1. Entwicklung einer Einzelzell-Strategie für die abundanzunabhängige Analyse unkultivierter MTB

Bisherige phylogenetische Analysen unkultivierter MTB basieren auf vergleichender Sequenzanalyse des 16S rRNA Gens aus magnetischen Anreicherungen (Amann *et al.*, 2006; Postec *et al.*, 2012; Woese & Fox, 1977). Diese enthalten allerdings verschiedene Spezies, wodurch hauptsächlich stark abundante MTB analysiert werden, während Informationen über niedrig abundante Bakterien nicht erfasst werden (Amann *et al.*, 2006). Des Weiteren bleibt die Herkunft der Sequenzen anonym und benötigt für die Korrelation zwischen Phylo- und Morphotyp weitere Methoden, wie zum Beispiel Fluoreszenz *in situ* Hybridisierung (FISH) (Lefèvre *et al.*, 2011a; Spring *et al.*, 1993). Durch die Verwendung auf Einzelzellen basierenden Techniken könnten diese Limitationen überwunden werden. So ermöglicht die Verwendung eines Mikrosortierers für die gezielte Analyse individueller MTB im Gegensatz zu FACS bereits die gleichzeitige morphologische Analyse während der Vereinzelung. Da direkte Sedimentproben nur wenige MTB enthalten und Sedimentpartikel die Sortierung stark erschweren, wird eine vorausgehende magnetische Anreicherung benötigt um den MTB-Anteil selektiv in der Probe zu erhöhen und störende Sedimentpartikel zu entfernen. Erste Sortierversuche erfolgten aufgrund der Verwendung von technisch limitierten long-distance Objektiven bei einer maximalen 60-fachen Vergrößerung und waren somit auf große und auffällige Morphologien, wie *Ca. M. bavaricum* beschränkt. Durch die Entwicklung eines speziell angefertigten Probenhalters konnten die Zellen unter mikroskopischer Kontrolle mit einem Objektiv mit 100facher Vergrößerung sortiert werden, was es erstmals ermöglichte auch kleine MTB wie Magnetospirillen abundanzunabhängig und zuverlässig zu sortieren. Des Weiteren musste während der Vereinzelung eine

Kontamination des Templates ausgeschlossen werden, da bereits geringste DNA-Verunreinigungen während der MDA amplifiziert werden kann. Durch mehrmaliges Aspirieren und Dispensieren wurden die Zielzellen in sterilt gefiltertem Standortwasser unter mikroskopischer Kontrolle „gewaschen“ und von sichtbaren Kontaminationen befreit. Da die Konzentration extrazellulärer DNA in marinen Proben gleich oder größer sein kann als die intrazelluläre DNA-Konzentration (Karl & Bjorkman, 2002; Rodrigue *et al.*, 2009), wurden die Zielzellen anschließend mehrfach in H₂O gewaschen. Die Verwendung eines Mikrosortierers und die verringerte morphologische Diversität innerhalb der magnetischen Anreicherung erlaubte es uns, obwohl bereits eine einzelne Zelle für eine MDA-Reaktion ausreichend ist, jeweils 5 morphologisch identische Zellen als Template zu verwenden um die Ausgangs-DNA-Konzentration und somit die Qualität der WGA-DNA zu erhöhen. Aus diesen Einzelzell-Genomen (SAGs, engl.: „single amplified genomes“) wurden mit universellen Primern (Lane, 1991) partielle 16S rRNA Gensequenzen amplifiziert und Klonbanken erstellt. Zur Qualitätssicherung wurden bis zu 50 Klone sequenziert um die 16S rRNA Gensequenz zu erhalten sowie die Kontaminationsfreiheit der SAGs für weiterführende Analysen zu gewährleisten.

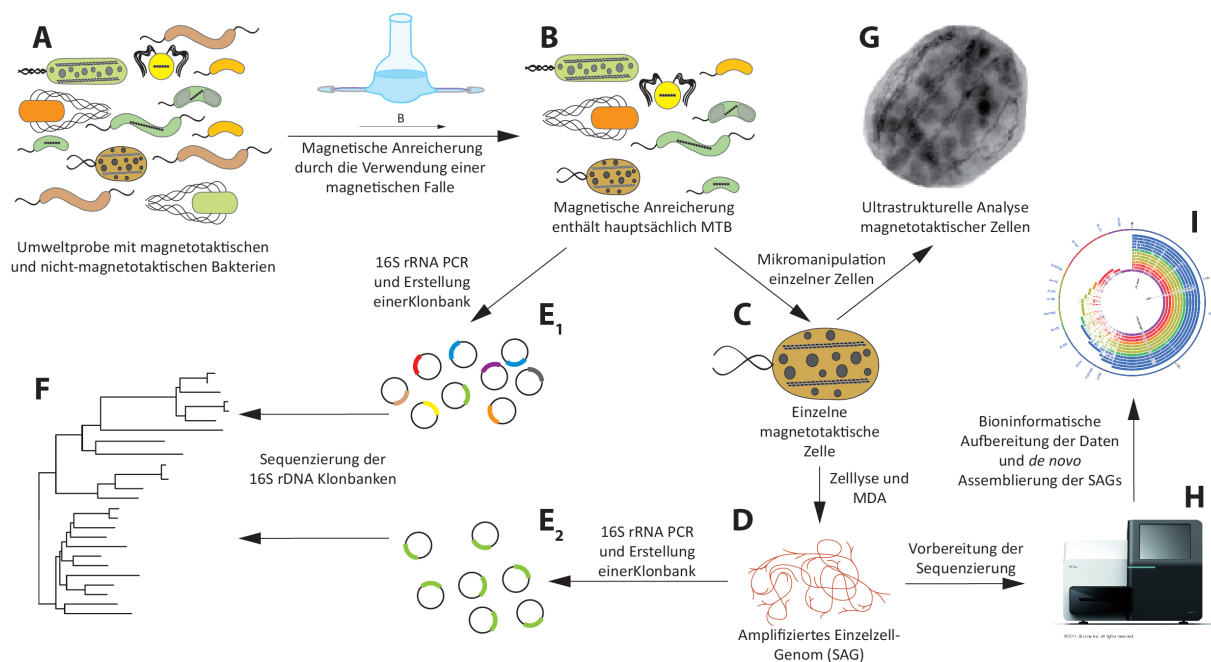


Abbildung 4: Schematische Darstellung der entwickelten Einzelzell-Strategie für die phylogenetische, morphologische und genomische sowie abundanzunabhängige Analyse unkultivierter magnetotaktischer Bakterien. Durch die magnetische Separation magnetotaktischer Bakterien aus einer Umweltprobe (A) erhielten wir eine magnetische Anreicherung diverser MTB (B). Durch die Mikromanipulation unter mikroskopischer Kontrolle wurden einzelne individuelle Zellen erhalten (C) und durch anschließender MDA ein amplifiziertes Einzelzell-Genom erhalten (D). Magnetische Anreicherungen (E₁) und Einzelzell-Genome (E₂) dienten als Template für 16S rRNA mit anschließender Klonbank-Erstellung für die phylogenetische Analyse (F). Um die Ultrastruktur mit dem Phylotyp zu korrelieren wurden individuelle FISH markierte und nicht-markierte Zellen via Mikromanipulation für elektronenmikroskopische Analysen sortiert (G). Durch die Sequenzierung individueller SAGs durch NGS-Systeme (H) mit anschließender bioinformatischer Nachbearbeitung, wurden Einzelzell-Genome *de novo* assembliert und analysiert (I).

2.1.2. Systematischer Vergleich von Einzelzell-Strategie mit metagenomischen Diversitäts-Analysen

Um die phylogenetische Diversität verschiedener Habitats systematisch zu analysieren, wurden, wie in Manuskript 1 dargestellt, 16S rRNA Gen-Metagenombanken mit dem auf WGA basierenden Einzelzell-Ansatz kombiniert (Abbildung 4), um die phylogenetische Diversität erschöpfend zu analysieren sowie die Einzelzell-Strategie zu validieren. Hierfür wurden jeweils ein marines Sediment aus dem Wattenmeer bei Cuxhaven (Cux) und ein limnisches Sediment aus dem Chiemsee (CS) verglichen. Aus allen SAGs und den magnetischen Anreicherungen wurden partielle 16S rRNA Gensequenzen amplifiziert und sequenziert. So konnten allen drei identifizierten Morphotypen (Cux-01-Cux-03) in den magnetischen Anreicherungen des marinen Habitats zweifelsfrei ihrem jeweiligen Phylotyp durch den Einzelzell-Ansatz zugeordnet werden, während 16S rRNA Genklonbanken diese nur partiell enthielten. In der limnischen Probe konnten hingegen fünf der sechs Phylotypen (CS-01-CS-05) durch den Einzelzell-Ansatz identifiziert werden, während die Klonbank lediglich 2 (CS-02 und CS-03) der abundantesten und einen zusätzlichen anonymen Phylotyp (CS-06) enthielt. Der Vergleich beider Techniken ergab, dass der WGA-Ansatz für die Analyse niedrig abundanter MTB dem klassischen Genbanken überlegen ist, während die Kombination beider Techniken höchstwahrscheinlich in der Lage ist die maximale Diversität innerhalb einer Probe zu erfassen.

2.1.3. Phylogenetische und ultrastrukturelle Analyse unkultivierter MTB

Von den in 2.1.2 identifizierten Phylotypen wiesen 2 eine 16S rDNA Sequenzidentität >97% auf und konnten einem unkultiviertem Magnetococcus Klon OTU-51 (CS-02) und *Ca. M. bavaricum* (CS-03) zugeordnet werden (Lin & Pan, 2010; Spring *et al.*, 1993). Die verbliebenen 6 Phylotypen wiesen eine Sequenzidentität unterhalb von 97% auf und repräsentieren somit neue Spezies. Die limnischen MTB CS-01, CS-05 und CS-06 werden wie die marinen MTB Cux-01, Cux-02 und Cux-03 phylogenetisch der Klasse der *Alphaproteobacteria* zugeordnet. Neben CS-03 konnte auch CS-04 dem tiefabzweigendem Phylum der *Nitrospirae* zugeordnet werden und besaß eine Sequenzidentität von 94% zu dem unkultivierten ovoiden *Nitrospirae Candidatus Magnetoovum mohavensis* (Lefèvre *et al.*, 2011a).

Neben der phylogenetischen Zuordnung ermöglicht der Einzelzell-Ansatz wie in Manuskript 1 und 2 beschrieben die gleichzeitige morphologische und ultrastrukturelle Analyse einzelner Zellen (Abbildung 4). Entsprechend ihrer phylogenetischen Zuordnung zu der Ordnung der *Magnetococcales* weisen Cux-01, Cux-02 und CS-02 eine kokkoide Zellform auf und synthetisieren die für magnetische Alphaproteobakterien typischen hexagonal prismatischen

Magnetosomen (Favre *et al.*, 2005). Interessanterweise konnten Cux-03 und CS-05 phylogenetisch den *Magnetococcales* zugeordnet werden, weisen allerdings eine vibrioide Zellmorphologie auf, die bereits mehrfach in vorherigen Studien unkultivierter MTB beobachtet aber nie phylogenetisch identifiziert werden konnte (Schüler, 1994; Spring *et al.*, 1995; Vali & Kirschvink, 1991). Beide MTB zeigen trotz ihres unterschiedlichen geografischen Ursprungs und unterschiedlicher Phylogenie überraschenderweise eine ähnliche Morphologie. So sind beide MTB mit einer Länge von 3,5 μm ähnlich groß, synthetisieren hexagonal prismatische Magnetosomen und bilden jeweils zwei charakteristische polare elektronendichte Einschlüsse. Diese Einschlüsse konnten durch EDX-Analysen als Phosphatgranula identifiziert werden, die in einzelnen Zellen bis zu zwei Drittel des Zellvolumens einnehmen. Granuläre Polyphosphate wurden bereits in anderen MTB wie dem MMP *Ca. M. multicellularis* identifiziert und könnten als Energiequelle, Phosphat- und Eisenspeicher fungieren (Achbergerová & Nahalka, 2011).

Das *Nitrospirae* CS-04 ähnelt mit seiner ovoiden Zellform und den projektilförmigen Magnetosomen, die in 4-5 Bündeln entlang der Zellachse in Ketten angeordnet sind dem phylogenetisch nahverwandte *Candidatus* *Magnetoovum mohavensis* (Lefèvre *et al.*, 2011a). Dennoch weisen beide MTB mit nur 94% eine geringe 16S rDNA-Sequenzidentität auf und repräsentieren somit jeweils eine neue phylogenetische Gruppe. Insgesamt deuten die Ergebnisse dieser Arbeit und die Identifikation weiterer magnetotaktischer *Nitrospirae* auf eine größere phylogenetische Diversität magnetotaktischer Bakterien innerhalb dieses Phylums hin als ursprünglich angenommen. Hinsichtlich seiner phylogenetischen Position und seinem Herkunftshabitat schlagen wir für das MTB CS-04 den Name *Candidatus* *Magnetoovum chiemensis* vor.

2.2. Etablierung genomischer Analyse einzelner unkultivierter MTB

Im Rahmen dieser Arbeit etablierten wir eine Methode für die Genomanalyse unkultivierter einzelner MTB mit dem Ziel das metabolische Potential und insbesondere die genetische Diversität der Magnetosomenbiosynthese zu analysieren.

In einem ersten Ansatz um genomische Informationen einzelner Zellen zu erhalten konstruierten wir eine Klonbank mit kleinen DNA-Fragmenten aus der Einzelzell WGA-DNA (Simon & Daniel, 2010) des unkultivierten MTB CS-05. Die Klonbank enthielt jedoch mit nur 27 Klonen und einer durchschnittlichen Insertgröße von 2 kb insgesamt nur 54 kb genomischer Information, was bei einer Genomgröße von 5 Mb lediglich 1% des Genoms entspricht. Die direkte Sequenzierung von Einzelzell WGA-DNA wurde bereits erfolgreich verwendet, um bakterielle Genome erfolgreich *de novo* zu assemblieren (Rodrigue *et al.*, 2009; Woyke *et al.*, 2010). Dennoch sind abundanzunabhängige Einzelzell-Techniken nicht

ausgereift und stellen keine Standardmethode dar. Neben den bereits besprochenen Kontaminationen während der MDA stellt die Sequenzassemblierung von Einzelzell WGA-DNA ein weiteres Problem dar. Während die Assemblierung genomischer DNA aus Reinkulturen gut etabliert ist, stellen *de novo* Assemblierungen aus WGA-DNA erhaltenen Sequenzierdaten aufgrund mehrerer Besonderheiten eine große Herausforderung dar. Die ungleichmäßige Amplifikation der chromosomalen DNA durch die MDA kann durch ein geringeres Verhältnis zwischen Reaktionsvolumen und eingesetzter DNA-Menge verringert werden (Rodrigue *et al.*, 2009; Swan *et al.*, 2011). Dies kann entweder durch die massive Verkleinerung des Reaktionsvolumens oder dem Einsetzen größerer DNA-Mengen erreicht werden (Marcy *et al.*, 2007). Um die Qualität der WGA-DNA zu erhöhen, verwendeten wir pro Ansatz 5 Zellen und führten die MDA-Reaktion in möglichst geringen Volumina (<1 µl) auf sogenannten AmpliGrids (Advalytix, München Deutschland) durch. Zudem führten wir vor der Sequenzassemblierung eine bioinformatische Normalisierung durch, um abundante und redundante Sequenzdaten zu beseitigen. Die bioinformatische oder enzymatische Entfernung dieser abundanten Bereiche hatte einen positiven Effekt auf die Assemblierung (Rodrigue *et al.*, 2009; Swan *et al.*, 2011). Des Weiteren wurde durch die konsequente Kombination zusammengehörender Sequenzdaten die Genomassemblierung verbessert. So gelang es Rinke und Kollegen im Rahmen des „Microbial Dark Matter“-Projektes die voraussichtliche Genomvollständigkeit, anhand von 139 Referenzgenen, mehrerer Einzelzell-Genome von durchschnittlich 40% auf über 90% steigern (Rinke *et al.*, 2013). Außerdem hatte der Assemblierungsalgorithmus einen entscheidenden Einfluss auf die Qualität der genomischen Daten. Die zuerst in Rahmen dieser Doktorarbeit verwendeten Assemblierungsprogramme CLC Genomics Workbench und Velvet (Zerbino & Birney, 2008; Zerbino, 2010) sind nicht auf WGA-DNA aus einzelnen Zellen spezialisiert, was in kleinen und stark fragmentierten Genomen resultierte. Durch die Verwendung des auf Einzelzell-DNA spezialisierten Programms SPAdes (Bankevich *et al.*, 2012; Nurk *et al.*, 2013) gelang es größere Einzelzell-Genome mit einer geringeren Fragmentierung für die Genomanalyse zu assemblieren. Im Rahmen dieser Arbeit wurden neben den SAGs der bereits vorgestellten MTB *Ca. M. bavaricum* und *Ca. M. chiemensis* auch die SAGs des multizellulären magnetotaktischen Prokaryoten *Candidatus Magnetomorum* HK-1 sowie des ungewöhnlichen ovoiden MTB *Candidatus Omnitrophus magneticus* analysiert (Tabelle 2) Die SAGs dieser unkultivierten MTB wurden wie in Manuskript 3 und 4 beschrieben anhand ihrer 16S rRNA Gensequenzen auf Kontaminationen und ihre Klonalität untersucht, nachfolgend sequenziert und die potentielle Genomabdeckung abgeschätzt (Rinke *et al.*, 2013). Die Genomabdeckung einzelner SAGs war mit durchschnittlich $51 \pm 10\%$ zu gering für genomische Analysen. Durch die speziesspezifische Kombination individueller

Sequenzdaten der SAGs wurden vorläufige Genome mit einer geschätzten Abdeckung von 74% bis zu 95% assembliert (Tabelle 2).

Tabelle 2: Generelle Informationen der Genome von *Candidatus* *Magnetoovum* *chiemensis*, *Candidatus* *Magnetobacterium* *bavaricum*, *Candidatus* *Omnitrophus* *magneticus*, *Candidatus* *Magnetomorum* *HK-1* im Vergleich zu *Candidatus* *Magnetobacterium* *casensis* (Lin *et al.*, 2014).

Parameter	<i>Candidatus</i> <i>Magnetoovum</i> <i>chiemensis</i> CS-04	<i>Candidatus</i> <i>Magnetobacterium</i> <i>bavaricum</i>	<i>Candidatus</i> <i>Omnitrophus</i> <i>magneticus</i> SKK01	<i>Candidatus</i> <i>Magnetomorum</i> <i>HK-1</i>	<i>Candidatus</i> <i>Magnetobacterium</i> <i>casensis</i>
Genomgröße (Mb)	3,9	6,3	3,4	14,3	3,4
G+C Gehalt (%)	40,4	47,40	35,80	34,7	48,90
Anzahl der Contigs	1402	4211	1120	3197	70
N50 (kb)	9,651	4,571	15,846	17,5	90,253
Maximale Contigröße (kb)	43,149	67,959	133,939	122,255	239,626
Genomvollständigkeit (%)	74,1	74,8	87,1	95,1	keine Angaben
Geschätzte Genomgröße (Mb)	5,3	8,4	3,9	15,5	3,4
Anzahl kodierender Sequenzen	4527	8277	3439	14451	3140
Anzahl der tRNAs	45	69	42	49	40
rRNA Operons	1	1	1	1	1
MAI-Größe(kb)	27,9	46	4,8	50,8	39,2
G+C Gehalt der MAI (%)	39,5	50,20	38,10	38,2	49,80
Anzahl putativer Magnetosomengene	21	30	6	51	31

2.2.1. Funktionelle Genomanalyse und Kultivierungsversuche unkultivierter magnetotaktischer *Nitrospirae*

Die Genome der magnetotaktischen *Nitrospirae* *Ca. M. bavaricum* und *Ca. M. chiemensis* waren mit einer Größe von 6,3 Mb bzw. 3,9 sowie einer geschätzten Abdeckung von je ca. 75% (Tabelle 2) ausreichend für eine funktionelle Genomanalyse. Anhand der identifizierten Gene wurde ein mannigfaltiges metabolisches Potential vorhergesagt.

So sind sowohl *Ca. M. bavaricum* als auch *Ca. M. chiemensis* anscheinend potentiell in der Lage Nitrat über die Denitrifikation oder die dissimilatorische Nitratreduktion zu Ammonium (Dong *et al.*, 2011) (DNRA, engl.: „dissimilatory nitrate reduction to ammonia“) als Elektronenakzeptor zu verwenden. Unter Stickstoff limitierten Bedingungen erlaubt der DNRA Stoffwechselweg die zytoplasmatische Reduktion von Nitrat, wodurch sich zwar die Energieausbeute verringert, das entstandene Ammonium jedoch wieder dem Metabolismus zugeführt werden kann (Dong *et al.*, 2011).

Die durch ultrastrukturelle Analysen identifizierten intrazellulärer Schwefelgranula in diesen Bakterien (Lefèvre *et al.*, 2011a; Spring *et al.*, 1993) sowie der Abbau der Einschlüsse unter aeroben Bedingungen in *Ca. M. bavaricum* (Jogler *et al.*, 2010) wiesen bereits auf einen Schwefel-oxidierenden Metabolismus hin. Mit der Sulfid:Quinon Oxidoreduktase (*sqr*), der dissimilatorische Sulfid Reduktase (*dsr*), der Adenosin 5'-Phosphosulfat Reduktase (*aprAB*) und der Adenosin 5'-Triphosphosphatsulfurylase (*sat*) wurden tatsächlich alle Enzyme für eine sukzessive Sulfidoxidation in den Genomen von *Ca. M. bavaricum* und *Ca. M. chiemensis* kodiert. Aufgrund der Bidirektionalität dieser Enzyme wird eine Reduktion von Sulfat zu Sulfid unter stark reduzierten Bedingungen postuliert (Zhou *et al.*, 2011). In

Anbetracht der bi-modalen vertikalen Verteilung von *Ca. M. bavaricum* in seinem Habitat, mit einem Maximum an der OATZ und einem weiteren in den anoxischen und stark reduzierten Sedimentschichten (Jogler *et al.*, 2010), könnte dieses MTB in der Lage sein in räumlicher Abhängigkeit von den Redox-Bedingungen zwischen Schwefel-Oxidation bzw. Reduktion zu wechseln, wie es für *Desulfovibrio desulfuricans* und *Desulfovibrio vulgaris* beschrieben wurde (Dannenbergh *et al.*, 1992; Dilling & Cypionka, 1990; Lin *et al.*, 2014). Die Vertikalverteilung von *Ca. M. mohaviensis* zeigte hingegen nur ein Maximum an der OATZ (Lefèvre *et al.*, 2011a), jedoch wurde diese Analyse mit einer geringeren Auflösung durchgeführt als für *Ca. M. bavaricum* (Jogler *et al.*, 2010), wodurch eventuell ein ähnliches zweites Maximum unterhalb der OATZ übersehen wurde.

Weiterhin sind *Ca. M. bavaricum* und *Ca. M. chiemensis* potentiell in der Lage autotroph zu wachsen, indem sie CO₂ über den Wood-Ljungdahl-Weg (WL-Weg) fixieren (Lin *et al.*, 2014). Während in *Ca. M. bavaricum* keine Gene für die Stickstofffixierung gefunden wurden, deutet die Identifikation von *nif*-Genen in *Ca. M. chiemensis* auf die Fähigkeit zur Diazotrophie hin. Obwohl die Identifikation eines Gens keinen Nachweis für dessen Expression darstellt, können dennoch wichtige Schlussfolgerungen über einen potentiellen Metabolismus und Kultivierungsansätze getroffen werden (Torsvik & Ovreas, 2002).

Aufgrund des vorhergesagten autotrophen und Schwefel-oxidierenden Metabolismus von *Ca. M. bavaricum* wurde eine entsprechende Strategie entwickelt (siehe Tabelle S1), um dieses Bakterium zu isolieren bzw. anzureichern. Magnetische Anreicherungen mit einer hohen *Ca. M. bavaricum* Abundanz wurden in unterschiedlichen Verdünnungsreihen (0-1.000 Zellen pro Ansatz) mit Thiosulfat als Elektronendonator unter mikroaeroben Bedingungen (2% O₂) mit Sauerstoff und/oder Nitrat als Elektronenakzeptor bei RT im Dunkeln inkubiert. Das Basalmedium bestand aus 5-10% Sedimentextrakt, dem Redoxpuffer Dithiothreitol, Fe(III)Citrat und einem Bicarbonat-Puffer mit 10% CO₂ in der Gasphase (Tabelle S1). Allerdings konnte trotz der Variation verschiedenster Substratkonzentrationen und Isolierungsmethoden, wie zum Beispiel verschiedenen Gradienten, bis auf eine einzige Ausnahme kein Wachstum magnetotaktischer Bakterien registriert werden. Nur mit dem Medium 2.1 (Tabelle S1) konnte ein vorübergehendes Wachstum eines ovoïden magnetotaktischen Bakteriums mit einer ähnlichen Morphologie und 16S rRNA Gensequenz zu *Ca. M. chiemensis* beobachtet werden. Jedoch wurde dieses Bakterium innerhalb weniger Tage von einer nicht-magnetischen Population überwachsen. Trotz mehrfacher Wiederholung der Kultivierung konnte das Ergebnis nicht reproduziert werden.

Ultrastrukturelle Analysen der Zellwand der *Nitrospirae* *Ca. M. bavaricum* und *Ca. M. mohaviensis* zeigten einen mehrschichtigen Aufbau bestehend aus Zytoplasmamembran, äußerer Membran, Peptidoglykan und einer dicken zweischichtigen äußeren Hülle, welche vermutlich aus Exopolysacchariden besteht (Jogler *et al.*, 2011;

Lefèvre *et al.*, 2011a). Interessanterweise identifizierten wir in dem *Ca. M. bavaricum* Genom zwei Gencluster, die möglicherweise die Biosynthese sporenhüllenähnlicher Polysaccharide kodieren (*spsBC₂E₂F₂G₂*). Diese sind ähnlich zu denen in dem Gram-negativen Bodenbakterium *Rhizobium leguminosarum*, welches für ihr Überleben in der Rhizosphäre, die erfolgreiche Symbiose mit Leguminosen sowie die Stickstofffixierung große Mengen Polysaccharide exportiert (Marczak *et al.*, 2013). Eine sporenhüllenähnliche Hülle erklärt auch die beobachtete ineffiziente Zelllyse dieses Bakteriums (Jogler *et al.*, 2011). Dies führte zu einer Unterrepräsentanz *Ca. M. bavaricum* spezifischer DNA in metagenomischen Klonbanken, obwohl diese MTB in magnetischen Anreicherungen hoch abundant war (Jogler *et al.*, 2011). Unsere metabolischen Vorhersagen für magnetotaktische *Nitrospirae* stimmen mit den genomischen Analysen des unkultivierten magnetotaktischen *Nitrospirae Candidatus Magnetobacterium casensis* überein, welche erst kurz vor Vollendung dieser Arbeit veröffentlicht wurden (Lin *et al.*, 2014). *Ca. M. casensis* stammt aus dem chinesischen See Lake Miyun und wurde durch einen massiven metagenomischen Ansatz analysiert. *Ca. M. casensis* ist mit einer 16S rRNA Genidentität von 98,2% eng mit *Ca. M. bavaricum* verwandt und weist ebenso hinsichtlich der Morphologie und Ultrastruktur eine hohe Ähnlichkeit auf (Lin *et al.*, 2014). Zusammenfassend kann für magnetotaktische *Nitrospirae* ein chemolithoautotropher und diazotropher Metabolismus vorhergesagt werden. Außerdem scheinen sie in der Lage zu sein in der Abhängigkeit von den Redox-Bedingungen zwischen Schwefel-Oxidation und Reduktion zu wechseln. Aufgrund der vorhergesagten metabolischen Variabilität aller magnetotaktischen *Nitrospirae* sind diese an schnell verändernde Umweltbedingungen an der OATZ angepasst, was ein entscheidender Wachstumsvorteil sein könnte.

2.2.2. Erstmalige Identifikation und phylogenetische, ultrastrukturelle und genomische Analyse eines MTB des *Omnitrophica* Phylums

Nach längerer Lagerung konnte in einem Mikrokosmos mit Chiemseesediment neben überwiegend (>90%) magnetotaktischen Kokken und Spirillen vereinzelt ein morphologisch auffälliges MTB beobachtet werden. Wie in Manuskript 2 beschrieben, konnte dieses MTB trotz seiner geringen Abundanz (<1%) aufgrund seiner auffälligen ovoiden Zellform und lichtbrechender intrazellulärer Einschlüsse gut von anderen MTB unterschieden und durch Einzelzelltechniken analysiert werden. In Hinsicht auf seine Motilität, Zellgröße, Zellmorphologie und der Biosynthese von bis zu 200 projektilförmiger Magnetosomen, die in mehreren Bündeln entlang der Zellachse organisiert sind, weist dieses Bakterium große Ähnlichkeiten zu MTB des *Nitrospirae* Phylums wie *Ca. M. mohavensis* und *Ca. M. chiemensis* auf (Lefèvre *et al.*, 2011a; Spring *et al.*, 1993). Trotz dieser hohen

Ähnlichkeiten wurde dieses MTB aufgrund seiner 16S und 23S rRNA Gensequenz sowie einem spezifischen Markergen (Gupta *et al.*, 2012) dem tiefabzweigendem Kandidatenphylum *Omnitrophica* (früher candidate division OP3) zugeordnet. Das Kandidatenphylum *Omnitrophica*, welches keinen kultivierten Vertreter enthält, basiert ursprünglich auf einer einzelnen 16S rRNA Gensequenz, die aus dem Sediment einer heißen Quelle des Yellowstone Nationalparks stammt (Hugenholtz *et al.*, 1998). Bisher konnten weitere *Omnitrophica* spezifische 16S rRNA Gensequenzen in aquatischen Habitaten wie marinen Sedimenten, in der Tiefsee, Süßwasser Seen, im Grundwasser, Nassreiskulturböden und methanogenen Bioreaktoren hauptsächlich in anoxischen Bereichen gefunden werden (Abulencia *et al.*, 2006; Brofft *et al.*, 2002; Derakshani *et al.*, 2001; Elshahed *et al.*, 2007; Huang *et al.*, 2010; Lehours *et al.*, 2007; Li & Wang, 2008; Macalady *et al.*, 2008; Madrid *et al.*, 2001; Röling *et al.*, 2001). Phylogenetische Analysen zeigten, dass die *Omnitrophica* zusammen mit den *Planctomycetes*, *Verrucomicrobia*, *Chlamydiae*, *Lentisphaerae* und *Poribacteria* ein monophyletisches Superphylum, das sogenannte „PVC Superphylum“ bilden (Pilhofer *et al.*, 2008; Wagner & Horn, 2006). Durch einen metagenomischen Ansatz gelang es, drei Fosmid-Klone mit insgesamt 105 kb Sequenzinformationen anhand *Omnitrophica* spezifischer 16S rRNA Gensequenzen zu identifizieren und zu analysieren (Glöckner *et al.*, 2010). Dieses MTB ist der erste beschriebene Morphotyp der dem *Omnitrophica* Phylum zugeordnet wird. Aufgrund seiner einzigartigen phylogenetischen Position und seines magnetotaktischen Verhaltens wurde für dieses MTB der Namen *Candidatus Omnitrophus magneticus* SKK-01 vorgeschlagen.

Anhand der 16S und 23S rRNA Gensequenzen wurden insgesamt 6 SAGs dem MTB *Ca. O. magneticus* zugeschrieben, individuell sequenziert und zu einem vorläufigen Genom mit einer Größe von 3,4 Mb und einer geschätzten Abdeckung von 87% assembliert (Tabelle 2). Jedoch konnten wir, trotz dieser hohen Genomabdeckung, im Gegensatz zu den durch Rinke und Kollegen beschriebenen Vertretern der *Omnitrophica* (Rinke *et al.*, 2013) für *Ca. O. magneticus* kein großes metabolisches Potential vorhersagen. So wurde nur eine dissimilatorische Sulfit Reduktase des Dissulfovirdin-Typs identifiziert, die in der Lage ist Sulfit unter reduzierten Bedingungen mit Elektronen aus der Hydrolisation von H₂ durch eine periplasmatische und membrangebundene Hydrogenase zu Sulfid zu reduzieren (Steuber & Kroneck, 1998). Tatsächlich konnten durch EDX-Analysen schwefelhaltige intrazelluläre Einschlüsse identifiziert werden, die diese Vorhersagen bestätigen. Ähnlich zu den MTB des *Nitrospirae* Phylums deuten genomische Analysen auf eine CO₂-Fixierung durch den reduktiven Citratzyklus sowie auf Diazotrophie hin.

Die Biosynthese projektilförmiger Magnetosomen durch *Ca. O. magneticus* sowie durch magnetotaktische *Nitrospirae* und *Deltaproteobacteria* verstärkt die Hypothese der monophyletischen Evolution der Magnetotaxis und des horizontalen Gentransfers zwischen

verschiedenen Phyla. Zudem wird vermutet, dass projektilförmige Magnetosomen die ursprüngliche Magnetosomenmorphologie darstellen und später in kompliziertere Formen wie kubo-oktaedrisch und elongiert prismatisch evolvierten (Abreu *et al.*, 2011; Lefèvre & Bazylinski, 2013). Trotz einer abgeschätzten Genomabdeckung von 87% konnten nur die partiellen Sequenzen der Magnetosomengene *mamEBMK* und *mad11* auf kleinen unzusammenhängenden Contigs gefunden werden, was eine MAI-Rekonstruktion verhinderte (Abbildung 5). Phylogenetische Analysen zeigten, dass die in *Ca. O. magneticus* identifizierten Magnetosomengene eine höhere Ähnlichkeit zu homologen Magnetosomengenen zu MTB des *Nitrospirae*-Phylums aufwiesen, als zu denen der Proteobakterien, während die rRNA Gensequenzen eindeutig den *Omnitrophica* innerhalb des PVC Superphylums zugeordnet wurden (Abbildung 7). Die Existenz homologer Magnetosomengene in phylogenetisch unterschiedlichen und durch nicht-magnetotaktische Bakterien getrennten Gruppen spricht gegen einen gemeinsamen magnetischen Vorfahren der *Proteobacteria*, *Nitrospirae* und *Omnitrophica*, sondern für eine Verteilung der Magnetotaxis durch horizontalen Gentransfer. Da die wesentlich aussagekräftigere Analyse der Tetranukleotidfrequenz erst ab einer Contiggröße von 20 kb möglich ist, die Magnetosomen enthaltenden Contigs aber wesentlich kleiner waren, wurde der G+C Prozentsatz zwischen der MAI und dem restlichen Genom verglichen. Der G+C Prozentsatz variierte nur minimal zwischen Magnetosomencontigs und dem restlichen Genom (Tabelle 2), was gegen einen kürzlich erfolgten horizontalen Gentransfer und für eine frühzeitige Adaption der Magnetosomengene in *Ca. O. magneticus* spricht. Aufgrund der hohen Genomabdeckung überrascht die geringe Anzahl identifizierter Magnetosomengene in *Ca. O. magneticus*. Dieser Widerspruch könnte darauf hinweisen, dass weitere Magnetosomengene eine geringe oder keine Homologie zu denen in magnetischen *Proteobacteria* oder *Nitrospirae* aufweisen.

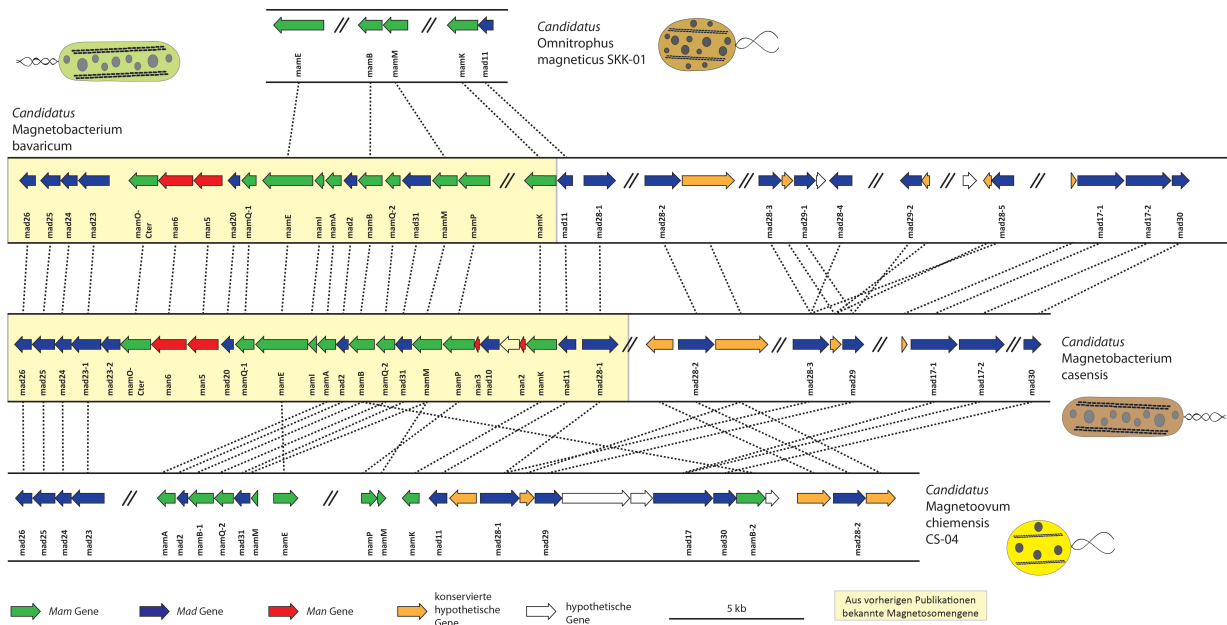


Abbildung 5: Molekulare Organisation identifizierter Magnetosomengene in *Ca. Omnitrophus magneticus* SKK-01 verglichen mit den *Nitrospirae* MTB *Ca. Magnetobacterium bavaricum*, *Ca. Magnetoovum chiemensis* und *Ca. Magnetobacterium casensis*. Verbindungsstriche zwischen Genen deuten homologe Gene an. Magnetosomengene die bereits publiziert wurden sind gelb hinterlegt.

2.2.3. Greigit- und Magnetitmagnetosomengene in einem multizellulären magnetotaktischen Prokaryoten

Wie in Manuskript 3 beschrieben konnte durch den Einsatz von Einzelzell-Techniken ein beinahe vollständiges Genom (95%) des multizellulären magnetotaktischen Prokaryoten *Candidatus Magnetomorum* HK-1 *de novo* assembliert werden. HK-1 wurde aus sandigen Sedimenten aus dem Wattenmeer bei Cuxhaven an der Nordsee angereichert. Trotz seiner morphologischen Ähnlichkeit zu dem MMP *Candidatus Magnetomorum litorale* (Wenter *et al.*, 2009), welcher ebenfalls in diesem Habitat gefunden wurde, gehört HK-1 aufgrund der 16S rRNA Gensequenz nicht derselben Spezies an, sondern hat eine hohe Sequenzidentität (99,3%) zum MMP *Candidatus Magnetomorum rongchengroseum*, welcher erst kürzlich in marinen Sedimenten des Sees Lake Yuehu in China gefunden wurde (Zhang *et al.*, 2014). Im Gegensatz zu dem bereits durch kultivierungsunabhängige Methoden genomisch analysierten MMP *Ca. M. multicellularis* lagen die meisten der identifizierten *mam* Gene in zwei homologen Kopien vor, die jeweils in zwei *mamAB*-ähnlichen Operons organisiert waren (Abbildung 6). Während ein Genset (Cluster 1) große Ähnlichkeiten zu den mutmaßlichen Greigitmagnetosomengenen von *Ca. M. multicellularis* aufwies (Abreu *et al.*, 2011), hatte das zweite Magnetosomengenopern (Cluster 2) eine ähnliche Operonorganisation und Gensequenz zu den Magnetitgenen des kultivierten Deltaproteobakteriums *Ca. D. magnetomortis* BW-1 (Abbildung 6) (Lefèvre *et al.*, 2011c;

Lefèvre *et al.*, 2013). Diese Ergebnisse deuten an, dass der Prozess der Magnetit- und der Greigitbiomineralisation durch genetisch voneinander getrennten *mamAB*-ähnlichen Operons gesteuert wird. Die ultrastrukturelle Identifikation von Magnetit- und Greigitpartikeln in der gleichen Zelle des nahverwandten MMP *Ca. M. rongchengrosum* (Zhang *et al.*, 2014) sind ein weiteres Indiz dafür, dass HK-1 in der Lage ist beide Minerale zu synthetisieren. Die höhere Identität der Greigitgene zwischen HK-1, *Ca. M. multicellularis* und *Ca. D. magnetomortis* BW-1 im Vergleich zu seinen eigenen Magnetitgenen, sowie die ähnliche Organisation der *mamAB*-ähnlichen Operons könnte auf eine sehr frühe Genduplikation mit anschließender Mutation in einem gemeinsamen Vorfahren mit späteren horizontalen Gentransfer hindeuten. Neben den *mamAB*-ähnlichen Operons identifizierten wir Homologe zu den erst kürzlich in anderen Deltaproteobakterien beschriebenen *mad* Genen, welche ebenfalls zum Teil in zwei Kopien vorlagen und unabhängige Operons bildeten (Cluster 3 und 4) (Abbildung 6). Interessanterweise war ein Genset von 18 *mad* Genen vorhanden, welches zuvor in

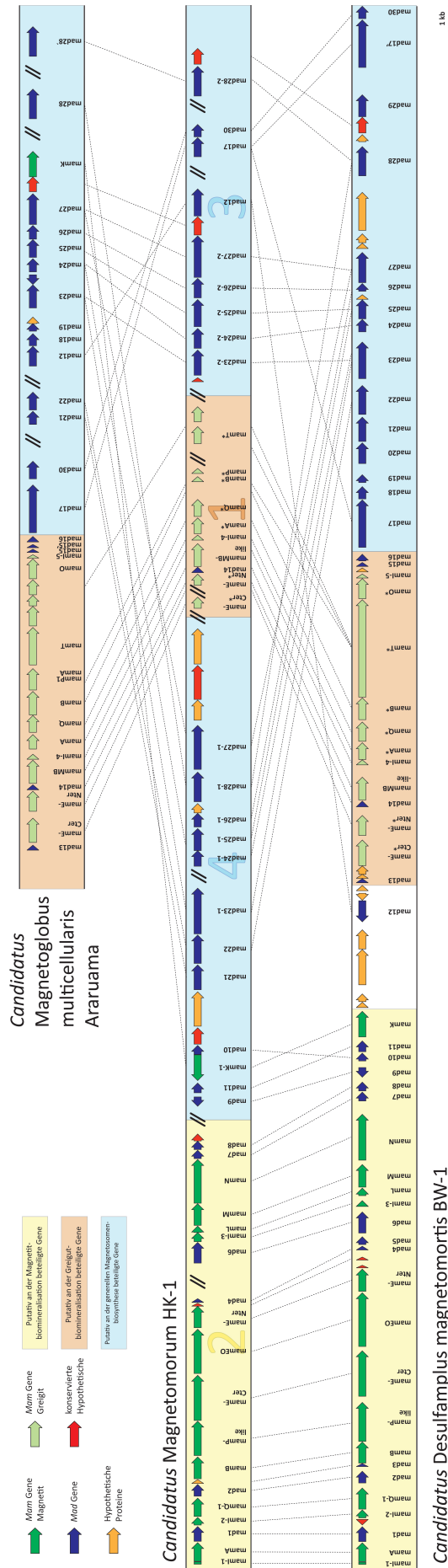


Abbildung 6: Molekulare Organisation identifizierter Magnetosomengene in *Ca. M. HK-1* verglichen mit den greigitproduzierenden MTB *Ca. D. magnetomortis* BW-1 und *Ca. M. multicellularis*. Verbindungsstriche zwischen Genen deuten homologe Gene an. An der Greigitbiosynthese beteiligte *mamAB*-ähnliche Operons sind orange hinterlegt, an der Magnetitbiosynthese beteiligte Operons sind gelb hinterlegt und Magnetosomengene die an der generellen Biosynthese beteiligt sind blau hinterlegt.

anderen magnetischen Deltaproteobakterien mit projektilförmigen Magnetitmagetosomen gefunden wurde (Lefèvre *et al.*, 2013), mit der Ausnahme von *mad20* in HK-1 vorhanden. Dies stimmt mit der Beobachtung projektilförmiger Magnetitmagetosomen in *Ca. M. rongchengroseum* und *Ca. M. litorale* überein. Der Klasse der *mad*-Gene wird ähnlich zu den Genen in den alphaproteobakteriellen *mamGFDC*, *mms6* und *mamXY* Operons eine Beteiligung an der Bestimmung der Magnetosomenmorphologie zugeschrieben (Lefèvre *et al.*, 2013).

2.2.4. Genetische Diversität der Magnetosomenbiosynthese unkultivierter *Nitrospirae*

Im Gegensatz zu kultivierten MTB, die nur 20-100 Magnetosomen pro Zelle synthetisieren können, sind MTB des phylogenetisch tiefabzweigenden *Nitrospirae* Phylums Fähig bis zu 1.000 Magnetitmagetosomen mit Projektilform herzustellen. Aufgrund dessen ist die genetische Determination der Magnetosomenbiosynthese in MTB des phylogenetisch tiefabzweigenden *Nitrospirae* Phylums von besonderem Interesse.

So beinhaltet das *Ca. M. bavaricum* Einzelzell-Genom die Magnetosomengene (*mamABEIKMOPQ*), die innerhalb eines *mamAB*-ähnlichen Operons organisiert waren und den bereits bekannten Sequenzen eines metagenomischen Klons entsprachen (Jogler *et al.*, 2011). Des Weiteren stimmten die Sequenzidentität der *mamAB*-ähnlichen Operons, die Genorganisation und der G+C Gehalt (~50%) zwischen *Ca. M. bavaricum* und *Ca. M. casensis* bis auf geringe Abweichungen ebenfalls überein (Abbildung 6, Tabelle 2). Diese große Ähnlichkeit der Magnetosomengene zwischen diesen *Nitrospirae*-Vertretern, die in geografisch getrennten Habitaten identifiziert wurden, sind ein Indiz für eine starke Konservierung der *mamAB*-ähnlichen Operons innerhalb der Gruppe der *Ca. Magnetobacteria*.

Ein partielles *mamAB*-ähnliches Operon in *Ca. M. chiemensis* mit den Magnetosomengenen (*mamABQME*) wies bis auf die Position von *mamE* eine ähnliche Genorganisation wie in *Ca. M. bavaricum* auf (Abbildung 5). Mit einem G+C Gehalt von 40% wich das *mamAB*-ähnliche Operon nur geringfügig von dem des Genoms ab, zeigte aber einen wesentlich geringeren G+C Gehalt verglichen zu *Ca. M. casensis* und *Ca. M. bavaricum* (Tabelle 2). Ebenso haben die Magnetosomenproteine mit ~50% eine wesentlich geringere Sequenzidentität zu *Ca. M. bavaricum* und *Ca. M. casensis*. In Hinsicht auf die 16S rRNA Gensequenzidentität von 94% zu seinem nächsten phylogenetischen Verwandten *Ca. M. litorale* weist dies auf eine größere genetische Diversität innerhalb der magnetotaktischen *Nitrospirae* hin.

Neben den in allen MTB präsenten *mam*-Genen wurden in allen magnetotaktischen *Nitrospirae* Homologe zu den zuvor in Deltaproteobakterien gefundenen *mad*-Genen identifiziert (Lefèvre *et al.*, 2013). Das Set von 18 *mad*-Genen, welches in allen magnetotaktischen Deltaproteobakterien die projektilförmige Magnetosomen biosynthetisieren vorhanden ist (Lefèvre *et al.*, 2013), war mit *mad2*, *mad10*, *mad11*, *mad17*, *mad20*, *mad23*, *mad24*, *mad25*, *mad26*, *mad28*, *mad29* und *mad30* nur partiell in magnetotaktischen *Nitrospirae* vorhanden. Jedoch sind die *mad*-Gene *mad23*, *mad24*, *mad25* und *mad26* in allen magnetischen Deltaproteobakterien und *Nitrospirae* vorhanden und sind in *Ca. M. bavaricum* und *Ca. M. casensis* Bestandteil des *mamAB*-ähnlichen Operons (Abbildung 5 und 6) (Jogler *et al.*, 2011; Lefèvre *et al.*, 2013; Lin *et al.*, 2014). Aufgrund ihrer Präsenz und konservierten Organisation in allen MTB mit projektilförmigen Magnetosomen (Abbildung 5 und 6) könnte es sein, dass diese Gene die spezifische Magnetosomenmorphologie determinieren. Auch außerhalb des *mamAB*-ähnlichen Operons wurden in allen *Nitrospirae* weitere Magnetosomengene gefunden. So konnten die putativ am Eisentransport beteiligten Gene *mad17* und *mad30* identifiziert werden. In *Ca. M. chiemensis* sind die Proteine Mad17, Mad30 sowie MamB in enger Nachbarschaft kodiert, was auf eine Interaktion dieser Proteine bei der Eisenaufnahme hindeuten könnte. Neben MamK ist außerdem das Aktin-ähnliche Mad28 in *Ca. M. bavaricum* in fünf Kopien, und in allen *Nitrospirae* in mindestens zwei Kopien kodiert (Abbildung 5). Der hohe Anteil zytoskeletaler Proteine könnte mit der Fähigkeit magnetischer *Nitrospirae* zusammenhängen, den starken magnetischen Interaktionen von bis zu 1.000 Magnetosomen pro Zelle standzuhalten und diese in mehreren Kettenbündeln zu organisieren. Vorläufige Versuche zur heterologe Expression eines MamK-eGFP Fusionsproteins in *M. gryphiswaldense* führte jedoch nicht zu der Bildung eines Filaments (Toro, persönliche Kommunikation) und könnte auf die Notwendigkeit weiterer Proteine und Interaktionspartner für die Filamentbildung hindeuten. Interessanterweise befinden sich *mamK* und ein *mad28* in allen *Nitrospirae* in direkter Nachbarschaft und sind immer durch ein *mad11* getrennt. Obwohl Mad11 keine signifikante Homologie zu anderen Proteinen hat und hierdurch keine potentielle Funktion vorhergesagt werden kann (Lefèvre *et al.*, 2013), ist es wahrscheinlich, dass die Interaktion zwischen Mad11 und den Aktin-ähnlichen Proteinen MamK und Mad28 für die Filamentbildung benötigt wird. In allen untersuchten *Nitrospirae* befindet sich ein weiteres *mad28* in der Nähe eines potentiellen Penizillin-Binde-Proteins (PBP1A), welches an der Peptidoglykansynthese beteiligt ist (Banzhaf *et al.*, 2012; Sauvage *et al.*, 2008). Magnetosomenketten in *Ca. M. bavaricum* liegen an der Zellmembran an und sind asymmetrisch in der Zelle angeordnet (Jogler *et al.*, 2011), jedoch nicht wie ursprünglich angenommen im größtmöglichen Abstand zueinander (Hanzlik *et al.*, 1996). Eine mögliche Funktion der Peptidoglykansynthese in der Zellteilung könnte auf einer Interaktion mit dem

Zytoskelett basieren. Eine Interaktion könnte aufgrund der asymmetrischen Anordnung des Zytoskeletts zu einer einseitigen Zellbiegung führen, welche nötig wäre, um die starke magnetische Interaktion zweier Tochterzellen während der Zellseparation zu überwinden (Katzmann *et al.*, 2011). Das Magnetosomengen *mad29* befindet sich in allen magnetischen *Nitrospirae* und Deltaproteobakterien und ist immer in der Nähe von *mad28* (Lefèvre *et al.*, 2013; Lin *et al.*, 2014). Mad29 ist homolog zu ATPasen und könnte daher Aktin-ähnliche Proteine bei der Hydrolyse von gebundenem ATP unterstützen und wäre somit an der Magnetosomenpositionierung wie es für *M. gryphiswaldense* beschrieben wurde beteiligt (Draper *et al.*, 2011).

Neben den *mam*- und *mad*-Genen konnten wir in *Ca. M. bavaricum* mit *man5* und *man6* zwei Gene der kürzlich entdeckten Klasse der *man*-Gene identifizieren (Lin *et al.*, 2014). Während diese Gene identisch zu ihren Homologen in *Ca. M. casensis* waren, konnten wir in *Ca. M. chiemensis* keine homologen Gene identifizieren. Daher könnte es sich bei den *man*-Genen weniger um *Nitrospirae*-spezifisch als um *Ca. Magnetobacterium*-spezifische Gene handeln. Des Weiteren wurden die Verwandtschaftsverhältnisse konservierter Mam und Mad Proteine, die im Rahmen dieser Arbeit in allen MTB identifiziert wurden, analysiert. Um Abweichungen individueller Proteine zu verringern erfolgte dies mit je 4 konkatenierten konservierten Proteinsequenzen, die in allen erhaltenen Genomsequenzen vorhanden waren (MamABEQ und Mad23-26).

Interessanterweise bilden die Mam und Mad-Proteine der *Nitrospirae* und *Omnitrophica* eine gemeinsame Gruppe und sind näher mit deltaproteobakteriellen Proteinen verwandt, die potentiell an der Greigitbiomineralisation beteiligt sind, als zu solchen für die Magnetitsynthese (Abbildung 7). Im Gegensatz zu den 16S rRNA Gensequenz Bäumen zweigen die Mam und Mad-Proteine innerhalb der Deltaproteobakterien ab und bilden keinen externen Zweig (Abbildung 7). Im Gegensatz zu seiner 16S rRNA Gensequenz sind die Mam-Proteine des magnetischen *Omnitrophica Ca. O. magneticus* nahverwandt mit den Mam-Proteinen des *Nitrospirae Ca. M. chiemensis*.

Diese phylogenetischen Analysen, die in dieser Weise bisher aufgrund der mangelhaften Datenlage noch nicht durchgeführt werden konnten, widersprechen der Hypothese der polyphyletischen Evolution der Magnetotaxis. Auch widerlegen sie die Hypothese eines gemeinsamen magnetotaktischen Vorfahren aller *Proteobacteria*, *Nitrospirae* und insbesondere *Omnitrophica* und unterstützen vielmehr die Hypothese des monophyletischen Ursprungs der Magnetotaxis und der Verbreitung dieser Eigenschaft via horizontalen Gentransfer.

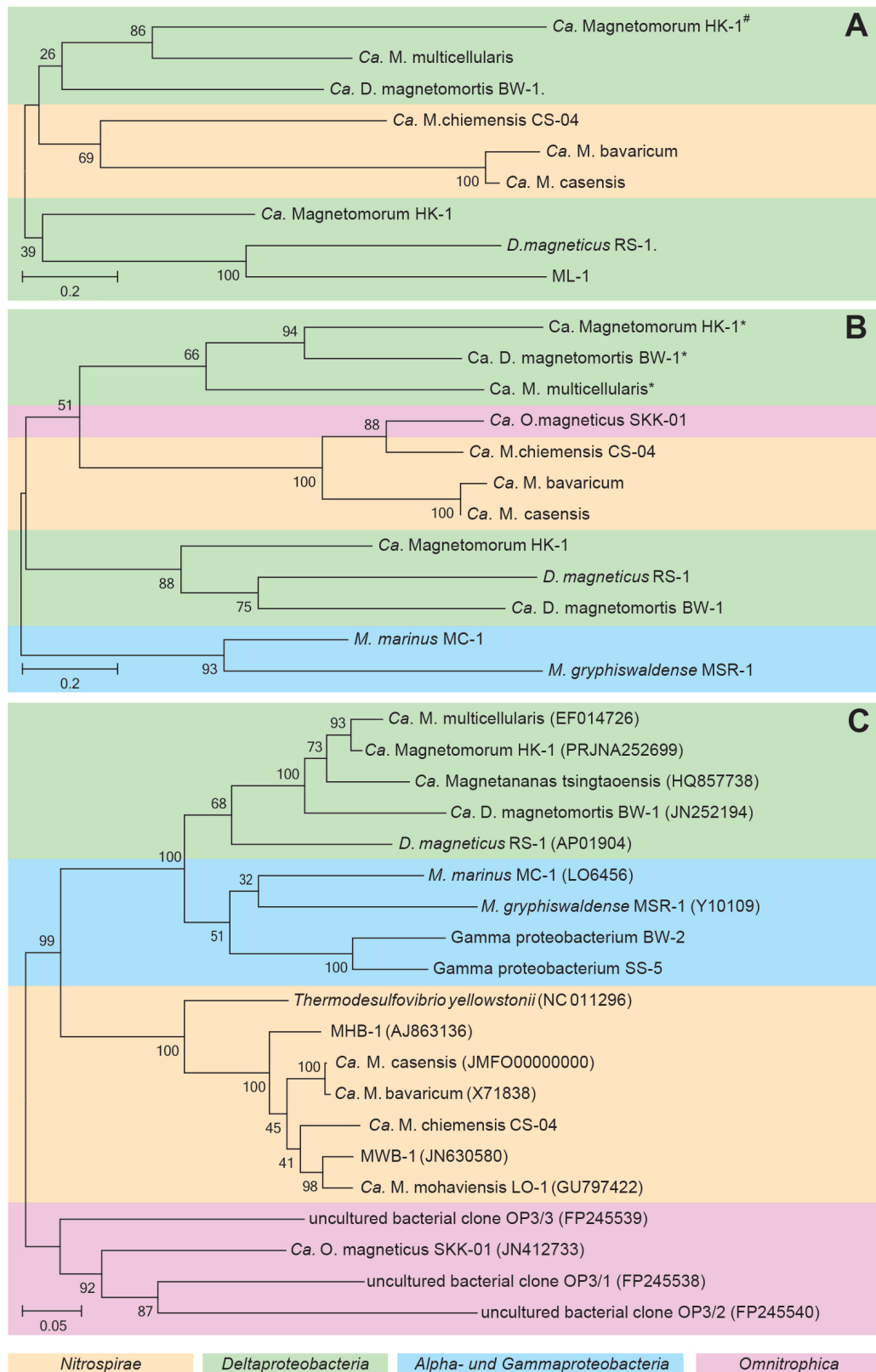


Abbildung 7: Phylogenetische Bäume konkatenierter Mad-Proteine (Mad23-26) **(A)**, konkatenierter Mam-Proteinen (MamABEQ) **(B)** und der 16S rRNA Gensequenzen **(C)** magnetotaktischer Bakterien der *Alphaproteobacteria*, *Gammaproteobacteria* (beide blau hinterlegt), *Deltaproteobacteria* (grün hinterlegt), *Nitrospirae* (gelb hinterlegt) und *Omnithrophica* (rosa hinterlegt). # = Mad-Proteine des Clusters 4 in *Ca. Magnetomorum* HK-1. * = Mam-Proteine die putativ an der Greigitzbiomineralisation beteiligt sind.

2.3. Ausblick

Im Rahmen dieser Doktorarbeit ist es erstmals gelungen, durch die Entwicklung eines abundanzunabhängigen Einzelzell-Ansatzes verschiedene unkultivierte magnetotaktische Bakterien morphologisch, phylogenetisch und genomisch zu analysieren. Durch die Rekonstruktion der MAI des multizellulären magnetischen Prokaryoten *Ca. Magnetomorum* HK-1 aus der Klasse der *Deltaproteobacteria* sowie der magnetischen *Nitrospirae* *Ca. M. bavaricum* und *Ca. M. chiemensis* konnte die genetische Diversität der Magnetosomenbiosynthese erweitert werden.

Darüber hinaus identifizierten wir mit *Ca. O. magneticus* das erste MTB, das phylogenetisch dem Kandidatenphylum *Omnitrophica* zugeordnet wird. Hierdurch wurde die erste Morphologie und die ersten Magnetosomengene dieses phylogenetisch tiefabzweigenden Phylums analysiert. Durch den Abgleich der Einzelzell-Genome mit Metagenombanken aus magnetischen Anreicherungen könnten nun in einem nächsten Schritt Anschlussklone identifiziert und durch überlappende Sequenzbereiche vorhandene Lücken in den Genomen geschlossen werden.

Basierend auf unseren Ergebnissen könnten Magnetosomengene dieser unkultivierten MTB unter Verwendung synthetischer Biologie heterolog in einem fremden Wirt, wie dem *M. gryphiswaldense* Stamm IK-1 und *Rhodospirillum rubrum* (Kolinko *et al.*, 2011; Kolinko *et al.*, 2014) expremiert werden, wodurch i) die genetischen Determinanten für die Biosynthese projektilförmiger Magnetosomen analysiert werden könnten sowie ii) projektilförmige Magnetosomenmorphologien für biotechnologische Anwendungen zur Verfügung stünden. So klonierte Kolinko *et al.*, 2014 alle Magnetosomen-Operons aus *M. gryphiswaldense* in Expressionsvektoren und transferierte diese in *R. rubrum*. Dies führte zur Magnetosomenbiosynthese durch diesen ursprünglich unmagnetischen Wirt. Durch den sukzessiven Austausch der Gene in den Expressionsvektoren die an der Kontrolle der Kristallgröße und Morphologie beteiligt sind durch konservierte *mad*-Gene, wie zum Beispiel *mad23*, *mad24*, *mad25* und *mad26*, könnte deren Funktion bei der Biosynthese projektilförmiger Magnetosomen offenbart werden. Durch weiterführende Expressionsstudien könnte die bisher weitestgehend unbekannt Funktionen der *mad* und *man*-Gene untersucht und ihre Beteiligung an der Biosynthese projektilförmiger Magnetosomen erörtert werden. Zudem könnte durch die Substitution des *mamAB*-Operons in den Expressionskassetten durch das putative Greigit *mamAB*-Operon aus *Ca. Magnetomorum* HK-1 und die heterologe Expression in verschiedenen magnetischen und nicht-magnetischen Wirten die genetische Kontrolle der Greigitbiomineralisation erörtert werden.

Obwohl die Existenz eines Gens innerhalb eines Genoms noch kein Beweis für dessen Expression oder Aktivität des Enzyms darstellt, lassen die in dieser Arbeit vorgestellten

genomischen Daten Rückschlüsse auf die potentielle Physiologie der MTB zu und dienen somit zielgerichteten Kultivierungsversuchen.

Weiterhin kann dieser Einzelzell-Ansatz für die morphologische, phylogenetische und genomische Analyse unkultivierter Bakterien auf andere auch nicht-magnetotaktische Bakterien übertragen werden.

3. Referenzen

- Abreu, F., Martins, J. L., Silveira, T. S., Keim, C. N., de Barros, H. G., Filho, F. J. & Lins, U. (2007).** 'Candidatus Magnetoglobus multicellularis', a multicellular, magnetotactic prokaryote from a hypersaline environment. *Int J Syst Evol Microbiol* **57**, 1318-1322.
- Abreu, F., Cantao, M. E., Nicolas, M. F., Barcellos, F. G., Morillo, V., Almeida, L. G., do Nascimento, F. F., Lefèvre, C. T., Bazylinski, D. A., AT, R. d. V. & Lins, U. (2011).** Common ancestry of iron oxide- and iron-sulfide-based biomineralization in magnetotactic bacteria. *ISME J* **5**, 1634–1640.
- Abreu, F., Morillo, V., Nascimento, F. F., Werneck, C., Cantao, M. E., Ciapina, L. P., de Almeida, L. G., Lefèvre, C. T., Bazylinski, D. A., de Vasconcelos, A. T. & Lins, U. (2014).** Deciphering unusual uncultured magnetotactic multicellular prokaryotes through genomics. *ISME J* **8**, 1055-1068.
- Abreu, F. P., Silva, K. T., Farina, M., Keim, C. N. & Lins, U. (2008).** Greigite magnetosome membrane ultrastructure in 'Candidatus Magnetoglobus multicellularis'. *Int Microbiol* **11**, 75-80.
- Abulencia, C. B., Wyborski, D. L., Garcia, J. A., Podar, M., Chen, W., Chang, S. H., Chang, H. W., Watson, D., Brodie, E. L., Hazen, T. C. & Keller, M. (2006).** Environmental whole-genome amplification to access microbial populations in contaminated sediments. *Appl Environ Microbiol* **72**, 3291-3301.
- Achbergerová, L. & Nahalka, J. (2011).** Polyphosphate-an ancient energy source and active metabolic regulator. *Microb Cell Fact* **10**, 63.
- Amann, R., Peplies, J. & Schüler, D. (2006).** Diversity and Taxonomy of Magnetotactic Bacteria. In *Magnetoreception and Magnetosomes in Bacteria*, pp. 25-36. Edited by D. Schüler. Heidelberg: Springer-Verlag.
- Amann, R. I., Ludwig, W. & Schleifer, K. H. (1995).** Phylogenetic identification and *in situ* detection of individual microbial cells without cultivation. *Microbiol Rev* **59**, 143-169.
- Bankevich, A., Nurk, S., Antipov, D., Gurevich, A. A., Dvorkin, M., Kulikov, A. S., Lesin, V. M., Nikolenko, S. I., Pham, S., Prjibelski, A. D., Pyshkin, A. V., Sirotkin, A. V., Vyahhi, N., Tesler, G., Alekseyev, M. A. & Pevzner, P. A. (2012).** SPAdes: a new genome assembly algorithm and its applications to single-cell sequencing. *J Comput Biol* **19**, 455-477.
- Banzhaf, M., van den Berg van Saparoea, B., Terrak, M., Fraipont, C., Egan, A., Philippe, J., Zapun, A., Breukink, E., Nguyen-Disteche, M., den Blaauwen, T. & Vollmer, W. (2012).** Cooperativity of peptidoglycan synthases active in bacterial cell elongation. *Mol Microbiol* **85**, 179-194.

Baumgartner, J., Bertinetti, L., Widdrat, M., Hirt, A. M. & Faivre, D. (2013). Formation of magnetite nanoparticles at low temperature: from superparamagnetic to stable single domain particles. *PLoS One* **8**, e57070.

Bazylinski, D. A., Frankel, R. B. & Jannasch, H. W. (1988). Anaerobic magnetite production by a marine magnetotactic bacterium. *Nature* **334**, 518-519.

Bazylinski, D. A., Frankel, R. B., Heywood, B. R., Mann, S., King, J. W., Donaghay, P. L. & Hanson, A. K. (1995). Controlled Biomineralization of Magnetite (Fe₃O₄) and Greigite (Fe₃S₄) in a Magnetotactic Bacterium. *Appl Environ Microbiol* **61**, 3232-3239.

Bazylinski, D. A. & Frankel, R. B. (2004). Magnetosome formation in prokaryotes. *Nat Rev Microbiol* **2**, 217-230.

Bazylinski, D. A., Williams, T. J., Lefèvre, C. T., Berg, R. J., Zhang, C. L., Bowser, S. S., Dean, A. J. & Beveridge, T. J. (2013a). *Magnetococcus marinus* gen. nov., sp. nov., a marine, magnetotactic bacterium that represents a novel lineage (*Magnetococcaceae* fam. nov., *Magnetococcales* ord. nov.) at the base of the *Alphaproteobacteria*. *Int J Syst Evol Microbiol* **63**, 801-808.

Bazylinski, D. A., Williams, T. J., Lefèvre, C. T., Trubitsyn, D., Fang, J., Beveridge, T. J., Moskowitz, B. M., Ward, B., Schübbe, S., Dubbels, B. L. & Simpson, B. (2013b). *Magnetovibrio blakemorei* gen. nov., sp. nov., a magnetotactic bacterium (*Alphaproteobacteria: Rhodospirillaceae*) isolated from a salt marsh. *Int J Syst Evol Microbiol* **63**, 1824-1833.

Bellini, S. (1963). Su di un particolare comportamento di batteri d'acqua dolce. *Microbiology Institute, University of Pavia*.

Blakemore, R. P. (1975). Magnetotactic bacteria. *Science* **190**, 377-379.

Blakemore, R. P., Maratea, D. & Wolfe, R. S. (1979). Isolation and pure culture of a freshwater magnetic spirillum in chemically defined medium. *J Bacteriol* **140**, 720-729.

Blakemore, R. P. (1982). Magnetotactic bacteria. *Annu Rev Microbiol* **36**, 217-238.

Brofft, J. E., McArthur, J. V. & Shimkets, L. J. (2002). Recovery of novel bacterial diversity from a forested wetland impacted by reject coal. *Environ Microbiol* **4**, 764-769.

Bruns, A., Cypionka, H. & Overmann, J. (2002). Cyclic AMP and acyl homoserine lactones increase the cultivation efficiency of heterotrophic bacteria from the central Baltic Sea. *Appl Environ Microbiol* **68**, 3978-3987.

Bruns, A., Nübel, U., Cypionka, H. & Overmann, J. (2003). Effect of signal compounds and incubation conditions on the culturability of freshwater bacterioplankton. *Appl Environ Microbiol* **69**, 1980-1989.

Caldwell, D. E., Wolfaardt, G. M., Korber, D. R. & Lawrence, J. R. (1997). Cultivation of microbial consortia and communities. In *Manuel of Environmental Microbiology*, pp. 79-90. Edited by M. V. Walter. Washington, D. C.: ASM Press.

Dannenberg, S., Kroder, M., Dilling, W. & Cypionka, H. (1992). Oxidation of H₂, organic compounds and inorganic sulfur compounds coupled to reduction of O₂ or nitrate by sulfate-reducing bacteria. *Arch Microbiol* **158**, 93-99.

Dean, F. B., Nelson, J. R., Giesler, T. L. & Lasken, R. S. (2001). Rapid amplification of plasmid and phage DNA using Phi 29 DNA polymerase and multiply-primed rolling circle amplification. *Genome Res* **11**, 1095-1099.

Dean, F. B., Hosono, S., Fang, L., Wu, X., Faruqi, A. F., Bray-Ward, P., Sun, Z., Zong, Q., Du, Y., Du, J., Driscoll, M., Song, W., Kingsmore, S. F., Egholm, M. & Lasken, R. S. (2002). Comprehensive human genome amplification using multiple displacement amplification. *Proc Natl Acad Sci U S A* **99**, 5261-5266.

DeLong, E. F., Frankel, R. B. & Bazylinski, D. A. (1993). Multiple evolutionary origins of magnetotaxis in bacteria. *Science* **259**, 803-806.

Derakshani, M., Lukow, T. & Liesack, W. (2001). Novel bacterial lineages at the (sub)division level as detected by signature nucleotide-targeted recovery of 16S rRNA genes from bulk soil and rice roots of flooded rice microcosms. *Appl Environ Microbiol* **67**, 623-631.

Dilling, W. & Cypionka, H. (1990). Aerobic respiration in sulfate-reducing bacteria. *FEMS Microbiol Lett* **71**, 123-127.

Dong, L. F., Sobey, M. N., Smith, C. J., Rusmana, I., Phillips, W., Stoff, A., Osborn, A. M. & Nedwell, D. B. (2011). Dissimilatory reduction of nitrate to ammonium, not denitrification or anammox, dominates benthic nitrate reduction in tropical estuaries. *Limnol Oceanogr* **56**, 279-291.

Draper, O., Byrne, M. E., Li, Z., Keyhani, S., Barrozo, J. C., Jensen, G. & Komeili, A. (2011). MamK, a bacterial actin, forms dynamic filaments *in vivo* that are regulated by the acidic proteins MamJ and LimJ. *Mol Microbiol* **82**, 342-354.

Edwards, R. (2014). *Naming Jack the Ripper*: Globe Pequot Press.

Elshahed, M. S., Youssef, N. H., Luo, Q., Najjar, F. Z., Roe, B. A., Sisk, T. M., Buhning, S. I., Hinrichs, K. U. & Krumholz, L. R. (2007). Phylogenetic and metabolic diversity of *Planctomycetes* from anaerobic, sulfide- and sulfur-rich Zodletone Spring, Oklahoma. *Appl Environ Microbiol* **73**, 4707-4716.

Faivre, D., Agrinier, P., Menguy, N., Zuddas, P., Pachana, K., Gloter, A., Laval, J.-Y. & Guyot, F. (2004). Mineralogical and isotopic properties of inorganic nanocrystalline magnetites. *Geochimica et Cosmochimica Acta* **68**, 4395-4403.

Faivre, D., Menguy, N., Guyot, F., Lopez, O. & Zuddas, P. (2005). Morphology of nanomagnetite crystals: Implications of formation conditions. *Am Min* **90**, 1793-1800.

Faivre, D. & Zuddas, P. (2007). Mineralogical and Isotopic Properties of Biogenic Nanocrystalline Magnetites. In *Magnetoreception and magnetosomes in bacteria*, pp. 175-196. Edited by D. Schüler. Heidelberg: Springer-Verlag.

Faivre, D. & Schüler, D. (2008). Magnetotactic bacteria and magnetosomes. *Chem Rev* **108**, 4875-4898.

Farina, M., Esquivel, D. M. S. & Lins de Barros, H. G. P. (1990). Magnetic iron-sulphur crystals from a magnetotactic microorganism. *Nature* **343**, 256-258.

Flies, C. B., Jonkers, H. M., de Beer, D., Bosselmann, K., Böttcher, M. E. & Schüler, D. (2005a). Diversity and vertical distribution of magnetotactic bacteria along chemical gradients in freshwater microcosms. *FEMS Microbiol Ecol* **52**, 185-195.

Flies, C. B., Peplies, J. & Schüler, D. (2005b). Combined approach for characterization of uncultivated magnetotactic bacteria from various aquatic environments. *Appl Environ Microbiol* **71**, 2723-2731.

Frankel, R. B., Bazylinski, D. A., Johnson, M. S. & Taylor, B. L. (1997). Magneto-aerotaxis in marine coccoid bacteria. *Biophys J* **73**, 994-1000.

Gich, F., Janys, M. A., König, M. & Overmann, J. (2012). Enrichment of previously uncultured bacteria from natural complex communities by adhesion to solid surfaces. *Environ Microbiol* **14**, 2984-2997.

Glöckner, J., Kube, M., Shrestha, P. M., Weber, M., Glöckner, F. O., Reinhardt, R. & Liesack, W. (2010). Phylogenetic diversity and metagenomics of candidate division OP3. *Environ Microbiol* **12**, 1218-1229.

Gnerre, S., Maccallum, I., Przybylski, D., Ribeiro, F. J., Burton, J. N., Walker, B. J., Sharpe, T., Hall, G., Shea, T. P., Sykes, S., Berlin, A. M., Aird, D., Costello, M., Daza, R., Williams, L., Nicol, R., Gnirke, A., Nusbaum, C., Lander, E. S. & Jaffe, D. B. (2011). High-quality draft assemblies of mammalian genomes from massively parallel sequence data. *Proc Natl Acad Sci U S A* **108**, 1513-1518.

Gorby, Y. A., Beveridge, T. J. & Blakemore, R. P. (1988). Characterization of the bacterial magnetosome membrane. *J Bacteriol* **170**, 834-841.

Grünberg, K., Wawer, C., Tebo, B. M. & Schüler, D. (2001). A large gene cluster encoding several magnetosome proteins is conserved in different species of magnetotactic bacteria. *Appl Environ Microbiol* **67**, 4573-4582.

Grünberg, K., Müller, E. C., Otto, A., Reszka, R., Linder, D., Kube, M., Reinhardt, R. & Schüler, D. (2004). Biochemical and proteomic analysis of the magnetosome membrane in *Magnetospirillum gryphiswaldense*. *Appl Environ Microbiol* **70**, 1040-1050.

Guo, F. F., Yang, W., Jiang, W., Geng, S., Peng, T. & Li, J. L. (2012). Magnetosomes eliminate intracellular reactive oxygen species in *Magnetospirillum gryphiswaldense* MSR-1. *Environ Microbiol* **14**, 1722-1729.

Gupta, R. S., Bhandari, V. & Naushad, H. S. (2012). Molecular Signatures for the PVC Clade (*Planctomycetes*, *Verrucomicrobia*, *Chlamydiae*, and *Lentisphaerae*) of *Bacteria* Provide Insights into Their Evolutionary Relationships. *Frontiers in Microbiology* **3**, 327.

Handelsman, J., Rondon, M. R., Brady, S. F., Clardy, J. & Goodman, R. M. (1998). Molecular biological access to the chemistry of unknown soil microbes: a new frontier for natural products. *Chemistry & biology* **5**, R245-249.

Hanzlik, M., Winklhofer, M. & Petersen, N. (1996). Spatial arrangement of chains of magnetosomes in magnetotactic bacteria. *Earth Planet Sci Lett* **145**, 125-134.

Huang, X. L., Chen, J. Y., Zhou, S. N., Xie, L. C. & Fu, C. S. (2010). [Prokaryote diversity in water environment of land-ocean ecotone of Zhuhai City]. *Ying Yong Sheng Tai Xue Bao* **21**, 452-457.

Hugenholtz, P., Pitulle, C., Hershberger, K. L. & Pace, N. R. (1998). Novel division level bacterial diversity in a Yellowstone hot spring. *J Bacteriol* **180**, 366-376.

Isambert, A., Menguy, N., Larquet, E., Guyot, F. & Valet, J.-P. (2007). Transmission electron microscopy study of magnetites in a freshwater population of magnetotactic bacteria. *Am Min* **92**, 621-630.

Jogler, C., Kube, M., Schübbe, S., Ullrich, S., Teeling, H., Bazylinski, D. A., Reinhardt, R. & Schüler, D. (2009a). Comparative analysis of magnetosome gene clusters in magnetotactic bacteria provides further evidence for horizontal gene transfer. *Environ Microbiol* **11**, 1267-1277.

Jogler, C., Lin, W., Meyerdierks, A., Kube, M., Katzmann, E., Flies, C., Pan, Y., Amann, R., Reinhardt, R. & Schüler, D. (2009b). Toward cloning of the magnetotactic metagenome: identification of magnetosome island gene clusters in uncultivated magnetotactic bacteria from different aquatic sediments. *Appl Environ Microbiol* **75**, 3972-3979.

Jogler, C. & Schüler, D. (2009). Genomics, genetics, and cell biology of magnetosome formation. *Annu Rev Microbiol* **63**, 501-521.

Jogler, C., Niebler, M., Lin, W., Kube, M., Wanner, G., Kolinko, S., Stief, P., Beck, A. J., De Beer, D., Petersen, N., Pan, Y., Amann, R., Reinhardt, R. & Schüler, D. (2010). Cultivation-independent characterization of '*Candidatus Magnetobacterium bavaricum*' via ultrastructural, geochemical, ecological and metagenomic methods. *Environ Microbiol* **12**, 2466-2478.

Jogler, C., Wanner, G., Kolinko, S., Niebler, M., Amann, R., Petersen, N., Kube, M., Reinhardt, R. & Schüler, D. (2011). Conservation of proteobacterial magnetosome genes and structures in an uncultivated member of the deep-branching *Nitrospirae* phylum. *Proc Natl Acad Sci U S A* **108**, 1134-1139.

Junge, K. (2008). Die Funktion der CDF-Transporter MamB und MamM beim magnetosomalen Eisentransport in *Magnetospirillum gryphiswaldense*. Bremen: In *Universität Bremen*.

Kao, C. M., Chen, C. Y., Chen, S. C., Chien, H. Y. & Chen, Y. L. (2008). Application of *in situ* biosparging to remediate a petroleum-hydrocarbon spill site: field and microbial evaluation. *Chemosphere* **70**, 1492-1499.

Karl, D. M. & Bjorkman, K. M. (2002). Dynamics of DOP. In *Biogeochemistry of Marine Dissolved Organic Matter*, pp. 315-319. Edited by D. A. Hansell & C. A. Carlson. San Diego: Academic press.

Katzmann, E., Scheffel, A., Gruska, M., Plitzko, J. M. & Schüler, D. (2010). Loss of the actin-like protein MamK has pleiotropic effects on magnetosome formation and chain assembly in *Magnetospirillum gryphiswaldense*. *Mol Microbiol* **77**, 208-224.

Katzmann, E., Müller, F. D., Lang, C., Messerer, M., Winklhofer, M., Plitzko, J. M. & Schüler, D. (2011). Magnetosome chains are recruited to cellular division sites and split by asymmetric septation. *Mol Microbiol* **82**, 1316-1329.

Kawaguchi, R., Burgess, J. G., Sakaguchi, T., Takeyama, H., Thornhill, R. H. & Matsunaga, T. (1995). Phylogenetic analysis of a novel sulfate-reducing magnetic bacterium, RS-1, demonstrates its membership of the *delta-Proteobacteria*. *FEMS Microbiol Lett* **126**, 277-282.

Kim, U. J., Shizuya, H., de Jong, P. J., Birren, B. & Simon, M. I. (1992). Stable propagation of cosmid sized human DNA inserts in an F factor based vector. *Nucleic Acids Res* **20**, 1083-1085.

Kleinstuber, S., Schleinitz, K. M., Breifeld, J., Harms, H., Richnow, H. H. & Vogt, C. (2008). Molecular characterization of bacterial communities mineralizing benzene under sulfate-reducing conditions. *FEMS Microbiol Ecol* **66**, 143-157.

Kogure, K., Simidu, U. & Taga, N. (1980). Distribution of viable marine bacteria in neritic seawater around Japan. *Can J Microbiol* **26**, 318-323.

Kolinko, I., Jogler, C., Katzmann, E. & Schüler, D. (2011). Frequent mutations within the genomic magnetosome island of *Magnetospirillum gryphiswaldense* are mediated by RecA. *J Bacteriol* **193**, 5328-5334.

Kolinko, I., Lohsse, A., Borg, S., Raschdorf, O., Jogler, C., Tu, Q., Pósfai, M., Tompa, E., Plitzko, J. M., Brachmann, A., Wanner, G., Müller, R., Zhang, Y. & Schüler, D. (2014). Biosynthesis of magnetic nanostructures in a foreign organism by transfer of bacterial magnetosome gene clusters. *Nat Nanotechnol* **9**, 193-197.

Komeili, A., Vali, H., Beveridge, T. J. & Newman, D. K. (2004). Magnetosome vesicles are present before magnetite formation, and MamA is required for their activation. *Proc Natl Acad Sci U S A* **101**, 3839-3844.

Komeili, A., Li, Z., Newman, D. K. & Jensen, G. J. (2006). Magnetosomes are cell membrane invaginations organized by the actin-like protein MamK. *Science* **311**, 242-245.

Lane, D. J. (1991). 16S/23S sequencing. In *Nucleic Acid Techniques in Bacterial Systematics*, pp. 115-175. Edited by E. Stackebrandt & M. G. Chichster. New York: Wiley & Sons.

Lasken, R. S. (2009). Genomic DNA amplification by the multiple displacement amplification (MDA) method. *Biochem Soc Trans* **37**, 450-453.

Lefèvre, C. T., Abreu, F., Schmidt, M. L., Lins, U., Frankel, R. B., Hedlund, B. P. & Bazylinski, D. A. (2010). Moderately thermophilic magnetotactic bacteria from hot springs in Nevada. *Appl Environ Microbiol* **76**, 3740-3743.

Lefèvre, C. T., Frankel, R. B., Abreu, F., Lins, U. & Bazylinski, D. A. (2011a). Culture-independent characterization of a novel, uncultivated magnetotactic member of the *Nitrospirae* phylum. *Environ Microbiol* **13**, 538-549.

Lefèvre, C. T., Frankel, R. B., Pósfai, M., Prozorov, T. & Bazylinski, D. A. (2011b). Isolation of obligately alkaliphilic magnetotactic bacteria from extremely alkaline environments. *Environ Microbiol* **13**, 2342-2350.

Lefèvre, C. T., Menguy, N., Abreu, F., Lins, U., Pósfai, M., Prozorov, T., Pignol, D., Frankel, R. B. & Bazylinski, D. A. (2011c). A cultured greigite-producing magnetotactic bacterium in a novel group of sulfate-reducing bacteria. *Science* **334**, 1720-1723.

Lefèvre, C. T., Vioria, N., Schmidt, M. L., Pósfai, M., Frankel, R. B. & Bazylinski, D. A. (2012). Novel magnetite-producing magnetotactic bacteria belonging to the *Gammaproteobacteria*. *ISME J* **6**, 440-450.

Lefèvre, C. T. & Bazylinski, D. A. (2013). Ecology, diversity, and evolution of magnetotactic bacteria. *Microbiol Mol Biol Rev* **77**, 497-526.

Lefèvre, C. T., Trubitsyn, D., Abreu, F., Kolinko, S., Jogler, C., de Almeida, L. G., de Vasconcelos, A. T., Kube, M., Reinhardt, R., Lins, U., Pignol, D., Schüler, D., Bazylnski, D. A. & Ginet, N. (2013). Comparative genomic analysis of magnetotactic bacteria from the *Deltaproteobacteria* provides new insights into magnetite and greigite magnetosome genes required for magnetotaxis. *Environ Microbiol* **15**, 2712-2735.

Lehours, A. C., Evans, P., Bardot, C., Joblin, K. & Gerard, F. (2007). Phylogenetic diversity of archaea and bacteria in the anoxic zone of a meromictic lake (Lake Pavin, France). *Appl Environ Microbiol* **73**, 2016-2019.

Li, R., Zhu, H., Ruan, J., Qian, W., Fang, X., Shi, Z., Li, Y., Li, S., Shan, G., Kristiansen, K., Li, S., Yang, H., Wang, J. & Wang, J. (2010). *De novo* assembly of human genomes with massively parallel short read sequencing. *Genome Res* **20**, 265-272.

Li, T. & Wang, P. (2008). [Bacterial and archaeal diversity in surface sediment from the south slope of the South China Sea]. *Wei Sheng Wu Xue Bao* **48**, 323-329.

Li, Y., Katzmann, E., Borg, S. & Schüler, D. (2012). The periplasmic nitrate reductase Nap is required for anaerobic growth and involved in redox control of magnetite biomineralization in *Magnetospirillum gryphiswaldense*. *J Bacteriol* **194**, 4847-4856.

Li, Y., Bali, S., Borg, S., Katzmann, E., Ferguson, S. J. & Schüler, D. (2013). Cytochrome cd1 nitrite reductase NirS is involved in anaerobic magnetite biomineralization in *Magnetospirillum gryphiswaldense* and requires NirN for proper d1 heme assembly. *J Bacteriol* **195**, 4297-4309.

Li, Y., Raschdorf, O., Silva, K. T. & Schüler, D. (2014a). The Terminal Oxidase cbb3 Functions in Redox Control of Magnetite Biomineralization in *Magnetospirillum gryphiswaldense*. *J Bacteriol* **196**, 2552-2562.

Li, Y., Sabaty, M., Borg, S., Silva, K. T., Pignol, D. & Schüler, D. (2014b). The oxygen sensor MgFnr controls magnetite biomineralization by regulation of denitrification in *Magnetospirillum gryphiswaldense*. *BMC Microbiol* **14**, 153.

Lin, W. & Pan, Y. (2009). Uncultivated magnetotactic cocci from yuandadu park in beijing, china. *Appl Environ Microbiol* **75**, 4046-4052.

Lin, W. & Pan, Y. (2010). Temporal variation of magnetotactic bacterial communities in two freshwater sediment microcosms. *FEMS Microbiology Lett* **302**, 85-92.

Lin, W., Jogler, C., Schüler, D. & Pan, Y. (2011a). Metagenomic analysis reveals unexpected subgenomic diversity of magnetotactic bacteria within the phylum *Nitrospirae*. *Appl Environ Microbiol* **77**, 323-326.

Lin, W., Li, B. & Pan, Y. (2011b). DMTB: a comprehensive online resource of 16S rRNA genes, ecological metadata, oligonucleotides, and magnetic properties of magnetotactic bacteria. *Chin Sci Bull* **56**, 476-478.

Lin, W., Wang, Y., Li, B. & Pan, Y. (2012). A biogeographic distribution of magnetotactic bacteria influenced by salinity. *ISME J* **6**, 475-479.

Lin, W., Wang, Y., Gorby, Y., Neilson, K. & Pan, Y. (2013). Integrating niche-based process and spatial process in biogeography of magnetotactic bacteria. *Sci Rep* **3**, 1643.

Lin, W., Deng, A., Wang, Z., Li, Y., Wen, T., Wu, L. F., Wu, M. & Pan, Y. (2014). Genomic insights into the uncultured genus 'Candidatus Magnetobacterium' in the phylum *Nitrospirae*. *ISME J*.

Lins, U., Freitas, F., Keim, C. N. & Farina, M. (2000). Electron Spectroscopic Imaging of Magnetotactic Bacteria: Magnetosome Morphology and Diversity. *Microsc Microanal* **6**, 463-470.

Lins, U., Freitas, S., De Barros, H., Esquivel, D. & Farina, M. (2003). Simple homemade apparatus for harvesting uncultured magnetotactic microorganisms. *Braz J Microbiol* **34**, 111-116.

Lohsse, A., Ullrich, S., Katzmann, E., Borg, S., Wanner, G., Richter, M., Voigt, B., Schweder, T. & Schüler, D. (2011). Functional analysis of the magnetosome island in *Magnetospirillum gryphiswaldense*: the *mamAB* operon is sufficient for magnetite biomineralization. *PLoS One* **6**, e25561.

Lohsse, A., Borg, S., Raschdorf, O., Kolinko, I., Tompa, E., Pósfai, M., Faivre, D., Baumgartner, J. & Schüler, D. (2014). Genetic dissection of the *mamAB* and *mms6* operons reveals a gene set essential for magnetosome biogenesis in *Magnetospirillum gryphiswaldense*. *J Bacteriol* **196**, 2658-2669.

Macalady, J. L., Dattagupta, S., Schaperdoth, I., Jones, D. S., Druschel, G. K. & Eastman, D. (2008). Niche differentiation among sulfur-oxidizing bacterial populations in cave waters. *ISME J* **2**, 590-601.

Madrid, V. M., Taylor, G. T., Scranton, M. I. & Chistoserdov, A. Y. (2001). Phylogenetic diversity of bacterial and archaeal communities in the anoxic zone of the Cariaco Basin. *Appl Environ Microbiol* **67**, 1663-1674.

Marcy, Y., Ishoey, T., Lasken, R. S., Stockwell, T. B., Walenz, B. P., Halpern, A. L., Beeson, K. Y., Goldberg, S. M. & Quake, S. R. (2007). Nanoliter reactors improve multiple displacement amplification of genomes from single cells. *PLoS Genet* **3**, 1702-1708.

Marczak, M., Dzwierzynska, M. & Skorupska, A. (2013). Homo- and heterotypic interactions between Pss proteins involved in the exopolysaccharide transport system in *Rhizobium leguminosarum* bv. trifolii. *Biol Chem* **394**, 541-559.

Martins, J. L., Silveira, T. S., Silva, K. T. & Lins, U. (2009). Salinity dependence of the distribution of multicellular magnetotactic prokaryotes in a hypersaline lagoon. *Int Microbiol* **12**, 193-201.

Martins, J. L., Silveira, T. S., Abreu, F., de Almeida, F. P., Rosado, A. S. & Lins, U. (2012). Spatiotemporal distribution of the magnetotactic multicellular prokaryote *Candidatus Magnetoglobus multicellularis* in a Brazilian hypersaline lagoon and in microcosms. *Int Microbiol* **15**, 141-149.

Meldrum, F. C., Mann, S., Heywood, B. R., Frankel, R. B. & Bazylinski, D. A. (1993). Electron microscopy study of magnetosomes in a cultured coccoid magnetotactic bacterium. *Proc Biol Sci* **251**, 231-236.

Murat, D., Quinlan, A., Vali, H. & Komeili, A. (2010). Comprehensive genetic dissection of the magnetosome gene island reveals the step-wise assembly of a prokaryotic organelle. *Proc Natl Acad Sci U S A* **107**, 5593-5598.

Nurk, S., Bankevich, A., Antipov, D., Gurevich, A. A., Korobeynikov, A., Lapidus, A., Prjibelski, A. D., Pyshkin, A., Sirotkin, A., Sirotkin, Y., Stepanauskas, R., Clingenpeel, S. R., Woyke, T., McLean, J. S., Lasken, R., Tesler, G., Alekseyev, M. A. & Pevzner, P. A. (2013). Assembling single-cell genomes and mini-metagenomes from chimeric MDA products. *J Comput Biol* **20**, 714-737.

Park, S. J., Kang, C. H., Chae, J. C. & Rhee, S. K. (2008). Metagenome microarray for screening of fosmid clones containing specific genes. *FEMS Microbiol Lett* **284**, 28-34.

Pikuta, E. V., Hoover, R. B., Bej, A. K., Marsic, D., Whitman, W. B., Cleland, D. & Krader, P. (2003). *Desulfonatronum thiodismutans* sp. nov., a novel alkaliphilic, sulfate-reducing bacterium capable of lithoautotrophic growth. *Int J Syst Evol Microbiol* **53**, 1327-1332.

Pilhofer, M., Rappl, K., Eckl, C., Bauer, A. P., Ludwig, W., Schleifer, K. H. & Petroni, G. (2008). Characterization and evolution of cell division and cell wall synthesis genes in the bacterial phyla *Verrucomicrobia*, *Lentisphaerae*, *Chlamydiae*, and *Planctomycetes* and phylogenetic comparison with rRNA genes. *J Bacteriol* **190**, 3192-3202.

Popp, F., Armiaige, J. P. & Schüler, D. (2014). Polarity of bacterial magnetotaxis is controlled by aerotaxis through a common sensory pathway. *Nat Commun*. Im Erscheinen.

Postec, A., Tapia, N., Bernadac, A., Joseph, M., Davidson, S., Wu, L. F., Ollivier, B. & Pradel, N. (2012). Magnetotactic bacteria in microcosms originating from the French Mediterranean Coast subjected to oil industry activities. *Microb Ecol* **63**, 1-11.

Raghunathan, A., Ferguson, H. R., Jr., Bornarth, C. J., Song, W., Driscoll, M. & Lasken, R. S. (2005). Genomic DNA amplification from a single bacterium. *Appl Environ Microbiol* **71**, 3342-3347.

Rappé, M. S. & Giovannoni, S. J. (2003). The uncultured microbial majority. *Annu Rev Microbiol* **57**, 369-394.

Raschdorf, O., Müller, F. D., Pòsfai, M., Pnitzko, J. M. & Schüler, D. (2013). The magnetosome proteins MamX, MamZ and MamH are involved in redox control of magnetite biomineralization in *Magnetospirillum gryphiswaldense*. *Mol Microbiol* **89**, 872-886.

Raschdorf, O., Pnitzko, J. M., Schüler, D. & Müller, F. D. (2014). A Tailored *galK* Counterselection System for Efficient Markerless Gene Deletion and Chromosomal Tagging in *Magnetospirillum gryphiswaldense*. *Appl Environ Microbiol* **80**, 4323-4330.

Rees, G. N., Harfoot, C. G. & Sheehy, A. J. (1998). Amino acid degradation by the mesophilic sulfate-reducing bacterium *Desulfobacterium vacuolatum*. *Arch Microbiol* **169**, 76-80.

Rinke, C., Schwientek, P., Sczyrba, A., Ivanova, N. N., Anderson, I. J., Cheng, J. F., Darling, A., Malfatti, S., Swan, B. K., Gies, E. A., Dodsworth, J. A., Hedlund, B. P., Tsiamis, G., Sievert, S. M., Liu, W. T., Eisen, J. A., Hallam, S. J., Kyrpides, N. C., Stepanauskas, R., Rubin, E. M., Hugenholtz, P. & Woyke, T. (2013). Insights into the phylogeny and coding potential of microbial dark matter. *Nature* **499**, 431-437.

Rodrigue, S., Malmstrom, R. R., Berlin, A. M., Birren, B. W., Henn, M. R. & Chisholm, S. W. (2009). Whole genome amplification and *de novo* assembly of single bacterial cells. *PLoS One* **4**, e6864.

Röling, W. F., van Breukelen, B. M., Braster, M., Lin, B. & van Verseveld, H. W. (2001). Relationships between microbial community structure and hydrochemistry in a landfill leachate-polluted aquifer. *Appl Environ Microbiol* **67**, 4619-4629.

Rong, C., Huang, Y., Zhang, W., Jiang, W., Li, Y. & Li, J. (2008). Ferrous iron transport protein B gene (*feoB1*) plays an accessory role in magnetosome formation in *Magnetospirillum gryphiswaldense* strain MSR-1. *Res Microbiol* **159**, 530-536.

Rong, C., Zhang, C., Zhang, Y., Qi, L., Yang, J., Guan, G., Li, Y. & Li, J. (2012). FeoB2 Functions in magnetosome formation and oxidative stress protection in *Magnetospirillum gryphiswaldense* strain MSR-1. *J Bacteriol* **194**, 3972-3976.

Sakaguchi, T., Arakaki, A. & Matsunaga, T. (2002). *Desulfovibrio magneticus* sp. nov., a novel sulfate-reducing bacterium that produces intracellular single-domain-sized magnetite particles. *Int J Syst Evol Microbiol* **52**, 215-221.

Sanger, F. & Coulson, A. R. (1975). A rapid method for determining sequences in DNA by primed synthesis with DNA polymerase. *J Mol Biol* **94**, 441-448.

Sanger, F., Nicklen, S. & Coulson, A. R. (1977). DNA sequencing with chain-terminating inhibitors. *Proc Natl Acad Sci U S A* **74**, 5463-5467.

Sauvage, E., Kerff, F., Terrak, M., Ayala, J. A. & Charlier, P. (2008). The penicillin-binding proteins: structure and role in peptidoglycan biosynthesis. *FEMS Microbiol Rev* **32**, 234-258.

Scheffel, A., Gardes, A., Grünberg, K., Wanner, G. & Schüler, D. (2008). The major magnetosome proteins MamGFDC are not essential for magnetite biomineralization in *Magnetospirillum gryphiswaldense* but regulate the size of magnetosome crystals. *J Bacteriol* **190**, 377-386.

Schleifer, K. H., Schüler, D., Spring, S., Weizenegger, M., Amann, R., Ludwig, W. & Köhler, M. (1991). The genus *Magnetospirillum* gen. nov., description of *Magnetospirillum gryphiswaldense* sp. nov. and transfer of *Aquaspirillum magnetotacticum* to *Magnetospirillum magnetotacticum* comb. nov. *Syst Appl Microbiol* **14**, 379-385.

Schübbe, S., Kube, M., Scheffel, A., Wawer, C., Heyen, U., Meyerdierks, A., Madkour, M. H., Mayer, F., Reinhardt, R. & Schüler, D. (2003). Characterization of a spontaneous nonmagnetic mutant of *Magnetospirillum gryphiswaldense* reveals a large deletion comprising a putative magnetosome island. *J Bacteriol* **185**, 5779-5790.

Schüler, D. (1990). Versuche zur Isolierung und Charakterisierung magnetotaktischer Bakterien. Greifswald: Ernst-Moritz-Arndt-Universität Greifswald.

Schüler, D. (1994). Isolierung und Charakterisierung magnetischer Bakterien - Untersuchungen zur Magnetitbiomineralisation in *Magnetospirillum gryphiswaldense*, pp. 1-125. München: TU München.

Schüler, D. (1999). Formation of magnetosomes in magnetotactic bacteria. *J Mol Microbiol Biotechnol* **1**, 79-86.

Schüler, D. & Bazylinski, D. A. (2007). Techniques for studying uncultured and cultured magnetotactic bacteria. In *Manual of Environmental Microbiology*, pp. 1129-1138. Edited by C. J. Hurst, R. L. Crawford, J. L. Garland, D. A. Lipson, M. A. L. & L. D. Setzenbach. Washington D.C.: ASM Press.

Schwarz, J. I., Lueders, T., Eckert, W. & Conrad, R. (2007). Identification of acetate-utilizing *Bacteria* and *Archaea* in methanogenic profundal sediments of Lake Kinneret (Israel) by stable isotope probing of rRNA. *Environ Microbiol* **9**, 223-237.

Shizuya, H., Birren, B., Kim, U. J., Mancino, V., Slepak, T., Tachiiri, Y. & Simon, M. (1992). Cloning and stable maintenance of 300-kilobase-pair fragments of human DNA in *Escherichia coli* using an F-factor-based vector. *Proc Natl Acad Sci U S A* **89**, 8794-8797.

Simmons, S. L., Sievert, S. M., Frankel, R. B., Bazylinski, D. A. & Edwards, K. J. (2004). Spatiotemporal distribution of marine magnetotactic bacteria in a seasonally stratified coastal salt pond. *Appl Environ Microbiol* **70**, 6230-6239.

Simon, C. & Daniel, R. (2010). Construction of small-insert and large-insert metagenomic libraries. *Methods Mol Biol* **668**, 39-50.

Siponen, M. I., Adryanczyk, G., Ginet, N., Arnoux, P. & Pignol, D. (2012). Magnetochrome: a c-type cytochrome domain specific to magnetotactic bacteria. *Biochem Soc Trans* **40**, 1319-1323.

Spring, S., Amann, R., Ludwig, W., Schleifer, K. H. & Petersen, N. (1992). Phylogenetic diversity and identification of nonculturable magnetotactic bacteria. *Syst Appl Microbiol* **15**, 116-122.

Spring, S., Amann, R., Ludwig, W., Schleifer, K. H., van Gernerden, H. & Petersen, N. (1993). Dominating role of an unusual magnetotactic bacterium in the microaerobic zone of a freshwater sediment. *Appl Environ Microbiol* **59**, 2397-2403.

Spring, S., Amann, R., Schleifer, K. H., Schüler, D., Poralla, K. & Petersen, N. (1995). Phylogenetic analysis of uncultured magnetotactic bacteria from the alpha-subclass of *Proteobacteria*. *Syst Appl Microbiol* **17**, 501-508.

Steuber, J. & Kroneck, P. M. H. (1998). Desulfoviridin, the dissimilatory sulfite reductase from *Desulfovibrio desulfuricans* (Essex): new structural and functional aspects of the membranous enzyme. *Inorganica Chimica Acta* **275**, 52–57.

Stolz, J. F. (1992). Magnetotactic bacteria: Biomineralization, ecology, sediment magnetism, environmental indicator. In *Biomineralization: process of iron and manganese; modern and ancient environments*, pp. 133-145. Edited by H. C. W. Skinner. Cremlingen-Destedt: Catena.

Suzuki, Y., Inagaki, F., Takai, K., Nealson, K. H. & Horikoshi, K. (2004). Microbial diversity in inactive chimney structures from deep-sea hydrothermal systems. *Microb Ecol* **47**, 186-196.

Swan, B. K., Martinez-Garcia, M., Preston, C. M., Sczyrba, A., Woyke, T., Lamy, D., Reinthaler, T., Poulton, N. J., Masland, E. D., Gomez, M. L., Sieracki, M. E., DeLong, E. F., Herndl, G. J. & Stepanauskas, R. (2011). Potential for chemolithoautotrophy among ubiquitous bacteria lineages in the dark ocean. *Science* **333**, 1296-1300.

Torsvik, V. & Ovreas, L. (2002). Microbial diversity and function in soil: from genes to ecosystems. *Curr Opin Microbiol* **5**, 240-245.

Uebe, R., Voigt, B., Schweder, T., Albrecht, D., Katzmann, E., Lang, C., Böttger, L., Matzanke, B. & Schüler, D. (2010). Deletion of a *fur*-like gene affects iron homeostasis and magnetosome formation in *Magnetospirillum gryphiswaldense*. *J Bacteriol* **192**, 4192-4204.

Uebe, R., Junge, K., Henn, V., Poxleitner, G., Katzmann, E., Plitzko, J. M., Zarivach, R., Kasama, T., Wanner, G., Pósfai, M., Böttger, L., Matzanke, B. & Schüler, D. (2011). The cation diffusion facilitator proteins MamB and MamM of *Magnetospirillum gryphiswaldense* have distinct and complex

functions, and are involved in magnetite biomineralization and magnetosome membrane assembly. *Mol Microbiol* **82**, 818-835.

Ullrich, S., Kube, M., Schübbe, S., Reinhardt, R. & Schüler, D. (2005). A hypervariable 130-kilobase genomic region of *Magnetospirillum gryphiswaldense* comprises a magnetosome island which undergoes frequent rearrangements during stationary growth. *J Bacteriol* **187**, 7176-7184.

Ullrich, S. & Schüler, D. (2010). Cre-lox-based method for generation of large deletions within the genomic magnetosome island of *Magnetospirillum gryphiswaldense*. *Appl Environ Microbiol* **76**, 2439-2444.

Vali, H., Förster, O., Amaratidis, G. & Petersen, N. (1987). Magnetotactic bacteria and their magnetofossils in sediments. *Earth Planet Sci Lett* **87**, 389-400.

Vali, H. & Kirschvink, J. L. (1991). Observations of magnetosome organization, surface structure, and iron biomineralization of undescribed magnetic bacteria. In *Iron biominerals*, pp. 97-116. Edited by R. B. Frankel & R. P. Blakemore. New York and London: Plenum press.

Wagner, M. & Horn, M. (2006). The *Planctomycetes*, *Verrucomicrobia*, *Chlamydiae* and sister phyla comprise a superphylum with biotechnological and medical relevance. *Curr Opin Biotechnol* **17**, 241-249.

Wahl, G. M., Lewis, K. A., Ruiz, J. C., Rothenberg, B., Zhao, J. & Evans, G. A. (1987). Cosmid vectors for rapid genomic walking, restriction mapping, and gene transfer. *Proc Natl Acad Sci U S A* **84**, 2160-2164.

Wang, Y., Lin, W., Li, J. & Pan, Y. (2013). High diversity of magnetotactic *Deltaproteobacteria* in a freshwater niche. *Appl Environ Microbiol* **79**, 2813-2817.

Wenter, R., Wanner, G., Schüler, D. & Overmann, J. (2009). Ultrastructure, tactic behaviour and potential for sulfate reduction of a novel multicellular magnetotactic prokaryote from North Sea sediments. *Environ Microbiol* **11**, 1493-1505.

Williams, T. J., Lefèvre, C. T., Zhao, W., Beveridge, T. J. & Bazylinski, D. A. (2011). *Magnetospira thiophila*, gen. nov. sp. nov., a new marine magnetotactic bacterium that represents a novel lineage within the *Rhodospirillaceae* (*Alphaproteobacteria*). *Int J Syst Evol Microbiol* **62**, 2443-2450.

Woese, C. R. & Fox, G. E. (1977). Phylogenetic structure of the prokaryotic domain: the primary kingdoms. *Proc Natl Acad Sci U S A* **74**, 5088-5090.

Wolfe, R. S., Thauer, R. K. & Pfennig, N. (1987). A 'capillary racetrack' method for isolation of magnetotactic bacteria. *FEMS Microbiol Ecol* **45**, 31-35.

Woyke, T., Xie, G., Copeland, A., Gonzalez, J. M., Han, C., Kiss, H., Saw, J. H., Senin, P., Yang, C., Chatterji, S., Cheng, J. F., Eisen, J. A., Sieracki, M. E. & Stepanauskas, R. (2009). Assembling the marine metagenome, one cell at a time. *PLoS One* **4**, e5299.

Woyke, T., Tighe, D., Mavromatis, K., Clum, A., Copeland, A., Schackwitz, W., Lapidus, A., Wu, D., McCutcheon, J. P., McDonald, B. R., Moran, N. A., Bristow, J. & Cheng, J. F. (2010). One bacterial cell, one complete genome. *PLoS One* **5**, e10314.

Zerbino, D. R. & Birney, E. (2008). Velvet: algorithms for *de novo* short read assembly using de Bruijn graphs. *Genome Res* **18**, 821-829.

Zerbino, D. R., McEwen, G. K., Margulies, E. H. & Birney, E. (2009). Pebble and rock band: heuristic resolution of repeats and scaffolding in the velvet short-read *de novo* assembler. *PLoS One* **4**, e8407.

Zerbino, D. R. (2010). Using the Velvet *de novo* assembler for short-read sequencing technologies. In *Curr Protoc Bioinformatics* Chapter 11:Unit 11.5.

Zhang, C., Meng, X., Li, N., Wang, W., Sun, Y., Jiang, W., Guan, G. & Li, Y. (2013). Two bifunctional enzymes with ferric reduction ability play complementary roles during magnetosome synthesis in *Magnetospirillum gryphiswaldense* MSR-1. *J Bacteriol* **195**, 876-885.

Zhang, R., Chen, Y. R., Du, H. J., Zhang, W. Y., Pan, H. M., Xiao, T. & Wu, L. F. (2014). Characterization and phylogenetic identification of a species of spherical multicellular magnetotactic prokaryotes that produces both magnetite and greigite crystals. *Res Microbiol* **165**, 481-489.

Zhou, J., He, Q., Hemme, C. L., Mukhopadhyay, A., Hillesland, K., Zhou, A., He, Z., Van Nostrand, J. D., Hazen, T. C., Stahl, D. A., Wall, J. D. & Arkin, A. P. (2011). How sulphate-reducing microorganisms cope with stress: lessons from systems biology. *Nat Rev Microbiol* **9**, 452-466.

4. Zusätzliche Informationen

Zusätzliche Tabellen

Tabelle S1: Kultivierungsansätze für die Isolierung von *Ca. M. bavaricum* aufgrund der in Kapitel 2.2.1. besprochenen funktionellen Genomanalyse.

Komponenten	1.1	1.2	1.1.1	1.1.2
Sedimentextrakt	10%	10%	10%	10%
Nitrat	2 mM	2 mM	2 mM	2 mM
Thiosulfat	10 mM	10 mM	10 mM	10 mM
NaHCO ₃	10 mM	10 mM	10 mM	10 mM
Fe(III)Citrat		10 µM	10 µM	10 µM
DTT			1 mM	1 mM
Wolfes Vitamin Lösung			0,1%	0,2%
Wolfes Mineral Lösung			0,1%	0,2%

Komponenten	2.1	2.2	2.3	2.4	2.5	2.6	2.7	2.8
Sedimentextrakt	10%	10%	10%	10%	10%	10%	10%	10%
Nitrat	2 mM	1 mM	4 mM	2 mM		8 mM	8 mM	8 mM
Thiosulfat	10 mM	10 mM	50 mM	50 mM	50 mM	25 mM		50 mM
NaHCO ₃	10 mM	10 mM	10 mM	10 mM	10 mM	10 mM	10 mM	10 mM
Fe(III)Citrat	10 µM	10 µM	25 µM	50 µM	50 µM	50 µM	50 µM	50 µM
DTT			1 mM	1 mM	1 mM	1 mM	1 mM	1 mM

Komponenten	3.1	3.2	3.3	3.4	3.5	3.6	3.7	3.8
Sedimentextrakt	10%	10%	10%	10%	10%	10%	10%	10%
Nitrat	8 mM	8 mM	8 mM	8 mM	8 mM	8 mM	8 mM	8 mM
Thiosulfat	10 mM	20 mM	30 mM	40 mM				
NaHCO ₃	10 mM	10 mM	10 mM	10 mM	10 mM	10 mM	10 mM	10 mM
Fe(III)Citrat	50 µM	50 µM	50 µM	50 µM	50 µM	50 µM	50 µM	50 µM
DTT			1 mM	1 mM	1 mM	1 mM	1 mM	1 mM
DMSO					5%	10%		
Laktat							0,5%	1%

Komponenten	4.1	4.2
Sedimentextrakt	10%	10%
Nitrat	1 mM	1 mM
Thiosulfat	10 mM	20 mM
NaHCO ₃	10 mM	10 mM
Fe(III)Citrat	10 µM	10 µM
DTT	1 mM	1 mM

Kapitel II

Publikationen und Manuskripte

1. Manuskript:

Clone libraries and single cell genome amplification reveal extended diversity of uncultivated magnetotactic bacteria from marine and freshwater environments.

Clone libraries and single cell genome amplification reveal extended diversity of uncultivated magnetotactic bacteria from marine and freshwater environments

Sebastian Kolinko,¹ Gerhard Wanner,¹
Emanuel Katzmann,¹ Felizitas Kiemer,¹
Bernhard M. Fuchs² and Dirk Schüler^{1*}

¹Biozentrum der Ludwigs-Maximilians-Universität,
Großhaderner Straße 2-4, 82 152 Planegg-Martinsried,
Germany.

²Max Planck Institute for Marine Microbiology,
Celsiusstr. 1, 28 359 Bremen, Germany.

Summary

Magnetotactic bacteria (MTB), which orient along the earth's magnetic field using magnetosomes, are ubiquitous and abundant in marine and freshwater environments. Previous phylogenetic analysis of diverse MTB has been limited to few cultured species and the most abundant and conspicuous members of natural populations, which were assigned to various lineages of the *Proteobacteria*, the *Nitrospirae* phylum as well as the candidate division OP3. However, their known phylogenetic diversity still not matches the large morphological and ultrastructural variability of uncultured MTB found in environmental communities. Here, we used analysis of 16S rRNA gene clone libraries in combination with microsorting and whole-genome amplification to systematically address the entire diversity of uncultured MTB from two different habitats. This approach revealed extensive and novel diversity of MTB within the freshwater and marine sediment samples. In total, single-cell analysis identified eight different phylotypes, which were only partly represented in the clone libraries, and which could be unambiguously assigned to their respective morphotypes. Identified MTB belonged to the *Alphaproteobacteria* (seven species) and the *Nitrospirae* phylum (two species). End-sequencing of a small insert library created from WGA-derived DNA of a novel conspicuous magnetotactic vibrio identified

genes with highest similarity to two cultivated MTB as well as to other phylogenetic groups. In conclusion, the combination of metagenomic cloning and single cell sorting represents a powerful approach to recover maximum bacterial diversity including low-abundant magnetotactic phylotypes from environmental samples and also provides access to genomic analysis of uncultivated MTB.

Introduction

Magnetotactic bacteria (MTB) are a diverse group of microorganisms, which are abundant and ubiquitous in chemically stratified aquatic or marine sediments (Flies *et al.*, 2005a; Faivre and Schüler, 2008). Common to all MTB is the presence of intracellular membrane-enclosed ferromagnetic nanocrystals of magnetite (Fe₃O₄) and/or greigite (Fe₃S₄), the magnetosomes (Bazylinski and Frankel, 2004; Jogler and Schüler, 2009; Lefèvre *et al.*, 2011b). The chain-like arrangement of these organelles allows the cells to navigate along the geomagnetic field lines in search for optimum growth conditions within chemical gradients in their stratified aquatic habitats (Frankel *et al.*, 1997; Bazylinski and Frankel, 2004; Faivre and Schüler, 2008).

MTB display a remarkable morphological, ultrastructural and phylogenetic diversity. Analysis of cultivated strains revealed them within the alpha, gamma and delta lineages of the *Proteobacteria* (Schleifer *et al.*, 1991; Kawaguchi *et al.*, 1995; Lefèvre *et al.*, 2012). In all tested cultivated MTB the genes responsible for magnetosome synthesis were identified within a large and more or less conserved genomic magnetosome island (MAI), which displays variability in different species with respect to gene content and molecular organization (Schübbe *et al.*, 2003; Ullrich *et al.*, 2005; Fukuda *et al.*, 2006; Richter *et al.*, 2007; Lefèvre *et al.*, 2012).

Despite of some recent impressive progress in isolation of novel strains, most MTB still cannot be cultivated in the lab, probably due to their lifestyle adapted to complex chemical gradients in stratified aquatic sediments, making cultivation-independent approaches

Received 25 July, 2012; revised 7 September, 2012; accepted 21 September, 2012. *For correspondence. E-mail dirk.schueler@lmu.de; Tel. (+49) 892 1807 4514; Fax (+49) 892 1807 4515.

indispensable. Unlike other uncultured bacteria, magnetotactic cells in environmental samples can be directly separated from non-MTB and inorganic matter by taking advantage of their unique magnetically directed motility (Wolfe *et al.*, 1987; Schüler and Bazylinski, 2007). Magnetic enrichment techniques, such as the 'capillary race-track' method and magnetic traps were successfully applied to collect cells for cultivation-independent phylogenetic analysis, which revealed the existence of novel uncultivated MTB belonging to the deep branching *Nitrospirae* phylum (Spring *et al.*, 1993; Flies *et al.*, 2005b; Lefèvre *et al.*, 2011a). Metagenomic analysis of magnetically collected MTB led to the identification of metabolic genes and large gene clusters homologous to the MAI of cultured MTB (Jogler *et al.*, 2010; Abreu *et al.*, 2011; Lin *et al.*, 2011a).

Whereas most studies of uncultivated MTB were limited to the analysis of highly abundant members of the community, genome amplification from single or few cells of low-abundant morphotypes revealed the existence of novel and extended phylogenetic diversity which had escaped detection by previous mass cloning approaches. For instance, a novel ovoid magnetic bacterium designated as SKK-01 could be assigned to the candidate division OP3, which so far only comprises uncultivated bacteria (Kolinko *et al.*, 2012). The combination of micromanipulation, whole-genome amplification (WGA) and screening of metagenomic libraries identified a magnetosome island in the uncultivated *Nitrospirae* '*Candidatus* Magnetobacterium bavaricum' (Mbav) (Jogler *et al.*, 2011). These studies indicated that the known phylogenetic and genomic diversity still only represents a minor part of the seemingly infinite morphological and ultrastructural variability observed in uncultured MTB from environmental communities.

While previous single-cell studies were limited to individual morphotypes, here we demonstrate that single-cell approaches and WGA can also be applied to the analysis of entire MTB communities. We show that maximum phylogenetic diversity from marine and freshwater habitats was recovered by a combination of single cell techniques and mass cloning strategies. By microsorting, morphotypes could be directly correlated to their corresponding phylotypes. A total of nine phylotypes, some of them putatively representing new genera and species, were assigned to the *Alphaproteobacteria* class (seven) and the *Nitrospirae* phylum (two). In addition, we demonstrate the use of small insert libraries from WGA-derived DNA for genomic analysis of single microsorted cells of a novel MTB.

Results

Diversity analysis by 16S rRNA gene clone libraries

For diversity analysis, MTB were magnetically collected from single microcosms obtained from two different

sampling sites, which were previously found to harbour a variety of diverse MTB: a marine intertidal mudflat sediment from the Wadden sea near Cuxhaven (*Cux*), (Flies *et al.*, 2005b; Wenter *et al.*, 2009), and a freshwater sediment from Lake Chiemsee (*CS*) (Spring *et al.*, 1993; Jogler *et al.*, 2010; Kolinko *et al.*, 2012).

Microscopy of hanging drops from *Cux* enrichments revealed three different magnetic morphotypes present in different relative abundances (Fig. 1, Table 1): An abundant bigger (~ 2.5 µm) coccus named *Cux*-01 with elongated prismatic magnetosomes contained both electron-dense and opaque granular inclusions, while a smaller (~ 1.5 µm), highly abundant coccus (*Cux*-02), also with elongated prismatic magnetosomes, had only electron dense granules. A magnetic large vibrio (*Cux*-03, 3.5 µm in length) with two characteristic polar electron dense inclusions was present in much lower numbers.

For phylogenetic analysis almost full-length 16S rRNA genes were amplified from magnetic enrichments applying universal eubacterial primers (Lane, 1991) and sub-cloned. From 50 tested clones, six different sequences were obtained, of which two gave best hits to uncultivated alphaproteo-MTBs from marine sediments of the Chinese sea (*Cux*-01: 94% identity to magnetococcus clone XSE-42 (Pan *et al.*, 2008), *Cux*-02: 96% identity to magnetococcus clone MRT-97), whereas the other sequences were not similar to known MTB.

Six distinct magnetic morphotypes with different relative abundances (Table 1) were identified in *CS* samples, which included a small (~ 1 µm) spirillum (*CS*-01), a small (~ 1.5 µm) (*CS*-02) and a large (~ 2.5 µm) (*CS*-04) coccus, two slightly distinct (with and without inclusions) large rods identical to the previously identified Mbav (*CS*-03) (Jogler *et al.*, 2010; 2011), and a large (~ 3.5 µm) vibrio with polar inclusions (*CS*-05) (Fig. 2, Table 1). Enrichments were dominated by *CS*-02 and *CS*-03 (Mbav), whereas *CS*-04 and *CS*-05 were present only in low numbers (Table 1). Although microscopy revealed the virtual absence of any non-MTB from magnetic enrichments, only a minor fraction (3 of 38) of subcloned 16S rRNA genes had similarity to known MTB (Table 1). Two sequences gave best hits to uncultivated alphaproteobacterial freshwater magnetic cocci, *CS*-02 to magnetic coccus clone OUT-51 (99% identity) (Lin and Pan, 2010) and *CS*-06 to the magnetic coccus clone 10 (99% identity) (Lin *et al.*, 2009). A third sequence proved to be identical to Mbav of the *Nitrospirae* phylum, which was consistently detected in previous analyses of the *CS* sampling site (Spring *et al.*, 1993; Jogler *et al.*, 2010). All other clones were most similar to various bacterial groups not known to be associated with MTB (data not shown).

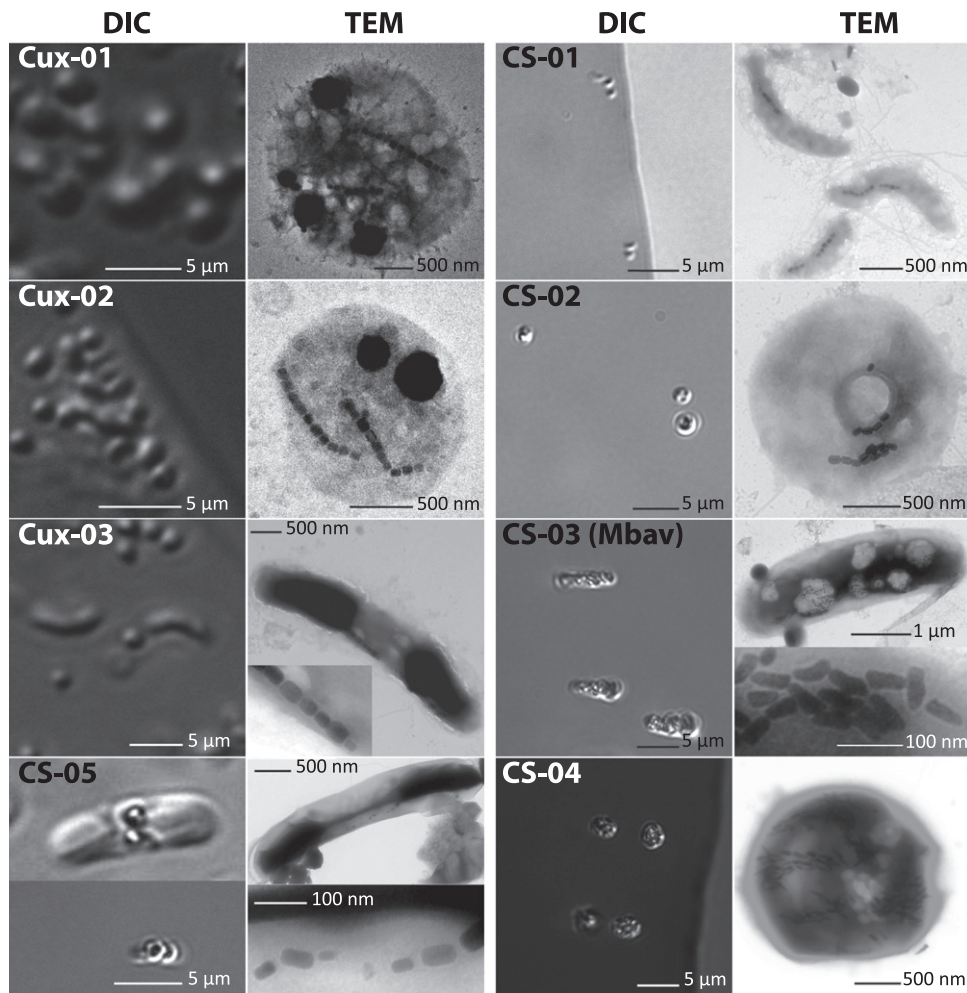


Fig. 1. Differential interference contrast (DIC) and transmission electron micrographs (TEM) of all identified MTB morphologies from freshwater (CS-01–CS-05) and marine (Cux-01–Cux-03) sediments.

Diversity analysis by microsorting

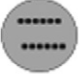




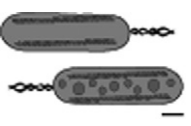
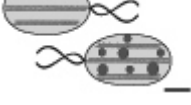

In previous studies microsorting was used only for large and morphologically conspicuous MTB cells, such as the giant rod Mbav and the big ovoid-shaped SKK-01 from candidate division OP3 (Jogler *et al.*, 2011; Kolinko *et al.*, 2012). However, our magnetic collections also contained very small spirilla-like MTB, which are more difficult to recognize by microscopy and to target by microsorting. To test if this technique could also be reliably applied to these small cells, an artificial mixture consisting of equal cell numbers ($\sim 10^6$ cells per ml each) of *E. coli* and spontaneous mutant strain *Magnetospirillum gryphiswaldense* MSR-1B (Schübbe *et al.*, 2003) was microsorted. As both strains were essentially non-motile and showed no magnetic response, their morphology was the only distinctive characteristic. For each morphotype, DNA from six independent MDA reactions on up to five cells served as a template for subsequent 16S PCR using universal eubac-

terial primers. All 16S rRNA gene sequences obtained from MDA reactions only matched their expected origin, and cross-contaminations were never observed, indicating that microsorting can also be applied with high accuracy to small cells.

Next, all different MTB morphotypes from *Cux* and *CS* magnetic collections were manually selected under microscopic control and washed in cell-free sample water and H_2O for at least 10 times to remove contaminants and extracellular DNA prior to MDA. For every morphotype four independent reactions with five cells per reaction were performed. From all reactions, subsequent 16S rRNA PCR using amplified DNA as template consistently yielded only one single phylotype, as shown by sequence analysis of 8 clones per clone library revealed and indicating the absence of contaminations (Fig. S1).

Microsorting and WGA of the three MTB morphotypes from *Cux* resulted in three different 16S rRNA gene sequences. Two of them obtained from the large (Cux-01)

Table 1. Overview over all MTB identified by magnetic collections and microsorting.

	Organism	Morphology	Abundance	Identical clones from clone library	Sequence obtained by microsorting	16S rDNA (bp)	Best nBLAST hit	Identity (%)
Marine	Cux-01		++	12	+	1467	Uncultured magnetococcus clone XSE-42 (EF379385)	94
	Cux-02		+++	21	+	1465	Uncultured magnetococcus clone MRT-97 (EF371493)	96
	Cux-03		+	0	+	1402	Uncultured magnetococcus clone CF22 (AJ863155)	94
Freshwater	CS-01		++	0	+	1467	Uncultured magnetospirillum Van25 ^a (HQ222269)	91
	CS-02		+++	2	+	1465	Uncultured magnetococcus clone OTU-51 (GQ468517)	99
	CS-03		++	5	+	1402	<i>Cand. Magnetobacterium bavaricum</i> (X71838)	~ 100
	CS-04		+	0	+	1516	<i>Cand. Magnetobacterium mohaviensis</i> LO-1 (GU979422)	94
	CS-05		+	0	+	1414	Uncultured magnetococcus clone TB24 (X81185)	90
	CS-06			1	-	919	Uncultured magnetococcus clone 10 (EU786575)	91

The relative abundance of morphotypes in magnetic collections is indicated as follows: +++ highly abundant (> 70%), ++ abundant, + rare morphotypes (< 1%). Bars indicate 1 μ m.

a. Not best hits.

and small coccus (Cux-02) matched the two anonymous MTB-like sequences obtained from the 16S rRNA clone library (99% cut-off, Table 1). The third sequence, which was not present in the clone library, originated from the large vibrio morphotype with polar electron dense inclusion (Cux-03) (Fig. 1). Cux-03 was assigned to the *Alphaproteobacteria* and had highest (94%) identity to an uncultured magnetic coccus clone CF22 from freshwater sediments near Bremen (North Germany) (Flies *et al.*, 2005b).

All five sequences obtained by WGA from microsorted magnetic enrichments from CS gave best hits to known MTB. Two sequences proved to be identical to anonymous clones from the corresponding library. One of them was obtained from the small and highly abundant magnetic coccus CS-02 with highest identity (99%) to

the uncultivated alphaproteobacterial freshwater magnetic coccus clone OTU-51. The other one obtained from the two CS-03 morphotypes (with and without sulfur inclusions) matched the known Mbav sequence as expected.

Three of the 16S rRNA sequences obtained by microsorting and WGA were not present in the corresponding clone library. The sequence amplified from the small spirillum CS-01 had an identity of 91% to *Magnetospirillum* sp. enrichment culture clone Van 25 and 89% identity to *M. gryphiswaldense*. The coccoid-shaped CS-04 yielded a best hit (94% identity) to '*Candidatus Magnetobacterium mohaviensis*' LO-1, which besides Mbav is another MTB previously shown to be affiliated with the *Nitrospirae* phylum (Lefèvre *et al.*, 2011a) (Fig. 4). The large vibrio CS-05 yielded a best hit to the uncultured

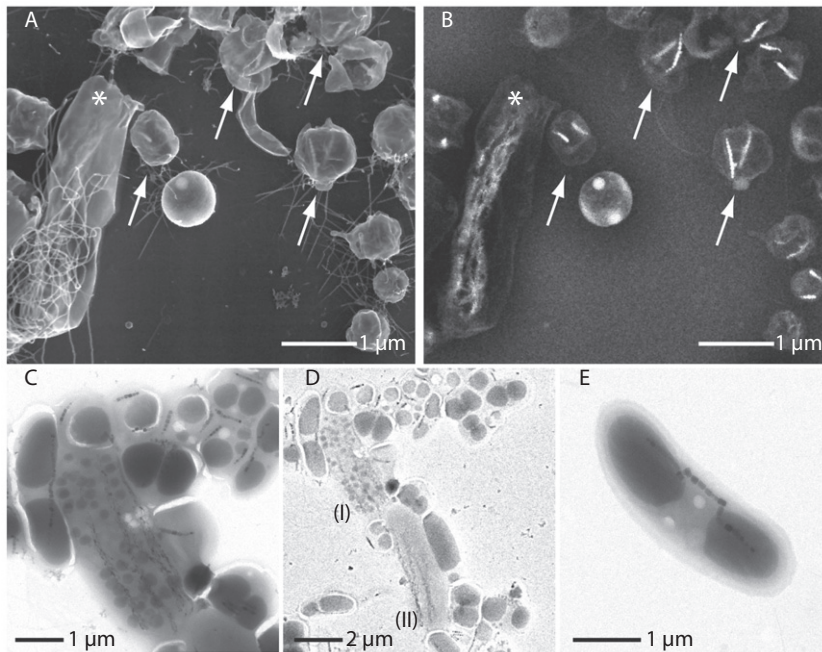


Fig. 2. Electron micrographs of magnetotactic cells from Lake Chiemsee CS sediments. SEM micrographs (accelerating voltage: 15 kV). Topographic SE image of surface structures of abundant magnetic cocci (arrow) and putative Mbav (asterisk) (A). The back-scattered electron image (B) reveals elongated prismatic magnetosomes in magnetic cocci and bullet-shaped magnetosomes in putative Mbav (B). Transmission electron micrographs of magnetic collections showing (C–D) morphological heterogeneity of Mbav cells; with (I) and without (II) intracellular inclusions (D). Micrograph of a CS-05 cell with two electron dense inclusions and prismatic magnetosomes (E).

alphaproteobacterium magnetococcus clone TB24, which was obtained from a freshwater pool (Spring *et al.*, 1995).

Ultrastructural and phylogenetic analysis of selected magnetic cells

For ultrastructural analysis, selected morphotypes from magnetic collections and those microsorted onto finder grids were further analysed by electron microscopy. CS-03 (Mbav) and CS-04, both belonging to the *Nitrospirae* phylum, also shared some ultrastructural similarities, such as the presence of bullet-shaped magnetosomes arranged in 3–5 chains as previously described (Fig. 1) (Spring *et al.*, 1993; Lefèvre *et al.*, 2011a). As observed for Mbav, also CS-04 cells displayed some morphological variability with respect to presence of putative sulfur globules (Fig. 2D) (Jogler *et al.*, 2010; Lefèvre *et al.*, 2011a).

In contrast to bipolar monotrichously flagellated cultivated magnetospirilla with cubo-octahedral magnetite crystals, the small spirillum CS-01 contained elongated magnetosome crystals and had a monopolar bundle of flagella (Fig. 1).

The highly abundant coccus CS-02 contained two chains of elongated prismatic magnetosomes (length 60 nm, width 40 nm) (Fig. 3). High-pressure frozen and freeze-substituted cells of CS-02 revealed a typical Gram-negative structure of the cell boundary, displaying an inner and an outer membrane. The outermost rough surface structure might represent a sheath or capsular structure (Fig. 3). Interestingly, the two parallel magnetosome

chains were arranged along a putative filamentous structure (approximately 11 nm in diameter) somehow resembling the cytoskeletal MamK filaments to which in *M. gryphiswaldense* and other MTB magnetosomes are attached (Jogler *et al.*, 2011; Katzmann *et al.*, 2011) (Fig. 3). Surfaces of the mineral cores became visible in particles where the magnetosome membrane layer was detached upon fractioning, as indicated by the smooth surface of the bare mineral crystal, as compared with presumably intact magnetosomes displaying a granular surface likely to be identical with the surface of the outer leaflet of the magnetosome membrane. Individual magnetosome particles appeared to be attached to the putative filament (Fig. 3 insert). The magnetosome membrane is clearly visible as a hollow membrane-like structure after apparent loss of magnetite cores during freeze fracturing (Fig. 3A).

Despite of their different phylogenetic affiliation, geographical origin and ecology, the two vibrioid morphotypes Cux-03 (marine) and CS-05 (freshwater) shared an intriguing morphological similarity. Both strains were about 3.5 µm in length and had one chain of elongated prismatic magnetosome crystals (115 ± 18 nm in length) that traverses the cell at its inner curvature. Magnetosome crystals consist of an iron oxide (likely magnetite), as indicated by coinciding signals for iron and oxygen, but not sulfur in energy-dispersive X-ray spectroscopy (EDX) (Fig. 3). In addition, they both displayed characteristic large electron dense inclusions at their poles (Fig. 3), which in CS-05 yielded colocalized signals for phosphorus and oxygen by EDX, identifying them as putative storage granules of phosphate (Silva *et al.*, 2008).

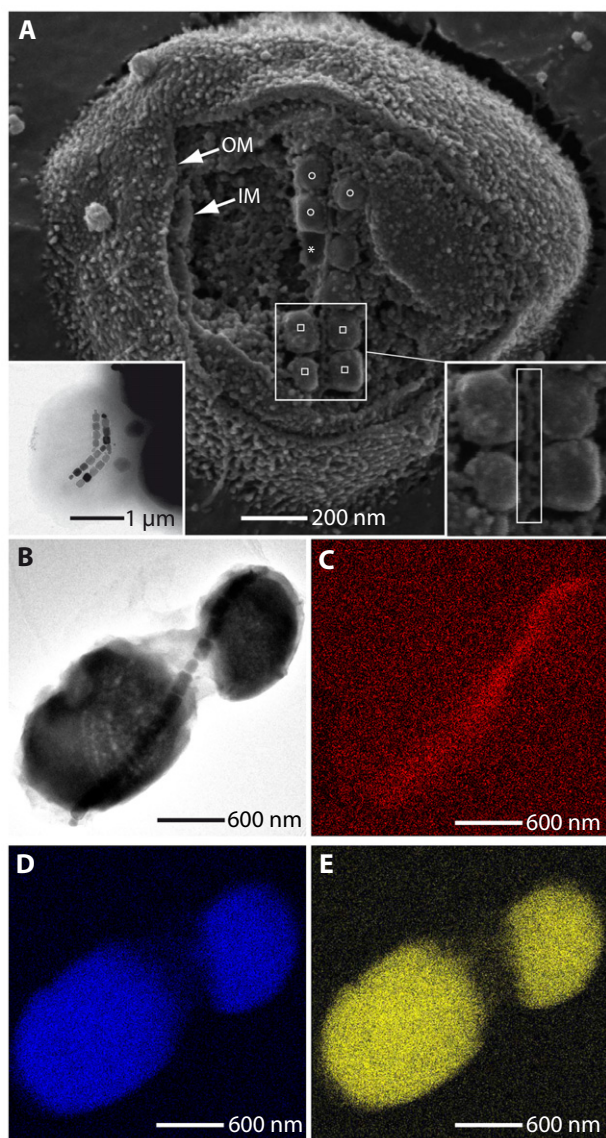


Fig. 3. Ultrastructural analysis.

A. SEM micrograph of a fractured frozen hydrated CS-02 cell. The cell has a Gram-negative cell wall with an outer (OM) and inner membrane (IM). Magnetosome particles displaying either the rough surface of the outer magnetosome membrane leaflet (□) or the smooth surface of the bare mineral core (○) are indicated. Magnetosomes form a chain arranged along a putative cytoskeletal filament (rectangular area in inset).

B–E. Ultrastructure of morphotype CS-05. TEM micrograph shows a magnetosome chain traversing the cell with its polar electron dense inclusions (B). Energy dispersive X-ray spectroscopy (EDX) revealed Fe content within magnetosomes highlighting the magnetosome chain traversing the cell (C) and oxygen and phosphor rich components of the cell, which coincide with its polar electron dense inclusions (D and E).

Genomic analysis of microsorted CS-05

Despite their morphological resemblance, CS-05 and Cux-03 share an identity of only 90% in their 16S rRNA genes and affiliate with different branches within the

Alphaproteobacteria (Fig. 4). Similar morphotypes were reported previously from magnetic collections from various environments, but their phylogenetic assignment was not identified (Vali and Kirschvink, 1991; Schüller, 1994; Spring and Schleifer, 1995; Flies *et al.*, 2005b), and nothing is known about the genetics and ecophysiology of these characteristic MTBs. To obtain first genomic information, double-amplified DNA from two subsequent MDA reactions on microsorted CS-05 cells was used for the generation of a small insert library (SIL) as described previously (Simon and Daniel, 2010). Endsequencing of all 27 clones (average insert size ~ 2 kb, read length ~ 800 bp) revealed hits to 38 different genes (Table 2). Seventy-five per cent showed highest similarity to proteobacterial genes, while the others yielded hits to *Archaea* (10%), *Firmicutes* (3%), *Cyanobacteria* (3%), *Planctomycetales* (1.5%), *Chlorobiaceae* (1.5%) and unknown bacteria (6%). Notably, 13 genes generated hits to the cultivated MTB *Magnetococcus* MC-1 and *Desulfovibrio magneticus* RS-1.

In addition to eight hypothetical genes, 30 genes have predicted functions, with eight involved in signal transduction, six related to the electron transport chain, whereas other genes are involved in DNA organization and repair (8%), protein biosynthesis (8%), metal ion translocation (5%), lipid and cell wall biosynthesis (5%) and regulation (2.5%) (Table 2). As expected from the small sample size, which is likely to represent less than 1% coverage, if assuming a characteristic genome size of about 5 Mb, no putative *mam* genes involved in magnetosome formation were identified.

Discussion

So far phylogenetic analysis of uncultivated MTB was mostly achieved by 16S rRNA PCR amplification on DNA from complex multispecies magnetic enrichments followed by mass cloning and screening of libraries (Ludwig and Schleifer, 1994; Amann *et al.*, 2006; Postec *et al.*, 2012). This technique relies on high cell numbers and detects only highly abundant MTB, while low abundant representatives are likely to be missed (Amann *et al.*, 2006). In addition, obtained sequences are anonymous, and the correlation of phylo- to morphotypes requires FISH and fluorescence microscopy. Recently, single cell techniques facilitated the amplification and *de novo* assembly of whole genomes from uncultivated marine, freshwater and symbiotic bacteria, allowing to link morphological and genomic information (Rodrigue *et al.*, 2009; Woyke *et al.*, 2010; Chitsaz *et al.*, 2011) Microsorting and WGA were also applied for the phylogenetic and ultrastructural analysis of large and morphologically conspicuous, abundant MTB from *Nitrospirae* (Jogler *et al.*, 2010; 2011), but also led to the discovery of novel

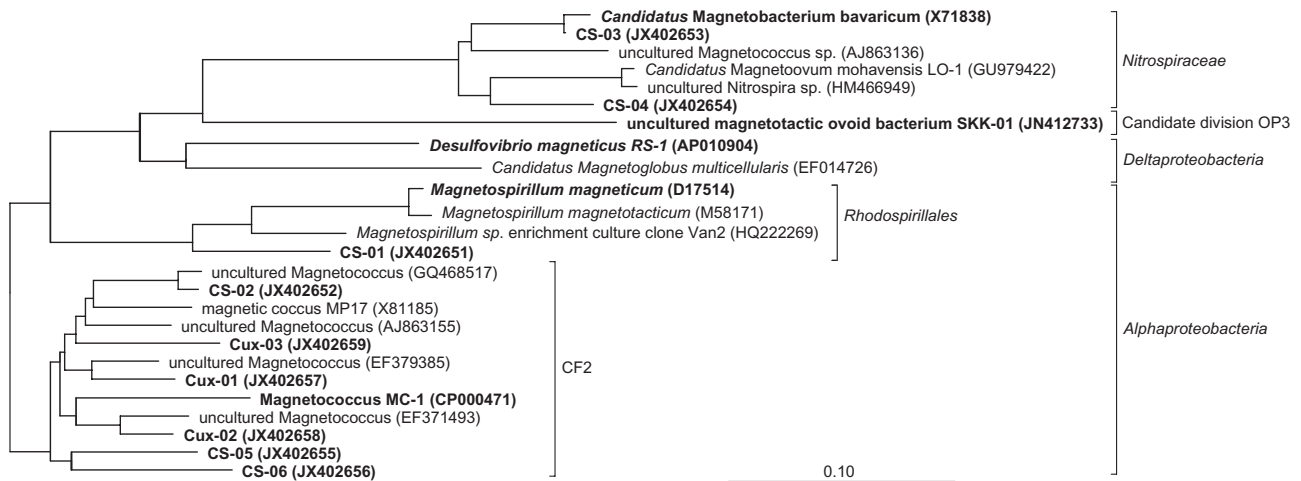


Fig. 4. Phylogenetic tree of 16S rRNA gene sequences retrieved from magnetic collections from Lake Chiemsee (CS) and Cuxhaven (Cux) by mass cloning and microsorting showing their phylogenetic affiliation.

low-abundant MTB (Kolinko *et al.*, 2012). Here, we used a combination of mass cloning of 16S rRNA genes and microsorting followed by WGA to target all MTB species present in magnetic collections from two environmental samples. We demonstrated that microsorting is not confined to large and morphologically conspicuous cells, but can also reliably be applied to other members of MTB communities such as small spirilla and cocci, as well as to high and low abundant MTB.

All three morphotypes present in the marine sample (*Cux*) could be linked to three different alphaproteobacterial species. Two of them were also represented in the clone library, whereas the least abundant morphotype (*Cux*-03) was missing. In the freshwater sample (*CS*) five of six MTB phylotypes were identified by single cell sorting, whereas clone library revealed only two of the most abundant MTB, but in addition identified one anonymous phylotype that was missed by single cell sorting. In conclusion, single cell sorting is more effective in the detection of low abundant MTB, whereas the combination of the two methods is likely to reveal maximum diversity.

It should be noted, however, that the identified species may not necessarily represent the entire MTB diversity present in the environment, because magnetic collections under our conditions are likely biased for aerotolerant and highly motile MTB. Second, microcosms stored in the lab are known to change in MTB community composition (Flies *et al.*, 2005a), as illustrated by the absence of MMP and SKK-01-like bacteria, which were previously observed in the same marine and freshwater sampling sites respectively (Wenter *et al.*, 2009; Kolinko *et al.*, 2012). Thus, the somewhat higher diversity observed in the freshwater sample (6 versus 4) phylotypes in the marine sample might rather result from the lower stability of marine samples, as marine and freshwater phylotypes

are about equally represented (122 versus 125 16S rRNA sequences) in the MTB databases (<http://database.biomnsl.com/index.html>) (Lin *et al.*, 2011b). Performing similar experiments on environmental samples *in situ* and under less selective conditions (e.g. by performing all steps in the absence of oxygen) is likely to reveal considerably higher diversity from various environments.

In total we identified nine different phylotypes. Whereas two of them (CS-02 and CS-03) are relatively closely related to previously identified MTB, six (*Cux*-01, *Cux*-02, *Cux*-03, CS-01, CS-04 and CS-05) displayed sequence divergence well beyond the species level (< 97% identity). Sequences of CS-01, CS-05 and CS-06 show very low identities to known MTB, and thus might each represent a new genus within the *Alphaproteobacteria* (Fig. 4).

Among the novel and more divergent MTB is the ovoid-shaped CS-04 affiliated with the *Nitrospirae* phylum. Although its morphology is strongly resembling that of the other *Nitrospirae* MTB LO-1 and MWB-1, which also exhibit an ovoid cell shape and bullet-shaped magnetosomes arranged in bundles of chains, CS-04 is not very closely related to them at the 16S rRNA level (94% identity to LO-1, 91% to MWB-1) (Lefèvre *et al.*, 2011a; Lin *et al.*, 2012). This suggests that the phylogenetic diversity within this group is higher than initially assumed and further indicates a wider geographic distribution of ovoid *Nitrospirae* MTB.

Another example for novel diversity is represented by the species *Cux*-03 and CS-05. Despite their different geographic origin and ecology (marine versus freshwater) both strains share considerable morphological similarity. Similar morphotypes were repeatedly reported but not identified in previous studies (Vali and Kirschvink, 1991; Schüller, 1994; Spring *et al.*, 1995). The closest 16S rRNA relatives of *Cux*-03 and CS-05 are two

Table 2. Results of BLAST analysis of protein fragments encoded by endsequences against the NCBI database.

Clone	Best hit	Coverage (%)	Identity (%)	E-value	Accession
A02	Cytochrome C class I [MC-1]	75	52	6.0E-50	YP866892
	SMC domain containing protein [<i>Syntroothermus</i>]	48	53	5.0E-05	YP00370187
A03	Cytochrome C monodhaem variants family [<i>Burkholderia</i>]	30	48	1.0E-22	ZP09753705
	Transposase IS66 [unc. <i>Bacterium</i>]			2.0E-87	CAX837781
A04	Cation diffusion facilitator family transport [<i>Halorubrum</i>]	47	33	9.0E-12	YP00256586
	Cobalt/zinc/cadmium efflux pump [<i>Thermococcus</i>]	35	33	2.0E-20	YP00476298
	Similar to type IV pillus assembly PilZ [unc. <i>Bacterium</i>]	18	57	7.0E-46	CAX84240
	PAS/PAC sensor hybrid histidine kinase [MC-1]	59	51	3.0E-49	YP866289
A05	Hypothetical protein Neut_222 [<i>Neutrosomonas</i>]	44	47	2.0E-51	YP748404
A08	Pyruvate phosphate dikinase [MC-1]	99	60	1.0E-125	YP866101
	Sensor histidine kinase [RS-1] ^a	37	27	1.0E-04	YP00295553
A09	Phosphoesterase PA-phosphatase related [<i>Lutiella</i>]	45	28	0.22	ZP03633678
A10	Response regulator modulated CheB methyltransferase [<i>Cyanothece</i>]	86	49	1.0E-38	YP00388954
	Response regulator modulated CheB methyltransferase [MC-1] ^a	86	48	1.0E-38	YP865749
A11	Unnamed protein product [<i>Synechococcus</i>]	89	46	7.0E-09	YP400828
A12	Hypothetical protein ThithDRAFT [<i>Thioalkalivibrio</i>]	95	42	1.0E-67	ZP08929740
	Hypothetical protein ThithDRAFT 16_16 [<i>Thioalkalivibrio</i>]	34	45	1.0E-21	ZP08929741
B01	DNA repair ATPase-like protein [<i>Acidaminococcus</i>]	66	69	2.0E-07	YP00339991
	Response regulator receiver [MC-1]	35	44	1.0E-21	YP867106
B02	Hypothetical protein VCO395_A2678 [<i>Vibrio cholerae</i>]	96	46	2.0E-39	YP001218556
B04	Putative hydrolase [<i>Pseudomonas</i>]	35	70	1.0E-37	EGM116298
B08	SMC domain protein [<i>Singulisphaera</i>]	47	28	2.0E-09	ZP09568834
B09	Aspartate carbamoyltransferase [MC-1]	52	71	8.0E-90	YP864038
B11	NADH dehydrogenase [<i>Chlorobium</i>]	49	78	2.0E-88	YP00195891
	Hypothetical protein Neut_222 [<i>Nitrosomonas</i>]	44	47	2.0E-51	YP748404
	Multi-sensor hybrid histidine kinase [MC-1] ^a	79	26	6.0E-24	YP866850
C02	Putative serin/threonin proter phosphatase-like protein [MC-1]	29	42	2.0E-21	YP866040
	Putative GAF sensor protein	32	35	1.0E-09	YP864160
C04	30s ribosomal protein S5 [MC-1]	45	77	1.0E-64	YP864789
	<i>rplP</i> gene product [MC-1] ^a	39	80	1.0E-68	YP864779
C05	Unnamed protein product [<i>Desulfovibrio africanus</i>]	97	49	1.0E-37	YP00505256
C06	ABC transporter [MC-1]	46	46	1.0E-26	YP866032
	Molybdopterine oxidoreductase	33	44	1.0E-18	YP865545
C07	Two-component hybrid sensor and regulator [RS-1] ^a	32	33	2.0E-27	YP00295229
	Molybdopterine oxidoreductase	93	61	1.0E-75	YP865545
C08	Hypothetical protein [<i>Nitrosococcus</i>]	26	55	1.0E-22	YP00376112
C09	tRNA delta(2)-isopentenylpyrophosphate transferase [<i>Pelobacter</i>]	63	55	1.0E-68	YP358505
C10	Cobalt/zinc/cadmium efflux pump [<i>Thermococcus</i>]	35	33	2.0E-20	YP00476292
	Similar to type IV pillus assembly PilZ [unc. <i>Bacterium</i>]	18	57	7.0E-46	CAX84240
	O-antigen polymerase [MC-1]	20	45	1.0E-07	YP864509
D04	Sensory box protein/sigma-54 [unc. <i>Bacterium</i>]	79	69	5.0E-125	CAX84064
	ATP-dependent protease LON [RS-1] ^a	26	33	1.0E-08	YP00295245
D07	Hypothetical protein XVE_4190 [<i>Xanthomonas</i>]	95	63	1.0E-86	ZP08180168
	Hypothetical protein DMR-36100 [RS-1] ^a	34	46	1.0E-25	YP00295498
	Hypothetical protein Mmc_2715 [MC-1] ^a	95	63	2.0E-23	YP866614
D09	Rhodanese-like sulfurtransferase PspE [<i>Cupriavidus</i>]	29	96	5.0E-68	ZP09627450

a. Not best hits.

different uncultured magnetic cocci, and despite of their morphological resemblance Cux-03 and CS-05 share only relatively low 16S identity with each other (90%). This provides a further example that morphologically similar MTB are not necessarily closely related, as it was also shown before for the phylogenetically divergent uncultivated MTB LO-1 and SKK-01 (Lefèvre *et al.*, 2011a; Kolinko *et al.*, 2012). Vice versa, CS-05 remarkably is the first rod or vibrio-shaped species found to branch within the so-called CF2 group, which so far was thought to comprise only coccoid MTB. However, unas-

signed 16S rDNA sequences (TB24) with 90% identity to CS-05 were previously reported from magnetic collections from freshwater that also contained vibrioid MTB (Spring *et al.*, 1995), suggesting that related species are more abundant in various environments.

The most characteristic feature shared by Cux-03 and CS-05 is the presence of large inclusions identified as granules of phosphate, which in some cells were found to occupy up to two-thirds of the cell volume. As in other bacteria, polyphosphate granules may serve as energy source, or as phosphate or chelated metal storage

(Achbergerová and Nahalka, 2011), a similar function in MTB can be hypothesized. We also were able to obtain first genomic information of CS-05 by end-sequencing of 27 clones of a DNA library generated from the amplified genomes of few cells. Future analysis of near complete genome data will likely generate insights into the putative metabolism of this organism. In addition, it demonstrates that single cell analysis is not limited to ultrastructure and conserved phylogenetic marker genes of uncultured MTB, but in future studies can be applied for the complete genomic analysis of, in theory, all microscopically detectable members of environmental MTB communities.

Experimental procedures

Bacterial strains, media and growth conditions

Escherichia coli DH5 α strains were cultivated in liquid lysogeny broth at 37°C under aerobic conditions. Liquid cultures of *Magnetospirillum* MSR-1B were cultivated in FSM medium at 30°C under aerobic conditions as described previously (Schübbe *et al.*, 2003).

Sediment sampling and magnetic collections

Freshwater sediments from Lake Chiemsee (CS, Germany, Bavaria) (47°51'08"N, 12°24'00"E) were collected in July 2010 from 10–20 m depth applying a bottom sampler. Aquaria were filled with 18–25 l of sediment slurry and covered with the same volume of sample water. To allow stratification, microcosms were stored at room temperature for several months. The sediment colour in the oxic sediment layers (~ 4 mm) was brownish, and then greyish down to 10 mm depth and below changed to black. Marine sediment cores were collected at low tide from an intertidal flat from the German Wadden see near Cuxhaven (Cux), Germany (53°53'32"N, 8°40'45"E) in April 2010. Stratified sandy sediments were overlaid with sea water and stored at RT in the dark without disturbing stratification. The sediment colour was brownish in the upper 5 mm of oxic sediment, then greyish down to 3–4 cm depth and below changed to black due to a high FeS content.

Magnetic enrichments from the freshwater sample (CS) were performed as previously described (Jogler *et al.*, 2009). In brief, MTB were magnetically collected from mud slurries containing 10 ml of sediment cores mixed with 30 ml of sample water. Magnetic collections were transferred into a magnetic trap for further enrichment. Marine MTB were enriched by applying the south pole of a magnet 2 cm above the sediment for 20 min. Enriched cells were directly used for downstream analysis.

Micromanipulation and WGA

Micromanipulation and WGA of single cells was performed as previously described (Kolinko *et al.*, 2012). In brief, single cells were microsorted and washed under strict microscopic control to remove contaminations and extracellular DNA and

transferred onto an AmpliGrid AG480F (Beckman Coulter, Krefeld, Germany) for subsequent WGA.

Determination of 16S rRNA gene sequences and phylogenetic analysis

The 16S rRNA genes were amplified using universal eubacteria-specific primers 27F and 1492R (Lane, 1991) and 50 ng of WGA derived DNA or a magnetic enrichment (~ 10⁶ cells) served as template. PCR products were cloned into pJET1.2/blunt Cloning Vector (Fermentas, Waltham, MA, USA) and sequenced with an ABI system according to the instructions of the manufacturer. Alignment of gene sequences was performed with the AlignX algorithm of the Vector NTI software version 11.0 (Invitrogen, Carlsbad, CA, USA). No chimerical sequences were identified using the Bellerophon algorithm (Huber *et al.*, 2004).

16S rRNA gene sequences from WGA experiments were analysed using the ARB software package version 5.2 (Ludwig *et al.*, 2004) and the SILVA SSU Ref database release 108 from April 2011 (Pruesse *et al.*, 2007). Briefly, nearly full-length 16S rRNA gene sequences were automatically aligned using the SINA aligner (Pruesse *et al.*, 2012) and manual refinement was carried out taking into account the secondary structure information of the native rRNA. For initial classification, MTB sequences were added to the corresponding guide trees of the SSU SILVA data set using the ARB parsimony tool. Based on this information, final tree reconstruction was performed with selected reference sequences and a larger number of their close relatives to stabilize tree topology. Reference sequences of MTB were selected from the DMTB database (<http://database.biomnsl.com/>). In total, 1020 sequences of the SSU data set were used to reconstruct a neighbour joining tree (ARB neighbour joining tool). Sequences described in this study can also be downloaded from the databases of the INSDC, comprising DDBJ, EMBL and GenBank.

Construction of a small insert partial genomic library

A small insert library of amplified genomic DNA was constructed similar as described previously (Simon and Daniel, 2010). In brief, WGA-derived DNA from CS-05 cells was amplified by a second round of WGA, enzymatically debranched and size selected for subcloning into pJET1.2/blunt Cloning Vector (Fermentas, Waltham, MA, USA) following the specifications of the manufacturer. All clones were prepared for end-sequencing applying specific pJet primers and sequenced with an ABI system according to the instructions of the manufacturer. Sequences were analysed against the NCBI database applying the xBLAST algorithm (Altschul *et al.*, 1997).

Light and electron microscopy

Magnetic collections were examined by hanging drop assay (Frankel *et al.*, 1997; Schüler and Bazylinski, 2007) using a SM-LUX (Leitz, Wetzlar, Germany) phase-contrast microscope. For ultrastructural analysis magnetically responsive cells were transferred to grids. For TEM of CS-05, single cells were sorted onto finder grids under microscopic control.

Transmission electron microscopy (TEM) was performed with a FEI Tecnai F20 (200 kV) TEM equipped with an Eagle charge-coupled-device camera (4096 by 4096 pixels). Cells were adsorbed on carbon-coated copper grids (Plano, Wetzlar, Germany). Images were acquired using EMMenu 4.0 and FEI software. For structural analysis, sorted cells were examined with a Zeiss AURIGA® high-resolution field-emission scanning electron microscope operated at 25 keV. SE and BSE images were simultaneously recorded with the chamber SE and QBSD detectors. For energy-dispersive X-ray (EDX) analysis (point analysis and EDX mapping) a Bruker QUANTAX double detector system (2 × 30 mm² XFlash®) was used at a working distance of 6 mm and 25 kV.

For high-pressure freezing, aluminium platelets were filled with concentrated cell suspensions and the cells immobilized by high-pressure freezing (Leica HPM100). For cryo-scanning electron microscopy high-pressure frozen samples were fractured with a Leica EM MED020, sublimated for 1–2 min at –95°C and coated with 3 nm tungsten, transferred to the scanning electron microscope and examined at 1 kV.

Acknowledgements

This work was supported by Deutsche Forschungsgemeinschaft (grant DFG Schu1080/9-1 and 11-1 to D.S.). We thank Silvia Dobler for excellent technical assistance.

References

- Abreu, F., Cantão, M.E., Nicolás, M.F., Barcellos, F.G., Morillo, V., Almeida, L.G., *et al.* (2011) Common ancestry of iron oxide- and iron-sulfide-based biomineralization in magnetotactic bacteria. *ISME J* **5**: 1634–1640.
- Achbergerová, L., and Nahalka, J. (2011) Polyphosphate-an ancient energy source and active metabolic regulator. *Microb Cell Fact* **10**: 63.
- Altschul, S.F., Madden, T.L., Schaffer, A.A., Zhang, J., Zhang, Z., Miller, W., and Lipman, D.J. (1997) Gapped BLAST and PSI-BLAST: a new generation of protein database search programs. *Nucleic Acids Res* **25**: 3389–3402.
- Amann, R., Peplies, J., and Schüler, D. (2006) Diversity and Taxonomy of Magnetotactic Bacteria. In *Magnetoreception and Magnetosomes in Bacteria*. Schüler, D. (ed.). Heidelberg: Springer-Verlag, pp. 25–36.
- Bazylinski, D.A., and Frankel, R.B. (2004) Magnetosome formation in prokaryotes. *Nat Rev Microbiol* **2**: 217–230.
- Chitsaz, H., Yee-Greenbaum, J.L., Tesler, G., Lombardo, M.J., Dupont, C.L., Badger, J.H., *et al.* (2011) Efficient *de novo* assembly of single-cell bacterial genomes from short-read data sets. *Nat Biotech* **29**: 915–921.
- Faivre, D., and Schüler, D. (2008) Magnetotactic bacteria and magnetosomes. *Chem Rev* **108**: 4875–4898.
- Flies, C.B., Jonkers, H.M., de Beer, D., Bosselmann, K., Böttcher, M.E., and Schüler, D. (2005a) Diversity and vertical distribution of magnetotactic bacteria along chemical gradients in freshwater microcosms. *FEMS Microbiol Ecol* **52**: 185–195.
- Flies, C.B., Peplies, J., and Schüler, D. (2005b) Combined approach for characterization of uncultivated magnetotactic bacteria from various aquatic environments. *Appl Environ Microbiol* **71**: 2723–2731.
- Frankel, R.B., Bazylinski, D.A., Johnson, M.S., and Taylor, B.L. (1997) Magneto-aerotaxis in marine coccoid bacteria. *Biophys J* **73**: 994–1000.
- Fukuda, Y., Okamura, Y., Takeyama, H., and Matsunaga, T. (2006) Dynamic analysis of a genomic island in *Magnetospirillum* sp. strain AMB-1 reveals how magnetosome synthesis developed. *FEBS Lett* **580**: 801–812.
- Huber, T., Faulkner, G., and Hugenholtz, P. (2004) Bellerophon: a program to detect chimeric sequences in multiple sequence alignments. *Bioinformatics* **20**: 2317–2319.
- Jogler, C., and Schüler, D. (2009) Genomics, genetics, and cell biology of magnetosome formation. *Annu Rev Microbiol* **63**: 501–521.
- Jogler, C., Lin, W., Meyerdieks, A., Kube, M., Katzmann, E., Flies, C., *et al.* (2009) Toward cloning of the magnetotactic metagenome: identification of magnetosome island gene clusters in uncultivated magnetotactic bacteria from different aquatic sediments. *Appl Environ Microbiol* **75**: 3972–3979.
- Jogler, C., Niebler, M., Lin, W., Kube, M., Wanner, G., Kolinko, S., *et al.* (2010) Cultivation-independent characterization of ‘*Candidatus* Magnetobacterium bavaricum’ via ultrastructural, geochemical, ecological and metagenomic methods. *Environ Microbiol* **12**: 2466–2478.
- Jogler, C., Wanner, G., Kolinko, S., Niebler, M., Amann, R., Petersen, N., *et al.* (2011) Conservation of proteobacterial magnetosome genes and structures in an uncultivated member of the deep-branching *Nitrospirae* phylum. *Proc Natl Acad Sci USA* **108**: 1134–1139.
- Katzmann, E., Müller, F.D., Lang, C., Messerer, M., Winkhofer, M., Plitzko, J.M., and Schüler, D. (2011) Magnetosome chains are recruited to cellular division sites and split by asymmetric septation. *Mol Microbiol* **82**: 1316–1329.
- Kawaguchi, R., Burgess, J.G., Sakaguchi, T., Takeyama, H., Thornhill, R.H., and Matsunaga, T. (1995) Phylogenetic analysis of a novel sulfate-reducing magnetic bacterium, RS-1, demonstrates its membership of the *delta-Proteobacteria*. *FEMS Microbiol Lett* **126**: 277–282.
- Kolinko, S., Jogler, C., Katzmann, E., Wanner, G., Peplies, J., and Schüler, D. (2012) Single-cell analysis reveals a novel uncultivated magnetotactic bacterium within the candidate division OP3. *Environ Microbiol* **14**: 1709–1721.
- Lane, D.J. (1991) 16S/23S sequencing. In *Nucleic Acid Techniques in Bacterial Systematics*. Stackebrandt, E., and Goodfellow, M. (eds). Chichester, UK: Wiley, pp. 115–175.
- Lefèvre, C.T., Frankel, R.B., Abreu, F., Lins, U., and Bazylinski, D.A. (2011a) Culture-independent characterization of a novel, uncultivated magnetotactic member of the *Nitrospirae* phylum. *Environ Microbiol* **13**: 538–549.
- Lefèvre, C.T., Menguy, N., Abreu, F., Lins, U., Posfai, M., Prozorov, T., *et al.* (2011b) A cultured greigite-producing magnetotactic bacterium in a novel group of sulfate-reducing bacteria. *Science* **334**: 1720–1723.
- Lefèvre, C.T., Vilorio, N., Schmidt, M.L., Posfai, M., Frankel, R.B., and Bazylinski, D.A. (2012) Novel magnetite-producing magnetotactic bacteria belonging to the *Gammaproteobacteria*. *ISME J* **6**: 440–450.

- Lin, W., and Pan, Y. (2010) Temporal variation of magnetotactic bacterial communities in two freshwater sediment microcosms. *FEMS Microbiol Lett* **302**: 85–92.
- Lin, W., Li, J., Schüller, D., Jogler, C., and Pan, Y. (2009) Diversity analysis of magnetotactic bacteria in Lake Miyun, northern China, by restriction fragment length polymorphism. *Syst Appl Microbiol* **32**: 342–350.
- Lin, W., Jogler, C., Schüller, D., and Pan, Y. (2011a) Metagenomic analysis reveals unexpected subgenomic diversity of magnetotactic bacteria within the phylum *Nitrospirae*. *Appl Environ Microbiol* **77**: 323–326.
- Lin, W., Li, B., and Pan, Y. (2011b) DMTB: a comprehensive online resource of 16S rRNA genes, ecological metadata, oligonucleotides, and magnetic properties of magnetotactic bacteria. *Chin Sci Bull* **56**: 476–478.
- Lin, W., Li, J., and Pan, Y. (2012) Newly isolated but uncultivated magnetotactic bacterium of the phylum *Nitrospirae* from Beijing, China. *Appl Environ Microbiol* **78**: 668–675.
- Ludwig, W., and Schleifer, K.H. (1994) Bacterial phylogeny based on 16S and 23S rRNA sequence analysis. *FEMS Microbiol Rev* **15**: 155–173.
- Ludwig, W., Strunk, O., Westram, R., Richter, L., Meier, H., Yadukumar, et al. (2004) ARB: a software environment for sequence data. *Nucleic Acids Res* **32**: 1363–1371.
- Pan, H., Zhu, K., Song, T., Yu-Zhang, K., Lefèvre, C.T., Xing, S., et al. (2008) Characterization of a homogeneous taxonomic group of marine magnetotactic cocci within a low tide zone in the China Sea. *Environ Microbiol* **10**: 1158–1164.
- Postec, A., Tapia, N., Bernadac, A., Joseph, M., Davidson, S., Wu, L.F., et al. (2012) Magnetotactic bacteria in microcosms originating from the French Mediterranean Coast subjected to oil industry activities. *Microb Ecol* **63**: 1–11.
- Pruesse, E., Quast, C., Knittel, K., Fuchs, B.M., Ludwig, W., Peplies, J., and Glöckner, F.O. (2007) SILVA: a comprehensive online resource for quality checked and aligned ribosomal RNA sequence data compatible with ARB. *Nucleic Acids Res* **35**: 7188–7196.
- Pruesse, E., Peplies, J., and Glöckner, F.O. (2012) SINA: Accurate high-throughput multiple sequence alignment of ribosomal RNA genes. *Bioinformatics* **28**: 1823–1829.
- Richter, M., Kube, M., Bazylinski, D.A., Lombardot, T., Glöckner, F.O., Reinhardt, R., and Schüller, D. (2007) Comparative genome analysis of four magnetotactic bacteria reveals a complex set of group-specific genes implicated in magnetosome biomineralization and function. *J Bacteriol* **189**: 4899–4910.
- Rodrigue, S., Malmstrom, R.R., Berlin, A.M., Birren, B.W., Henn, M.R., and Chisholm, S.W. (2009) Whole genome amplification and *de novo* assembly of single bacterial cells. *PLoS ONE* **4**: e6864.
- Schleifer, K.H., Schüller, D., Spring, S., Weizenegger, M., Amann, R., Ludwig, W., and Köhler, M. (1991) The genus *Magnetospirillum* gen. nov., description of *Magnetospirillum gryphiswaldense* sp. nov. and transfer of *Aquaspirillum magnetotacticum* to *Magnetospirillum magnetotacticum* comb. nov. *Syst Appl Microbiol* **14**: 379–385.
- Schübbe, S., Kube, M., Scheffel, A., Wawer, C., Heyen, U., Meyerdierts, A., et al. (2003) Characterization of a spontaneous nonmagnetic mutant of *Magnetospirillum gryphiswaldense* reveals a large deletion comprising a putative magnetosome island. *J Bacteriol* **185**: 5779–5790.
- Schüller, D. (1994) Isolierung und Charakterisierung magnetischer Bakterien – Untersuchungen zur Magnetitbiomineralisation in *Magnetospirillum gryphiswaldense*, pp. 1–125. München: TU München.
- Schüller, D., and Bazylinski, D.A. (2007) Techniques for studying uncultured and cultured magnetotactic bacteria. In *Manual of Environmental Microbiology*. Hurst, C.J., Crawford, R.L., Garland, J.L., Lipson, D.A., Mills, A.L., and Setzenbach, L.D. (eds). Washington DC, USA: ASM Press, pp. 1129–1138.
- Silva, K.T., Abreu, F., Keim, C.N., Farina, M., and Lins, U. (2008) Ultrastructure and cytochemistry of lipid granules in the many-celled magnetotactic prokaryote, ‘*Candidatus* Magnetoglobus multicellularis’. *Micron* **39**: 1387–1392.
- Simon, C., and Daniel, R. (2010) Construction of small-insert and large-insert metagenomic libraries. *Methods Mol Biol* **668**: 39–50.
- Spring, S., and Schleifer, K.H. (1995) Diversity of magnetotactic bacteria. *Syst Appl Microbiol* **18**: 147–153.
- Spring, S., Amann, R., Ludwig, W., Schleifer, K.H., van Gemerden, H., and Petersen, N. (1993) Dominating role of an unusual magnetotactic bacterium in the microaerobic zone of a freshwater sediment. *Appl Environ Microbiol* **59**: 2397–2403.
- Spring, S., Amann, R., Ludwig, W., Schleifer, K.H., Schüller, D., Poralla, K., and Petersen, N. (1995) Phylogenetic analysis of uncultured magnetotactic bacteria from alpha-subclass of *Proteobacteria*. *Syst Appl Microbiol* **17**: 501–508.
- Ullrich, S., Kube, M., Schübbe, S., Reinhardt, R., and Schüller, D. (2005) A hypervariable 130-kilobase genomic region of *Magnetospirillum gryphiswaldense* comprises a magnetosome island which undergoes frequent rearrangements during stationary growth. *J Bacteriol* **187**: 7176–7184.
- Vali, H., and Kirschvink, J.L. (1991) Observations of magnetosome organization, surface structure, and iron biomineralization of undescribed magnetic bacteria. In *Iron Biominerals*. Frankel, R.B., and Blakemore, R.P. (eds). New York: Plenum Press, pp. 97–116.
- Wenter, R., Wanner, G., Schüller, D., and Overmann, J. (2009) Ultrastructure, tactic behaviour and potential for sulfate reduction of a novel multicellular magnetotactic prokaryote from North Sea sediments. *Environ Microbiol* **11**: 1493–1505.
- Wolfe, R.S., Thauer, R.K., and Pfennig, N. (1987) A ‘capillary racetrack’ method for isolation of magnetotactic bacteria. *FEMS Microbiol Ecol* **45**: 31–35.
- Woyke, T., Tighe, D., Mavromatis, K., Clum, A., Copeland, A., Schackwitz, W., et al. (2010) One bacterial cell, one complete genome. *PLoS ONE* **5**: e10314.

Supporting information

Additional Supporting Information may be found in the online version of this article:

Fig. S1. Schematic of experimental set-up of the combined approach to recover diversity from magnetic collections and genomic analysis of single cells. After a magnetic enrichment from an environmental sample (A) a selective enriched collection of MTB was obtained (B). Using universal eubacterial primers almost full-length 16S rRNA genes were amplified and subcloned for sequencing (C). Every MTB morphotype was selected by single cell sorting applying micromanipulation under microscopic control (D). Genomic

DNA of selected cells were amplified using the viral Φ 29 DNA-polymerase by multiple displacement amplification (MDA). Amplified DNA served as template for 16S rRNA PCR allowing phylogenetic analysis of selected morphotypes (E). For genetic analysis of microsorted CS-05 cells genomic DNA was amplified a second time by the MDA, enzymatically debranched, checked for contaminations and subcloned for analysis (F).

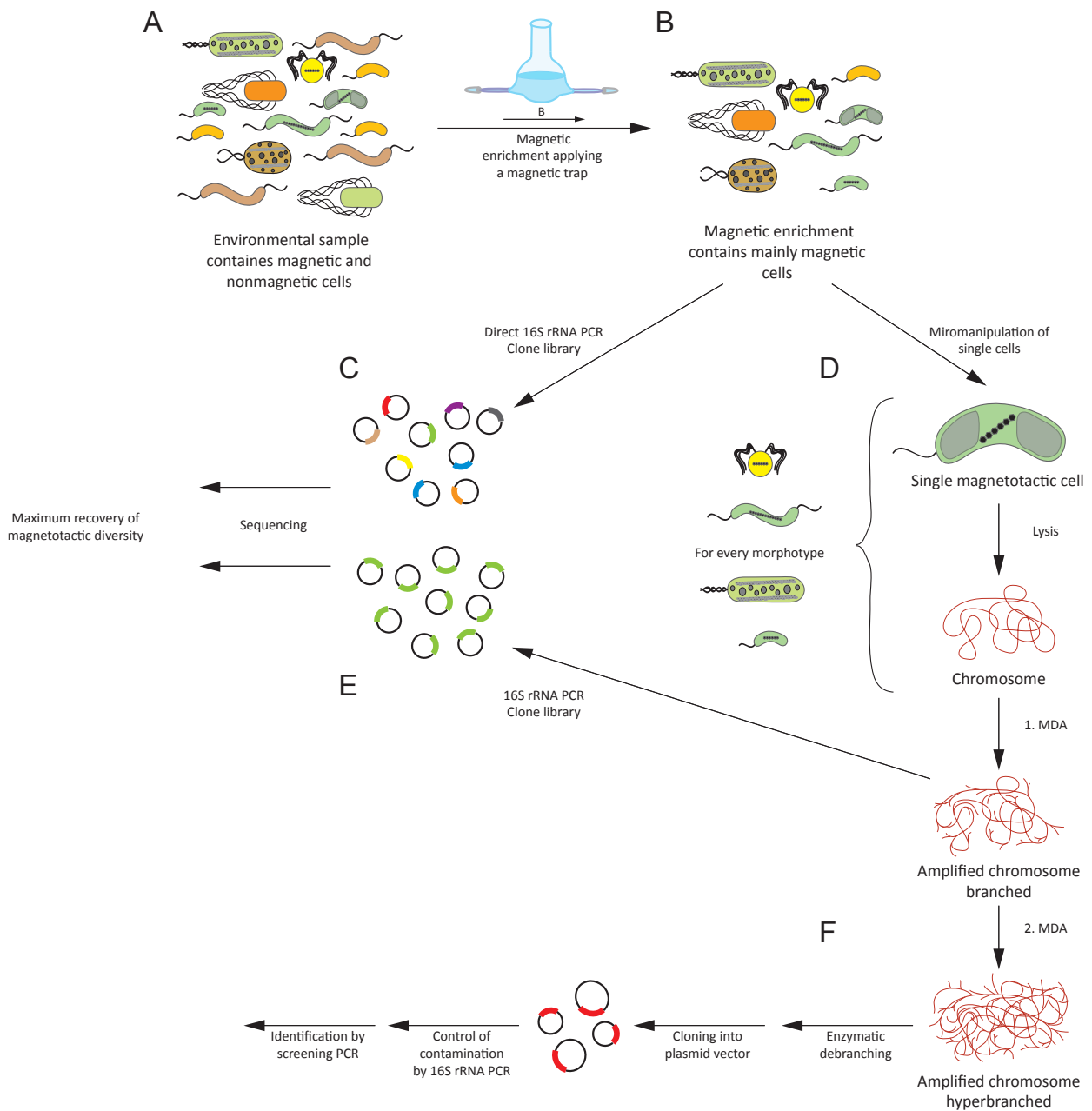


Fig.S1. Schematic of experimental setup of the combined approach to recover maximum diversity from magnetic collections and genomic analysis of single cells.

After a magnetic enrichment we obtained from an environmental sample (A) a selective enriched collection of MTB (B). Using universal eubacterial primers almost full length 16S rRNA genes were amplified and subcloned for sequencing (C). Every MTB morphotype was selected by single cell sorting applying micromanipulation under microscopic control (D). Genomic DNA of selected cells were amplified using the viral $\Phi 29$ DNA-polymerase by multiple displacement amplification (MDA). Amplified DNA served as template for 16S rRNA PCR allowing phylogenetic analysis of selected morphotypes (E). For genetic analysis of microsorted CS-05 cells genomic DNA was amplified a second time by the MDA, enzymatically debranched, checked for contaminations and subcloned for analysis (F).

2. Manuskript:

Single-cell analysis reveals a novel uncultivated magnetotactic bacterium within the candidate division OP3.

Single-cell analysis reveals a novel uncultivated magnetotactic bacterium within the candidate division OP3

Sebastian Kolinko,¹ Christian Jogler,^{1†}
Emanuel Katzmann,¹ Gerhard Wanner,¹
Jörg Peplies² and Dirk Schüler^{1*}

¹Ludwig-Maximilians-Universität Munich, Microbiology,
Großhaderner Str. 2-4, 82152 Planegg-Martinsried,
Germany.

²Ribocon GmbH, 28359 Bremen, Germany.

Summary

Magnetotactic bacteria (MTB) are a diverse group of prokaryotes that orient along magnetic fields using membrane-coated magnetic nanocrystals of magnetite (Fe₃O₄) or greigite (Fe₃S₄), the magnetosomes. Previous phylogenetic analysis of MTB has been limited to few cultivated species and most abundant members of natural populations, which were assigned to *Proteobacteria* and the *Nitrospirae* phyla. Here, we describe a single cell-based approach that allowed the targeted phylogenetic and ultrastructural analysis of the magnetotactic bacterium SKK-01, which was low abundant in sediments of Lake Chiemsee. Morphologically conspicuous single cells of SKK-01 were micromanipulated from magnetically collected multi-species MTB populations, which was followed by whole genome amplification and ultrastructural analysis of sorted cells. Besides intracellular sulphur inclusions, the large ovoid cells of SKK-01 harbour ~175 bullet-shaped magnetosomes arranged in multiple chains that consist of magnetite as revealed by TEM and EDX analysis. Sequence analysis of 16 and 23S rRNA genes from amplified genomic DNA as well as fluorescence *in situ* hybridization assigned SKK-01 to the candidate division OP3, which so far lacks any cultivated representatives. SKK-01 represents the first morphotype that can be assigned to the OP3 group as well as the first magnetotactic member of the PVC superphylum.

Introduction

Magnetotactic bacteria (MTB) are a heterogeneous group of prokaryotes, which synthesize membrane-enclosed crystals of magnetite (Fe₃O₄) or greigite (Fe₃S₄) (Bazylinski and Frankel, 2004). These organelles, called magnetosomes, are organized in chains and cause the cell to align along the Earth's geomagnetic field lines (Frankel *et al.*, 1997). It is assumed that magnetotaxis facilitates navigation of the microaerophilic and anaerobic MTB in chemically stratified limnic or marine sediments (Frankel *et al.*, 1997; Bazylinski and Frankel, 2004; Faivre and Schüler, 2008).

Magnetosome biomineralization and magnetotaxis are complex traits, which are under strict genetic control (Grünberg *et al.*, 2001; 2004; Jogler and Schüler, 2009; Murat *et al.*, 2010). Genes controlling magnetotaxis were identified within a large genomic magnetosome island (MAI) (Schübbe *et al.*, 2003; Ullrich *et al.*, 2005; Fukuda *et al.*, 2006; Richter *et al.*, 2007), which so far was found to be generally conserved in all cultivated and uncultivated MTB (Jogler *et al.*, 2009a,b; 2011; Abreu *et al.*, 2011).

Magnetotactic bacteria display a great diversity with respect to cell shapes such as spirilla, cocci, vibrios, ovoid, rod-shaped and multicellular bacteria, as well as to magnetosome morphologies including hexa and cubo-octahedral, elongated-prismatic and bullet-shaped crystals that are aligned in single or multiple chains (Bazylinski and Frankel, 2004; Jogler and Schüler, 2009). The morphological and ultrastructural variability is also matched by a broad phylogenetic diversity of MTB, and magnetotactic representatives have been identified in several lineages (Amann *et al.*, 2006). Most MTB, such as the cultivated magnetospirilla, vibrios and cocci, as well as many uncultivated magnetotactic cocci have been assigned to *Alphaproteobacteria* (Schleifer *et al.*, 1991; Sakaguchi *et al.*, 2002; Bazylinski *et al.*, 2004; Jogler and Schüler, 2009). A recent study (Lefèvre *et al.*, 2011a) indicates the existence of three newly cultured MTB belonging to the Deltaproteobacteria class. Other MTB including strain *Desulfovibrio magneticus* RS-1 (Kawaguchi *et al.*, 1995) and a number of uncultured multicellular magnetotactic prokaryotes (Esquivel *et al.*, 1983; Abreu *et al.*,

Received 31 July, 2011; revised 7 September, 2011; accepted 7 September, 2011. *For correspondence. E-mail dirk.schueler@lmu.de; Tel. (+49) 892 1807 4514; Fax (+49) 892 1807 4515. †Present address: Harvard Medical School, Boston, MA 02115, USA.

2007; Wenter *et al.*, 2009) were then assigned to the *Deltaproteobacteria*. Recently, two MTB belonging to the *Gammaproteobacteria* were isolated (Lefèvre *et al.*, 2011b). Outside the *Proteobacteria*, MTB so far have been found only within the deep branching *Nitrospirae* phylum (Spring *et al.*, 1993; Flies *et al.*, 2005a; Jogler *et al.*, 2010; Lefèvre *et al.*, 2010; 2011c; Lin *et al.*, 2011).

Because of the adaptation to complex chemical gradients in stratified sediments, only a relative small number of MTB has been isolated in axenic culture. However, in contrast to most other uncultivated microorganisms, MTB can be directly collected from environmental samples and separated from sediment particles and other microorganisms by using their magnetically directed motility (Flies *et al.*, 2005a). Magnetic enrichment such as 'capillary racetrack' technique (Wolfe *et al.*, 1987; Schüller *et al.*, 1999) had been applied in several cultivation-independent studies for the morphological and phylogenetic analysis of MTB in environmental samples (Spring *et al.*, 1994; Flies *et al.*, 2005a,b; Schüller and Bazylinski, 2007; Jogler and Schüller, 2009). Recently, metagenomic analysis of magnetically collected MTB revealed that magnetosome genes are also clustered in uncultivated MTB (Jogler *et al.*, 2009b; Lin *et al.*, 2011). By screening large-insert libraries (Jogler *et al.*, 2009b) several clones from uncultivated MTB were found to contain MAI-like genes with homology to those of cultivated *Alphaproteobacteria*. Homologous magnetosome genes were recently also identified by pyrosequencing of DNA from an uncultivated deltaproteobacterial multicellular magnetotactic prokaryotes (Abreu *et al.*, 2011). By combining micromanipulation with whole genome amplification (WGA) and screening of metagenomic libraries, genomic MAI-like clusters with homology to proteobacterial magnetosome genes were also identified in the uncultivated *Nitrospirae* '*Candidatus* Magnetobacterium bavaricum' (Mbav) (Spring *et al.*, 1993). These findings suggested that the origin of magnetotaxis was monophyletic and genes controlling magnetosome formation were transferred horizontally between *Proteobacteria* and representatives of the *Nitrospirae* phylum (Jogler *et al.*, 2009a; 2011; Abreu *et al.*, 2011). However, previous studies on uncultivated MTB mostly relied on high cell numbers, and thus were limited to the analysis of most abundant representatives (Amann *et al.*, 1995). On the other hand, the sporadic microscopic observation of rare individual magnetotactic cells with conspicuous and unique morphologies, but unknown phylogenetic assignment (Vali and Kirschvink, 1991; Schüller, 1994; Flies *et al.*, 2005a; Lin *et al.*, 2009) suggested that the diversity of low abundant MTB in aquatic environments might be underestimated, and known bacterial lineages may not fully represent the true phylogenetic distribution of magnetotaxis.

Using a novel approach that allowed the targeted phylogenetic and ultrastructural analysis of individual MTB

cells, we here describe a novel uncultivated ovoid magnetotactic bacterium designated strain SKK-01, which was low abundant in freshwater sediments of Lake Chiemsee. WGA from microsorted cells followed by PCR analysis of the 16S and 23S rRNA genes assigned SKK-01 to candidate division OP3 (Hugenholtz *et al.*, 1998), which so far lacks any cultivated representatives and was characterized solely based on environmental marker sequences derived from metagenomic clones of unknown origin. Thus, SKK-01 not only is the first identified magnetotactic representative of OP3 division, but also represents the first morphotype that can be assigned to this group.

Results

Description and sediment distribution of SKK-01

Sediment collected from Lake Chiemsee contained various morphotypes of MTB including spirilla, cocci, vibrios and characteristic large rods described as '*Cand.* Magnetobacterium bavaricum' (Mbav) (Spring *et al.*, 1993; Jogler *et al.*, 2010; 2011). Upon prolonged laboratory storage, small magnetococci and spirilla became predominant (> 90%) in the microcosms. After 12–18 months of incubation at room temperature, we occasionally observed individual conspicuous MTB in microscopic samples from two of ten microcosms collected from the same sampling site in 2008 and 2009 respectively. These cells, named SKK-01, accounted for < 1% of total MTB and could be easily recognized by their conspicuous ovoid 'melon'-shaped morphology, their characteristic large size (up to 3.7 by 2.3 μm), the presence of several refractile inclusions and unusually fast ($126 \pm 35 \mu\text{m s}^{-1}$) N-seeking swimming motility, which together distinguished SKK-01 from all other more abundant MTB present in the sample (Movie S1).

We determined the vertical distribution of SKK-01 in undisturbed sediments by counting magnetically responsive cells from different horizons in cores taken from SKK-01-positive microcosms, similar as described before (Flies *et al.*, 2005b). Whereas other MTB, mostly magnetotactic cocci and spirilla, were abundant in high numbers between 2.3×10^6 and $2.3 \times 10^7 \text{ cm}^{-3}$ within the first mm of sediment with a maximum at 7–8 mm (Fig. 1), SKK-01 was detected in much lower numbers with a peak distribution of $1.3 \times 10^5 \text{ cm}^{-3}$ at 10 mm depth (Fig. 1), very much reminiscent to the distribution of Mbav (Jogler *et al.*, 2010). The presence of SKK-01 coincided with a transition in colour of the stratified sediment from 10 to 12 mm, indicating a change from oxic to reduced conditions (Fig. 1, asterisk).

Phylogenetic analysis of single SKK-01 cells

The low abundance of SKK-01 among magnetically collected MTB prevented its identification by conventional

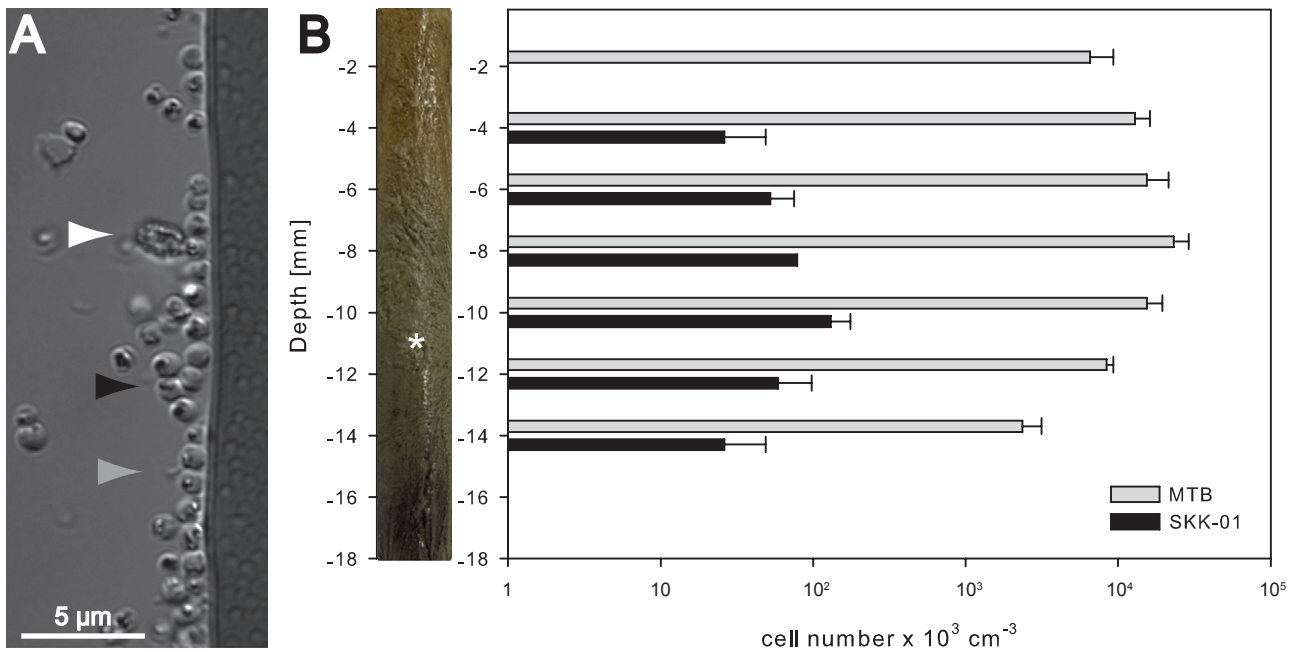


Fig. 1. A. Differential interference contrast (DIC) light micrographs of north-seeking MTB in a hanging drop, magnetically enriched from a microcosm sampled from Lake Chiemsee. A large ovoid cell of the low abundant strain SKK-01 (white arrow) is visible among numerous magnetic cocci (black arrow) and spirilla (grey arrow). B. Vertical distribution of total MTB and strain SKK-01 in sediment layers of a microcosm from sediments from Lake Chiemsee. Cell counts were done in triplicates, with line extensions representing the positive standard deviation. A representative SKK-01 containing sediment core from a microcosm is shown (*), illustrating the vertical chemical stratification indicated by different colours.

mass PCR and shotgun cloning (Amann *et al.*, 1995), and we were unable to further increase its proportion by magnetic enrichment. Therefore, we applied single-cell sorting by micromanipulation followed by WGA using multiple displacement amplification (MDA) (Hutchison and Venter, 2006), similar as described previously (Jogler *et al.*, 2010; 2011) (Fig. S1). SKK-01 cells were manually selected under strict microscopic control based on their conspicuous morphology from suspensions of magnetically collected MTB (Fig. S1, Movie S2). Due to its low abundance SKK-01 could not always be separated from other predominant MTB in the first sorting step. However, cells that were accidentally co-aspired could be easily eliminated by repeated dilution and resorting (Movie S2). Five cells per

reaction were found to be sufficient as template in each subsequent MDA reaction, which yielded ~600 ng DNA per each reaction.

Aliquots of 60 ng of amplified SKK-01 DNA were directly used as template in subsequent PCR. PCR with universal eubacterial 16S rRNA gene primers 27f and 1492r (Table 1) (Lane, 1991) yielded amplicons of the expected size, whereas no products were obtained from negative controls including empty WGA reactions and such containing only filtered extracellular sorting fluid. Sequencing of 40 subcloned PCR products amplified from three independent WGA reactions yielded all identical sequences, indicating that the amplified DNA originated from a single phylotype.

Table 1. Primers for PCR amplification of 16S and 23S rRNA genes used in this study.

Primer	Orientation	Binding position	Sequence (5'-3')
27f	Forward	16S 27–47	AGAGTTTGGATCCTGGCTCAG
1492r	Reverse	16S 1492–1501	GGTTACCTTGTTACGACTT
SK-03	Forward	23S 44–60	AGCGGATGAAGGACGTG
SK-04	Forward	23S 46–63	GCGATGAAGGACGTACTA
SK-05	Forward	23S 465–483	GAGGGAAAGGTGAAAAGAA
SK-08	Forward	23S 1090–1104	WGCGTAAYAGCTCAC
SK-11	Reverse	23S 2498–2512	AGCYGACATCGAGG
SK-12	Reverse	23S 2652–2668	CGGTCTCTCGTACTAA
SK-13	Reverse	23S 2744–2759	CTTAGATGCYTTACAGC

Whereas 16S rRNA gene sequences obtained from micromanipulated cells of the most abundant magnetotactic morphotypes present within the same magnetic collections assigned them next to well known alphaproteobacterial MTB (mainly uncultivated magnetococci, data not shown), initial blastn searches of as SKK-01-derived sequences against the GenBank database unexpectedly did not indicate any close relationship to known MTB sequences. Instead, they generated top hits to other, exclusively uncultivated bacteria from aquatic environments (Table 2). Best hit (91% identity) was found to the unaffiliated uncultivated clone d0-62 from a profoundal lake sediment, followed by a number of anonymous environmental sequences with no phylogenetic assignment. Among the next top hits, high identity (84%) was found to clone LPBBBM90 (FJ902074) that had been assigned to the candidate division OP3 (Hugenholtz *et al.*, 1998), and several other environmental sequences assigned to this group (Table 2). Closest cultured relative (81% identity) was *Pelobacter acetylenicus* strain WoAcy1 (Liesack and Finster, 1994), an obligate anaerobe that belongs to the order of *Desulfuromonadales* within the *Deltaproteobacteria*.

To confirm affiliation of SKK-01 with the candidate division OP3, comparative 16S rRNA gene sequence analysis was conducted that unambiguously supported our initial findings (Fig. 2). In comparison to the reference groups considered (*Chlamydia*, *Verrucomicrobia*, *Planctomycetes*, *Nitrospirae*), the phylogenetic analysis of the SKK-01 16S rRNA gene sequence showed stable and monophyletic grouping with other OP3-classified sequences and also close relation to the profoundal lake sediment clone (AM409855) could be confirmed. We wanted to further confirm the affiliation of SKK-01 by the 23S rRNA gene as a second phylogenetic marker (Ludwig and Schleifer, 1994; de la Haba *et al.*, 2011). Because we failed to amplify any product from SKK-01-derived WGAs using universal eubacterial primers 11a and 97ar (Van Camp *et al.*, 1993), we deduced a set of primers from 23S rRNA sequences of large metagenomic fragments OP3/1, OP3/2 and OP3/3, which had been recently assigned to OP3 division based on analysis of their complete rRNA operons (Glöckner *et al.*, 2010). Primers SK-03, -04, -05, -07, -08, -11, -12 and -13 yielded products of expected sizes in various combinations (Table 1 and Fig. S2), yielding a single contiguous sequence covering 2.9 kb of the 23S rRNA gene. Phylogenetic analysis fully supported the OP3 affiliation of SKK-01, even though the backbone branching patterns of the main groups showed inconsistencies between the 16S and 23S rRNA gene trees, a common phenomenon in phylogenetic analysis (Ludwig, 2010).

Table 2. Selected top nBLAST hits of SKK-01 16S rDNA.

Similarity	Description	Sampling site (reference)	Accession number GenBank
91%	Uncultured bacterium, clone d0-62	Profundal sediment, freshwater, Lake Kinnert Israel	AM409855
88%	Uncultured bacterium clone PL 188	Sea sediments, marine, Arabian Sea	FJ268555
85%	Uncultured organism clone MAT-CR-M4-A08	Mat community, Hypersaline Candelaria lagoon, Puerto Rico (Isenbarger <i>et al.</i> , 2008)	EU245642
85%	Uncultured bacterium clone MD2896-B143	Subseafloor sediments, marine, South China Sea	EU385743
85%	Uncultured bacterium C1_B035	Hydrothermal sediments, marine, Guaymas Basin (Teske <i>et al.</i> , 2002)	AF4_19696
85%	Uncultured bacterium clone ORI-860-27-P_S101-103_272B07	Subseafloor sediment, marine, Taiwan	GU553782
84%	Uncultured bacterium clone MD2896-B233	Subseafloor sediments, marine, South China Sea	EU385809
84%	Uncultured bacterium clone ORI-860-27-P_S101-103_272B04	Subseafloor sediment, marine, Taiwan	GU553779
84%	Uncultured bacterium clone HDB_SIPO629	Saturated zone, Hanford site, 300 Area	HM187166
84%	Uncultured candidate division OP3 bacterium clone LPBBBM90	Sediment biomat, phreatic limestone sinkhole, freshwater, Mexico	FJ902074
82%	Candidate division OP3 clone OPB2	Hot Spring, freshwater, Yellowstone National Park (Hugenholtz <i>et al.</i> , 1998)	AF027088
82%	Uncultured candidate division OP3 bacterium clone Z17M5B	Biomat, 17 m depth of a phreatic sinkhole, freshwater, Mexico	FJ484461
81%	Uncultured candidate division OP3 bacterium clone Z273MB20	Biomat, 273 m depth of a phreatic sinkhole, freshwater, Mexico	FJ484653
81%	<i>Pelobacter acetylenicus</i> WoAcy1	Creek sediment, freshwater, Germany (Schink, 1985; Liesack and Finster, 1994)	X70955
80%	Uncultured bacterium clone OP3/1	Flooded paddy soil, freshwater, Italy (Glöckner <i>et al.</i> , 2010)	FP245538
79%	Uncultured bacterium clone OP3/3	Flooded paddy soil, freshwater, Italy (Glöckner <i>et al.</i> , 2010)	FP245540
79%	Uncultured bacterium clone OP3/3	Flooded paddy soil, freshwater, Italy (Glöckner <i>et al.</i> , 2010)	FP245539

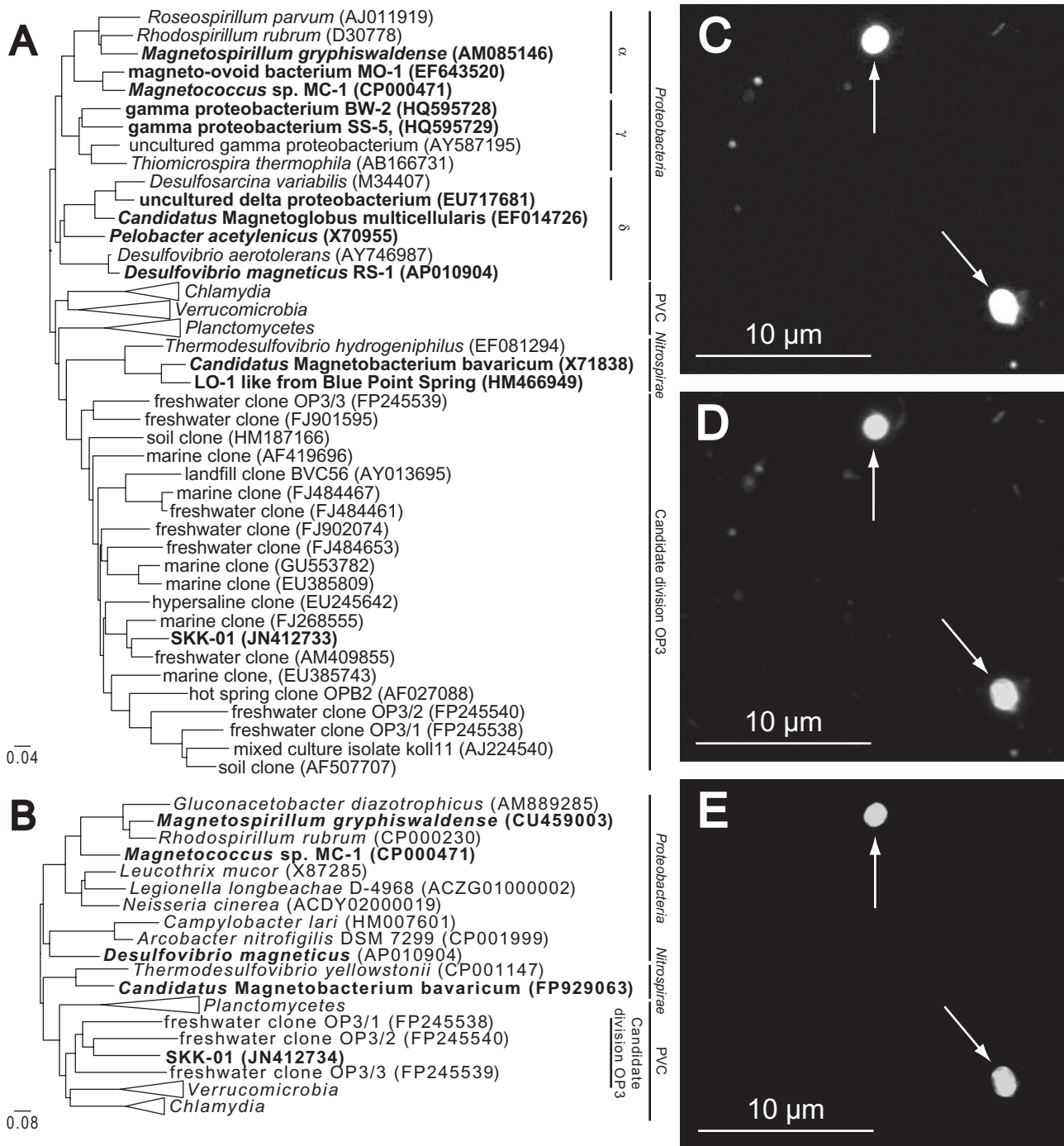


Fig. 2. Phylogenetic trees of 16S (A) and 23S (B) rRNA gene sequences showing the phylogenetic affiliation of SKK-01 from Lake Chiemsee sediment and other selected references of the heterogeneous group of MTB. INSDC accession numbers are given in parentheses. Magnetotactic bacteria are highlighted in bold. Scale bar indicates estimated sequence divergence. Fluorescence *in situ* hybridization (FISH) of magnetically collected cells from Lake Chiemsee sediments. C. Fluorescence of a 4',6-diaminodino-2-phenylindole (DAPI) staining, all cells are stained. D. Epifluorescence of Cy3 labelled oligonucleotide eubacteria-specific probes Eub 338 I–III. All cells hybridized. E. Epifluorescence of fluorescein (FITC) labelled probe MO401. All cells of SKK-01 morphotype hybridized with the specific probe MO401 (white arrows) whereas the accompanying cells were not stained.

Fluorescence in situ hybridization

To further authenticate its 16S rRNA gene sequence by fluorescent *in situ* hybridization (FISH), we designed the SKK-01 specific oligonucleotide probe MO401 (5'-CGG GGATGAATGCAAATGGG-3'). MO401 was assigned to fluorescence class I, revealed by comparison with the *E. coli* 16S rRNA gene sequence (Behrens *et al.*, 2003). Control of the probe sequence with 'probe match' (Cole *et al.*, 2009) of the RDP-II database suggested no hybridization with any other sequence. As the bioinformatic tool 'probe check' (Loy *et al.*, 2008) predicted only three mismatches to sequences of the genus *Photorhabdus*, we performed a control hybridization to exclude potential cross-hybridizations. However, hybridization of MO401 to cells of *Photorhabdus luminescence* strain TT01 yielded no fluorescence signal, irrespective of the formamide concentration used (data not shown).

Hybridization of all MTB cells in magnetic collections with MO401 in the presence of 50% formamide yielded a reliable fluorescence signal, which was exclusively associated with cells of the SKK-01 morphotype (Fig. 2). In contrast, counterstaining with DAPI and co-hybridization with eubacterial probes EUB3381–III (Amann *et al.*, 1990; Alm *et al.*, 1996; Daims *et al.*, 1999) (Fig. 2) also recognized all other morphotypes in the samples (Fig. 2).

Because of its strong morphological resemblance to the uncultivated magnetotactic Nitrospirae MTB LO-1 (Lefèvre *et al.*, 2011c) and the co-occurrence with cells of Mbav within the same sample, we wanted to differentiate SKK-01 from Nitrospira-like MTB. Therefore, SKK-01 cells were co-hybridized with the oligonucleotide probe Mbavp originally designed for detection of Mbav (Spring *et al.*, 1993), which was found to hybridize also with cells of the uncultivated MHB-1 (Flies *et al.*, 2005a) and LO-1 (Lefèvre *et al.*, 2011c). If magnetically collected cells were hybridized with Mbavp, a signal was detected only for Mbav cells, whereas SKK-01 cells were not recognized by the Mbavp probe (Fig. S3).

Morphology and ultrastructure of SKK-01

The ovoid cells of SKK-01 are $2.5 \pm 1.0 \mu\text{m}$ in length by $1.9 \pm 0.7 \mu\text{m}$ in width ($n = 47$). DIC microscopy revealed the intracellular presence of numerous light refractive inclusions (Fig. 3A). To unambiguously correlate the phenotype of single cells with information with their ultrastructure, microsorted individual fluorescence-marked SKK-01 cells as well as unhybridized cells of this morphotype were sorted onto finder grids, which allows to locate and target single cells by electron microscopy (Fig. S1). Analysis of fluorescence-marked and unmarked cells revealed that beside magnetosomes, SKK-01 cells had numerous

(35 ± 7 per cell) spherical intracellular inclusions that were $\sim 0.3 \mu\text{m}$ in size and occupied a major proportion of the cell volume. Using energy-dispersive X-ray spectroscopy (EDX) these inclusions were identified as sulphur (Fig. 3E). Whereas flagella were difficult to discern by TEM of the few sorted cells, 'Ryu-staining' (Ryu, 1937; Heimbrook *et al.*, 1989) revealed that SKK-01 cells have two polar filaments or tufts of flagella (Fig. 3B).

Similar to the magnetotactic Nitrospirae MTB Mbav and LO-1 (Jogler *et al.*, 2011; Lefèvre *et al.*, 2011c), SKK-01 has bullet-shaped magnetosomes that are organized in multiple bundles of 5–7 magnetosome chains traversing the cell along its length (Fig. 4A and B). Each cell produced 175 ± 15 crystals with a size varying between 40 and 185 nm (110 ± 23 nm) in length and 37 ± 5 nm in width ($n = 360$), with magnetosomes between 90 and 120 nm length accounting for 62% of all particles. Interestingly, magnetosome crystals have similar dimensions (106 ± 22 nm) as well as an almost congruent size distribution compared with those of Mbav (Fig. 4C and E). Bundles of magnetosomes were also visible as dark structures in epifluorescence micrographs of SKK-01 cells stained with various dyes, suggesting an arrangement of magnetosome chains closely adjacent to the cell membrane (Fig. 4B), similar as shown for Mbav (Katzmann *et al.*, 2010; Jogler *et al.*, 2011) and other MTB. Element mapping by energy-dispersive X-ray spectroscopy revealed a signal for iron and oxygen coinciding with magnetosome crystals, but the absence of a sulphur signal, which is consistent with the presence of an iron-oxide, such as magnetite or maghemite (Fig. 3F–G).

Discussion

Up to now, the known phylogenetic distribution of magnetotaxis has been limited to *Proteobacteria* and the deep branching Nitrospirae phyla. Here we present first evidence that MTB also occur within the candidate OP3 division, which was originally defined based on a single 16S rRNA gene sequence obtained from Obsidian Pool sediment, a hot spring in Yellowstone National Park (Hugenholtz *et al.*, 1998). Only very limited information is available for members of the candidate division OP3, which so far contains no cultured representatives. OP3-like 16S rRNA gene sequences were exclusively found in aquatic environments, such as marine sediments, hypersaline deep sea, freshwater lakes, aquifers, flooded paddy soils and methanogenic bioreactors, in which OP3 bacteria appear to thrive within anoxic zones (Derakshani *et al.*, 2001; Madrid *et al.*, 2001; Röling *et al.*, 2001; Brofft *et al.*, 2002; Abulencia *et al.*, 2006; Elshahed *et al.*, 2007; Lehours *et al.*, 2007; Li and Wang, 2008; Macalady *et al.*, 2008; Huang *et al.*, 2010). In a recent study it was found that three large metagenomic clones, which were

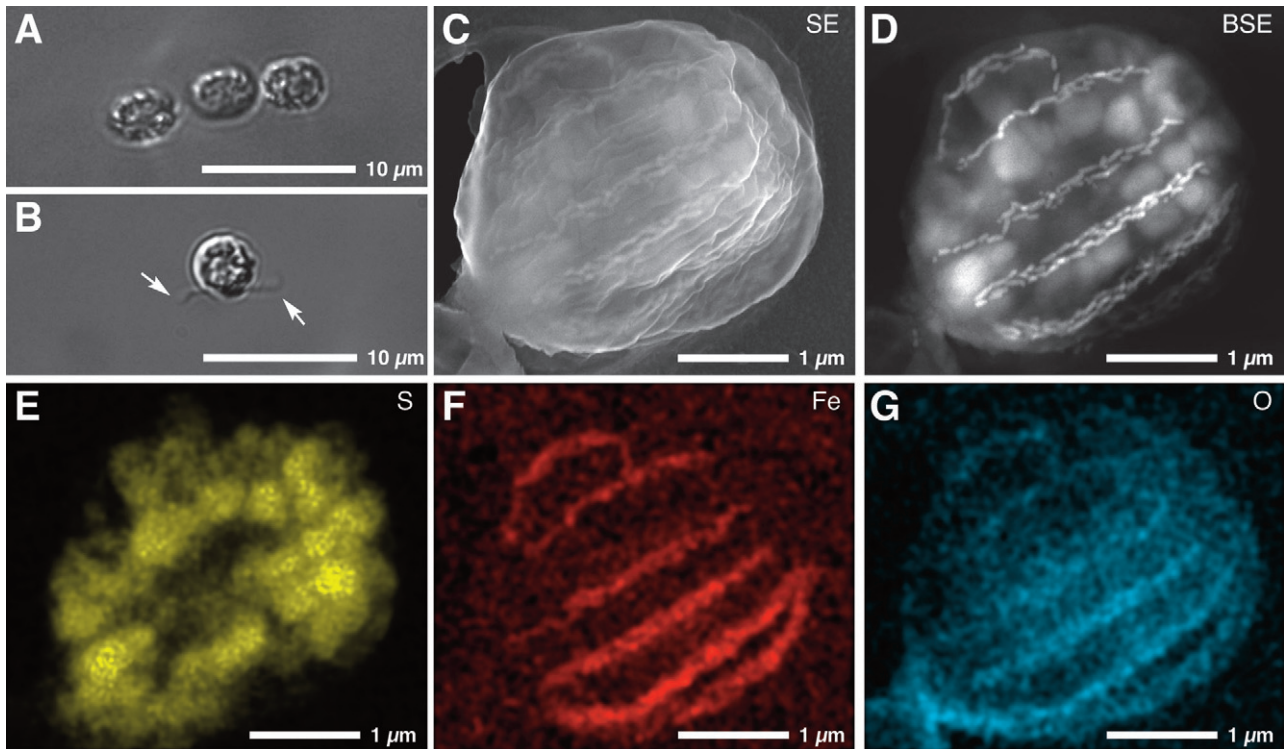


Fig. 3. Morphology and ultrastructure of SKK-01.

A. Differential interference contrast (DIC) light micrograph of microsorted cells of strain SKK-01 showing numerous intracellular inclusions.

B. DIC light micrograph of a Ryu stained cell of SKK-01 showing two polar filaments or tufts of flagella (arrows).

C–G. Comparative ultrastructural analysis of a microsorted SKK-01 cell.

C. Scanning electron microscopy shows large and numerous inclusions and bullet-shaped magnetosomes.

D. The back-scattered electron image of SKK-01 reveals bullet-shaped magnetosomes organized in multiple bundles and in addition numerous large and spherical inclusions (electron dense elements can be distinguished based on their high yield of back-scattered electrons that results in a bright signal). Elements mapping using Energy dispersive X-ray spectroscopy (EDX) revealing sulfur containing intracellular inclusions (E) Fe content within magnetosomes highlighting chains parallel to the long axis of the cell (F) and oxygen rich components of the cell, which coincide with magnetosome chains (G).

assigned to the OP3 candidate division based on analysis of their complete rRNA operons, shared a high proportion of ORFs with best matches to homologues from *Deltaproteobacteria* rather than to those of members of the PVC superphylum. This raised speculations that OP3 bacteria may have evolved metabolic capabilities similar to those of *Deltaproteobacteria* (Glöckner *et al.*, 2010). It was also noted by Glöckner and colleagues that OP3 bacteria were frequently detected in anoxic environments that are defined by the redox cycling of iron, manganese and other metals, and/or sulphur as major drivers of microbial activity (Glöckner *et al.*, 2010). These general characteristics apparently are also shared by the novel magnetotactic bacterium SKK-01 with respect of its occurrence within the suboxic layers of the sediment as well as the intracellular presence of numerous sulphur and iron-rich inclusions. From this it might be speculated that SKK-01 may couple sulphur oxidation to the reduction of iron or other electron acceptors for anaerobic respiration.

SKK-01 displays a remarkable morphological similarity to uncultivated MTB from the *Nitrospirae* phylum, such

as Mbav with respect to shape and size distribution of the bullet-shaped magnetosome crystals (Spring *et al.*, 1993; Jogler *et al.*, 2010), and to LO-1 in terms of overall morphology and ultrastructure as well as motility characteristics (Lefèvre *et al.*, 2011c). However, based on analysis of the 16S and 23S rRNA genes, the phylogenetic affiliation of SKK-01 is clearly distinct from the *Nitrospirae* affiliated MTB. Thus, the observed similarity of bullet-shaped magnetosomes between SKK-01 and MTB of the *Nitrospirae* might reinforce the hypothesis of horizontal genetic exchange between the two phyla or a general adaption to common niche. It was speculated by Abreu and colleagues 2011 that this crystal morphology is the first to appear and it evolved in more complicated structures as cubo-octahedral observed in the most 'recent' group of *Proteobacteria* (e.g. *Alpha* and *Gammaproteobacteria*). The fact that SKK-01 is found in a deeper branching group than the *Nitrospirae* reinforces the hypothesis that the common ancestor of all MTB could biomineralize bullet-shaped crystals, taking in consideration the postulated monophyletic evolution of the

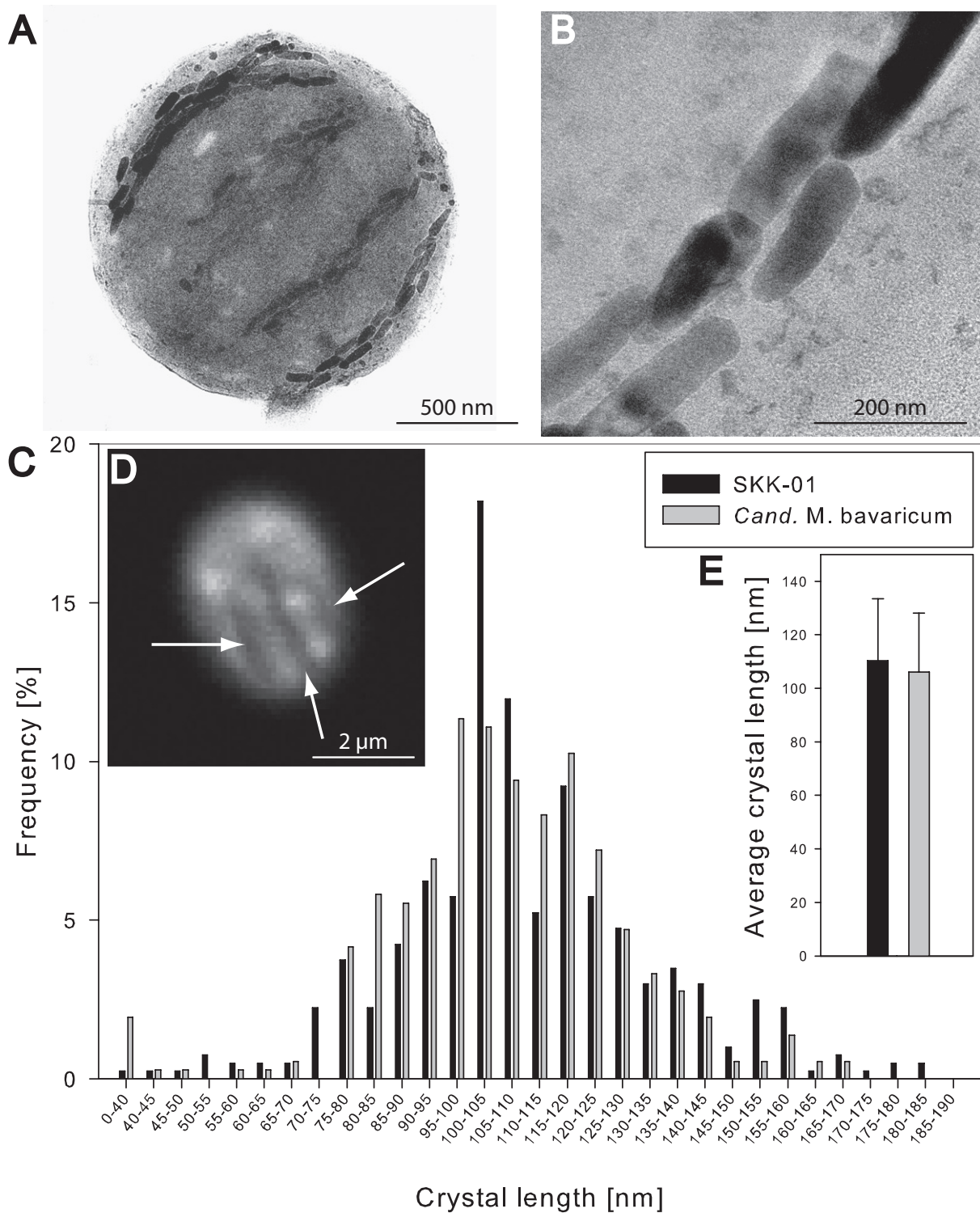


Fig. 4. Analysis of magnetosomes from SKK-01. A. Transmission electron micrograph of a SKK-01 cell with bullet-shaped magnetosomes traversing the cell in five chains. B. Highly magnified micrograph of bullet-shaped magnetosomes of SKK-01. C. Size distributions from SKK-01 and Mbav were obtained by analysis of 360 crystals. D. Light micrograph of a Cy3 epifluorescence stained cell of SKK-01. Magnetosome chains are visible as dark regions traversing the cell along its length. E. Length distributions of bullet shaped magnetosome crystals from SKK-01 and the unrelated magnetotactic bacterium Mbav obtained by analysis of 360 crystals.

magnetotactic behaviour (Abreu *et al.*, 2011; Jogler *et al.*, 2011).

Previous phylogenetic analyses revealed that OP3 together with the candidate division *Poribacteria* and the *Planctomycetes*, *Verrucomicrobia*, *Chlamydiae* and *Lentisphaerae* form a monophyletic clade referred to as the 'PVC superphylum' (Wagner and Horn, 2006; Pilhofer *et al.*, 2008). Our comparative 16S and 23S rRNA-gene sequence analysis yielded congruent results and suggest that SKK-01 along with other OP3 bacteria belongs to PVC superphylum.

All knowledge about OP3 candidate division so far has been derived exclusively from the analysis of anonymous 16S rRNA gene sequences and metagenomic clones, whereas the corresponding bacteria have remained undetected. Consequently, nothing is known about morphologies and numbers of OP3 bacteria in natural environments. Thus, our identification of SKK-01 also represents the first assignment of a cell morphotype to this group.

So far, MTB similar to SKK-01 have not been reported by previous studies of uncultivated MTB, in which the low representation of SKK-like bacteria likely prevented their detection by conventional cultivation-independent approaches based on mass PCR (Amann *et al.*, 2006). In contrast, our method enabled the targeted analysis of very low abundant MTB by microsorting of individual cells followed by WGA and PCR of phylogenetic marker genes. In addition, microsorting also allowed authenticating the obtained phylogenetic information by FISH as well as by the targeted ultrastructural analysis of phylo-stained single cells, thus providing unambiguous correlation between genomic information, morphology and ultrastructure of individual cells. Similar approaches might be used also for the combined phylogenetic, ultrastructural, genomic and even cultivational analysis of single cells of other yet-uncultivated and under-represented bacteria. In particular, single cell-based genome analyses of other uncultivated MTB from various habitats are likely to reveal further unexpected diversity that may extend towards other lineages. The genetic analysis of magnetotaxis and their phylogenetic distribution in diverse lineages will also reveal further information about the direction and mechanisms of presumed horizontal gene transfer of magnetosome genes (Jogler *et al.*, 2009a,b; 2011; Abreu *et al.*, 2011).

Experimental procedures

Sediment sampling and magnetic collections

Freshwater sediments from Lake Chiemsee (Germany, Bavaria) (latitude: 47°51'08"N; longitude 12°24'00"E) were collected from the same sampling site in June 2008 and July 2009 from 10–20 m depth applying a bottom sampler. Aquaria were filled with 18–25 l sediment slurry and covered

with the same volume of sample water. To allow stratification these microcosms were stored at room temperature for several months. The sediment colour was brownish in the oxic sediment layers (~4 mm), then greyish down to 10 mm depth and below changed to black colour due to a high FeS content. Magnetic two-step enrichments for downstream analysis were performed as previously described (Jogler *et al.*, 2009b). In brief, MTB were magnetically collected from mud slurries containing 10 ml of sediment cores mixed with 30 ml sample water. Magnetic collections were transferred into a magnetic trap for further enrichment. The distribution of MTB and SKK-01 in the sediment was determined by microscopic counting of magnetically responsive cells in horizontally sliced sediment cores as previously described (Flies *et al.*, 2005b; Jogler *et al.*, 2010).

Micromanipulation based WGA

As described previously by Jogler and colleagues (Jogler *et al.*, 2011), custom-made plastic frames mounted to microscopic slides served as sorting devices for micromanipulation. Three droplets of 10 µl containing magnetic collected cells, filter-sterilized (0.2 µm pore size) sample water and pure H₂O were placed next to each other onto the sorting device and covered with 900 µl mineral oil (Bio-Rad, Hercules, CA, USA) to prevent evaporation. The prepared sorting device was placed next to an Advantix AmpliGrid AG480F (Advantix, Munich, Germany) into a double slide holder of an IX81 microscope (Olympus, Tokyo, Japan) equipped with a 100_UPLSAPO100XO objective for differential interference contrast (DIC) microscopy. Under microscopic control at 1000 × magnification SKK-01-like cells were transferred successively from magnetic collections to filter-sterilized (0.2 µm pore size) sample water and then into H₂O. At each step, cells were at least 10 times aspirated and dispensed by the glass capillary to remove contaminants and extracellular DNA (Fig. S1, Movie S2). Washed cells were directly transferred into 0.45 µl of sample buffer (illustra GenomiPhi V2 DNA amplification kit, GE Healthcare, Little Chalfont, UK) covered with 5 µl of sealing solution (Advantix). Loaded AmpliGrids were inserted into an AmpliSpeed cyclor (Advantix), which was calibrated to work at 4°C. Samples were heated to 98°C for 6 min and stored at 4°C for 10 min. Reaction buffer with enzyme mix (0.45 µl) was added to the sample buffer by pipetting it onto the sealing solution. The WGA reaction was carried out at 30°C for 4 h.

Determination of 16S and 23S rRNA gene sequences and phylogenetic analysis

The 16S rRNA gene was amplified from WGA experiments of SKK-01 cells using Bacteria-specific primers 27F and 1492R (Lane, 1991) (Table 2). The 23S rRNA gene was amplified using primers listed in Table 1 deduced from conserved regions of 23S rRNA genes of metagenomic OP3 clones (Glöckner *et al.*, 2010). PCR products were cloned into pJET1.2/blunt Cloning Vector (Fermentas, Waltham, MA, USA) and sequenced with an ABI system according to the instructions of the manufacturer. Alignment of gene sequences was performed with the AlignX algorithm of the

Vector NTI software version 11.0 (Invitrogen, Carlsbad, CA, USA). Sequences were negatively checked for chimera using the Bellerophon algorithm (Huber *et al.*, 2004).

16S/23S rRNA gene sequences were analysed using the ARB software package version 5.2 (Ludwig *et al.*, 2004) and the corresponding SILVA SSU Ref and LSU Ref databases release 106 from April 2010 (Pruesse *et al.*, 2007). Briefly, nearly full length 16S and 23S rRNA gene sequences of strain SKK-01 were automatically aligned according to the SILVA SSU and LSU reference alignments and manual refinement was carried out taking into account the secondary structure information of the native rRNA. For initial classification, SKK-01 sequences were added to the corresponding guide trees of the SSU and LSU SILVA datasets using the ARB parsimony tool.

Based on this information, final tree reconstruction was performed with selected reference sequences and a larger number of their close relatives to stabilize tree topologies. Reference sequences of MTB were selected from the DMTB database (<http://database.biomnsl.com/>). In total, 1020 and 160 sequences of the SSU and LSU datasets, respectively, were used to reconstruct maximum likelihood trees using the RAxML tool version 7.0.3 (Stamatakis, 2006) with the GTR-GAMMA model and based on 1475 and 2689 valid columns of the SSU and LSU alignments, respectively (highly variable positions were filtered out using positional variability filters based on all sequences of the domain Bacteria within the complete SSU and LSU SILVA datasets). General tree topologies were evaluated by parallel maximum distance analysis (ARB neighbour joining tool). Partial sequences were added to the tree using the ARB parsimony tool. For better clarity, only selected sequences and groups are shown in the figure. Sequences described in this study can also be downloaded from the databases of the INSDC, comprising DDBJ, EMBL and GenBank (corresponding accession numbers are listed in Fig. 2).

Fluorescence in situ hybridization

The SKK-01 specific oligonucleotide probe MO401 was designed with Vector NTI 11.0 (Invitrogen) and verified by *Probecheck* (Cole *et al.*, 2009) and *Probe Match* (Loy *et al.*, 2008). Based on data available for *E. coli*, accessibility of the target site and the fluorescence class of the probe were checked (Behrens *et al.*, 2003). For Co-hybridization probes Eub338 I–III (Amann *et al.*, 1990; Alm *et al.*, 1996; Daims *et al.*, 1999) and Mbavp (Spring *et al.*, 1993) were used. Probes were labelled either with carboxymethylrhodamine (Cy3) or fluorescein (FITC) as a fluorescent dye. FISH was performed as described (Pernthaler *et al.*, 2001). *Photorhabdus luminescence* TT01 (kindly provided by R. Heermann, LMU) was used as a negative control.

Light, fluorescence and electron microscopy

Magnetic collections were examined by hanging drop assay (Frankel *et al.*, 1997; Schüler and Bazylinski, 2007) using a SM-LUX (Leitz, Wetzlar, Germany) phase contrast microscope. Fluorescence microscopy was performed with an IX81 inverted microscope (Olympus) using a 100_ UPLSAPO100X objective.

For ultrastructural analysis, phylo-stained cells applying probe MO401 and unstained cells were sorted onto finder grids under fluorescence and light microscopic control.

Transmission electron microscopy (TEM) was performed with a FEI Tecnai F20 (200 kV) TEM equipped with an Eagle charge-coupled-device camera (4096 by 4096 pixels). Cells (either negatively stained by uranyl acetate or left unstained) were adsorbed on carbon-coated copper grids (Plano, Wetzlar, Germany). Images were acquired using EMMenu 4.0 and FEI software. For structural analysis, sorted cells were examined with a Zeiss AURIGA high-resolution field-emission scanning electron microscope operated at 25 keV. SE- and BSE images were simultaneously recorded with the chamber SE and QBSD detectors. For energy-dispersive X-ray (EDX) analysis (point analysis and EDX mapping) a Bruker QUANTAX double detector system (2 × 30 mm² XFlash) was used at a working distance of 6 mm and 25 kV.

Acknowledgements

This work was supported by Deutsche Forschungsgemeinschaft (Grant DFG Schu1080/11-1 to D.S.).

References

- Abreu, F., Martins, J.L., Silveira, T.S., Keim, C.N., de Barros, H.G., Filho, F.J., and Lins, U. (2007) '*Candidatus Magnetoglobus multicellularis*', a multicellular, magnetotactic prokaryote from a hypersaline environment. *Int J Syst Evol Microbiol* **57**: 1318–1322.
- Abreu, F., Cantao, M.E., Nicolas, M.F., Barcellos, F.G., Morillo, V., Almeida, L.G., *et al.* (2011) Common ancestry of iron oxide- and iron-sulfide-based biomineralization in magnetotactic bacteria. *ISME J* **5**: 1634–1640.
- Abulencia, C.B., Wyborski, D.L., Garcia, J.A., Podar, M., Chen, W., Chang, S.H., *et al.* (2006) Environmental whole-genome amplification to access microbial populations in contaminated sediments. *Appl Environ Microbiol* **72**: 3291–3301.
- Alm, E.W., Oerther, D.B., Larsen, N., Stahl, D.A., and Raskin, L. (1996) The oligonucleotide probe database. *Appl Environ Microbiol* **62**: 3557–3559.
- Amann, R., Peplies, J., and Schüler, D. (2006) Diversity and taxonomy of magnetotactic bacteria. In *Magnetoreception and Magnetosomes in Bacteria*. Schüler, D. (ed.). Heidelberg: Springer-Verlag Berlin, pp. 25–36.
- Amann, R.I., Binder, B.J., Olson, R.J., Chisholm, S.W., Devereux, R., and Stahl, D.A. (1990) Combination of 16S rRNA-targeted oligonucleotide probes with flow cytometry for analyzing mixed microbial populations. *Appl Environ Microbiol* **56**: 1919–1925.
- Amann, R.I., Ludwig, W., and Schleifer, K.H. (1995) Phylogenetic identification and *in situ* detection of individual microbial cells without cultivation. *Microbiol Rev* **59**: 143–169.
- Bazylinski, D.A., and Frankel, R.B. (2004) Magnetosome formation in prokaryotes. *Nat Rev Microbiol* **2**: 217–230.
- Bazylinski, D.A., Dean, A.J., Williams, T.J., Long, L.K., Middleton, S.L., and Dubbels, B.L. (2004) Chemolithoau-

- totrophy in the marine, magnetotactic bacterial strains MV-1 and MV-2. *Arch Microbiol* **182**: 373–387.
- Behrens, S., Rühlend, C., Inacio, J., Huber, H., Fonseca, A., Spencer-Martins, I., *et al.* (2003) *In situ* accessibility of small-subunit rRNA of members of the domains Bacteria, Archaea, and Eucarya to Cy3-labeled oligonucleotide probes. *Appl Environ Microbiol* **69**: 1748–1758.
- Brofft, J.E., McArthur, J.V., and Shimkets, L.J. (2002) Recovery of novel bacterial diversity from a forested wetland impacted by reject coal. *Environ Microbiol* **4**: 764–769.
- Cole, J.R., Wang, Q., Cardenas, E., Fish, J., Chai, B., Farris, R.J., *et al.* (2009) The Ribosomal Database Project: improved alignments and new tools for rRNA analysis. *Nucleic Acids Res* **37**: D141–D145.
- Daims, H., Bruhl, A., Amann, R., Schleifer, K.H., and Wagner, M. (1999) The domain-specific probe EUB338 is insufficient for the detection of all Bacteria: development and evaluation of a more comprehensive probe set. *Syst Appl Microbiol* **22**: 434–444.
- Derakshani, M., Lukow, T., and Liesack, W. (2001) Novel bacterial lineages at the (sub)division level as detected by signature nucleotide-targeted recovery of 16S rRNA genes from bulk soil and rice roots of flooded rice microcosms. *Appl Environ Microbiol* **67**: 623–631.
- Elshahed, M.S., Youssef, N.H., Luo, Q., Najar, F.Z., Roe, B.A., Sisk, T.M., *et al.* (2007) Phylogenetic and metabolic diversity of *Planctomycetes* from anaerobic, sulfide- and sulfur-rich Zodletone Spring, Oklahoma. *Appl Environ Microbiol* **73**: 4707–4716.
- Esquivel, D.M.S., Lins de Barros, H.G.P., Farina, M., Aragaõ, P.H.A., and Danon, J. (1983) Microorganismes magnétotactiques de la region de Rio de Janeiro. *Biol Cell* **47**: 227–234.
- Faivre, D., and Schüler, D. (2008) Magnetotactic bacteria and magnetosomes. *Chem Rev* **108**: 4875–4898.
- Flies, C.B., Peplies, J., and Schüler, D. (2005a) Combined approach for characterization of uncultivated magnetotactic bacteria from various aquatic environments. *Appl Environ Microbiol* **71**: 2723–2731.
- Flies, C.B., Jonkers, H.M., de Beer, D., Bosselmann, K., Böttcher, M.E., and Schüler, D. (2005b) Diversity and vertical distribution of magnetotactic bacteria along chemical gradients in freshwater microcosms. *FEMS Microbiol Ecol* **52**: 185–195.
- Frankel, R.B., Bazylinski, D.A., Johnson, M.S., and Taylor, B.L. (1997) Magneto-aerotaxis in marine coccoid bacteria. *Biophys J* **73**: 994–1000.
- Fukuda, Y., Okamura, Y., Takeyama, H., and Matsunaga, T. (2006) Dynamic analysis of a genomic island in *Magnetospirillum* sp. strain AMB-1 reveals how magnetosome synthesis developed. *FEBS Lett* **580**: 801–812.
- Glöckner, J., Kube, M., Shrestha, P.M., Weber, M., Glöckner, F.O., Reinhardt, R., and Liesack, W. (2010) Phylogenetic diversity and metagenomics of candidate division OP3. *Environ Microbiol* **12**: 1218–1229.
- Grünberg, K., Wawer, C., Tebo, B.M., and Schüler, D. (2001) A large gene cluster encoding several magnetosome proteins is conserved in different species of magnetotactic bacteria. *Appl Environ Microbiol* **67**: 4573–4582.
- Grünberg, K., Müller, E.C., Otto, A., Reszka, R., Linder, D., Kube, M., *et al.* (2004) Biochemical and proteomic analysis of the magnetosome membrane in *Magnetospirillum gryphiswaldense*. *Appl Environ Microbiol* **70**: 1040–1050.
- de la Haba, R.R., Marquez, M.D., Papke, R.T., and Ventosa, A. (2011) Multilocus sequence analysis (MLSA) of the family *Halomonadaceae*. *Int J Syst Evol Microbiol* (Epub ahead of print).
- Heimbrook, M.E., Wang, W.L., and Campbell, G. (1989) Staining bacterial flagella easily. *J Clin Microbiol* **27**: 2612–2615.
- Huang, X.L., Chen, J.Y., Zhou, S.N., Xie, L.C., and Fu, C.S. (2010) Prokaryote diversity in water environment of land-ocean ecotone of Zhuhai City. *Ying Yong Sheng Tai Xue Bao* **21**: 452–457.
- Huber, T., Faulkner, G., and Hugenholtz, P. (2004) Bellerophon: a program to detect chimeric sequences in multiple sequence alignments. *Bioinformatics* **20**: 2317–2319.
- Hugenholtz, P., Pituille, C., Hershberger, K.L., and Pace, N.R. (1998) Novel division level bacterial diversity in a Yellowstone hot spring. *J Bacteriol* **180**: 366–376.
- Hutchinson, C.A., 3rd, and Venter, J.C. (2006) Single-cell genomics. *Nat Biotechnol* **24**: 657–658.
- Isenbarger, T.A., Finney, M., Rios-Velazquez, C., Handelsman, J., and Ruvkun, G. (2008) Miniprimer PCR, a new lens for viewing the microbial world. *Appl Environ Microbiol* **74**: 840–849.
- Jogler, C., and Schüler, D. (2009) Genomics, genetics, and cell biology of magnetosome formation. *Annu Rev Microbiol* **63**: 501–521.
- Jogler, C., Kube, M., Schübbe, S., Ullrich, S., Teeling, H., Bazylinski, D.A., *et al.* (2009a) Comparative analysis of magnetosome gene clusters in magnetotactic bacteria provides further evidence for horizontal gene transfer. *Environ Microbiol* **11**: 1267–1277.
- Jogler, C., Lin, W., Meyerdieks, A., Kube, M., Katzmann, E., Flies, C., *et al.* (2009b) Toward cloning of the magnetotactic metagenome: identification of magnetosome island gene clusters in uncultivated magnetotactic bacteria from different aquatic sediments. *Appl Environ Microbiol* **75**: 3972–3979.
- Jogler, C., Niebler, M., Lin, W., Kube, M., Wanner, G., Kolinko, S., *et al.* (2010) Cultivation-independent characterization of ‘*Candidatus Magnetobacterium bavaricum*’ via ultrastructural, geochemical, ecological and metagenomic methods. *Environ Microbiol* **12**: 2466–2478.
- Jogler, C., Wanner, G., Kolinko, S., Niebler, M., Amann, R., Petersen, N., *et al.* (2011) Conservation of proteobacterial magnetosome genes and structures in an uncultivated member of the deep-branching Nitrospira phylum. *Proc Natl Acad Sci USA* **108**: 1134–1139.
- Katzmann, E., Scheffel, A., Gruska, M., Plietzko, J.M., and Schüler, D. (2010) Loss of the actin-like protein MamK has pleiotropic effects on magnetosome formation and chain assembly in *Magnetospirillum gryphiswaldense*. *Mol Microbiol* **77**: 208–224.
- Kawaguchi, R., Burgess, J.G., Sakaguchi, T., Takeyama, H., Thornhill, R.H., and Matsunaga, T. (1995) Phylogenetic analysis of a novel sulfate-reducing magnetic bacterium, RS-1, demonstrates its membership of the delta-Proteobacteria. *FEMS Microbiol Lett* **126**: 277–282.
- Lane, D.J. (1991) 16S/23S sequencing. In *Nucleic Acid Techniques in Bacterial Systematics*. Stackebrandt, E.,

- and Chichster, M.G. (eds). New York, USA: Wiley & Sons, pp. 115–175.
- Lefèvre, C.T., Abreu, F., Schmidt, M.L., Lins, U., Frankel, R.B., Hedlund, B.P., and Bazylinski, D.A. (2010) Moderately thermophilic magnetotactic bacteria from hot springs in Nevada. *Appl Environ Microbiol* **76**: 3740–3743.
- Lefèvre, C.T., Frankel, R.B., Posfai, M., Prozorov, T., and Bazylinski, D.A. (2011a) Isolation of obligately alkaliphilic magnetotactic bacteria from extremely alkaline environments. *Environ Microbiol* **13**: 2342–2350.
- Lefèvre, C.T., Vitoria, N., Schmidt, M.L., Posfai, M., Frankel, R.B., and Bazylinski, D.A. (2011b) Novel magnetite-producing magnetotactic bacteria belonging to the Gammaproteobacteria. *ISME J* (Epub ahead of print).
- Lefèvre, C.T., Frankel, R.B., Abreu, F., Lins, U., and Bazylinski, D.A. (2011c) Culture-independent characterization of a novel, uncultivated magnetotactic member of the *Nitrospirae* phylum. *Environ Microbiol* **13**: 538–549.
- Lehours, A.C., Evans, P., Bardot, C., Joblin, K., and Gerard, F. (2007) Phylogenetic diversity of archaea and bacteria in the anoxic zone of a meromictic lake (Lake Pavin, France). *Appl Environ Microbiol* **73**: 2016–2019.
- Li, T., and Wang, P. (2008) Bacterial and archaeal diversity in surface sediment from the south slope of the South China Sea. *Wei Sheng Wu Xue Bao* **48**: 323–329.
- Liesack, W., and Finster, K. (1994) Phylogenetic analysis of five strains of Gram-negative, obligately anaerobic, sulfur-reducing bacteria: Description of *Desulfuromoea* gen. nov., including the species *D. kysingii* sp. nov., *D. bakii* sp. nov. and *D. succinoxidans* sp. nov. *Int J Syst Bacteriol* **44**: 753–758.
- Lin, W., Li, J., Schüller, D., Jogler, C., and Pan, Y. (2009) Diversity analysis of magnetotactic bacteria in Lake Miyun, northern China, by restriction fragment length polymorphism. *Syst Appl Microbiol* **32**: 342–350.
- Lin, W., Jogler, C., Schüller, D., and Pan, Y. (2011) Metagenomic analysis reveals unexpected subgenomic diversity of magnetotactic bacteria within the phylum Nitrospirae. *Appl Environ Microbiol* **77**: 323–326.
- Loy, A., Arnold, R., Tischler, P., Rattei, T., Wagner, M., and Horn, M. (2008) probeCheck – a central resource for evaluating oligonucleotide probe coverage and specificity. *Environ Microbiol* **10**: 2894–2898.
- Ludwig, W. (2010) Molecular Phylogeny of Microorganisms: is rRNA Still a Useful Marker? *Molecular Phylogeny of Microorganisms*. Oren, A., and Papke, R.T. (eds). Norfolk: Caister Academic Press, pp. 65–84.
- Ludwig, W., and Schleifer, K.H. (1994) Bacterial phylogeny based on 16S and 23S rRNA sequence analysis. *FEMS Microbiol Rev* **15**: 155–173.
- Ludwig, W., Strunk, O., Westram, R., Richter, L., Meier, H., Yadukumar, et al. (2004) ARB: a software environment for sequence data. *Nucleic Acids Res* **32**: 1363–1371.
- Macalady, J.L., Dattagupta, S., Schaperdoth, I., Jones, D.S., Druschel, G.K., and Eastman, D. (2008) Niche differentiation among sulfur-oxidizing bacterial populations in cave waters. *ISME J* **2**: 590–601.
- Madrid, V.M., Taylor, G.T., Scranton, M.I., and Chistoserdov, A.Y. (2001) Phylogenetic diversity of bacterial and archaeal communities in the anoxic zone of the Cariaco Basin. *Appl Environ Microbiol* **67**: 1663–1674.
- Murat, D., Quinlan, A., Vali, H., and Komeili, A. (2010) Comprehensive genetic dissection of the magnetosome gene island reveals the step-wise assembly of a prokaryotic organelle. *Proc Natl Acad Sci USA* **107**: 5593–5598.
- Pernthaler, J., Glöckner, F.O., Schönhuber, W., and Amann, R. (2001) Fluorescence *in situ* hybridization (FISH) with rRNA-targeted oligonucleotide probes.
- Pilhofer, M., Rappl, K., Eckl, C., Bauer, A.P., Ludwig, W., Schleifer, K.H., and Petroni, G. (2008) Characterization and evolution of cell division and cell wall synthesis genes in the bacterial phyla *Verrucomicrobia*, *Lentisphaerae*, *Chlamydiae*, and *Planctomycetes* and phylogenetic comparison with rRNA genes. *J Bacteriol* **190**: 3192–3202.
- Pruesse, E., Quast, C., Knittel, K., Fuchs, B.M., Ludwig, W., Peplies, J., and Glöckner, F.O. (2007) SILVA: a comprehensive online resource for quality checked and aligned ribosomal RNA sequence data compatible with ARB. *Nucleic Acids Res* **35**: 7188–7196.
- Richter, M., Kube, M., Bazylinski, D.A., Lombardot, T., Glockner, F.O., Reinhardt, R., and Schüller, D. (2007) Comparative genome analysis of four magnetotactic bacteria reveals a complex set of group-specific genes implicated in magnetosome biomineralization and function. *J Bacteriol* **189**: 4899–4910.
- Röling, W.F., van Breukelen, B.M., Braster, M., Lin, B., and van Verseveld, H.W. (2001) Relationships between microbial community structure and hydrochemistry in a landfill leachate-polluted aquifer. *Appl Environ Microbiol* **67**: 4619–4629.
- Ryu, E. (1937) A simple method of staining bacterial flagella. *Kitasato Arch Exp Med* **14**: 218–219.
- Sakaguchi, T., Arakaki, A., and Matsunaga, T. (2002) *Desulfovibrio magneticus* sp. nov., a novel sulfate-reducing bacterium that produces intracellular single-domain-sized magnetite particles. *Int J Syst Evol Microbiol* **52**: 215–221.
- Schink, B. (1985) Fermentation of acetylene by an obligate anaerobe, *Pelobacter acetylenicus* sp. nov. *Arch Microbiol* **142**: 295–301.
- Schleifer, K.H., Schüller, D., Spring, S., Weizenegger, M., Amann, R., Ludwig, W., and Köhler, M. (1991) The genus *Magnetospirillum* gen. nov., description of *Magnetospirillum gryphiswaldense* sp. nov. and transfer of *Aquaspirillum magnetotacticum* to *Magnetospirillum magnetotacticum* comb. nov. *Syst Appl Microbiol* **14**: 379–385.
- Schübbe, S., Kube, M., Scheffel, A., Wawer, C., Heyen, U., Meyerdierks, A., et al. (2003) Characterization of a spontaneous nonmagnetic mutant of *Magnetospirillum gryphiswaldense* reveals a large deletion comprising a putative magnetosome island. *J Bacteriol* **185**: 5779–5790.
- Schüller, D. (1994) Isolierung und Charakterisierung magnetischer Bakterien – Untersuchungen zur Magnetitbiomineralisation in *Magnetospirillum gryphiswaldense*. Munich.
- Schüller, D., and Bazylinski, D.A. (2007) Techniques for studying uncultured and cultured magnetotactic bacteria. In *Manual of Environmental Microbiology*. Hurst, C.J., Crawford, R.L., Garland, J.L., Lipson, D.A., Mills, A.L., and Setzenbach, L.D. (eds). Washington DC, USA: ASM Press, pp. 1129–1138.
- Schüller, D., Spring, S., and Bazylinski, D.A. (1999) Improved technique for the isolation of magnetotactic spirilla from a

- freshwater sediment and their phylogenetic characterization. *Syst Appl Microbiol* **22**: 466–471.
- Spring, S., Amann, R., Ludwig, W., Schleifer, K.H., van Gemerden, H., and Petersen, N. (1993) Dominating role of an unusual magnetotactic bacterium in the microaerobic zone of a freshwater sediment. *Appl Environ Microbiol* **59**: 2397–2403.
- Spring, S., Amann, R., Schleifer, K.H., Schüller, D., Poralla, K., and Petersen, N. (1994) Phylogenetic analysis of uncultured magnetotactic bacteria from the alpha-subclass of *Proteobacteria*. *Syst Appl Microbiol* **17**: 501–508.
- Stamatakis, A. (2006) RAxML-VI-HPC: maximum likelihood-based phylogenetic analyses with thousands of taxa and mixed models. *Bioinformatics* **22**: 2688–2690.
- Teske, A., Hinrichs, K.U., Edgcomb, V., de Vera Gomez, A., Kysela, D., Sylva, S.P., *et al.* (2002) Microbial diversity of hydrothermal sediments in the Guaymas Basin: evidence for anaerobic methanotrophic communities. *Appl Environ Microbiol* **68**: 1994–2007.
- Ullrich, S., Kube, M., Schübbe, S., Reinhardt, R., and Schüller, D. (2005) A hypervariable 130-kilobase genomic region of *Magnetospirillum gryphiswaldense* comprises a magnetosome island which undergoes frequent rearrangements during stationary growth. *J Bacteriol* **187**: 7176–7184.
- Vali, H., and Kirschvink, J.L. (1991) Observations of magnetosome organization, surface structure, and iron biomineralization of undescribed magnetic bacteria. In *Iron Biominerals*. Frankel, R.B., and Blakemore, R.P. (eds). New York and London: Plenum Press, pp. 97–116.
- Van Camp, G., Chapelle, S., and De Wachter, R. (1993) Amplification and sequencing of variable regions in bacterial 23S ribosomal RNA genes with conserved primer sequences. *Curr Microbiol* **27**: 147–151.
- Wagner, M., and Horn, M. (2006) The *Planctomycetes*, *Verrucomicrobia*, *Chlamydiae* and sister phyla comprise a superphylum with biotechnological and medical relevance. *Curr Opin Biotechnol* **17**: 241–249.
- Wenter, R., Wanner, G., Schüller, D., and Overmann, J. (2009) Ultrastructure, tactic behaviour and potential for sulfate reduction of a novel multicellular magnetotactic prokaryote from North Sea sediments. *Environ Microbiol* **11**: 1493–1505.
- Wolfe, R.S., Thauer, R.K., and Pfennig, N. (1987) A 'capillary racetrack' method for isolation of magnetotactic bacteria. *FEMS Microbiol Ecol* **45**: 31–35.

Supporting information

Additional Supporting Information may be found in the online version of this article:

Fig. S1. Schematic representation of the strategy that was used for phylogenetic and ultrastructural analysis of the low abundant MTB SKK-01. By two-step magnetic collection from a sediment microcosm (A), a highly purified sample was obtained containing a mixture of various MTB (B). Micrograph of a single microsorted SKK-01 cell in a glass capillary (gc) under microscopic control (C). Genomic DNA of microsorted cells was amplified using the viral Φ 29 DNA-polymerase by MDA. Amplified DNA served as template for 16S rRNA PCR for subsequent phylogenetic analysis (D) and deduction of a specific probe for phylo-staining of SKK-01 by FISH cells among diverse magnetically collected MTB (E). To correlate phylogeny and morphology, individual epifluorescence-marked and unmarked cells were sorted onto finder grids via micromanipulation (F), allowing ultrastructural analysis by electron microscopy (G).

Fig. S2. Schematic map of primer binding sites within the SKK-01 23S rRNA gene. Binding positions and orientations are indicated by arrows.

Fig. S3. Fluorescence *in situ* hybridization (FISH) of magnetically collected MTB with the SKK-01 specific oligonucleotide probe MO401. A. Fluorescence of a 4',6-diaminodino-2-phenylindole (DAPI) stained magnetically collected cells from Lake Chiemsee sediments. B. Epifluorescence of the fluorescein isothiocyanate (FITC) labelled with the oligonucleotide probe *Mbavp*. Only cells of *Mbav* are fluorescent, whereas SKK-01 cells are not recognized. C. Epifluorescence of the Cy3-labelled probe MO401. All cells of SKK-01 hybridized with the specific probe MO401 whereas the accompanying cells were not stained.

Movie S1. Movement of a SKK-01 cell among other MTB in a horizontal magnetic field of reversing direction. Cells were observed in a hanging drop at 400 × magnification by phase contrast microscopy.

Movie S2. Microsorting of SKK-01 cells from a mixture of magnetically collected MTB. Details are indicated in the movie and explained in the text.

Please note: Wiley-Blackwell are not responsible for the content or functionality of any supporting materials supplied by the authors. Any queries (other than missing material) should be directed to the corresponding author for the article.

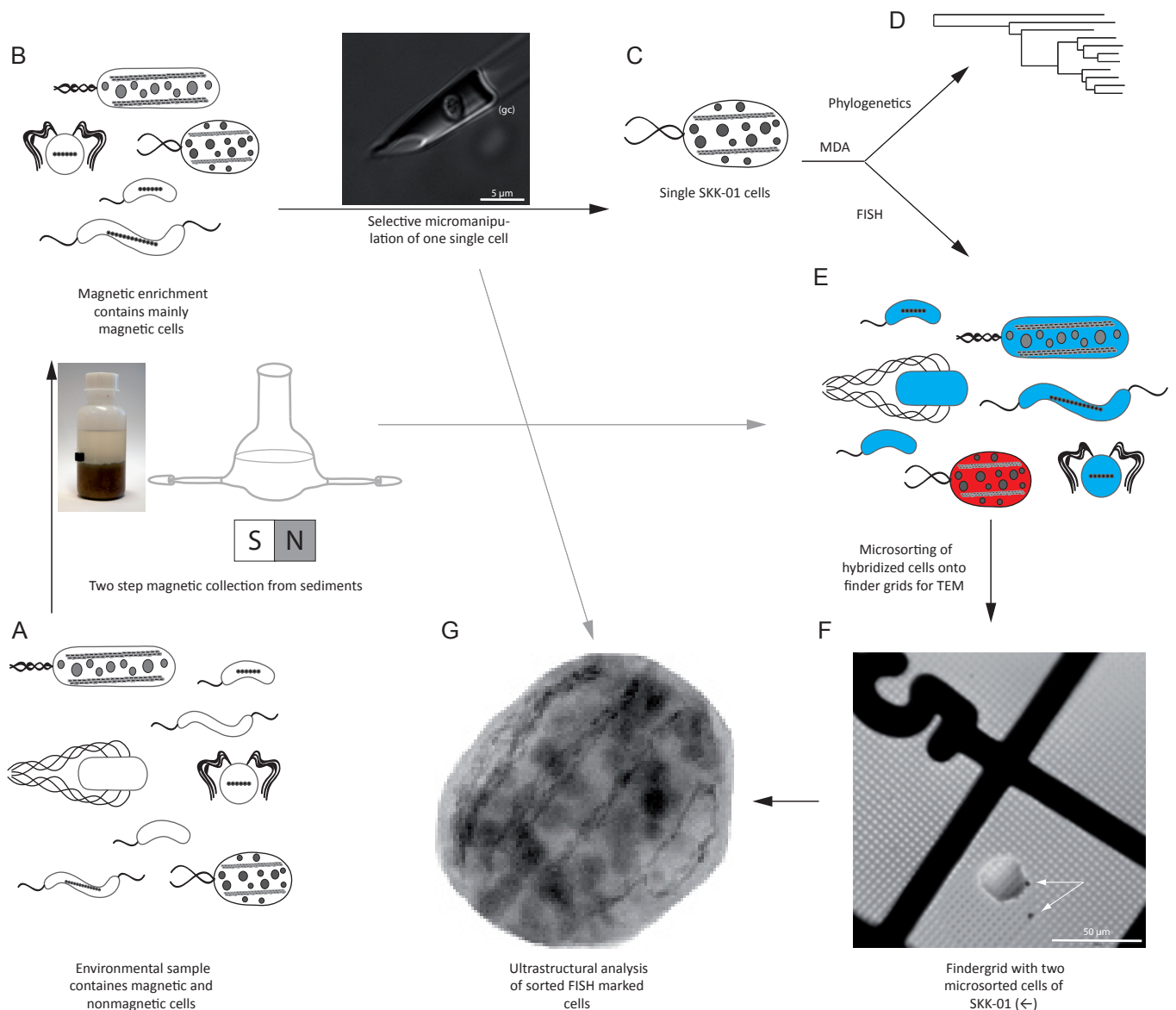


Fig. S1. Schematic representation of the strategy that was used for phylogenetic and ultrastructural analysis of the low abundant MTB SKK-01. By two-step magnetic collection from a sediment microcosm (A), a highly purified sample was obtained containing a mixture of various MTB (B). Micrograph of a single microsorted SKK-01 cell in a glass capillary (gc) under microscopic control (C). Genomic DNA of microsorted cells was amplified using the viral Φ 29 DNA-polymerase by MDA. Amplified DNA served as template for 16S rRNA PCR for subsequent phylogenetic analysis (D) and deduction of a specific probe for phylo-staining of SKK-01 by FISH cells among diverse magnetically collected MTB (E). To correlate phylogeny and morphology, individual epifluorescence-marked and unmarked cells were sorted onto finder grids via micromanipulation (F), allowing ultrastructural analysis by electron microscopy (G).

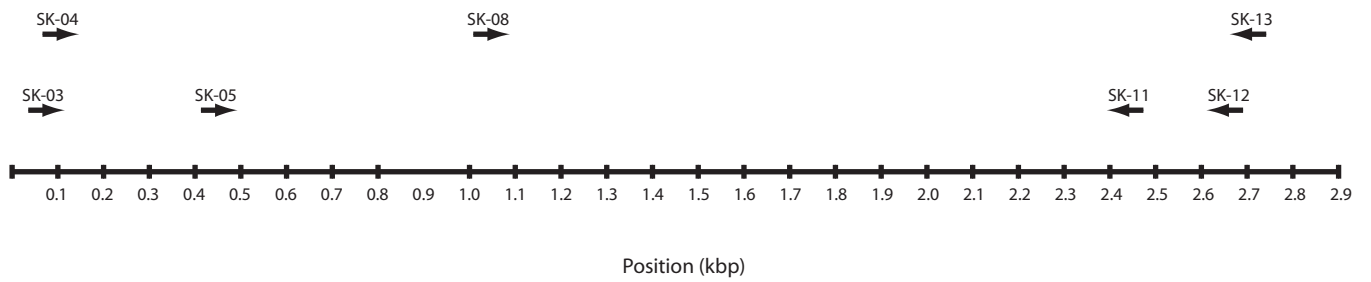


Fig. S2. Schematic map of primer binding sites within the SKK-01 23S rRNA gene. Binding positions and orientations are indicated by arrows.

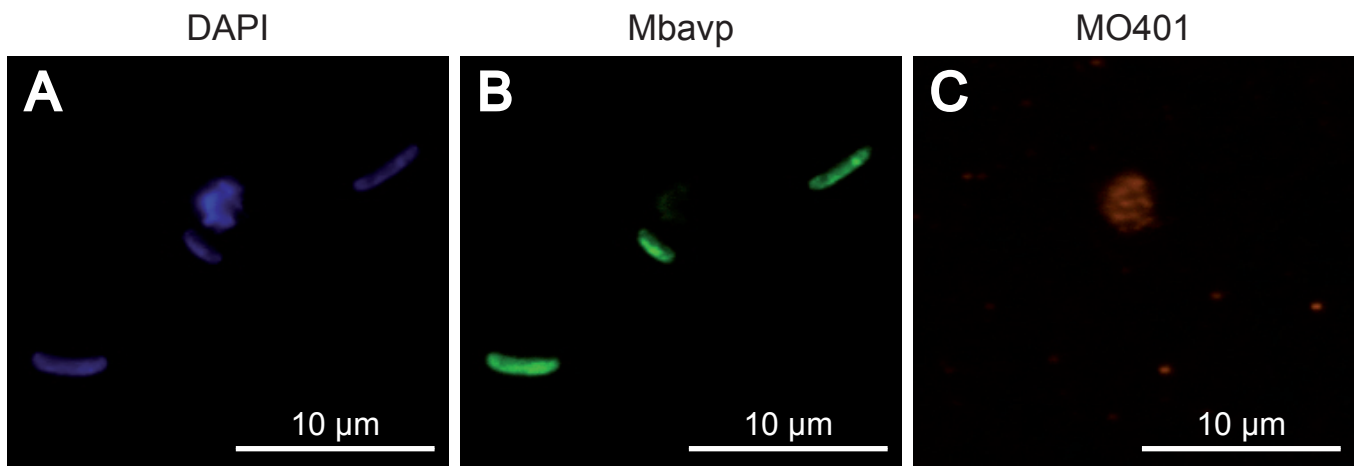


Fig. S3. Fluorescence in situ hybridization (FISH) of magnetically collected MTB with the SKK-01 specific oligonucleotide probe MO401. A. Fluorescence of a 4',6-diaminodino-2-phenylindole (DAPI) stained magnetically collected cells from Lake Chiemsee sediments. B. Epifluorescence of the fluorescein isothiocyanate (FITC) labelled with the oligonucleotide probe Mbavp. Only cells of Mbav are fluorescent, whereas SKK-01 cells are not recognized. C. Epifluorescence of the Cy3-labelled probe MO401. All cells of SKK-01 hybridized with the specific probe MO401 whereas the accompanying cells were not stained.

3. Manuskript:

Single-cell genomics reveals potential for magnetite and greigite biomineralization in an uncultivated multicellular magnetotactic prokaryote.

Single-cell genomics reveals potential for magnetite and greigite biomineralization in an uncultivated multicellular magnetotactic prokaryote

Sebastian Kolinko,^{1*} Michael Richter,²
Frank-Oliver Glöckner,^{2,3} Andreas Brachmann¹ and
Dirk Schüler^{1,4**}

¹Ludwig-Maximilians-Universität Munich, Microbiology,
Großhaderner Str. 2-4, 82152 Planegg-Martinsried,
Germany.

²Microbial Genomics and Bioinformatics Research
Group, Max Planck Institute for Marine Microbiology,
Bremen, Germany.

³Jacobs University Bremen, Bremen, Germany.

⁴Department of Microbiology, University Bayreuth,
Bayreuth, Germany.

Summary

For magnetic orientation, magnetotactic bacteria biosynthesize magnetosomes, which consist of membrane-enveloped magnetic nanocrystals of either magnetite (Fe₃O₄) or greigite (Fe₃S₄). While magnetite formation is increasingly well understood, much less is known about the genetic control of greigite biomineralization. Recently, two related yet distinct sets of magnetosome genes were discovered in a cultivated magnetotactic deltaproteobacterium capable of synthesizing either magnetite or greigite, or both minerals. This led to the conclusion that greigite and magnetite magnetosomes are synthesized by separate biomineralization pathways. Although magnetosomes of both mineral types co-occurred in uncultured multicellular magnetotactic prokaryotes (MMPs), so far only one type of magnetosome genes could be identified in the available genome data. The MMP *Candidatus Magnetomorum* strain HK-1 from coastal tidal sand flats of the North Sea (Germany) was analysed by a targeted single-cell approach. The draft genome assembly resulted in a size of 14.3 Mb and an estimated completeness of 95%. In addition to genomic features consistent with a sulfate-reducing lifestyle, we identified numerous genes putatively involved in magnetosome biosynthesis. Remarkably, most *mam*

orthologues were present in two paralogous copies with highest similarity to either magnetite or greigite type magnetosome genes, supporting the ability to synthesize magnetite and greigite magnetosomes.

Introduction

Magnetotactic bacteria (MTB) biosynthesize magnetosomes, which serve as geomagnetic field sensors that facilitate the cells' search for optimum growth conditions within chemical gradients in their stratified aquatic habitats (Frankel *et al.*, 1997; Bazylinski and Frankel, 2004). Magnetotactic bacteria display a great morphological and phylogenetic diversity, and have been found within the alpha, gamma and delta lineages of the *Proteobacteria*, as well as in the deep-branching phyla *Nitrospirae* and *Omnitrophica* (Kolinko *et al.*, 2012; Lefèvre and Bazylinski, 2013). Magnetosome particles biosynthesized by various MTB also display a large variability with respect to crystal morphologies, including hexa- and cubooctahedral, elongated-prismatic, and bullet shapes (Bazylinski and Frankel, 2004; Jogler and Schüler, 2009). Depending on the species, the ferromagnetic crystals were found to consist either of the magnetic minerals magnetite (Fe₃O₄) or greigite (Fe₃S₄) (Bazylinski and Frankel, 2004; Jogler and Schüler, 2009). Genes controlling the biosynthesis of magnetite magnetosomes have been first identified in the Alphaproteobacterium *Magnetospirillum gryphiswaldense* (Grünberg *et al.*, 2001) and its close relatives, in which they are involved in vesicle formation, iron transport and crystallization, redox control, and magnetosome alignment (Jogler and Schüler, 2009; Lefèvre and Bazylinski, 2013).

In *M. gryphiswaldense*, the > 30 magnetosome genes are clustered mostly in several operons within a large genomic magnetosome island (MAI) (Schübbe *et al.*, 2003; Ullrich *et al.*, 2005; Richter *et al.*, 2007; Lefèvre *et al.*, 2013a). Similar MAI-like clusters were found in all other known magnetite forming MTB in the alpha, gamma and delta lineages of the *Proteobacteria* (Ullrich *et al.*, 2005; Nakazawa *et al.*, 2009; Lefèvre *et al.*, 2012), as well as in uncultivated MTB from the deep-branching phylum *Nitrospirae* (Jogler *et al.*, 2011).

In some uncultivated MTB, magnetite and greigite magnetosome crystals were found to co-occur within the

Received 17 June, 2014; accepted 25 July, 2014. For correspondence. *E-mail Sebastian.Kolinko@gmx.de; Tel. (+49) 8921 8074 504. **E-mail dirk.schueler@uni-bayreuth.de; Tel. (+49) 0 921/55 2728; Fax +(49) 0 921/55 2727.

same cell, which suggested that the formation of both magnetosome types is controlled by separate biomineralization processes (Bazylnski *et al.*, 1995). Later, it was observed that the cultivated deltaproteobacterium *Candidatus Desulfamplus magnetomortis* BW-1 in highly reducing growth conditions (i.e. in the presence of 0.3 mM sulfide) biomineralized mostly greigite magnetosomes, whereas under more oxidizing conditions predominantly magnetite magnetosomes were synthesized (Lefèvre *et al.*, 2011a; 2013a). In the same study, it was also found that most magnetosome genes in BW-1 are present in two divergent copies and form two separate clusters. This suggested that one set of genes may be responsible for the biomineralization of magnetite magnetosomes, whereas the second set may control greigite magnetosome production and that the two gene sets might be regulated differentially (Lefèvre *et al.*, 2011a). However, the homology between the two sets of genes also implied that biomineralization of magnetite and greigite magnetosomes did not evolve independently, and not polyphyletic as speculated earlier (Delong *et al.*, 1993; Abreu *et al.*, 2011; Lefèvre *et al.*, 2013a).

One of the most intriguing morphologies among the MTB is represented by uncultivated multicellular magnetotactic prokaryotes (MMPs), which were first discovered in a brackish lagoon near Rio de Janeiro City (Brazil) (Esquivel *et al.*, 1983; Farina *et al.*, 1983) and later found to inhabit various marine coastal environments worldwide (Keim *et al.*, 2004; 2007; Wenter *et al.*, 2009; Zhou *et al.*, 2011; Zhang *et al.*, 2014). Multicellular magnetotactic prokaryotes are large (3–12 µm) aggregates of 10–40 genetically identical cells that are arranged around an acellular internal compartment. All MMPs were found affiliated with the *Deltaproteobacteria* and have a putatively sulfate-reducing metabolism (Wenter *et al.*, 2009; Abreu *et al.*, 2014). In early studies, greigite magnetosomes were only discovered in cells of MMPs, each forming clusters of cubical to rectangular crystals (Amann *et al.*, 1990; Farina *et al.*, 1990; Pósfai *et al.*, 1998) or several parallel chains of bullet-shaped magnetosomes (Wenter *et al.*, 2009; Zhou *et al.*, 2011). A single magnetosome gene cluster comprising 10 putative *mam* genes was identified in magnetically collected cells that were highly enriched in the greigite-producing MMP *Candidatus Magnetoglobus multicellularis* (Abreu *et al.*, 2011). Identified genes were most closely related to the greigite gene cluster in BW-1 and remotely related to gene clusters of magnetite-producing MTB, leading to the conclusion that these genes are responsible for greigite biomineralization (Abreu *et al.*, 2011; Lefèvre *et al.*, 2011a). However, MMPs from Itaipu Lagoon (Brazil) and the coastal lagoon Lake Yuehu (China) were previously shown to form magnetite magnetosomes as well, either exclusively or together with greigite magnetosomes in

individual cells (Keim *et al.*, 2007; Zhou *et al.*, 2011). This co-occurrence of magnetite and greigite crystals in MMPs raised the question whether they also may contain two separate sets of genes independently controlling the biosynthesis of either magnetite or greigite magnetosomes. Yet, besides its single greigite-type gene cluster, no genes with close similarity to known magnetite genes of other MTB were identified in the nearly complete draft genome of MMP *Ca. M. multicellularis* (Abreu *et al.*, 2011; 2014; Lefèvre *et al.*, 2013a).

Here we report the discovery of two divergent magnetosome gene clusters in uncultivated marine MMPs from a coastal tidal mud flat of the North Sea, Germany. Targeted genomic analysis of four single MMP aggregates by magnetic collection followed by micromanipulation identified two divergent *mamAB*-like operons. The first gene cluster comprises genes similar to greigite magnetosome genes in *Ca. M. multicellularis*, whereas the second comprises genes most closely related to magnetite magnetosome genes in the deltaproteobacterium BW-1. Both clusters in addition contain several *mad* genes, which were recently identified in other MTB from the *Deltaproteobacteria* (Lefèvre *et al.*, 2013a).

Results and discussion

Sandy sediment cores collected at low tide from an intertidal flat in the German Wadden Sea near Cuxhaven (53°53'32"N, 8°40'45"E) in August 2010 contained MMPs morphologically virtually identical to *Candidatus Magnetomorphum litorale*, which was identified recently from the same sampling site (Wenter *et al.*, 2009). After magnetic enrichment, as described in Wenter and colleagues (2009), 12 living MMPs were concentrated in 20 µl sterile liquid, and could be easily identified among other MTB by their conspicuous shape, large size and characteristic 'ping-pong' motion (Rodgers *et al.*, 1990). MMPs were individually sorted by micromanipulation for subsequent whole genome amplification (WGA) as previously described (Kolinko *et al.*, 2012). Four WGA reactions were set up, each from one MMP aggregate comprising 20–30 cells, resulting in four single amplified genomes (SAGs). Polymerase chain reaction amplification of a small-subunit rRNA gene yielded a single product from each SAG, indicating clonality and the absence of contaminations. The low natural abundance of MMPs in our samples prevented any extensive ultrastructural and chemical analysis of the magnetosome crystals.

All 16S rRNA genes were identical to each other and had the highest identity (96.8%) to *Ca. M. litorale* clone MMP, the greigite-synthesizing MMP identified previously from the same sampling site (Simmons *et al.*, 2007; Wenter *et al.*, 2009), followed by 99.3% identity to

Candidatus Magnetomorum sp. 1–7, an uncultivated spherical MMP producing both magnetite and greigite magnetosomes (Zhang *et al.*, 2014). This sequence divergence to MMPs previously sampled from the same site indicates some genetic variability or heterogeneity of local MMP populations possibly even beyond the species level, despite the morphological identity to *Ca. M. litorale* described by Wenter and colleagues (2009). In the following, we refer to the MMP analysed in this study as *Candidatus Magnetomorum* strain HK-1.

For Illumina MiSeq sequencing, shotgun libraries were constructed from individual SAGs with the Nextera DNA Sample Preparation Kit (Illumina) according to the instructions of the manufacturer. Digital normalization of sequencing data was performed as previously described (Swan *et al.*, 2011) to reduce WGA-based amplification bias prior to *de novo* assembly by the SPAdes Genome Assembler (Bankevich *et al.*, 2012). Obtained *de novo* assemblies were validated by BLAST (Altschul *et al.*, 1997) and single copy marker gene analysis (Rinke *et al.*, 2013). Draft SAGs had sizes of 6, 10, 11 and 10 Mb with genome completeness of 60, 57, 45 and 60%, respectively, which were estimated by the presence or absence of 139 bacterial single copy marker genes (Rinke *et al.*, 2013). In contrast to the observed minor variation in genome completeness between individual SAGs, marker gene distribution showed a high diversity (not shown), indicating that different regions of the genome were covered by the individual SAGs. Combining sequencing reads of the four SAGs (> 97% nucleotide identity) further improved *de novo* assemblies significantly, as shown by an increased N50-value of 18.2 kb. Overall, this resulted in a combined draft genome with a size of 14.3 Mb and an estimated genome completeness of 95%.

Several general genomic features of HK-1 substantiate the suggested sulfate-reducing lifestyle of *Ca. Magnetomorum* (Wenter *et al.*, 2009). For instance, we detected full-length genes homologous to *dsrA* (dissimilatory sulfate reductase subunit alpha), *dsrB* (dissimilatory sulfate reductase subunit beta) and *aprA* (APS reductase) of *Ca. M. multicellularis*, (Abreu *et al.*, 2014). We identified 22 *mam* genes in the draft genome of HK-1 encoding proteins, which displayed variable degrees of amino acid (aa) similarity 43–80% to magnetosome genes from *Ca. M. multicellularis* and *Ca. D. magnetomortis* (Table 1). Remarkably, most orthologues were present in two paralogous copies, which appeared to form two separate clusters and were less similar to each other than to *mam* genes of distinct MTB (Table 2). A partial *mamAB*-like operon termed *cluster 1* was identified on a single contig (4.3 kb) with homologues to the known magnetosome genes *mamE***I***MB***Q***A***B***P1** and *mad14* (Fig. 1). Genes were most similar (71 ± 9% aa similarity) (Table 1) to genes putatively involved in greigite magnetosome

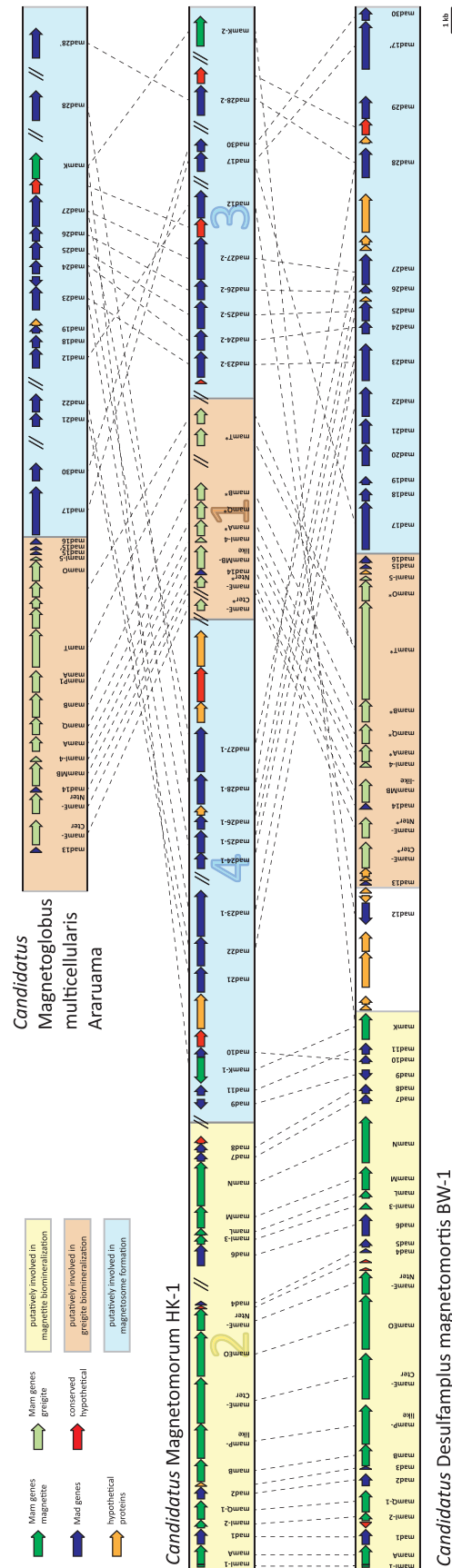


Fig. 1. Molecular organization of identified magnetosome genes in *Ca. Magnetomorum* strain HK-1 compared with the greigite-producing MTB *Ca. Desulfamplus magnetomortis* strain BW-1 and *Ca. Magnetoglobus multicellularis* strain Araruama (Lefevre and Bazylinski, 2013; Lefevre *et al.*, 2013a). Bars between clusters indicate homologous genes. *MamAB*-like operons putatively involved in greigite biomineralization are indicated by orange, *mamAB*-like operons putatively involved in magnetite production are indicated by yellow, and gene cluster putatively involved in general magnetosome biosynthesis are highlighted in blue.

Table 1. Comparison of known Mam and Mad proteins identified in the draft genome of *Ca. Magnetomorum* strain HK-1 with those of all MTB.

Putative protein	Accession number	Magnetotactic bacterium with protein with highest sequence identity ^a	Accession number	Identity (%)	E-value	Magnetotactic bacterium with second highest sequence identity ^a	Accession number	Identity (%)	E-value	Magnetotactic bacterium with third highest sequence identity [#]	Accession number	Identity (%)	E-value
MamE-Nter*, partial	HK1_001784	MMP	ADV17396	79.87	6.12E-84	BW-1	CCO06706	70.59	7.41E-66	MMP (mamO*)	ADV17386	51.66	9.65E-43
Mad14	HK1_001785	BW-1	CCO06707	34.57	2.06E-06								
MamMB*	HK1_001786	MMP	ADV17395	58.68	1.88E-130	BW-1	CCO06708	51.03	1.45E-91				
MamI-4*	HK1_001787	BW-1	CCO06709	71.19	2.72E-10								
MamA*	HK1_001788	MMP	ADV17394	73.00	1.71E-104	BW-1	CCO06710	49.25	1.56E-74	LM-1	AEX00088	26.79	1.71E-20
MamQ*	HK1_001789	MMP	ADV17393	73.89	5.51E-110	BW-1	CCO06711	52.99	2.62E-72				
MamB*	HK1_001790	MMP	ADV17392	79.75	2.05E-105	BW-1	CCO06712	67.36	7.08E-86	LM-1	AEX00091	37.83	6.03E-38
Magnetosome protein, similar to OMM13 of MMP	HK1_003129	MMP	ETR64738	64.93	1.25E-75	MMP	ETR64740	61.02	1.61E-53	BW-1	CCO06713	59.46	1.95E-50
mamE-Cter*, partial	HK1_006086	MMP	ETR64748	56.15	3.24E-64	BW-1	CCO06705	48.13	1.55E-51	BW-1	CCO06713	28.49	1.55E-51
MamT*	HK1_007740	MMP	ETR64741	60.39	1.98E-155	BW-1	CCO06713	44.03	5.78E-49				
MamI-3	HK1_003568	BW-1	CCO06685	42.20	7.32E-28	RS-1	YP_002955481	44.00	1.69E-08	FH-1	AGG16208	40.87	3.75E-08
MamI-1	HK1_000730	BW-1	CCO06668	77.78	5.23E-11	FH-1	AGG16237	51.35	4.13E-05				
MamA	HK1_000731	BW-1	AET24905	46.93	3.30E-71	ML-1	AFX88975	43.86	1.58E-66	FH-1	AGG1619	44.62	2.12E-59
Mad1	HK1_000732	BW-1	CCO06668	53.69	2.19E-63	RS-1	YP_002955492	48.76	2.08E-61	ML-1	AFZ77011	45.20	5.42E-48
MamI-2	HK1_000733	BW-1	AET24919	53.15	1.06E-32	RS-1	YP_002955491	49.55	3.49E-29	ML-1	AFZ77012	45.61	1.05E-19
MamQ	HK1_000734	BW-1	AET24916	42.81	2.08E-65	FH-1	AGG16199	43.73	1.22E-49	RS-1	AP_002955490	41.86	2.10E-43
Mad2	HK1_000735	BW-1	CCO06674	70.00	1.22E-77	RS-1	YP_002955489	66.67	2.01E-75	ML-1	AFZ77013	64.85	2.76E-73
MamB	HK1_000737	BW-1	CCO06676	63.14	9.78E-117	RS-1	YP_002955488	57.49	1.01E-112	FH-1	AGG16201	57.14	1.10E-112
MamP-like	HK1_000738	BW-1	AET24923	49.10	2.42E-136	ML-1	AFZ77015	40.24	1.67E-50	FH-1	AGG16202	44.53	6.41E-50
MamE-Cter	HK1_000739	BW-1	CCO06678	43.61	4.63E-165	ML-1	AFZ77017	41.63	7.90E-121	FH-1	AGG16203	42.92	3.14E-113
MamEO	HK1_000740	BW-1	CCO06679	47.74	8.12E-108	ML-1	AFZ77018	45.31	6.84E-63	FH-1	AGG16204	45.13	1.59E-61
MamE-Nter	HK1_000741	BW-1	CCO06680	50.49	4.74E-95	RS-1	YP_002955484	47.04	3.23E-75	ML-1	AFZ77020	46.18	5.12E-73
Mad4	HK1_000743	ML-1	AFZ77022	40.30	3.62E-20	RS-1	YP_002955500	40.19	2.34E-16	BW-1	CCO06682	54.55	3.02E-13
Mad8	HK1_003562	RS-1	YP_002955477	49.09	1.33E-22	FH-1	AGG16212	50.49	2.39E-22	ML-1	AFZ77028	50.53	3.25E-08
Mad7	HK1_003563	RS-1	YP_002955478	33.33	4.23E-09	FH-1	AGG16211	37.76	4.27E-09	BW-1	CCO06690	36.80	5.67E-09
MamN	HK1_003564	BW-1	CCO06688	45.25	2.47E-166	MV-1	CAV30813	37.59	1.17E-77	MSR-1	YP_008938249	33.48	2.27E-74
MamM	HK1_003565	BW-1	CCO06687	56.14	7.91E-110	RS-1	YP_002955479	38.10	2.43E-69	FH-1	ADD16210	38.23	6.33E-69
MamL	HK1_003566	BW-1	CCO06686	65.28	3.24E-27	RS-1	YP_002955480	54.95	1.36E-21	FH-1	AGG16209	52.75	4.31E-20
Mad6	HK1_003569	FH-1	AGG16207	52.67	5.10E-112	RS-1	YP_002955482	52.67	5.27E-112	ML-1	AFZ77023	51.42	2.56E-110

Mad28-2	HK1_003334	MMP	ETR69845	63.40	7.65E-166	RS-1	YP_002955461	50.91	3.87E-117	FH-1	AGG16228	50.91	8.80E-117
Mad24-1	HK1_005202	BW-1	CCO06724	26.90	2.14E-10	MMP	ETR64730	25.14	2.07E-08				
Mad25-1	HK1_005203	MMP	ETR70753	41.55	1.68E-43	BW-1	CCO06725	42.63	5.94E-38	MMP	ETR64729	34.58	5.32E-33
Mad26-1	HK1_005204												
Mad28-1	HK1_005206	MMP	AFX88998	49.10	2.34E-124	FH-1	AGG16228	46.30	2.10E-115	RS-1	YP_002955461	49.69	2.44E-115
Mad27-1	HK1_005207	MMP	ADV17377	48.67	3.71E-136	BW-1	CCO06728	48.43	4.23E-131	FH-1	AGG16231	45.59	7.88E-129
Mad23-1	HK1_005509	RS-1	YP_002955466	42.09	4.04E-90	BW-1	CCO06723	37.80	6.84E-79	MMP	ADV17381	43.10	3.97E-68
Mad22	HK1_005510	BW-1	CCO06722	22.64	4.03E-09	MMP	AFX88997	25.19	3.20E-06	ML-1	AFZ77036	19.63	1.16E-05
Mad21-1	HK1_005511	MMP	AFX88996	25.43	1.93E-08								
conserved hypothetical protein	HK1_005513	Mbav	FQ377626	31.10	1.52E-29								
Mad10	HK1_005514	RS-1	YP_002955470	37.72	3.90E-19	ML-1	AFZ77033	39.05	8.80E-18	BW-1	CCO06719	39.25	7.22E-17
MamK-1	HK1_005515	MMP	ETR64725	75.71	0.00E+00	ML-1	AFZ77032	65.92	4.08E-169	BW-1	CCO06694	64.45	7.86E-168
Mad11	HK1_005516	ML-1	AFZ77031	28.26	1.10E-08								
Mad9	HK1_005517	ML-1	AFZ77030	55.64	2.93E-49	BW-1	CCO06691	55.22	4.01E-47	RS-1	YP_002955475	57.89	4.53E-47
MamK-2	HK1_005096	MMP	ETR69056	90.91	8.01E-152	ML-1	AFZ77032	41.69	3.07E-74	BW-1	AET24913	40.18	5.07E-70
Mad12	HK1_006937	MMP	ADV17383	77.45	2.09E-157	BW-1	CCO06700	42.86	4.56E-69	BW-1	CCO06747	42.12	5.53E-63
magnetosome protein, similar to OMM2 of MMP	HK1_006938	MMP	ETR64726	47.20	3.36E-41								
Mad27-2	HK1_006939	MMP	ETR64727	66.19	0.00E+00	BW-1	CCO06728	51.84	6.54E-140	FH-1	AGG16231	40.54	0.00
Mad26-2	HK1_006940	MMP	ETR64728	42.29	6.43E-37	BW-1	CCO06727	38.95	4.05E-12	RS-1	YP_002955463	26.62	5.47E-11
Mad25-2	HK1_006941	MMP	ETR64729	58.45	2.87E-78	BW-1	CCO06725	39.90	1.62E-35	Mbav	AFX60119	34.74	4.94E-26
Mad24-2	HK1_006942	MMP	ETR64730	46.70	1.64E-46	BW-1	CCO06724	27.04	3.44E-10	Mbav	AFX60119	24.84	2.02E-08
Mad23-2	HK1_006943	MMP	ETR64731	70.27	1.63E-48	RS-1	YP_002955466	56.07	2.12E-34	BW-1	CCO06723	53.21	1.64E-33
Mad17	HK1_007976	ML-1	AFX88974	63.54	1.70E-35								
Mad30	HK1_007977	ML-1	AGG16192	61.03	5.08E-93	BW-1	AGG16188	31.78	4.22E-36	MMP	ETR64734	32.72	142E-35

a. BW-1 = *Ca. Desulfamplus magnetomortis*. FH-1 = bacterium FH-1. Mbav = *Ca. Magnetobacterium bavaricum*. MC-1 = *Magnetococcus marinus*. ML-1 = delta *Proteobacterium* ML-1. MMP = *Ca. Magnetoglobus multicellularis*. MSR-1 = *Magnetospirillum gryphiswaldense*. MV-1 = *Magnetovibrio blakemorei*. RS-1 = *Desulfovibrio magneticus*. Proteins are classified in the order they appear in the genome of *Ca. Magnetomorum* HK-1.

Colours indicate putative affiliation with magnetite biomineralization (yellow), greigite biomineralization (red) and general magnetosome biosynthesis (blue). *Putatively involved in greigite biomineralization.

Table 2. Comparison of Mam proteins putatively involved in magnetite biomineralization to those putatively involved in greigite biomineralization of *Candidatus Magnetomorum* HK-1.

Proteins in magnetite biomineralization	Accession number	Proteins in greigite biomineralization	Accession number	Identity (%)	E-value
MamA	HK1_000731	MamA*	HK1_001788	25.00	1.62E-23
MamQ	HK1_000734	MamQ*	HK1_001789	30.29	5.20E-23
MamB	HK1_000737	MamMB*	HK1_001786	27.45	1.69E-18
MamE-Cter	HK1_000739	MamE-Cter*	HK1_006086	43.42	7.62E-37
MamEO	HK1_000740	MamE-Cter*	HK1_006086	45.77	2.17E-40
MamM	HK1_003565	MamMB*	HK1_001786	32.14	5.77E-15

*Putatively involved in greigite biomineralization.

biomineralization from *Ca. M. multicellularis* and *Ca. D. magnetomortis* (Abreu *et al.*, 2011; Lefèvre *et al.*, 2013a). Cluster 1 is syntenic to the greigite gene cluster in *Ca. M. magnetoglobus* (Fig. 1), indicating a strong conservation among both MMPs. Additionally, a partial magnetosome gene *mamT** and an orthologous gene to OMM13 with high similarity to greigite genes of *Ca. M. magnetoglobus* were found on small contigs (Fig. 1, Table 1).

The second gene cluster (cluster 2, Fig. 1) comprises two contigs (12.2 kb and 5.6 kb) and has a similar gene order to the magnetite gene clusters in BW-1 and *Desulfovibrio magneticus* RS-1 (Lefèvre *et al.*, 2013a). The identified *mamIAIQBPPEEOILMN*, *mad1*, *mad2*, *mad6* and *mad7* genes are most similar to magnetosome genes of magnetite-producing *Deltaproteobacteria*, with identities ranging between 44% and 78% ($55.0 \pm 11\%$), indicating a putative function in magnetite biomineralization (Table 1). Together, these results suggest that the two gene clusters may control the biomineralization of magnetite and greigite magnetosomes separately. Despite the strong morphological similarity, no magnetite crystals were identified in *Ca. M. litorale*, which might be due to the absence of a magnetite gene cluster or strong reducing environmental conditions omitting the formation of magnetite particles. Future studies on MMP collected from diverse sampling locations have to show the impact of environmental conditions on the mineralization process of magnetosomes.

Besides the *mamAB*-like operons, we identified on different contigs homologues to the recently discovered *mad* genes, with highest similarity to *mad* genes from magnetic *Deltaproteobacteria*, particularly to *Ca. M. multicellularis*. One gene cluster (termed cluster 3; Fig. 1) comprises a *mad12* gene and a putative *mad23–mad27*-operon, with synteny and high identity ($58 \pm 14\%$) to a gene cluster in *Ca. M. magnetoglobus* (Lefèvre *et al.*, 2013a). A further gene set (termed cluster 4) contains homologues to *mad24–mad28*, but with a divergent gene order compared with *Ca. M. magnetoglobus*, and shows highest similarity to those from rod-shaped magnetotactic *Deltaproteobacteria* (Fig. 1, Table 1). Interestingly, a set of

18 *mad* genes, which were present in MTB of the *Deltaproteobacteria* class that biomineralizes bullet-shaped magnetite magnetosomes, was also present in *Ca. Magnetomorum* HK-1, with *mad20* being the only exception (Table 1) (Lefèvre *et al.*, 2013a). This is consistent with the observation of bullet-shaped magnetosomes in other closely related MMPs (Fig. 1) (Wenter *et al.*, 2009; Zhou *et al.*, 2011), indicating the presence of these genes. In the draft genome of *Ca. M. Multicellularis*, only 10 of these *mad* genes were present, which might explain the absence of bullet-shaped magnetosomes.

Of note, we also identified several divergent gene copies coding for the actin-like proteins MamK (HK1_005515, HK1_005096) and Mad28 (HK1_005206, HK1_003334), which might be associated with the ability of MMPs to biomineralize numerous chains of magnetosomes within a single cell. Whereas the monocistronic *mamK* was found on a contig (9.8 kb) together with *mad* genes *mad9*, *mad11*, *mad21*, *mad22* and *mad23*, the first *mad28* (*mad28-1*) was part of an operon together with *mad24*, *mad25* and *mad27* on an 8.7 kb contig (Fig. 1). Similar to *Ca. M. multicellularis* (Lefèvre *et al.*, 2013a), a second *mad28* (*mad28-2*) was found in a contig that does not contain other *mam* genes.

The origin and evolution of greigite magnetosome genes still remain elusive. Greigite biomineralization in some MTB, such as *Ca. D. magnetomortis* (Lefèvre *et al.*, 2011a), may reflect their sulfate-reducing lifestyle adapted to more reducing conditions, prevalent also on the ancient anoxic earth at the time when *Proteobacteria* emerged (Anbar *et al.*, 2007; Lefèvre *et al.*, 2013b).

The correlation of well-defined magnetosome morphologies, including cubooctahedral and elongated prismatic of the later-diverging *Alpha*- and *Gammaproteobacteria* (Devouard *et al.*, 1998; Lefèvre *et al.*, 2012), and the biomineralization of less morphologically consistent bullet-shaped magnetosomes in MTB of the *Deltaproteobacteria* and the deep-branching phyla *Nitrospirae* and *Omnitrophica* (Jogler *et al.*, 2011; Lefèvre *et al.*, 2011b; Kolinko *et al.*, 2012), led to the hypothesis that

bullet-shaped magnetosomes represent the more ancient crystal morphology (Lefèvre *et al.*, 2013b). However, greigite-producing MTB so far were found only in the deeply diverging *Deltaproteobacteria*, but not in the deep-branching phyla. Therefore, the higher identity of the greigite gene cluster of HK-1 to greigite genes of other MTB than to its own magnetite genes may indicate ancient gene duplication followed by subsequent mutation in a common ancestor and an acquirement via horizontal gene transfer by HK-1. This hypothesis appears to be supported by the high synteny of *mamAB*-like gene clusters between the magnetic *Deltaproteobacteria* *Ca. M. desulfamplus*, *Ca. M. multicellularis* and strain HK1. So far, it is not clear whether the apparent absence of a homologous magnetite gene cluster in *Ca. M. multicellularis* was caused by spontaneous loss of these genes, as frequently observed for other MTB during cultivation, (Schübbe *et al.*, 2003), or whether it simply escaped detection due to the partial incompleteness (10% missing) of the draft genome (Abreu *et al.*, 2014).

Overall, our study provides first evidence for the occurrence of two divergent magnetosome gene clusters in MMPs. This strongly suggests that *Ca. Magnetomorum* HK-1 and probably other, if not all MMPs, have the potential to synthesize either greigite and magnetite magnetosomes or both.

Acknowledgements

We thank Antonio Fernandez-Guerra for excellent assistance. This work was supported by the Deutsche Forschungsgemeinschaft (Grant DFG Schu1080/11-1 to D.S.). This Whole Genome Shotgun project has been deposited at DDBJ/EMBL/GenBank under the accession JPDT00000000. The version described in this paper is version JPDT01000000. The sequence associated contextual (meta) data are MIGS (Yilmaz *et al.*, 2011) compliant.

References

Abreu, F., Cantao, M.E., Nicolas, M.F., Barcellos, F.G., Morillo, V., Almeida, L.G., *et al.* (2011) Common ancestry of iron oxide- and iron-sulfide-based biomineralization in magnetotactic bacteria. *ISME J* **5**: 1634–1640.

Abreu, F., Morillo, V., Nascimento, F.F., Werneck, C., Cantao, M.E., Ciapina, L.P., *et al.* (2014) Deciphering unusual uncultured magnetotactic multicellular prokaryotes through genomics. *ISME J* **8**: 1055–1068.

Altschul, S.F., Madden, T.L., Schaffer, A.A., Zhang, J., Zhang, Z., Miller, W., and Lipman, D.J. (1997) Gapped BLAST and PSI-BLAST: a new generation of protein database search programs. *Nucleic Acids Res* **25**: 3389–3402.

Amann, R.L., Binder, B.J., Olson, R.J., Chisholm, S.W., Devereux, R., and Stahl, D.A. (1990) Combination of 16S rRNA-targeted oligonucleotide probes with flow cytometry for analyzing mixed microbial populations. *Appl Environ Microbiol* **56**: 1919–1925.

Anbar, A.D., Duan, Y., Lyons, T.W., Arnold, G.L., Kendall, B., Creaser, R.A., *et al.* (2007) A whiff of oxygen before the great oxidation event? *Science* **317**: 1903–1906.

Bankevich, A., Nurk, S., Antipov, D., Gurevich, A.A., Dvorkin, M., Kulikov, A.S., *et al.* (2012) SPAdes: a new genome assembly algorithm and its applications to single-cell sequencing. *J Comput Biol* **19**: 455–477.

Bazyliński, D.A., and Frankel, R.B. (2004) Magnetosome formation in prokaryotes. *Nat Rev Microbiol* **2**: 217–230.

Bazyliński, D.A., Frankel, R.B., Heywood, B.R., Mann, S., King, J.W., Donaghay, P.L., and Hanson, A.K. (1995) Controlled biomineralization of magnetite (Fe(*inf*3)O(*inf*4)) and greigite (Fe(*inf*3)S(*inf*4)) in a magnetotactic bacterium. *Appl Environ Microbiol* **61**: 3232–3239.

Delong, E.F., Frankel, R.B., and Bazyliński, D.A. (1993) Multiple evolutionary origins of magnetotaxis in bacteria. *Science* **259**: 803–806.

Devouard, B., Pósfai, M., Hua, X., Bazyliński, D.A., Frankel, R.B., and Buseck, P.R. (1998) Magnetite from magnetotactic bacteria: size distributions and twinning. *Am Min* **83**: 1387–1398.

Esquivel, D.M.S., Lins de Barros, H.G.P., Farina, M., Aragaõ, P.H.A., and Danon, J. (1983) Microorganismes magnétotactiques de la region de Rio de Janeiro. *Biol Cell* **47**: 227–234.

Farina, M., Lins de Barros, H., Esquivel, M.S., and Danon, J. (1983) Ultrastructure of a magnetotactic bacterium. *Biol Cell* **48**: 85–88.

Farina, M., Esquivel, D.M., and De Barros, H.G. (1990) Magnetic iron-sulfur crystals from a magnetotactic microorganism. *Nature* **343**: 256–258.

Frankel, R.B., Bazyliński, D.A., Johnson, M.S., and Taylor, B.L. (1997) Magneto-aerotaxis in marine coccoid bacteria. *Biophys J* **73**: 994–1000.

Grünberg, K., Wawer, C., Tebo, B.M., and Schüler, D. (2001) A large gene cluster encoding several magnetosome proteins is conserved in different species of magnetotactic bacteria. *Appl Environ Microbiol* **67**: 4573–4582.

Jogler, C., and Schüler, D. (2009) Genomics, genetics, and cell biology of magnetosome formation. *Annu Rev Microbiol* **63**: 501–521.

Jogler, C., Wanner, G., Kolinko, S., Niebler, M., Amann, R., Petersen, N., *et al.* (2011) Conservation of proteobacterial magnetosome genes and structures in an uncultivated member of the deep-branching *Nitrospirae* phylum. *Proc Natl Acad Sci USA* **108**: 1134–1139.

Keim, C.N., Abreu, F., Lins, U., Lins de Barros, H., and Farina, M. (2004) Cell organization and ultrastructure of a magnetotactic multicellular organism. *J Struct Biol* **145**: 254–262.

Keim, C.N., Martins, J.L., de Barros, H.L., Lins, U., and Farina, M. (2007) Structure, behavior, ecology and diversity of multicellular magnetotactic prokaryotes. In *Magnetoreception and Magnetosomes in Bacteria*. Schüler, D. (ed.). Heidelberg, Germany: Springer-Verlag Berlin, pp. 103–132.

Kolinko, S., Jogler, C., Katzmann, E., Wanner, G., Peplies, J., and Schüler, D. (2012) Single-cell analysis reveals a novel uncultivated magnetotactic bacterium within the candidate division OP3. *Environ Microbiol* **14**: 1709–1721.

Lefèvre, C.T., and Bazyliński, D.A. (2013) Ecology, diversity,

- and evolution of magnetotactic bacteria. *Microbiol Mol Biol Rev* **77**: 497–526.
- Lefèvre, C.T., Menguy, N., Abreu, F., Lins, U., Pósfai, M., Prozorov, T., *et al.* (2011a) A cultured greigite-producing magnetotactic bacterium in a novel group of sulfate-reducing bacteria. *Science* **334**: 1720–1723.
- Lefèvre, C.T., Pósfai, M., Abreu, F., Lins, U., Frankel, R.B., and Bazylinski, D.A. (2011b) Morphological features of elongated-anisotropic magnetosome crystals in magnetotactic bacteria of the *Nitrospirae* phylum and the *Deltaproteobacteria* class. *Earth Planet Sci Lett* **312**: 194–200.
- Lefèvre, C.T., Vilorio, N., Schmidt, M.L., Pósfai, M., Frankel, R.B., and Bazylinski, D.A. (2012) Novel magnetite-producing magnetotactic bacteria belonging to the *Gammaproteobacteria*. *ISME J* **6**: 440–450.
- Lefèvre, C.T., Trubitsyn, D., Abreu, F., Kolinko, S., Jogler, C., de Almeida, L.G., *et al.* (2013a) Comparative genomic analysis of magnetotactic bacteria from the *Deltaproteobacteria* provides new insights into magnetite and greigite magnetosome genes required for magnetotaxis. *Environ Microbiol* **15**: 2712–2735.
- Lefèvre, C.T., Trubitsyn, D., Abreu, F., Kolinko, S., de Almeida, L.G., de Vasconcelos, A.T., *et al.* (2013b) Monophyletic origin of magnetotaxis and the first magnetosomes. *Environ Microbiol* **15**: 2267–2274.
- Nakazawa, H., Arakaki, A., Narita-Yamada, S., Yashiro, I., Jinno, K., Aoki, N., *et al.* (2009) Whole genome sequence of desulfovibrio magneticus strain RS-1 revealed common gene clusters in magnetotactic bacteria. *Genome Res* **19**: 1801–1808.
- Pósfai, M., Buseck, P.R., Bazylinski, D.A., and Frankel, R.B. (1998) Reaction sequence of iron sulfide minerals in bacteria and their use as biomarkers. *Science* **280**: 880–883.
- Richter, M., Kube, M., Bazylinski, D.A., Lombardot, T., Glöckner, F.O., Reinhardt, R., and Schüler, D. (2007) Comparative genome analysis of four magnetotactic bacteria reveals a complex set of group-specific genes implicated in magnetosome biomineralization and function. *J Bacteriol* **189**: 4899–4910.
- Rinke, C., Schwientek, P., Sczyrba, A., Ivanova, N.N., Anderson, I.J., Cheng, J.F., *et al.* (2013) Insights into the phylogeny and coding potential of microbial dark matter. *Nature* **499**: 431–437.
- Rodgers, F.G., Blakemore, R.P., Blakemore, N.A., Frankel, R.B., Bazylinski, D.A., Maratea, D., and Rodgers, C. (1990) Intercellular junctions, motility and magnetosome structure in a multicellular magnetotactic prokaryote. In *Iron Biominerals*. Frankel, R.B., and Blakemore, R.P. (eds). New York, NY, USA: Plenum Press, pp. 231–237.
- Schübbe, S., Kube, M., Scheffel, A., Wawer, C., Heyen, U., Meyerdierks, A., *et al.* (2003) Characterization of a spontaneous nonmagnetic mutant of *Magnetospirillum gryphiswaldense* reveals a large deletion comprising a putative magnetosome island. *J Bacteriol* **185**: 5779–5790.
- Simmons, S.L., Bazylinski, D.A., and Edwards, K.J. (2007) Population dynamics of marine magnetotactic bacteria in a meromictic salt pond described with qPCR. *Environ Microbiol* **9**: 2162–2174.
- Swan, B.K., Martinez-Garcia, M., Preston, C.M., Sczyrba, A., Woyke, T., Lamy, D., *et al.* (2011) Potential for chemolithoautotrophy among ubiquitous bacteria lineages in the dark ocean. *Science* **333**: 1296–1300.
- Ullrich, S., Kube, M., Schübbe, S., Reinhardt, R., and Schüler, D. (2005) A hypervariable 130-kilobase genomic region of *Magnetospirillum gryphiswaldense* comprises a magnetosome island which undergoes frequent rearrangements during stationary growth. *J Bacteriol* **187**: 7176–7184.
- Wenter, R., Wanner, G., Schüler, D., and Overmann, J. (2009) Ultrastructure, tactic behaviour and potential for sulfate reduction of a novel multicellular magnetotactic prokaryote from North Sea sediments. *Environ Microbiol* **11**: 1493–1505.
- Yilmaz, P., Kottmann, R., Field, D., Knight, R., Cole, J.R., Amaral-Zettler, L., *et al.* (2011) Minimum information about a marker gene sequence (MIMARKS) and minimum information about any (x) sequence (MlXS) specifications. *Nat Biotechnol* **29**: 415–420.
- Zhang, R., Chen, Y.R., Du, H.J., Zhang, W.Y., Pan, H.M., Xiao, T., and Wu, L.F. (2014) Characterization and phylogenetic identification of a species of spherical multicellular magnetotactic prokaryotes that produces both magnetite and greigite crystals. *Res Microbiol*. doi:10.1016/j.resmic.2014.07.012.
- Zhou, K., Pan, H., Zhang, S., de Barros, H.L., Xiao, T., and Wu, L.F. (2011) Occurrence and microscopic analyses of multicellular magnetotactic prokaryotes from coastal sediments in the Yellow Sea. *Chin J Oceanol Limnol* **29**: 246–251.

Supporting information

Additional Supporting Information may be found in the online version of this article at the publisher's web-site:

Table S1. General draft genome features of *Ca. Magnetomorum* HK-1.

Table S1. General draft genome features of *Ca. Magnetomorum* HK-1.

Parameter	<i>Candidatus</i>
	<i>Magnetomorum</i> HK-1
Total genome size (Mb)	14.3
GC content (%)	34.6
Number of contigs	3036
N50 (kb)	18.2
Maximum contig length (kb)	122.255
Genome completeness (%)	95
Estimated genome size (Mb)	15.1
Number of coding sequences (CDS)	11,022
Number of tRNAs	47
Number of copies of rRNA operon	1
Total MAI size (kb)	50.8
GC content MAI (%)	38.2
Number of putative magnetosome genes	51

4. Manuskript:

Single-cell analysis of phylogenetic deep-branching MTB reveal a conserved set of proteobacterial magnetosome genes.

Single-cell analysis of phylogenetic deep-branching MTB reveal a conserved set of proteobacterial magnetosome genes

Sebastian Kolinko^{1*)}, Michael Richter²⁾, Frank-Oliver Glöckner^{2,3)}, Andreas Brachmann¹⁾,
Dirk Schüler^{1,4*)}

¹⁾ Ludwig Maximilian University Munich, Dept. Biology I, LMU Biozentrum, Großhaderner Str. 2-4, 82152 Planegg-Martinsried, Germany

²⁾ Max Planck Institute for Marine Microbiology, Microbial Genomics and Bioinformatics Research Group, Celsiusstr. 1, 28359 Bremen, Germany.

³⁾ Jacobs University Bremen gGmbH, Campusring 1, 28759 Bremen, Germany.

⁴⁾ University Bayreuth, Dept. Microbiology, Germany.

^{*)} Corresponding author

Keywords: WGA; micromanipulation; single cell analysis; magnetotactic; single amplified genomes; multicellular magnetotactic prokaryote; MMP

Running Title: Genomic analysis of an uncultivated multicellular magnetotactic prokaryote.

Correspondence: Dirk Schüler, Lehrstuhl für Mikrobiologie, Gebäude NW I, Universitätsstraße 30, 95447 Bayreuth, Germany.

E-Mail: dirk.schueler@uni-bayreuth.

Material and Methods

Sampling

Freshwater sediments were collected from Lake Chiemsee (Germany, Bavaria) (47°51'08"N, 12°24'00"E) and stored at room temperature as previously described (Kolinko *et al.*, 2012). Magnetic enrichments from microcosms were performed as previously described (Jogler *et al.*, 2010) and analyzed/checked for the presence of morphologically conspicuous MTB like *Ca. M. bavaricum*, SKK-01 and CS-04.

Whole genome amplification (WGA) and single amplified genome (SAG) screening

Micromanipulation and WGA of single cells was performed as previously described (Kolinko *et al.*, 2012). Briefly, single conspicuous cells were selected and washed under strict microscopic control via micromanipulation to eliminate contaminations and extracellular DNA for subsequent WGA. UV irradiation of WGA sample and reaction buffers (illustra GenomiPhi V2 DNA amplification kit, GE Healthcare, Little Chalfont, UK) were performed as previously described (Woyke *et al.*, 2011) for decontamination. The WGA reaction was carried out at 30°C for 10 h. Partial 16S rRNA genes were amplified from SAGs applying bacteria-specific primers 27F and 1492R (Lane, 1991), cloned into pJET1.2/blunt Cloning Vector (Fermentas, Waltham, MA, USA) and sequenced with an ABI system according to the instructions of the manufacturer to identify SAGs for whole genome amplification.

Genome completeness estimation

Genome size and completeness was estimated using a set of 139 conserved single copy genes (CSCG), that have been determined from finished bacterial genome sequences ($n = 1516$) in the IMG database (Markowitz *et al.*, 2012; Rinke *et al.*, 2013). These genes occurred only once in at least 90% of all genomes, based on hits to the protein family (Pfam) database (Punta *et al.*, 2012). The estimated genome completeness of individual and

combined SAGs was estimated as the ratio of identified CSCGs to total CSCGs, and was used to calculate the estimated complete genome size by division the estimated genome coverage by the total assembly size (Rinke *et al.*, 2013).

Phylogenetic analysis

Alignments of sequences were performed using ClustlW multiple alignment accessory application in the MEGA version 6 sequence alignment editor (Tamura *et al.*, 2013).

Phylogeny was analyzed as previously described (Abreu *et al.*, 2014). In brief, phylogenetic trees were constructed using MEGA version 6 applying the maximum likelihood method based on the Whelon and Goldman model (Whelan & Goldman, 2001). The tree with the highest log likelihood is shown. Bootstrap values were calculated with 1000 replicates. The tree topology space was searched using the best by Subtree Pruning and Regrafting algorithms, from five random starting trees generated by the BioNJ algorithm (Guindon & Gascuel, 2003; Guindon *et al.*, 2010).

Results

Sandy freshwater sediments were collected from 10-20 m depth from Lake Chiemsee (47°51'08"N, 12°24'00"E) and following a prolonged storage of 18 months at RT were analyzed for MTB. One microcosm contained occasionally (<1% abundance) conspicuous ovoid 'melon'-shaped magnetic responsive morphotypes, virtually identical to the previously described uncultivated magnetotactic bacterium SKK-01 (Kolinko *et al.*, 2012). Following magnetic enrichment and targeted micromanipulation of single cells as described by Kolinko *et al.*, 2012, whole genome amplification (WGA) reactions were set up, each with 5 identical cells as template, resulting in six single amplified genomes (SAGs). PCR amplification employing universal eubacterial primers 27f and 1492r (Lane, 1991) to SAGs yielded an identical single product, indicating clonality and the absence of contaminations and qualified SAGs for individual sequencing and *de novo* assembly. Each SAG contains a full rRNA gene operon with the standard 16S, 23S-5S arrangements of rRNA genes and were identical to the partial 16S and 23S rRNA genes of the uncultivated magnetotactic bacterium SKK-01 that had been previously assigned to the deep-branching candidate division OP3 (Hugenholtz *et al.*, 1998; Kolinko *et al.*, 2012). The candidate division OP3 belongs to the *Planctomycetes-Verrucomicrobia-Chlamydiae* (PVC) superphylum and was recently renamed into candidate phylum *Omnitrophica* (Rinke *et al.*, 2013; Wagner & Horn, 2006). A recently described conserved PVC signature gene of unknown function (Gupta *et al.*, 2012) (NP_219933) was detected in individual SAGs and encoded a hypothetical protein (SAG1675_1). In the following we refer to this MTB as *Candidatus* *Omnitrophus* *magneticus* strain SKK-01.

Besides SKK-01, large magnetotactic rods virtually identical to the previously identified *Candidatus* *Magnetobacterium* *bavaricum* were abundant in the same microcosm and were selected for targeted analysis. Six WGA reactions each with 5 identical cells were set up as described above, followed by 16S rRNA gene screening for clonality and subsequent individual *de novo* assembling after sequencing of obtained SAGs. Individual 16S and 23S rRNA genes from SAGs were identical to those of *Ca. M. bavaricum* (Jogler *et al.*, 2010;

Spring *et al.*, 1993) a large rod-shaped MTB belonging to the deep-branching phylum *Nitrospirae*.

A further microcosm with sediment from Lake Chiemsee contained a large magnetotactic coccus morphologically resembling the previously described uncultivated MTB CS-04, which also was first identified by single-cell techniques (Kolinko *et al.*, 2013). Clonality and the absence of contaminations of four WGA reactions were verified by identical 16S rRNA genes amplified by PCR. Individual sequencing and genome assembly obtained full length 16S rRNA genes, which were most similar (99.9% identity) to the *Nitrospirae* MTB CS-04 from Lake Chiemsee (Kolinko *et al.*, 2013). *Candidatus* Magnetoovum chiemensis strain CS-04. *De novo* assemblies were validated by BLAST (Altschul *et al.*, 1997), tetra-nucleotide frequency and single copy marker gene analysis (Rinke *et al.*, 2013). The size of obtained SAGs ranged between 0.6 Mb and 3.7Mb (2.3 ± 0.9 Mb) composed of an average of 2100 ± 1221 contigs with an average size of 1327 ± 657 bp. The estimated genome completeness of SAGs varied between 7.3% and 60% ($44.5 \pm 0.2\%$) (Figure 1). SAGs contained primarily small contigs, indicated by a N50-value <3 kb (2.9 ± 2.1 kb) and an average contig size <1.5 kb, which prevented the identification of large contiguous magnetosome gene clusters (Figure S1). By combining individual SAGs of *Ca. O. magneticus*, *Ca. M. bavaricum* and *Ca. M. chiemensis* increased the draft genome sizes (3.9, 6.3 and 3.4 Mb) and estimated genome completeness (74, 75 and 87%) significantly, facilitating automatic gene annotation and magnetosome gene cluster detection.

General metabolic features/metabolic reconstruction

Functional analysis of the draft genomes revealed besides the common genomic potential of autotrophy and respiratory growth a metabolic variation between organisms.

A putative versatile metabolism was identified in the draft genome of *Ca. M. bavaricum*, which can utilize both oxidized nitrogen and sulfur compounds as electron acceptor. *Ca. M. bavaricum* can utilize oxidized nitrogen substrates as terminal electron acceptors applying either denitrification (DN) or dissimilatory nitrate reduction to ammonia (DNRA) (Dong *et al.*, 2011), which were fully reconstructed from the draft genome of *Ca. M. bavaricum*. Under nitrogen limiting conditions the DNRA pathway is used to reduce cytoplasmatic nitrate to nitrite by a membrane bound nitrate reductase (Nar) (SAG4_002195-SAG4_002187) and further reduced by a cytoplasmic nitrite reductase (NirB) (SAG4_006891) to ammonia. For denitrification, periplasmic nitrate is successively reduced to its gaseous products nitrous oxide (N₂O) and N₂ by the nitrate reductase (Nap) (SAG4_006956), nitrite reductase (NirS) (SAG4_007402), nitric oxide reductase (FprA)(SAG_000686), and nitrous oxide reductase (Nos)(SAG4_007532), which were found to be encoded in the draft genome. The utilization of nitrate or nitrite as nitrogen source by assimilatory nitrate reduction was indicated by the presence of an assimilatory nitrate reductase (SAG4_001651). In contrast to *Ca. M. casensis* no genes involved in nitrogen fixation were identified in *Ca. M. bavaricum* (Lin *et al.*, 2014).

Sulfur globule accumulation and consumption under oxic conditions in the cytoplasm indicated the ability of sulfur-oxidizing metabolism of *Ca. M. bavaricum* in a previous study (Jogler *et al.*, 2010). Whereas no genes encoding sulfur oxidation proteins (Sox) were found, a gene coding for a putative sulfide:quinine oxidoreductase (SAG4_006205) was identified, which is postulated to oxidize sulfide to elemental sulfur (Dahl *et al.*, 2005). Genes coding for a dissimilatory sulfite reductase (*dsr*) (SAG4_005384, SAG4_000906), which further oxidizes sulfur to sulfite. The oxidation of sulfite to sulfate is proposed to be mediated by an adenosine 5'-phosphosulfate (APS) reductase (Apr) and adenosine 5'-triphosphate (ATP) sulfurylase (Sat) (SAG4_003142- SAG4_003143) (Holkenbrick). The previously identified

Ribulose-1,5-bisphosphat-carboxylase (RuBisCo) like protein of *Ca. M. bavaricum* was found to be encoded in our draft genome (Sag4_004452) with a similar, yet distinct amino acid composition to RLPs involved in thiosulfate oxidation (Jogler *et al.*, 2010).

Additionally, an assimilatory sulfate reducing pathway with genes coding for Sat (SAG4_003142) and Cys (SAG4_008196, SAG4_006026) was present in *Ca. M. bavaricum*. Identical to *Ca. M. casensis* (Lin 2014), we identified genes coding for CO₂-fixation via the reductive acetyl-CoA pathway (Wood-Ljungdahl pathway) and the reductive citric acid cycle in *Ca. M. bavaricum*, indicative for autotrophic growth.

Ca. M. bavaricum contains between 600 and 1,000 bullet-shaped magnetite magnetosomes per cell and needs to accumulate large amounts of extracellular iron for their biomineralization. We identified an iron transporter operon with two adjacent genes coding for a ferrous iron transporter protein A (FeoA) followed downstream by a gene encoding FeoB (SAG4_005787-SAG4-005789). These proteins had highest similarity to the magnetosome proteins Mad17 and Mad30 previously identified in *Ca. M. casensis* (Lin *et al.*, 2014). Besides a gene (SAG4_006900) coding for a general transporter for divalent metal ions of the NRAMP transporter family, we found genes encoding proteins with considerable similarities to TonB-dependent transporters. Additionally we identified the coding potential for bacterial ferritins (SAG4_005573, which are responsible for intracellular iron homeostasis. A phosphate-rich ferric hydroxide phase, similar to bacterial ferritins is hypothesized to be a precursor for magnetite mineralization (Baumgartner *et al.*, 2013).

-CS-04- Similar to *Ca. M. bavaricum* we identified in the draft genome of CS-04 genes coding for the DNRA pathway, including a (membrane bound) nitrate reductase (Nar) (SAG2_004472-SAG2_002275) and (cytoplasmatic) nitrite reductase (SAG2_002406). In contrast to *Ca. M. bavaricum* neither genes for a denitrification nor an assimilatory nitrate reducing pathway were found, but most genes involved/responsible in/for nitrogen fixation, like a *nif*-operon (*nifHDKNXHD1HD2BF,nifSU*) and a gene encoding a Nif-specific ferredoxin III (SAG2_003423 - SAG2_003431, SAG2_000687, and SAG2_002127).

Consistent with the presence of sulfur-rich inclusions (Kolinko *et al.*, 2013), genes encoding a sulfur oxidation pathway was identified in part with a putative sulfide:quinone oxidoreductase (SAG2_003639), a dissimilatory sulfite reductase (SAG2_001606, SAG2_004249), Sat and Apr (Sag2_00042-Sag2_000044). The incorporation of sulfur is driven by the assimilatory sulfate reduction. The identification of genes coding for all proteins necessary for CO₂-fixation via the Wood-Ljungdahl-pathway, imply autotrophy for CS-04. Congruent to the draft genome of *Ca. M. bavaricum* genes coding for Mad17, Mad30, a general metal²⁺ transporter (NRAMP), TonB-dependent transporters and bacterial ferritin were present in CS-04. Additionally we found genes coding for a ferric uptake regulator (Fur) (SAG2_003095) and FeoB (SAG2_004218) on discontinuous contigs.

In contrast to both *Nitrospirae* genomes described in this work, neither a dissimilatory nor an assimilatory nitrate reduction pathway were found in the genome of SKK-01. Although, genes governing nitrogen fixation were identified in part in SKK-01 with genes coding for NifBHD1HD2SUX (SAG01_000292, SAG01_000293, SAG01_000295, SAG01_000231, SAG01_001446) and a Nif specific ferredoxin III (SAG01_000294) encoded within an operon together with *nif* genes.

The identification of sulfur-rich inclusions in SKK-01, led to the hypothesis of a sulfur-oxidizing metabolism (Kolinko *et al.*, 2012). A reversible dissulfoviridin type dissimilatory sulfite reductase (dSiR) (SAG1_002184) was found in the draft genome. Under reducing conditions dSiR transfers 6 electrons from the hydrolysis of H₂ by a periplasmic and a membrane bound hydrogenase (SAG1_001262 - SAG1_001265) to sulfite reducing it to sulfide. Sulfur-oxidizing bacteria such as *Thiobacillus* oxidize sulfur components by a reverse reaction of dSiR (Steuber & Kroneck, 1998), which could be the case for SKK-01.

In contrast to *Ca. M. bavaricum* and CS-04, no genes encoding factors for CO₂ fixation via the Wood-Ljungdahl pathway were found for SKK-01. Analysis of the genome of SKK-01 identified two key genes coding for a fumarate reductase (SAG1_001169) and a 2-oxoglutarate ferredoxin oxidoreductase (SAG1_002145), implying CO₂-fixation through the reductive citric acid cycle.

Whereas SKK-01 synthesizes up to 200 bullet-shaped magnetosomes per cell, organized in multiple bundles of 5–7 magnetosome chains traversing the cell along its length (Kolinko *et al.*, 2012), genome analysis unexpectedly did not identify any iron uptake systems, besides an iron dependent repressor (SAG1_003364) and a TonB dependent receptor plug (SAG1_000510).

Cell wall biosynthesis

TEM micrographs of ultrathin sections of high-pressure frozen and freeze-substituted cells of *Ca. Magnetobacterium bavaricum* showed a multilayered cell boundary composing a cytoplasmic membrane, an outer membrane, one layer of peptidoglycan, and a bipartite outer layer resembling a capsular structure, which was hypothesized to consist of polysaccharides (Jogler *et al.* 2011). Besides genes involved in outer membrane and peptidoglycan biogenesis, which were found in all analyzed draft genomes, only *Ca. M. bavaricum* contained two sets of genes encoding for the biosynthesis of spore coat like polysaccharides (*spsBC₂E₂F₂G₂*) (SAG4_007242 – SAG4_007262), which were similar to those of *Rhizobium leguminosarum*. The Gram-negative soil bacterium *R. leguminosarum* was shown to produce large amounts of exopolysaccharide (EPS) that has been shown to be an important determinant of successful nitrogen-fixing symbiosis with legume plants (Marczak *et al.* 2013) and is hypothesized to be an important survival strategy in soil and rhizosphere (Bonomi *et al.* 2012).

These spore coat like polysaccharides could be the reason for poor chemical lysis as described previously (Jogler 2011). Although Mbav was the most abundant morphotype in MTB collections, 16S rRNA gene libraries revealed an underrepresentation of Mbav in fosmid libraries possibly due to its unusual cell structure (Jogler *et al.* 2011

Magnetosome biosynthesis

Contigs encoding magnetosome proteins in all draft genomes differed only slightly in respect of G+C content to their draft genomes. Whereas the MAI of *Ca. M. bavaricum* had a G+C content of 50%, those of CS-04 and SKK-01 had ~40%.

One contig (23,385 bp) in the draft genome of *Ca. M. bavaricum* contained a *mamAB*-like operon, which was almost identical (>99% nucleotide identity) to that found on a metagenomic clone of *Ca. M. bavaricum* (Jogler 2011) and had a similar gene order and high nucleotide identity (91.2%) to the *mamAB*-like operon in *Ca. M. casensis* (Lin 2014). The G+C content of the *mamAB*-like operon with 50.2% was slightly higher compared to the draft genome with 47.4% (Table 1) Magnetosome genes *mamK*, *mad11* and *mad28*, which were part of the *mamAB*-like operon in *Ca. M. casensis* were encoded on a small accessory contig (Figure 1).

The *mamAB*-like operon contained magnetosome genes *mamKPMQBAIEQO-Cter*, *man5*, *man6*, *mad2*, *mad11*, *mad20*, *mad28* and *mad23-26*, which were previously identified in various magnetotactic *Deltaproteobacteria* and *Nitrospirae* and encoded magnetosome proteins with high identities to *Ca. M. bavaricum* (>98%) and to *Ca. M. casensis* (>80%) (Table 2).

A partial *mamAB*-like operon is also present in the draft genome of CS-04 encoding magnetosome proteins MamEMQBAPM and Mad23-26 with an identity of approximately 50% to other magnetotactic *Nitrospirae* and *Deltaproteobacteria* (Table2).

In contrast to *Ca. M. bavaricum* and CS-04, only small discontinuous contigs with genes encoding magnetosome proteins were found in the draft genome of SKK-01, and therefore no larger magnetosome gene cluster (>1.5 kb) or gene order could be analyzed (Figure 1).

Encoded magnetosome proteins MamEKBM and Mad11 had a high identity of approximately 60% to their orthologs in magnetotactic *Nitrospirae* (Table 2), and therefore represent to our knowledge the first reported magnetosome proteins in the deep-branching candidate phylum *Omnitrophica*, which harbors no cultivated representatives so far. Furthermore, Mam and Mad proteins of SKK-01 seemed to be closely related to those of CS-04 within the deep-branching *Nitrospirae* (Figure 1, Figure 2).

Additionally we were able to identify several discontinuous contigs with magnetosome genes putatively involved in magnetosome biosynthesis outside the *mamAB*-like operons of *Ca. M. bavaricum* and *Ca. M. casensis*.

A small contig (~2 kb) in the genome of *Ca. M. bavaricum* and CS-04 contained a gene encoding a further Mad28 (Mad28-2) (SAG2_000493, SAG4_006080), which was accompanied downstream by a highly conserved gene (SAG2_000494, SAG4_006079). This gene encodes a putative penicillin binding protein (PBP) with a multimodular transpeptidase-transglycosylase activity. A homologous magnetosome gene tandem was found outside of the described *mamAB*-like operon of *M. casensis*, and is therefore highly conserved in magnetotactic *Nitrospirae* (Figure 1, Table 2, Table 3).

Another contig (4 kb) of *Ca. M. bavaricum* contained 5 genes organized in an operon, with 2 of them coding for actin-like proteins Mad28-3 (SAG4_001959) and Mad28-4 (SAG4_001964) and 1 encoding a putative ATPase Mad29 (SAG4_1962), and was therefore termed *mad28-29*-operon. The genes *mad28-3* and *mad29* are separated by a hypothetical gene (SAG4_001961), which was found to be highly conserved in magnetotactic *Nitrospirae* and encodes a protein putatively involved lipid A biosynthesis (Table 2). In *Ca. M. casensis* a homologous *mad28-29*-operon is present outside the MAI, and comprises as well a third *mad28* (Mcas_XA) and a *mad29* gene (Mcas_XB), which are separated by a homologous gene to SAG4_001961 (SAG_XC).

In CS-04 the *mad28-29*-operon is also present but is much larger (12,560 bp) and contains besides a second *mad28* (SAG2_000029), a gene encoding a hypothetical protein (SAG2_000028), a *mad29* (SAG2_000027), and several previously described magnetosome genes, like *mamKB*, *mad11*, *mad17*, and *mad30* (Figure 1). Noteworthy magnetosome genes involved in iron homeostasis *mad17*, *mad30* and *mamB*, are in close proximity. Two genes (SAG2_000030, SAG2_000021) had high identities to genes in other magnetotactic bacteria (Table 2). SAG2_000021 encodes a lipoprotein which is highly conserved in magnetotactic *Nitrospirae* and *Alphaproteobacteria* but is missing in the class of *Deltaproteobacteria*. The second gene encodes for a CheY-like protein (SAG2_000030) and

is similar to an orthologous gene in *Ca. M. bavaricum* (SAG4_005785), which is in close proximity to magnetosome genes *mad17-2* (SAG4_005788), *mad17-1* (SAG4_005789), and *mad30* (SAG4_005786) (Table 2) (Figure X). A third conserved hypothetical protein was located upstream of the two copies of *mad17* in *Ca. M. bavaricum* (SAG4_005790) and *Ca. M. casensis* (Mcas_XD) but was not identified in CS-04 (Figure X) (Table 2).

A highly conserved gene was identified in the *mamAB*-like operons of *Ca. M. bavaricum*, *Ca. M. casensis* (XY) and CS-04 (SAG2_000250), and was always localized between *mamM* and *mamQ-2* coding for a putative thioredoxin. This gene was also present in a gene cluster together with *mamK* and several *mad* genes of the recently described multicellular magnetotactic prokaryote *Ca. Magnetomorum* HK-1 (Kolinko et al. 2014). Due to its high conservation among MTB of the *Nitrospirae* phylum and presence in the *Deltaproteobacteria* class and absence of homologs in the *Alphaproteobacteria*, it was termed *mad31*. Thioredoxins are small ubiquitous proteins with a highly conserved active site sequence (Holmgren 1985, 95, Martin 1995) and possess functions in redox regulation and oxidative stress response (Zeller et al. 2006) and therefore may be involved in the maintenance of physico-chemical conditions necessary for magnetosome biomineralization.

Individual Mam and Mad protein of *Ca. M. bavaricum*, *Ca. M. casensis*, *Ca. Magnetoovum* CS-04, *Ca. Magnetotrophicum* SKK-01, *Ca. Magnetomorum* HK-1 together with *Ca. Magnetoglobus multicellularis*, *Ca. Desulfamplus magnetomortis* BW-1, *Desulfovibrio magneticus* RS-1, *Magnetospirillum gryphiswaldense* MSR-1 and *Magnetococcus marinus* MC-1, involved in magnetite and greigite biomineralization were analyzed separately (Figure S1) and in concatenation. Mam proteins of the *Nitrospirae* and the *Deltaproteobacteria* are more closely related to each other than to those of the *Alphaproteobacteria*. Noteworthy, individual and concatenated Mam and Mad magnetosome proteins of all *Nitrospirae* clustered within the *Deltaproteobacteria* and were more closely related to those putatively involved in greigite than to those in magnetite biomineralization, which was previously described for Mam proteins only (Abreu et al. 2014) (Figure X).

Mam and Mad proteins of SKK-01, the only known magnetotactic representative of the deep-branching candidate phylum *Omnitrophica*, seemed to be closely related to those of CS-04 within the deep-branching *Nitrospirae*.

Discussion

While the numbers of magnetic *Proteobacteria* in available axenic cultures are slightly increasing, MTB of the deep-branching phyla *Nitrospirae* and *Omnitrophica* have remained recalcitrant to cultivation attempts despite of considerable effort. However, a growing number of uncultivated MTB of the *Nitrospirae* phylum from diverse habitats in Germany, USA and China (Flies *et al.*, 2005; Kolinko *et al.*, 2013; Lefèvre *et al.*, 2011; Lin *et al.*, 2011; Lin *et al.*, 2014; Spring *et al.*, 1993) have been described and suggest a worldwide distribution. In contrast to nonmagnetic uncultivated microorganisms, MTB can be directly collected from environmental samples and separated from sediment particles and other microorganisms by using their magnetically directed motility (Flies *et al.*, 2005). Metagenomic analysis of magnetically collected MTB revealed highly conserved magnetotactic signature genes in MTB of the deep-branching phylum *Nitrospirae*, with homology to those in *Proteobacteria* (Jogler *et al.*, 2011). Recently, the genome of the uncultivated MTB *Ca. M. casensis* has been partly sequenced from highly enriched magnetic enrichments (Lin *et al.*, 2014). This genome sequencing approach uses highly enriched magnetic collections of uncultivated MTB and relied on high cell numbers, and thus are limited to abundant representatives. With most uncultivated MTBs with conspicuous and unique morphologies being low abundant, other abundance-independent techniques must be applied.

By the combination of micromanipulation, whole-genome amplification (WGA) and 16S rRNA PCR a novel ovoid MTB designated as SKK-01 of the deep-branching candidate phylum *Omnitrophica* (formerly candidate division OP3 (Rinke *et al.*, 2013)) was identified (Kolinko *et al.*, 2012). Recently, a cultivation-independent targeted approach applying single-cell techniques was used to recover draft genomes of several uncultivated bacteria from candidate phyla directly from environmental samples for functional analysis (Rinke *et al.*, 2013).

By targeted single-cell techniques combined with next generation sequencing, single amplified genomes (SAGs) from 3 conspicuous magnetic morphotypes were recovered and unambiguously assigned to *Ca. M. bavaricum*, *Ca. M. chiemensis* and *Ca. O. magneticus*

(Kolinko *et al.*, 2012; Kolinko *et al.*, 2013). The obtained draft genomes were 3.9, 6.3 and 3.4 Mb in size and had an estimated genome completeness of 74.1, 74.8 and 87.1%, respectively for *Ca. M. chiemensis*, *Ca. M. bavaricum* and *Ca. O. magneticus*, and were therefore sufficient for functional genome analysis.

General metabolism

All analyzed MTB shared a putative autotrophic lifestyle fixing CO₂ through the reverse citric acid cycle or the WL-pathway, which was only present in magnetic *Nitrospirae* *Ca. M. bavaricum* and *Ca. M. chiemensis* and is consistent with the identification of the WL-pathway and the reverse citric acid cycle in the draft genome of *Ca. M. casensis* (Lin *et al.*, 2014). The WL-pathway can be found in acetogens, methanogens and many sulfate reducers (Sousa *et al.*, 2013).

Despite ultrastructural identification of sulfur inclusions in magnetic *Nitrospirae* and their consumption during prolonged microaerobic storage in *Ca. M. bavaricum*, indicating a sulfur oxidizing metabolism (Jogler *et al.*, 2010; Kolinko *et al.*, 2012; Kolinko *et al.*, 2013) we identified genes coding for enzymes Sat, Apr and Dsr, which are involved in dissimilatory sulfate reduction, but were suggested to operate in reverse direction (Zhou *et al.*, 2011). Additionally, the oxidation of sulfide to sulfur is putatively catalyzed by the sulfide:quinone oxidoreductase, which was present in their draft genomes.

The reversibility of sulfur oxidation and the vertical distribution of *Ca. M. bavaricum* in sediments, forming two peaks, with one at the OATZ and the other close to the anoxic zone (Jogler *et al.*, 2010), suggesting electron shuttling between sulfate and sulfide depending on redox conditions, as reported for some bacteria, like *Desulfovibrio desulfuricans* und *Desulfovibrio vulgaris* (Cypionka, 1994; Dannenberg *et al.*, 1992; Dilling & Cypionka, 1990). The identification of a DNRA-pathway in both *Nitrospirae* and an additional DN-pathway in *Ca. M. bavaricum*, as well a partial respiratory chain, indicated an oxidation of reduced sulfur compounds at the OATZ with nitrate and oxygen respectively. In deeper, anaerobic and

therefore more reduced sediment layers they may use sulfate as terminal electron acceptor.

This findings as postulated for *Ca. M. casensis*(Lin *et al.*, 2014).

In contrast to *Ca. M. bavaricum* and *Ca. M. chiemensis*, a less metabolic flexibility was concluded the draft genome of *Ca. O. magneticus*. The presence of sulfur-rich inclusions indicated a sulfur oxidizing metabolism in the magnetotactic *Omnitrophica* SKK-01 and is in agreement with the identification of a dissimilatory sulfite reductase (dSiR). DSiR is postulated to be involved in the oxidation of sulfide under certain putatively more oxidized conditions(Steuber & Kroneck, 1998), as found at the OATZ where most SKK-01 cells were present in 10 mm sediment depth, coinciding with a transition in color of the stratified sediment, indicating a change from oxic to reduced conditions (Kolinko *et al.*, 2012).

Therefore a sulfur cycling between sulfate and sulfide, depending on redox conditions may be performed by *Ca. O. magneticus*, similar to *Ca. M. bavaricum* and *Ca. M. chiemensis*, but further studies need to prove this hypothesis of energy-conservation for deep-branching MTB. *Ca. M. bavaricum* and *Ca. M. chiemensis* display complex metabolic strategies similar to *Ca. M. casensis*, allowing them to quickly adapt to changing environmental conditions which may lead to a growth advantage of these microorganisms.

The accumulation of large amounts of iron is required for magnetosome biosynthesis, therefore the intracellular iron content may account for up to 4% of the dry weight.

Ca. M. bavaricum and *Ca. M. chiemensis* seem to accumulate ferrous iron applying the NRAMP and Feo system, which is supported by the identification of genes of the NRAMP transporter family and genes *feoA* (*mad17*) and *feoB* (*mad30*) in both genomes. Whereas *mad17*, *mad30* and a *mamB* were contiguously present in *Ca. M. chiemensis*, two *mad17* genes upstream of a *mad30* in *Ca. M. bavaricum*, which were found together on one contig. The uptake of ferric iron occurs probably through TonB-dependent transporters, despite the absence of genes governing siderophore biosynthesis.

The *mamAB* operon of magnetite-producing contains a conserved set of core genes (*mamABEIKLMOPQ*), which encode the minimal set of universal functions for magnetosome biosynthesis (Lefèvre *et al.*, 2013; Lohsse *et al.*, 2014; Murat *et al.*, 2010) and crystal formation in a heterologous host (Kolinko *et al.*, 2014).

Genomic analysis identified these genes (*mamABEIKMOPQ*) in the draft genome of *Ca. M. bavaricum* organized in a *mamAB*-like operon, and showed insignificant divergences compared with a previously described partial *mamAB-like* operon of a metagenomic clone (Jogler *et al.*, 2011) and only minor divergences to the full *mamAB-like* operon of *Ca. M. casensis* with respect to gene order, G+C content (~50%) and average sequence identity (Lin *et al.*, 2014). These remarkable similarities between *Ca. M. bavaricum* and *Ca. M. casensis*, which were found at geographic distant habitats, indicate a strong conservation of the *mamAB*-operon in the `Ca. Magnetobacterium` genus.

The *mam* genes (*mamABQME*) found in the partial *mamAB*-operon of CS-04 were arranged similar to *Ca. M. bavaricum*, except for *mamE* being located upstream of *mamM* and not downstream of *mamA*. Further, partial magnetosome genes *mamP* and a second *mamM* were found together on a small contig.

In contrast to the `Ca. Magnetobacterium` genus, magnetosome genes *mamK* and a second *mamB* were found in the *mad28-29*-operon. This divergence is reflected by significant sequence divergences at the 16S rRNA gene level and a differing G+C content (40%) between CS-04 and bacteria of the `Ca. Magnetobacterium` genus and may suggest a higher diversity within this group as previously speculated (Kolinko *et al.*, 2013).

Despite, the draft genome of SKK-01 had the highest estimated genome completeness among our data set, only few partial magnetosome genes (*mamEBMK*) could be identified on small discontinuous contigs and therefore no gene order could be analyzed. This contradiction suggests that accessory/further magnetosome genes of the deep-

branching candidate phylum Omnitrophica, share low or even no homology/identity to those found in the *Proteobacteria* and *Nitrospirae*.

So far, greigite magnetosome formation is only described for MTB of the *Deltaproteobacteria* and was never observed for MTB of the *Nitrospirae* phylum. According to this observation no gene-cluster with any homology to greigite magnetosome genes was found in our draft-genomes, contraindicating a genetic potential for greigite biomineralization in *Nitrospirae* MTB.

However, a number of previous identified alphaproteobacterial magnetosome genes, such as *mamHRSTNOLJ* were not found in the draft genomes, including *Ca. M. casensis*.

Interestingly, we identified several genes in all draft genomes with great homology to *mad* genes, either interspacing *mam* genes or found on contigs harboring homologs to *mam* genes. Lefèvre et al found a set of 18 *mad* genes specific to magnetotactic *Deltaproteobacteria* that biomineralize bullet-shaped magnetosomes (Lefèvre et al., 2013). By including our draft genomes of deep-branching MTB and the draft genome of *Ca. M. casensis* we were able to refine/reduce this set to ~11 proteins, including Mad2, Mad10, Mad11, Mad17, Mad23, Mad24, Mad25, Mad26, Mad28, Mad29 and Mad30. The genes coding for Mad11 and Mad20 were also present in the genome of *Ca. M. casensis* but mistakenly annotated as *man1* and *man4*.

Due the ubiquitous presence of *mad* genes in bullet-shape magnetosome forming and deep-branching MTB, this group of genes should be redefined as “magnetosome associated deep-branching”.

The putative magnetosome gene *mad11* is conserved in all deep-branching MTB and the *Deltaproteobacteria* and is always accompanying *mamK* (Lefèvre et al., 2013), including *Desulfovibrio magneticus*, *Ca. Magnetomortis desulfamplus*, bacterium FH-1 and in the recently published draft genome of the magnetotactic multicellular prokaryote *Ca.*

Magnetomorum HK-1 (Kolinko et al. 2014 in review), indicating a function in magnetosome chain formation. Despite, no conserved domain or motif could be identified and no function

for Mad11 was predicted, an accessory function in magnetosome biosynthesis can be hypothesized.

A small cluster comprising magnetosome genes *mad23*, *mad24*, *mad25* and *mad26* was found in all *Nitrospirae* and *Deltaproteobacteria* genomes of MTB synthesizing bullet-shaped magnetosomes. Except for Mad23, which is putatively involved in protein interaction, no functions are predicted for Mad24, Mad25 and Mad26. Nonetheless, it is possible that these genes specific to the deep-branching MTB might govern accessory functions, like control of size, shape and organization of magnetosomes, similar to the *GFDC*-operon in magnetic *Alphaproteobacteria*.

The magnetic *Nitrospirae* *Ca. M. bavaricum*, *Ca. M. casensis* and CS-04 biosynthesize multiple chains of magnetosomes traversing the cell along their cell length axis (Hanzlik *et al.*, 1996; Lin *et al.*, 2014; Spring *et al.*, 1993). Apparently, all MAIs contained a gene encoding the actin-like protein MamK, which forms a cytoskeletal element and is hypothesized to be involved in magnetosome chain assembly (Katzmann *et al.*, 2010; Komeili *et al.*, 2006). Noteworthy, we found up to 5 copies of *mad28* randomly scattered in our draft genomes and *Ca. M. casensis* respectively, which codes for the actin-like protein Mad28 (Lefèvre *et al.*, 2013). This high amount of potential cytoskeletal proteins might be associated with the ability of magnetic *Nitrospirae* to withstand strong magnetic interactions caused by up to 1,000 magnetosomes arranged in multiple chains.

Preliminary heterologous expression of a MamK-eGFP fusion protein of *Ca. M. bavaricum* in *M. gryphiswaldense* did not result in filament formation (Toro *et al.* unpublished data) and may indicate the necessity of accessory proteins in this bacterium. These observations are consistent with the demonstration of filamentous structures in *Ca. M. bavaricum* by cryo-SEM and –TEM, which unlikely to alphaproteobacterial filaments did not form a network of filament bundles but appeared to form ordered tubular structures with a hollow interior, around which the individual magnetosome strands are arranged (Jogler *et al.* 2011).

Interestingly, *mad28-2* is accompanied by a conserved gene coding for a membranous putative penicillin binding protein (PBP1A), which is involved in peptidoglycan synthesis as a

multimodular transpeptidase-transglycosylase (Banzhaf *et al.*, 2012; Sauvage *et al.*, 2008). Magnetosome chains in *Ca. M. bavaricum* are closely adjacent to the cell membrane and are asymmetrically distributed around the cells length axis (Jogler *et al.*, 2011) and not separated by the maximum possible distance from each other as previously postulated (Hanzlik *et al.*, 1996). The interaction of cytoskeletal elements with peptidoglycan synthesis would therefore cause a unidirectional cell bending, which is necessary during cell division to overcome the magnetostatic interactions between separating daughter chains, as described for *M. gryphiswaldense* (Katzmann *et al.*, 2011).

The gene *mad29* coding for a putative ATPase was another gene which was found to be located downstream of a *mad28* homolog in all magnetic Nitrospirae and the *Deltaproteobacteria Ca. D. magnetomortis* and *D. magneticus* (Lefèvre *et al.*, 2013). As an ATPase Mad29 may be involved in hydrolyzation of ATP putatively bound to polymerized Mad28 filaments and therefore in magnetosome repositioning as described for *M. gryphiswaldense* (Draper *et al.*, 2011).

Phylogenetic trees revealed that magnetosome proteins such as MamE, MamB, MamM, MamK and Mad11 of SKK-01 branch together with their homologs of MTB-relatives from the *Nitrospirae*, forming a branch within the class of magnetic *Deltaproteobacteria*. Due to the fact that these three magnetotactic groups are phylogenetically distantly related and separated by non-magnetotactic species a common magnetotactic ancestor for *Proteobacteria*, *Nitrospirae* and *Omnitrophica* seems very unlikely, as this scenario depends on multiple events of loss of magnetosome genes in all three phyla.

Another possibility represents the horizontal gene transfer of magnetosome genes between MTB of the *Proteobacteria*, *Nitrospirae* and *Omntitrophica*. In contrast to phylogenetic trees based on magnetosome proteins, phylogenetic 16S and 23S rRNA gene trees showed a clear separate branching of SKK-01 from *Nitrospirae* and *Proteobacteria* within the PVC superphylum (Kolinko *et al.*, 2013). Horizontal gene transfer of conserved magnetosome genes between *Proteobacteria*, *Nitrospirae* and *Omnitrophica* provides a more likely explanation of this contradiction. Metagenomic clones, which were assigned to the candidate

phylum *Omnitrophica* based on rRNA analysis, contained a high proportion of ORFs with best matches to homologues to *Deltaproteobacteria* and may have evolved similar capabilities (Glöckner *et al.*, 2010). The observed minor difference in G+C content between MAI (35.8%) and draft genome (38.1%) in SKK-01 argues against a recent horizontal gene transfer event and rather for an ancient event of transfer.

References

Abreu, F., Morillo, V., Nascimento, F. F. & other authors (2014). Deciphering unusual uncultured magnetotactic multicellular prokaryotes through genomics. *ISME J* **8**, 1055-1068.

Altschul, S. F., Madden, T. L., Schaffer, A. A., Zhang, J., Zhang, Z., Miller, W. & Lipman, D. J. (1997). Gapped BLAST and PSI-BLAST: a new generation of protein database search programs. *Nucleic Acids Res* **25**, 3389-3402.

Banzhaf, M., van den Berg van Saparoea, B., Terrak, M. & other authors (2012). Cooperativity of peptidoglycan synthases active in bacterial cell elongation. *Mol Microbiol* **85**, 179-194.

Baumgartner, J., Morin, G., Menguy, N., Perez Gonzalez, T., Widdrat, M., Cosmidis, J. & Faivre, D. (2013). Magnetotactic bacteria form magnetite from a phosphate-rich ferric hydroxide via nanometric ferric (oxyhydr)oxide intermediates. *Proc Natl Acad Sci U S A* **110**, 14883-14888.

Cypionka, H. (1994). Novel metabolic capacities of sulfate-reducing bacteria, and their activities in microbial mats. In *Microbial Mats*, pp. 367-376. Edited by L. Stal & P. Caumette. Berlin: Springer Heidelberg.

Dahl, C., Engels, S., Pott-Sperling, A. S., Schulte, A., Sander, J., Lubbe, Y., Deuster, O. & Brune, D. C. (2005). Novel genes of the *dsr* gene cluster and evidence for close interaction of Dsr proteins during sulfur oxidation in the phototrophic sulfur bacterium *Allochromatium vinosum*. *J Bacteriol* **187**, 1392-1404.

Dannenberg, S., Kroder, M., Dilling, W. & Cypionka, H. (1992). Oxidation of H₂, organic compounds and inorganic sulfur compounds coupled to reduction of O₂ or nitrate by sulfate-reducing bacteria. *Arch Microbiol* **158**, 93-99.

Dilling, W. & Cypionka, H. (1990). Aerobic respiration in sulfate-reducing bacteria. *FEMS Microbiol Lett* **71**, 123-127.

Dong, L. F., Sobey, M. N., Smith, C. J., Rusmana, I., Phillips, W., Stoff, A., Osborn, A. M. & Nedwell, D. B. (2011). Dissimilatory reduction of nitrate to ammonium, not denitrification or anammox, dominates benthic nitrate reduction in tropical estuaries. *Limnol Oceanogr* **56**, 279-291.

Draper, O., Byrne, M. E., Li, Z., Keyhani, S., Barrozo, J. C., Jensen, G. & Komeili, A. (2011). MamK, a bacterial actin, forms dynamic filaments *in vivo* that are regulated by the acidic proteins MamJ and LimJ. *Mol Microbiol* **82**, 342-354.

Flies, C. B., Peplies, J. & Schüler, D. (2005). Combined approach for characterization of uncultivated magnetotactic bacteria from various aquatic environments. *Appl Environ Microbiol* **71**, 2723-2731.

Glöckner, J., Kube, M., Shrestha, P. M., Weber, M., Glöckner, F. O., Reinhardt, R. & Liesack, W. (2010). Phylogenetic diversity and metagenomics of candidate division OP3. *Environ Microbiol* **12**, 1218-1229.

Guindon, S. & Gascuel, O. (2003). A simple, fast, and accurate algorithm to estimate large phylogenies by maximum likelihood. *Systematic biology* **52**, 696-704.

Guindon, S., Dufayard, J. F., Lefort, V., Anisimova, M., Hordijk, W. & Gascuel, O. (2010). New algorithms and methods to estimate maximum-likelihood phylogenies: assessing the performance of PhyML 3.0. *Systematic biology* **59**, 307-321.

Gupta, R. S., Bhandari, V. & Naushad, H. S. (2012). Molecular Signatures for the PVC Clade (*Planctomycetes*, *Verrucomicrobia*, *Chlamydiae*, and *Lentisphaerae*) of *Bacteria* Provide Insights into Their Evolutionary Relationships. *Frontiers in Microbiology* **3**, 327.

Hanzlik, M., Winklhofer, M. & Petersen, N. (1996). Spatial arrangement of chains of magnetosomes in magnetotactic bacteria. *Earth Planet Sci Lett* **145**, 125-134.

Hugenholtz, P., Pitulle, C., Hershberger, K. L. & Pace, N. R. (1998). Novel division level bacterial diversity in a Yellowstone hot spring. *J Bacteriol* **180**, 366-376.

Jogler, C., Niebler, M., Lin, W. & other authors (2010). Cultivation-independent characterization of '*Candidatus Magnetobacterium bavaricum*' via ultrastructural, geochemical, ecological and metagenomic methods. *Environ Microbiol* **12**, 2466-2478.

Jogler, C., Wanner, G., Kolinko, S., Niebler, M., Amann, R., Petersen, N., Kube, M., Reinhardt, R. & Schüler, D. (2011). Conservation of proteobacterial magnetosome genes and structures in an uncultivated member of the deep-branching *Nitrospirae* phylum. *Proc Natl Acad Sci U S A* **108**, 1134-1139.

Katzmann, E., Scheffel, A., Gruska, M., Plitzko, J. M. & Schüler, D. (2010). Loss of the actin-like protein MamK has pleiotropic effects on magnetosome formation and chain assembly in *Magnetospirillum gryphiswaldense*. *Mol Microbiol* **77**, 208-224.

Katzmann, E., Müller, F. D., Lang, C., Messerer, M., Winklhofer, M., Plitzko, J. M. & Schüler, D. (2011). Magnetosome chains are recruited to cellular division sites and split by asymmetric septation. *Mol Microbiol* **82**, 1316-1329.

Kolinko, I., Lohsse, A., Borg, S. & other authors (2014). Biosynthesis of magnetic nanostructures in a foreign organism by transfer of bacterial magnetosome gene clusters. *Nature Nanotechnol* **9**, 193-197.

Kolinko, S., Jogler, C., Katzmann, E., Wanner, G., Peplies, J. & Schüler, D. (2012). Single-cell analysis reveals a novel uncultivated magnetotactic bacterium within the candidate division OP3. *Environ Microbiol* **14**, 1709-1721.

Kolinko, S., Wanner, G., Katzmann, E., Kiemer, F., B, M. F. & Schuler, D. (2013). Clone libraries and single cell genome amplification reveal extended diversity of uncultivated magnetotactic bacteria from marine and freshwater environments. *Environ Microbiol* **15**, 1290-1301.

Komeili, A., Li, Z., Newman, D. K. & Jensen, G. J. (2006). Magnetosomes are cell membrane invaginations organized by the actin-like protein MamK. *Science* **311**, 242-245.

Lane, D. J. (1991). 16S/23S sequencing. In *Nucleic Acid Techniques in Bacterial Systematics*, pp. 115-175. Edited by E. Stackebrandt & M. G. Chichster: Wiley & Sons, New York.

Lefèvre, C. T., Frankel, R. B., Abreu, F., Lins, U. & Bazylnski, D. A. (2011). Culture-independent characterization of a novel, uncultivated magnetotactic member of the *Nitrospirae* phylum. *Environ Microbiol* **13**, 538-549.

Lefèvre, C. T., Trubitsyn, D., Abreu, F. & other authors (2013). Comparative genomic analysis of magnetotactic bacteria from the Deltaproteobacteria provides new insights into magnetite and greigite magnetosome genes required for magnetotaxis. *Environ Microbiol* **15**, 2712-2735.

Lin, W., Jogler, C., Schüler, D. & Pan, Y. (2011). Metagenomic analysis reveals unexpected subgenomic diversity of magnetotactic bacteria within the phylum *Nitrospirae*. *Appl Environ Microbiol* **77**, 323-326.

Lin, W., Deng, A., Wang, Z., Li, Y., Wen, T., Wu, L. F., Wu, M. & Pan, Y. (2014). Genomic insights into the uncultured genus 'Candidatus Magnetobacterium' in the phylum *Nitrospirae*. *ISME J*.

Lohsse, A., Borg, S., Raschdorf, O., Kolinko, I., Tompa, E., Pósfai, M., Faivre, D., Baumgartner, J. & Schüler, D. (2014). Genetic dissection of the mamAB and mms6 operons reveals a gene set essential for magnetosome biogenesis in *Magnetospirillum gryphiswaldense*. *J Bacteriol* **196**, 2658-2669.

Markowitz, V. M., Chen, I. M., Palaniappan, K. & other authors (2012). IMG: the Integrated Microbial Genomes database and comparative analysis system. *Nucleic Acids Res* **40**, D115-122.

Murat, D., Quinlan, A., Vali, H. & Komeili, A. (2010). Comprehensive genetic dissection of the magnetosome gene island reveals the step-wise assembly of a prokaryotic organelle. *Proc Natl Acad Sci U S A* **107**, 5593-5598.

- Punta, M., Coggill, P. C., Eberhardt, R. Y. & other authors (2012).** The PFAM protein families database. *Nucleic Acids Res* **40**, D290-301.
- Rinke, C., Schwientek, P., Sczyrba, A. & other authors (2013).** Insights into the phylogeny and coding potential of microbial dark matter. *Nature* **499**, 431-437.
- Sauvage, E., Kerff, F., Terrak, M., Ayala, J. A. & Charlier, P. (2008).** The penicillin-binding proteins: structure and role in peptidoglycan biosynthesis. *FEMS Microbiol Rev* **32**, 234-258.
- Sousa, F. L., Thiergart, T., Landan, G., Nelson-Sathi, S., Pereira, I. A., Allen, J. F., Lane, N. & Martin, W. F. (2013).** Early bioenergetic evolution. *Philosophical transactions of the Royal Society of London Series B, Biological sciences* **368**, 20130088.
- Spring, S., Amann, R., Ludwig, W., Schleifer, K. H., van Gemerden, H. & Petersen, N. (1993).** Dominating role of an unusual magnetotactic bacterium in the microaerobic zone of a freshwater sediment. *Appl Environ Microbiol* **59**, 2397-2403.
- Steuber, J. & Kroneck, P. M. H. (1998).** Desulfoviridin, the dissimilatory sulfite reductase from *Desulfovibrio desulfuricans* (Essex): new structural and functional aspects of the membranous enzyme. *Inorganica Chimica Acta* **275**, 52–57.
- Tamura, K., Stecher, G., Peterson, D., FilipSKI, A. & Kumar, S. (2013).** MEGA6: Molecular Evolutionary Genetics Analysis version 6.0. *Molecular biology and evolution* **30**, 2725-2729.
- Wagner, M. & Horn, M. (2006).** The *Planctomycetes*, *Verrucomicrobia*, *Chlamydiae* and sister phyla comprise a superphylum with biotechnological and medical relevance. *Curr Opin Biotechnol* **17**, 241-249.
- Whelan, S. & Goldman, N. (2001).** A general empirical model of protein evolution derived from multiple protein families using a maximum-likelihood approach. *Molecular biology and evolution* **18**, 691-699.
- Woyke, T., Sczyrba, A., Lee, J., Rinke, C., Tighe, D., Clingenpeel, S., Malmstrom, R., Stepanauskas, R. & Cheng, J. F. (2011).** Decontamination of MDA reagents for single cell whole genome amplification. *PLoS One* **6**, e26161.
- Zhou, J., He, Q., Hemme, C. L. & other authors (2011).** How sulphate-reducing microorganisms cope with stress: lessons from systems biology. *Nat Rev Microbiol* **9**, 452-466.

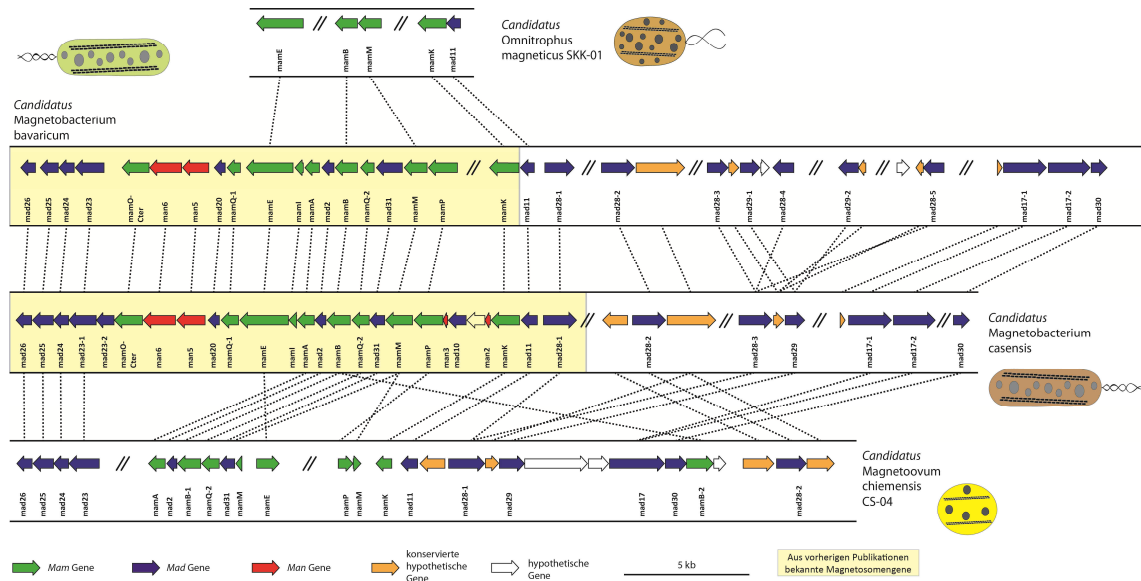


Figure 1: Schematic comparison of magnetosome gene clusters of *Ca. Magnetobacterium bavaricum*, *Ca. Magnetobacterium casensis*, *Ca. Magnetovum chiemensis* and *Ca. Omnitrophus magneticus*.

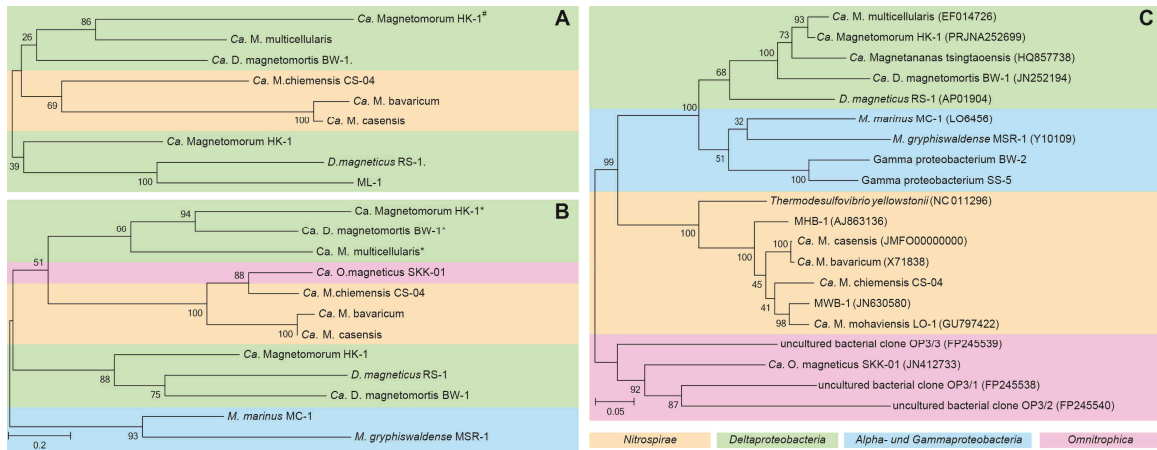


Figure 2: Phylogenetic Maximum-Likelihood tree based on concatenated amino-acid sequences of Mad (A) and Mam (B) genes. * Magnetosome genes likely involved in greigite biomineralization. # mad genes closely associated to putatively mam genes likely involved in greigite biomineralization in Ca. Magnetomorphum strain HK-1. (C) Phylogenetic tree of 16S rRNA gene sequences

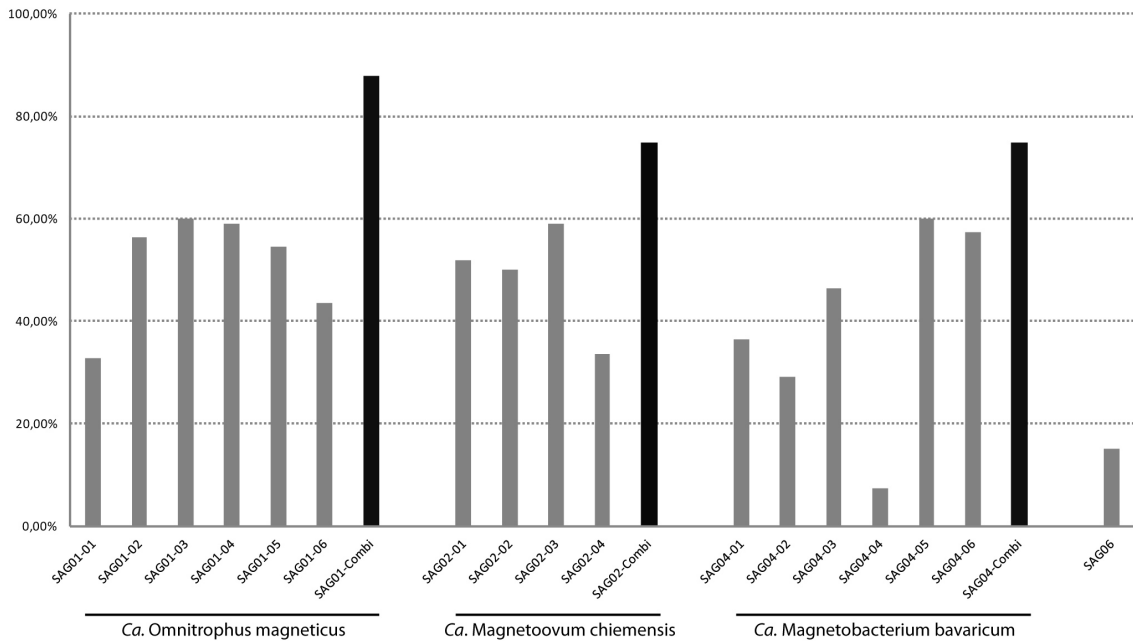


Figure S1 alternative 1: Estimated genome completeness for single amplified genomes (gray) and combined draft genomes (black) [SAG01 entspricht SKK01)(Magnetoovum hydrogenophilus), SAG02 entspricht CS04 (Ovoides *Nitrospirae* aus dem Chiemsee) *Ca. Magnetoovum sulfurreducens* und SAG04 entspricht Mbav

Table 1. General genomic features of the draft genomes of *Ca. Omnitrophus magneticus* SKK1, *Ca. Magnetoovum chiemensis* CS-04, *Ca. Magnetobacterium bavaricum*, and for comparison *Ca. Magnetobacterium casensis* (Lin *et al.*, 2014)

Parameter	<i>Candidatus</i> <i>Magnetoovum</i> <i>chiemensis</i> CS-04	<i>Candidatus</i> <i>Magnetobacterium</i> <i>bavaricum</i>	<i>Candidatus</i> <i>Omnitrophus</i> <i>magneticus</i> SKK01	<i>Candidatus</i> <i>Magnetomorum</i> HK-1	<i>Candidatus</i> <i>Magnetobacterium</i> <i>casensis</i>
Genomgröße (Mb)	3.9	6.3	3.4	14.3	3.4
G+C Gehalt (%)	40.4	47.40	35.80	34.7	48.90
Anzahl der Contigs	1402	4211	1120	3197	70
N50 (kb)	9.651	4.571	15.846	17.5	90.253
Maximale Contigröße (kb)	43.149	67.959	133.939	122.255	239.626
Genomvollständigkeit (%)	74.1	74.8	87.1	95.1	N/A
Geschätzte Genomgröße (Mb)	5.3	8.4	3.9	15.5	3.4
Anzahl kodierender Sequenzen	4527	8277	3439	14451	3140
Anzahl der tRNAs	45	69	42	49	40
rRNA Operons	1	1	1	1	1
MAI-Größe(kb)	27.9	46	4.8	50.8	39.2
G+C Gehalt der MAI (%)	39.5	50.20	38.10	38.2	49.80
Anzahl putativer Magnetosomene	21	30	6	51	31

Table 2: Comparison of Mam, Mad, Man and putative magnetosome proteins involved in magnetosome formation identified in the draft genome of *Ca. M. bavaricum* against draft genomes of *Ca. Magnetoovum chiemensis* CS-04, *Ca. M. casensis*, *Ca. Omnitrophus magneticus* SKK-01 and the Genbank database.

Putative protein	Accession number	Bacetrium with protein with highest sequence identity	Accession	Identity [%]	E-Value	Bacetrium with protein with second highest sequence identity	Accession	Identity [%]	E-Value	Bacetrium with protein with third highest sequence identity	Accession	Identity [%]	E-Value
Man6	orf7_glimmer3	Mbav	FQ377626	100.00	0.00E+00	Mcas	fig 798577.3.peg. 716	82.41	0.00E+00				
Man5 Cter	orf8_glimmer3	Mbav	FQ377626	100.00	2.70E-62	Mcas	fig 798577.3.peg. 717	73.08	4.75E-42				
Man5 Nter	orf9_glimmer3	Mbav	FQ377626	100.00	4.50E-169	Mcas	fig 798577.3.peg. 717	84.13	2.96E-133				
Man4 hypothetical protein MamO Cter	orf10_glimmer3	Mbav	FQ377626	100.00	1.07E-80	Mcas	fig 798577.3.peg. 718	91.10	1.64E-72				
MamQ-1	orf11_glimmer3	Mbav	FQ377626	100.00	7.88E-126	Mcas	fig 798577.3.peg. 719	88.72	4.54E-145	SAG2	YP_361264	43.51	1.00E-61
MamE	orf12_glimmer3	Mbav	FQ377626	99.45	4.23E-118	Mcas	fig 798577.3.peg. 720	90.61	2.59E-116	SAG2	SAG2_001748	39.98	1.44E-41
MamI	orf13_glimmer3	Mbav	FQ377626	100.00	7.27E-42	Mcas	XXX fig 798577.3.peg. 722	93.67	1.79E-43	SAG2	Magnetofaba australis IT-1 AHG23891	43.59	1.55E-11
MamA	orf14_glimmer3	Mbav	FQ377626	98.77	3.93E-55	Mcas	fig 798577.3.peg. 722	90.61	2.59E-116	SAG2	SAG2_000254	41.89	1.44E-17
MamB	orf16_glimmer3	Mbav	FQ377626	99.63	3.33E-180	Mcas	fig 798577.3.peg. 724	93.01	8.97E-170	SAG2	SAG2_000252	65.56	7.89E-121
MamQ-2	orf17_glimmer3	Mbav	FQ377626	99.45	9.35E-136	Mcas	fig 798577.3.peg. 725	82.56	1.01E-121	SAG2	SAG2_000251	37.30	6.03E-43
MamM	orf19_glimmer3	Mbav	FQ377626	100.00	0.00E+00	Mcas	fig 798577.3.peg. 727	94.79	0.00E+00	SAG1	WGA_2131_0	64.54	1.83E-65
MamP	orf20_glimmer3	Mbav	FQ377626	98.54	0.00E+00	Mcas	fig 798577.3.peg. 728	79.48	0.00E+00	SAG2	SAG2_002945	57.22	3.20E-72
MamK	SAG4_006134	Mbav	AFX60119	97.48	1.10E-78	Mcas	fig 798577.3.peg. 733	96.82	3.24E-109	SAG1	SAG1_WGA_9 31_1	65.19	8.98E-86
Mad26	orf2_glimmer3	Mbav	FQ377626	93.01	8.45E-112	Mcas	fig 798577.3.peg. 710	81.22	2.49E-113	SAG2	SAG2_002159	31.55	1.17E-24
Mad25	orf3_glimmer3	Mbav	FQ377626	100.00	1.60E-148	Mcas	fig 798577.3.peg. 711	80.83	9.78E-132	SAG2	SAG2_002158	41.21	1.27E-40
Mad24	orf4_glimmer3	Mbav	FQ377626	100.00	1.49E-122	Mcas	fig 798577.3.peg. 712	87.75	5.92E-124	SAG2	Cand. Magnetoglobus multicellularis ETR64730	27.39	1.85E-10
Mad23	orf5_glimmer3	Mbav	FQ377626	100.00	7.18E-32	Mcas	fig 798577.3.peg. 713	65.96	5.12E-26				
Mad2	orf15_glimmer3	Mcas	fig 798577.3.peg. 723	95.49	1.05E-91	SAG2	SAG2_000253 fig 798577.3.peg. 726	28.21	2.67E-16	ML-1	AFZ77013	28.33	2.49E-08
Thioredoxin	orf18_glimmer3	Mbav	FQ377626	100.00	2.65E-127	Mcas	fig 798577.3.peg. 734	87.22	4.45E-115	SAG2	SAG2_000250	38.10	2.60E-40
Mad11	SAG4_006135	Mcas	fig 798577.3.peg. 735	61.29	9.77E-72	SAG1	SAG1_WGA_9 31_0	27.23	1.45E-20	SAG2	SAG2_000031	27.23	1.45E-20
Mad28-1	SAG4_006136	Mcas	fig 798577.3.peg. 735	80.52	0.00E+00	Mcas	XXX fig 798577.3.peg. 735	76.96	0.00E+00	MLMS-1	WP_00729099 5	63.80	1.32E-148
Mad28-4	SAG4_001692	Mcas	fig 798577.3.peg. 735	91.72	0.00E+00	Mcas	fig 798577.3.peg. 735	91.40	0.00E+00	MLMS-1	WP_00729099 5	66.77	6.11E-142
Mad28-3	SAG4_001959	Mcas	fig 798577.3.peg. 735	92.68	0.00E+00	Mcas	fig 798577.3.peg. 735	91.40	0.00E+00	MLMS-1	WP_00729099 5	66.45	3.98E-141
Mad29-1	SAG4_001962	Mcas	XXX fig 798577.3.peg. 735	87.67	0.00E+00	SAG2	SAG2_000027 fig 798577.3.peg. 735	47.65	2.81E-91	BW-1	CCO06735	42.91	2.31E-78
Mad28-4	SAG4_001964	Mcas	fig 798577.3.peg. 735	92.68	0.00E+00	Mcas	fig 798577.3.peg. 735	91.40	0.00E+00	MLMS-1	WP_00729099 5	66.45	3.98E-141
Mad28-6, partial	SAG4_004173	Mcas	fig 798577.3.peg. 735	70.59	7.27E-58	Mcas	fig 798577.3.peg. 735	59.06	9.83E-49	MLMS-1	WP_00729099 5	61.76	3.21E-20
Mad30	SAG4_005787	Mcas	1239 fig 798577.3.peg. 908	91.94	1.51E-159	SAG2	SAG2_000023 fig 798577.3.peg. 909	53.44	9.76E-93	FH-1	AGG16216	50.94	2.94E-67
Mad17-1	SAG4_005788	Mcas	fig 798577.3.peg. 908	86.13	0.00E+00	Mcas	fig 798577.3.peg. 909	79.42	0.00E+00	SAG2	SAG2_000024	53.18	0.00E+00
Mad17-2	SAG4_005789	Mcas	fig 798577.3.peg. 908	88.26	0.00E+00	Mcas	fig 798577.3.peg. 909	79.69	0.00E+00	SAG2	SAG2_000024	52.80	0.00E+00
Mad28-2	SAG4_006080	Mcas	735	96.88	0.00E+00	SAG2	SAG2_000493	56.08	1.51E-136	MLMS-1	WP_00729099 5	58.56	1.61E-138
Mad29-2	SAG4_006507	Mcas	735	89.67	0.00E+00	SAG2	SAG2_000027	46.98	4.42E-90	BW-1	CCO06735	41.89	1.31E-76

Table 3: Comparison of Mam, Mad, and putative magnetosome proteins involved in magnetosome formation identified in the draft genome of *Ca. Magnetoovum chiemensis* CS-04 against draft genomes of *Ca. M. bavaricum*, *Ca. M. casensis*, *Ca. Omnitrophus magneticus* SKK-01 and the Genbank database.

Putative protein	Accession number	Bacetrium with protein with highest sequence identity	Accession	Identity [%]	E-Value	Bacetrium with protein with second highest sequence identity	Accession	Identity [%]	E-Value	Bacetrium with protein with third highest sequence identity	Accession	Identity [%]	E-Value	
MamK	extra_04	Mcas	fig 798577.3.peg.711	62.92	2.04E-78	Mbav	orf16_glimmer3	62.36	2.18E-80	ML-1	AFZ77032	57.23	2.80E-64	
MamB-2	SAG2_000022	AMB-1	YP_420341	44.22	7.44E-84	SO-1	WP_008622202	43.22	1.06E-84	MV-1	CAV30807	42.16	3.94E-74	
Mad30	SAG2_000023	Mcas	fig 798577.3.peg.1239	59.07	1.68E-97	Mbav	SAG4_005787	55.13	7.20E-97	FH-1	AGG16216	45.02	9.62E-62	
Mad17	SAG2_000024	Mcas	fig 798577.3.peg.908	55.06	0.00E+00	Mbav	SAG4_005788	54.00	0.00E+00	BW-1	AET24920	53.69	0.00E+00	
Mad29	SAG2_000027	Mbav	SAG4_001962	47.65	2.85E-91	Mcas	XXX	46.28	2.35E-89	BW-1	CCO06735	48.00	5.79E-89	
MamE	SAG2_000247	SAG1	WGA_1071_0	73.27	6.78E-85	Mcas	fig 798577.3.peg.720	53.73	1.69E-96	Mbav	FCQ377626	52.12	2.60E-87	
MamM-1	SAG2_000249	Mbav	FCQ377626	41.41	1.69E-29	Mcas	orf19_glimmer3	41.41	2.38E-29	SS-5	AFX88990	53.73	4.14E-22	
MamQ-II	SAG2_000251	Mcas	fig 798577.3.peg.725	40.13	3.91E-35	Mbav	FCQ377626	38.75	6.18E-35	Mbav	orf16_glimmer3	37.50	3.29E-35	
MamB-1	SAG2_000252	Mbav	FCQ377626	67.12	3.58E-130	Mcas	fig 798577.3.peg.724	67.12	3.58E-130	Mbav	orf16_glimmer3	65.56	5.32E-111	
putative MamA	SAG2_000254	Mbav	FCQ377626	52.85	5.00E-69	Mcas	fig 798577.3.peg.722	51.30	4.20E-68	Mbav	Crystal Structure Of Mama Protein	3VTX_A	55.35	3.81E-54
Mad28-2	SAG2_000493	MLMS-1	WP_007290995	56.85	3.28E-129	AHT2	YP_003690005	56.25	2.58E-126	Mbav	SAG4_006080	56.08	1.64E-137	
MamP, partial	SAG2_002945	Mbav	FCQ377626	57.22	5.40E-72	Mcas	fig 798577.3.peg.728	57.22	1.56E-65	Mbav	Crystal Structure Of MamP in Complex With Iron(ii)	4JJ3_A	44.00	3.43E-42
MamM-2	SAG2_002946	Mcas	727	55.21	1.73E-26	Mbav	FCQ377626	54.17	3.93E-26	SS-5	AFX_88990	47.19	4.18E-22	
Mad28-1	SAG2_000029	Mcas	XXX	63.80	3.11E-65	Mbav	SAG4_006136	58.43	2.50E-137	AHT2	YP_003690005	55.43	1.86E-131	
Mad11	SAG2_000031	SAG1	SAG1_WGA_931_0	41.76	4.34E-45	Mcas	fig 798577.3.peg.733	28.79	4.87E-17	Mbav	SAG4_006135	25.79	1.13E-19	
Thioredoxin	SAG2_000250	Mbav	FCQ377626	38.10	1.47E-38	Mcas	XY	37.98	8.48E-48	MMP	SAG5_007197	27.94	4.99E-32	
Mad2	SAG2_000253	Mcas	fig 798577.3.peg.723	29.91	2.43E-17	Mbav	orf15_glimmer3	28.21	2.82E+01	BW-1	AEX00095	33.62	1.20E-06	
Mad23	SAG2_002156	ML-1 [Candidatus Magnetoglobobus multicellularis str. Araruma]	AFZ77038	47.60	2.18E-58	Mcas	fig 798577.3.peg.713	45.61	1.03E-54	Mbav	FCQ377626	43.93	1.43E-55	
Mad24	SAG2_002157	ML-1 [Candidatus Magnetoglobobus multicellularis str. Araruma]	ADV17380	32.52	1.89E-16	Mcas	fig 798577.3.peg.712	28.17	3.45E-14	Mbav	orf4_glimmer3	27.46	2.52E-13	
Mad25 [SAG2_002158]	SAG2_002158	Mcas	fig 798577.3.peg.711	41.24	2.93E-37	Mbav	orf3_glimmer3	40.68	3.52E-39	BW-1	CCO06725	36.73	2.64E-24	
Mad26	SAG2_002159	Mcas	fig 798577.3.peg.710	34.09	2.20E-22	Mbav	orf2_glimmer3	32.58	9.19E-23	Mbav	Candidatus Magnetoglobobus multicellularis str. Araruma	ADV17378	33.98	1.61E-08

Table 4: Comparison of Mam and Mad magnetosome proteins involved in magnetosome formation identified in the draft genome of *Ca. Omnitrophus magneticus* SKK-01 against draft genomes of *Ca. M. bavaricum*, *Ca. M. casensis*, *Ca. Magnetoovum* CS-04 and the Genbank database.

Putative protein	Accession number	Bacetrium with protein with highest sequence identity			Bacetrium with protein with second highest sequence identity			Bacetrium with protein with third highest sequence identity					
		Accession	Identity [%]	E-Value	Accession	Identity [%]	E-Value	Accession	Identity [%]	E-Value			
Mad11	SAG1_WGA_9 31_0	SAG2	SAG2_000031	43.53	9.67E-41	Mcas	fig 798577.3.peg- 734	36.25	1.57E-21	Mbav	SAG4_006135	35.76	4.29E-19
MamK, partial	SAG1_WGA_9 31_1	Mbav	SAG4_006134 fig 798577.3.peg- 720	65.19	5.20E-84	Mcas	fig 798577.3.peg- 733	65.19	2.19E-81	MMP	ETR64725	62.22	8.68E-71
MamE	WGA_1071_0	Mcas		61.09	1.38E-101	SAG2	SAG2_000247 fig 798577.3.peg- 724	73.06	3.60E-83	Mbav	FQ377626	59.00	9.05E-92
MamB, partial	WGA_1430_0	SAG2	SAG2_000252	71.76	2.07E-39	Mcas		68.24	7.71E-31	Mbav	FQ377626	67.06	9.20E-30
MamM, partial	WGA_2131_0	Mcas		65.25	3.73E-64	Mbav	FQ377626	65.25	3.73E-64	LM-5	AEC03524	42.06	5.45E-24

5. Manuskript:

Conservation of proteobacterial magnetosome genes and structures in an uncultivated member of the deep-branching *Nitrospirae* phylum.

Conservation of proteobacterial magnetosome genes and structures in an uncultivated member of the deep-branching *Nitrospira* phylum

Christian Jogler^{a,1,2}, Gerhard Wanner^a, Sebastian Kolinko^a, Martina Niebler^a, Rudolf Amann^b, Nikolai Petersen^a, Michael Kube^c, Richard Reinhardt^{c,3}, and Dirk Schüler^{a,2}

^aLudwig Maximilians University, 82152 Munich, Germany; ^bMax Planck Institute for Marine Microbiology, 28359 Bremen, Germany; and ^cMax Planck Institute for Molecular Genetics, 14195 Berlin, Germany

Edited by Edward F. DeLong, Massachusetts Institute of Technology, Cambridge, MA, and approved November 30, 2010 (received for review August 26, 2010)

Magnetotactic bacteria (MTB) are a phylogenetically diverse group which uses intracellular membrane-enclosed magnetite crystals called magnetosomes for navigation in their aquatic habitats. Although synthesis of these prokaryotic organelles is of broad interdisciplinary interest, its genetic analysis has been restricted to a few closely related members of the *Proteobacteria*, in which essential functions required for magnetosome formation are encoded within a large genomic magnetosome island. However, because of the lack of cultivated representatives from other phyla, it is unknown whether the evolutionary origin of magnetotaxis is monophyletic, and it has been questioned whether homologous mechanisms and structures are present in unrelated MTB. Here, we present the analysis of the uncultivated “*Candidatus Magnetobacterium bavaricum*” from the deep branching *Nitrospira* phylum by combining micromanipulation and whole genome amplification (WGA) with metagenomics. Target-specific sequences obtained by WGA of cells, which were magnetically collected and individually sorted from sediment samples, were used for PCR screening of metagenomic libraries. This led to the identification of a genomic cluster containing several putative magnetosome genes with homology to those in *Proteobacteria*. A variety of advanced electron microscopic imaging tools revealed a complex cell envelope and an intricate magnetosome architecture. The presence of magnetosome membranes as well as cytoskeletal magnetosome filaments suggests a similar mechanism of magnetosome formation in “*Cand. M. bavaricum*” as in *Proteobacteria*. Altogether, our findings suggest a monophyletic origin of magnetotaxis, and relevant genes were likely transferred horizontally between *Proteobacteria* and representatives of the *Nitrospira* phylum.

Magnetotactic bacteria (MTB) are widespread aquatic microorganisms that use unique intracellular organelles called magnetosomes to navigate along the earth’s magnetic field while searching for growth-favoring microoxic zones within stratified sediments. In strains of *Magnetospirillum*, it was shown that magnetosomes consist of magnetite (Fe_3O_4) crystals enclosed by a dedicated phospholipid membrane. The magnetosome membrane (MM) contains a specific set of proteins (1–3), which direct the biomineralization of highly ordered crystals along actin-like cytoskeletal filaments that control the assembly and intracellular positioning of a linear magnetosome chain (4–7). Synthesis of magnetosomes has recently emerged as a model for prokaryotic organelle formation and biomineralization (8–11). The trait of magnetotaxis is widely spread among *Proteobacteria* including members from the α -, δ - and γ -subdivisions, as well as uncultivated species from the deep branching *Nitrospira* phylum (8). The presence of MTB within unrelated lines of various phylogenetic groups, as well as their stunning diversity with respect to magnetosome shape, composition, and intracellular organization lead to speculations of whether the evolutionary origin of magnetotaxis is polyphyletic. Thus, independent origins and subsequent convergent evolution were proposed for greigite and magnetite producing MTB (12), and it has been suggested that those MTB forming

magnetic crystals of divergent shapes or composition may use different mechanisms of magnetosome formation (13, 14).

Despite recent progress, magnetosome formation is not yet fully understood at the molecular and biochemical levels. Essential molecular factors, cellular structures, and processes leading to organelle formation and biomineralization have been characterized mostly in magnetospirilla. In *Magnetospirillum gryphiswaldense* most genes implicated in magnetosome synthesis were identified within several operons of a genomic magnetosome island (MAI) (15), which encodes functions in magnetosome membrane biogenesis, magnetosomal iron uptake, and control of magnetite crystallization (8, 10). Because of their conservation in other cultivated α -proteobacterial MTB (16, 17), it has been suggested that the MAI may have been transferred horizontally, which was further corroborated by the recent discovery of homologous gene clusters in metagenomic clones (18) and the δ -proteobacterial *Desulfovibrio magneticus* RS-1 (19). However, the limited genetic information about magnetosome formation that has been confined to a few cultivated MTB mainly of the α -*Proteobacteria*, is in striking disparity to the fact that MTB are a noncoherent and phylogenetically heterogeneous group. Because of the lack of cultivated representatives it has remained unknown whether homologous mechanisms and structures are used by divergent MTB from deep branching phyla outside the *Proteobacteria*.

One of the most intriguing systems for studying magnetosome formation in distantly related, nonproteobacterial MTB is the uncultivated “*Candidatus Magnetobacterium bavaricum*” (Mbav) from the deep branching *Nitrospira* phylum. Mbav has been identified originally within suboxic sediment layers of Bavarian lakes (20, 21), but a variety of related MTB were subsequently shown to display a wider global distribution (22–24). A recent cultivation-independent analysis of Mbav revealed first insights into its metabolic and genetic characteristics, suggesting that Mbav might be a chemolithoautotroph, obtaining energy from the oxidation of reduced sulfur compounds (21).

Compared to other MTB, Mbav is unique with respect to its large size (3–10 μm) and distinct cell biology, in particular to its numerous (up to 1,000) magnetosomes, which have a bullet-shaped, kinked morphology and are organized in multiple bundles

Author contributions: C.J., R.A., R.R., and D.S. designed research; C.J., G.W., S.K., M.N., N.P., and M.K. performed research; G.W., R.A., N.P., M.K., and R.R. contributed new reagents/analytic tools; C.J., G.W., S.K., M.N., R.A., N.P., M.K., R.R., and D.S. analyzed data; and C.J., G.W., and D.S. wrote the paper.

The authors declare no conflict of interest.

This article is a PNAS Direct Submission.

Data deposition: The sequence reported in this paper has been deposited in the GenBank database (accession no. [FQ377626](http://www.ncbi.nlm.nih.gov/nuccore/FQ377626)).

¹Present address: Harvard Medical School, Boston, MA 02115.

²To whom correspondence may be addressed. E-mail: christian_jogler@hms.harvard.edu or dirk.schueler@lrz.uni-muenchen.de.

³Present address: Max Planck Institute for Plant Breeding Research, 50829 Cologne, Germany.

This article contains supporting information online at www.pnas.org/lookup/suppl/doi:10.1073/pnas.1012694108/-DCSupplemental.

of chains (20, 21, 25). Because previous studies failed to detect a membrane around magnetosomes of Mbav, it was speculated that non- α MTB producing bullet-shaped magnetite crystals might use different biomineralization mechanisms based on “templates” that might be fundamentally divergent from the MM-dependent mechanism in magnetospirilla and related MTB (13, 14).

Here, we describe an approach for targeted subgenomic and ultrastructural analysis of *Candidatus M. bavaricum*. By combining whole genome amplification of DNA from few Mbav cells collected by micromanipulation with screening of metagenomic libraries, we demonstrate the presence of a putative genomic magnetosome island with homology to that in *Proteobacteria*. In addition, the detection of structures such as a magnetosome membrane as well as putative cytoskeletal magnetosome filaments suggests a similar mechanism of magnetosome formation in uncultivated MTB of the deep-branching *Nitrospira* phylum as in *Proteobacteria*.

Results

Magnetosomes of “*Candidatus M. bavaricum*” Are Enclosed by a Membrane and Arranged Along a Cytoskeletal Filamentous Structure.

Magnetic mass collections from sediment samples highly enriched in Mbav cells (>40%, Fig. 1A) were subjected to several advanced high-resolution imaging techniques. Transmission electron microscopy (TEM) and SEM of high-pressure frozen and freeze-substituted cells revealed a number of unusual ultrastructural characteristics (Figs. 1 and 2 and Figs. S1 and S2). In addition to a peptidoglycan layer and the outer membrane (OM) and inner membrane (IM), the multilayered cell boundary exhibits an unusually wide periplasmic space and a bipartite outer layer resembling a capsular structure, which forms ridges and star-like extensions (Fig. 1; see Fig. S1 for further details). Sulfur globuli and polyhydroxybutyrate (PHB)-like granules are present within the cytoplasm (Fig. 1B and Fig. S2). Cells have a single bundle of \approx 40 flagella (15–20 nm in diameter), which originate from different discrete spots of one cell pole (Figs. 1G and 2D). Overall, the cell wall structure resembles that of related representatives of the *Nitrospira* phylum, such as *Nitrospira marina* (26), *N. moscoviensis* (27), and *N. defluvii* (28), whereas the bipartite outer layer seems to be a distinct feature of the Mbav cell envelope.

As revealed by different imaging techniques, cells contained multiple chains of magnetosomes (Figs. 1A and 2). In contrast to previous studies, we found that the morphology and size of crystals was more variable including bullet-shaped, conical, or blunted polyheders, which had kinked or bent appearances. In SEM micrographs of fractured cells, magnetosomes appeared in densely packed bundles of several individual strands (Fig. 2A). SEM of focused ion beam sections of cryopreparations (Fig. 2F), and high-pressure frozen and freeze-substituted (Fig. 2G) cells revealed that the magnetosome bundles consist of three to six (mostly five) individual magnetosome strands that are arranged around a central core and form a regular rosette-like bundle (Fig. 2F), which is situated 20–50 nm beneath the cytoplasmic membrane. In cross-sections, between two and six of such magnetosome bundles appeared to be distributed preferentially within a roughly semi-circular segment along the periphery of cells (Fig. 2G). Individual strands maintain nearly identical positions in 3D reconstructions by serial focused ion beam (FIB) sectioning (Fig. 2G and Movie S1). This argues against a twisted “braid-like” helical structure, which was described in previous studies (e.g., ref. 25). Instead, individual strands within a bundle appear aligned parallel to each other.

Intriguingly, TEM of ultrathin sections of high-pressure frozen and freeze-substituted cells revealed that strands are aligned parallel to a filamentous structure (Fig. 2B, asterisks). At higher magnification this filament is bound by two electron dense layers, which suggests that filaments may form a tubular structure with a diameter of 12–13 nm (Fig. 2C). Filaments closely adjacent to magnetosome particles were also seen in cryo-SEM of tangential-fractured cells (Fig. 2D) and 3D reconstructions of FIB “sections” (Movies S1 and S2). In its appearance, intracellular position, and dimensions these filamentous structures are strongly

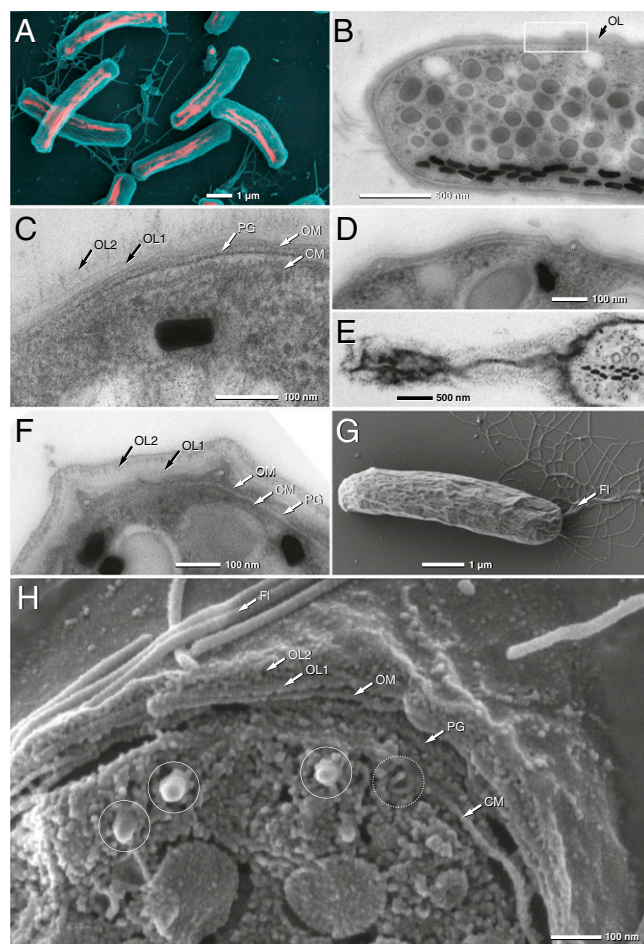


Fig. 1. Scanning (SEM) and transmission electron (TEM) micrographs of “*Candidatus M. bavaricum*” cells (Mbav). (A) SEM micrograph of Mbav by simultaneous detection of secondary (blue) and backscattered electrons (red). Chains of magnetite crystals are visible (red). (B–D) TEM micrographs of ultrathin sections of high-pressure frozen and freeze-substituted cells showing the multilayered cell boundary (B, framed area). CM, cytoplasmic membrane; OM, outer membrane; PG, peptidoglycan; OL1, inner part of outer layer; OL2, outer part of outer layer; asterisks, ridges or papillae of periplasmic space. (E) FIB section showing a network of extensions of ridges. (F and G) TEM and SEM of conventionally fixed samples (FI, flagella). (H) High-resolution SEM of a high-pressure frozen, cryofractured, and frozen hydrated Mbav cell. Solid circle, magnetosome crystals; dotted circle, empty magnetosome membrane vesicles.

reminiscent of the cytoskeletal magnetosome filament (MF) that has been previously discovered in cultivated magnetospirilla (4–6).

Most notably, in TEM thin sections, individual crystals were found to be surrounded by a membranous structure that displays a laminate appearance (Fig. 2B and C). Its thickness of 3–4 nm appeared somewhat lower than that of the cytoplasmic membrane (CM) (6–7 nm), which might be due to the fact that the innermost electron dense layer cannot be discerned against the dark background of the adjacent magnetite crystals. This membranous layer was found in all analyzed thin sections of Mbav and resembles the MM of magnetospirilla detected by the same method (29). Hollow, concave membrane-like structures were also visible by cryo-SEM of cross-fractured cells of Mbav (Figs. 1H and 2E). Because of their size and close vicinity to magnetosome crystals, they are likely to represent empty MM vesicles from which the magnetite core was lost during freeze fracturing.

Altogether, these data suggest that Mbav has a complex and distinct subcellular structure with respect to cell wall architecture and organization of the magnetosome chains. However, structures

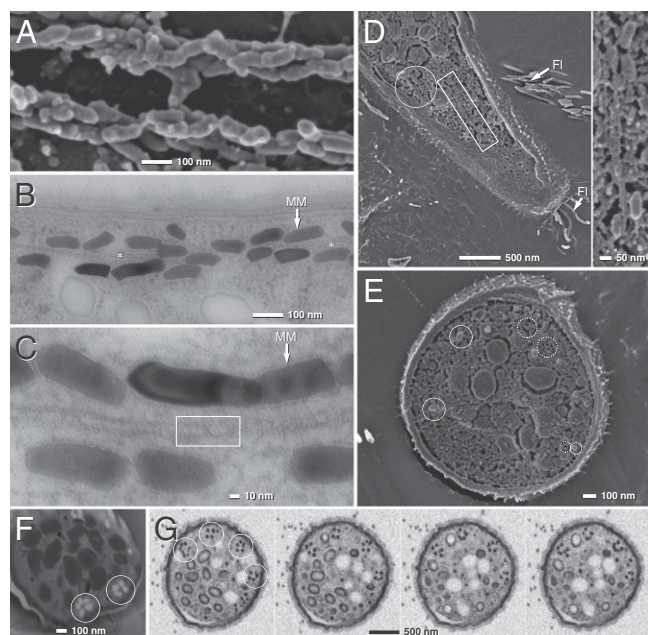


Fig. 2. TEM and SEM micrographs of Mbav magnetosome chains (see Fig. S3 for an enlarged version at higher resolution). (A) SEM micrograph of a cryofractured cell (after chemical fixation) showing two bundles of magnetosome strands. (B and C) TEM ultrathin sections of high-pressure frozen and freeze-substituted cells showing strands of magnetosomes aligned parallel to a tubular filamentous structure (asterisk, framed area; MM, magnetosome membrane). (D and E) Cryo-SEM (frozen hydrated) of tangential (D) and cross-fractured (E) cells of Mbav (rectangular frame, magnetosomes aligned along MF; solid circles, magnetosomes crystals; dotted circle, empty MM vesicles). (F and G) SEM of focused ion beam (FIB) sections (F), and high-pressure frozen and freeze-substituted (G) Mbav cells. Circles indicate several rosette-like magnetosome bundles. Different micrographs in G represent selected sections from FIB-milling series (every 10th section is shown from left to right). Each section has a thickness of 8 nm.

highly reminiscent of the MM and the MF in α -proteobacterial MTB are clearly present.

Single-Cell Sorting and Whole Genome Amplification (WGA). To identify putative magnetosome genes, we initially attempted a similar approach as was successfully used for the identification of MAI clusters from metagenomic large-insert libraries (18). However, screening of more than 10,000 clones from six independently constructed fosmid libraries based on magnetically highly enriched Mbav cells failed to detect any clones harboring genes with similarity to known magnetosome proteins. Although in our environmental MTB collections Mbav was the most abundant morphotype (>40%), 16S rRNA gene libraries revealed that Mbav was only poorly represented in fosmid libraries constructed from these collections (<1%). Possibly, this bias was caused by poor DNA recovery due to the unusual cell structure of Mbav (21). All our attempts to increase the relative proportion of Mbav DNA by fluorescence-assisted cell sorting, filtration, and selective lysis were unsuccessful (experimental details available on request). Therefore, we had to develop an alternative strategy, which combined WGA of individually sorted Mbav cells with highly stringent PCR screening of metagenomic fosmid libraries with Mbav-specific primers deduced from WGA sequences (Fig. S4). In addition to Mbav cells, the only other abundant morphotypes present in our magnetic collections were magnetotactic cocci that could be easily distinguished from the conspicuous large (5–10 μ m) rod-like Mbav cells (Fig. S5). This facilitated their strictly selective separation using micromanipulation with microscopic control over every sorting step (Figs. S5 and S6 A–D and Movie S3). Mbav cells were collected from

a 5- μ L droplet, containing the heterogeneous mixture of magnetically collected MTB and subjected to washing steps by two subsequent transfers into water droplets to eliminate potential extracellular DNA contaminations. Between 1 (Movie S3) and 1,000 (Movie S4) Mbav cells were collected into a single capillary, in which cells remained intact and viable upon release into water droplets (Movie S5). For WGA, washed cells were transferred to 0.75- μ L droplets of lysis buffer on Ampligrids (Fig. S6C). Five to 10 individually sorted Mbav cells per WGA reaction yielded sufficient amounts of DNA for subsequent sequence analysis. A total of 3.8 μ g of DNA was amplified from 158 cells sorted in 10 independent reactions, which were pooled to reduce stochastic amplification bias. Analysis of the corresponding 16S rRNA gene library (25 clones) before pyrosequencing exclusively revealed 100% identical *Candidatus M. bavaricum* sequences. This indicates that the separation was highly specific for target cells, which were free from contaminating DNA.

Identification of a Magnetosome Gene Cluster of *Candidatus M. bavaricum* by WGA-Enabled Screening of Metagenomic Libraries.

Pyrosequencing generated a total of 118.95 Mb of sequence information. However, only 39% of the obtained sequence data could be assembled (1,061 contigs; average size 556 bp) resulting in about 0.6 Mb. This is likely to represent only a fraction of the Mbav genome, if a genome size between 2 Mb (as for its closest sequenced relative *Thermodesulfobivibrio yellowstonii* NC_011296), and about 5 Mb (like most other MTB) is assumed. Most likely the limited amount of DNA available for the pyrosequencing approach (3.8 μ g) resulted in short read lengths and poor assembly, which prevented the analysis of entire genes or operons. However, two contigs of 529 bp (no. 1) and 570 bp (no. 2) were found to display partial similarity to known magnetosome proteins MamE (no. 1; 50% identities in 60 aa) and MamP (no. 2; 38% identities in 76 aa). Using primers targeting these regions, about 10,000 clones from metagenomic fosmid libraries (18, 21) were PCR screened. Five clones, which previously had escaped our initial screening because of the lack of endsequence similarities, were identified from which either identical sequences of *mamE* (1 clone), or *mamP* (1 clone), or both (3 clones) could be amplified.

Sequencing, assembly, and gene prediction of *mamE* and *mamP*-positive clones yielded a contig of 37 kb with 34 putative genes [Fig. 3 and National Center for Biotechnology Information (NCBI) FQ377626]. The mismatch-free overlap (99.99% sequence identity) of five individual fosmids with an insert size of about 35 kb, 24 kb, 35 kb, 24 kb, and 27 kb, respectively, indicates a clonal origin of the amplified Mbav DNA. This was further verified in two independent control experiments (Fig. S7). The G+C content of 49.7% is within the range of 46.9–50.2% as determined for metagenomic fosmid clones containing phylogenetic marker genes (16S rRNA) from Mbav-like MTB (21, 30), but differs significantly from the related *T. yellowstonii* (34%), although it is well below the range of percentage of G+C found in MTB thus far (54.8–65.1%) (8). Out of the 34 identified genes, 14 encode hypothetical proteins, and 2 share no similarity to the NCBI database (Table S1). Among the genes related to proteins of known functions, 2 encode transposases, 3 are related to transcriptional regulation, whereas 4 might be related to metabolic functions (lyase, oxidoreductase, polysaccharide biosynthesis, and pyruvate phosphorylation; Table S1). Four genes encode proteins with the highest identity to *T. yellowstonii* (Table S1).

Most remarkably, the contig contains a 18-kb cluster of 22 genes of which some display striking homology to known magnetosome genes of proteobacterial MTB (Fig. 3 and Tables S1 and S2). Their short intergenic distance and identical transcriptional direction suggest that they may be part of a common putative operon as in all other MTB analyzed so far. Whereas 8 of the 22 genes encode proteins with greatest similarity to MTB (on the basis of BlastP analysis against the NCBI database), only 5 of them (MameIBMP) are most similar to known magnetosome genes (Table S1 and Fig. S8). Among them, MamI, which has been implicated in the formation of magnetosome vesicles in α -proteobacterial magneto-

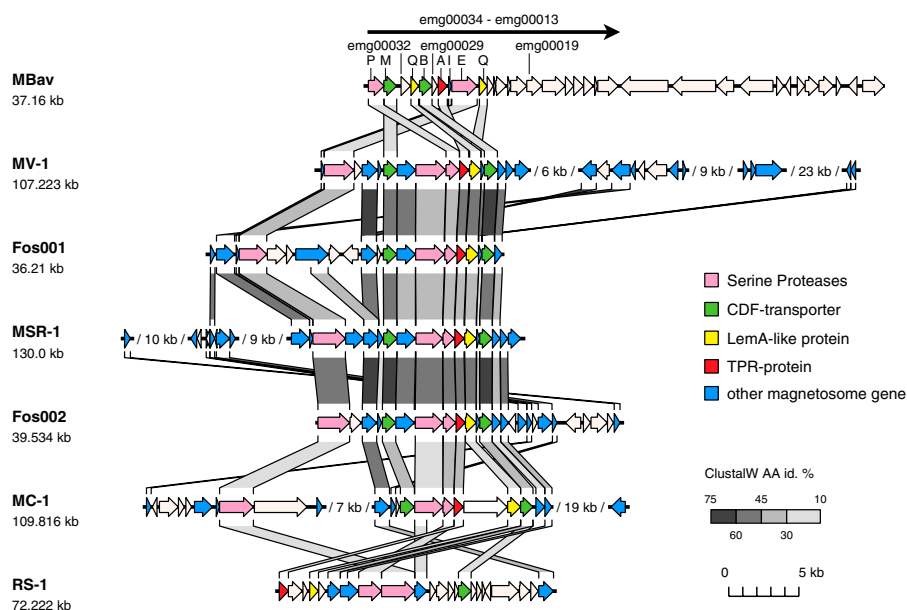


Fig. 3. Molecular organization of sections from putative magnetosome islands of Mbav and selected other MTB (Mbav, *Candidatus M. bavaricum*; MV-1, magnetic vibrio; Fos001+002, metagenomic MTB clones; MSR-1, *Magnetospirillum gryphiswaldense*; MC-1, magnetic coccus; RS-1, *Desulfovibrio magneticus*). The black arrow on Top indicates the extension of a putative magnetosome operon in Mbav. Different colored arrows indicate characteristic features of proteins encoded by known magnetosome genes, whereas equivalent genes are connected by stripes of various shadings, which indicate different degrees of identity (id) as calculated from ClustalW alignments of encoded proteins. Alignments were generated with TRAPPIST, a Python-based toolbox for alignment, analysis, and visualization of genomes or genome segments.

spirilla (10) is least conserved (23–35% identity; Fig. S9), but shares significant and exclusive similarity to MamI homologs from all other analyzed MTB including *Desulfovibrio magneticus*, in which it escaped detection in previous studies (10, 19, 31).

Two genes of this putative operon (emg00025 and emg00031) were annotated as *mamQ-I* and *mamQ-II*, respectively, because they share similarity to all MamQ homologs, although the database comparison shows the highest similarity to a LemA-like protein from non-MTB. For the same reasons, the TPR domain protein (emg00028) was annotated as MamA, which was reported to be involved in magnetosome “activation” in *M. magneticum* (32). MamE and MamP are PDZ-containing putative serine proteases (33). Whereas MamP was implicated in the control of magnetite crystal size and number, MamE is thought to be involved in magnetosome formation by directing the proper localization of a subset of magnetosome proteins (10). MamM and MamB share homology with cation diffusion facilitator (CDF) transporters (34, 35) and are assumed to mediate iron transport into the magnetosome compartment (8). Multiple sequence comparisons were performed with all identified Mam homologs of Mbav to analyze their phylogenetic relation to magnetosome proteins from other MTB (Figs. S8 and S11). As an example, regardless of the algorithm used, Mbav MamB, and MamM CDF transporters cluster together with MamB and MamM proteins of MTB, which form a phylogenetically distinct branch separately from other CDF proteins, such as iron transporting FieF-like proteins (35) (Fig. S11). All other analyzed magnetosome genes display comparable branching patterns (Fig. S8). This demonstrates homology of magnetosome proteins from the *Nitrospira* phylum with those of proteobacterial origin, suggesting a horizontal gene transfer (HGT) between both phyla.

In addition to the 8 genes with clear homology to known α -proteobacterial magnetosome proteins, the Mbav magnetosome cluster comprises 14 further genes, which either intersperse the *mam* homologs (emg00032–emg00029) or are mostly located downstream of them (emg00024–emg00013). The majority of them (10 genes) encode hypothetical proteins, or share only weak similarity (22–27%) to proteins of known function, such as proteins involved in polysaccharide biosynthesis and chromosome condensation. Interestingly, 3 of these 14 genes encode proteins that share the highest similarity to *Desulfovibrio magneticus* (28–29%), whereas one of them (emg00029) encodes a hypothetical membrane protein and is localized between *mamA* and *mamB*. One further putative membrane protein encoded by

orf emg00019 shares the highest identity with a bacterium not known to produce magnetosomes.

Discussion

On the basis of their unusual characteristics such as magnetosome arrangement, distinct cell biology and distant phylogenetic position, and lacking any genetic information, it has been questioned whether nonproteobacterial MTB from deep-branching phyla such as *Nitrospira* share homologous structures and genetic mechanisms of biomineralization with magnetotactic *Proteobacteria* (13).

Whereas our magnetic mass collection enabled the application of advanced imaging techniques, the poor representation and unknown identity of Mbav DNA in multispecies large-insert libraries from those enrichments hampered the metagenomic analysis of magnetosome formation. Therefore, for the confident identification and targeted analysis of magnetosome genes from Mbav, we had to resort to an alternative strategy based on WGA of individually sorted cells. Such targeted WGA approaches have recently been demonstrated to be functional for other cultivated and uncultivated MTB (36).

Genomes from several uncultured bacteria have been partly sequenced from single or few cells (for instance ref. 37, 38). However, despite recent improvements in genome recovery and normalization procedures (39), single-cell genome sequencing has not yet become a routine technique, and only recently the first gap-free reconstruction of an entire genome from a single polyploid bacterium was demonstrated (40). Unlike the large contigs of >0.5 Mb reported in some of these studies, our WGA approach yielded only relatively short average contig lengths, most likely due to poor DNA recovery from lysis-recalcitrant Mbav cells (21) and consequent amplification bias due to limiting amounts of template DNA. However, the obtained sequences allowed the identification of true Mbav clones in existing multispecies metagenomic libraries. Whereas neither of the two complementary approaches (WGA and metagenomics) alone was successful, their combination led to first insights into the genetic control of magnetosome formation in a nonproteobacterial MTB from the deep-branching *Nitrospira* phylum. Similar strategies could be applied as an efficient and economical approach for targeted genomic analysis of further MTB or other low-abundant environmental bacteria with conspicuous morphologies.

Whereas in one study organic material and several polypeptides with homology to known magnetosome proteins copurified with isolated magnetite crystals of the δ -proteobacterium

D. magneticum RS-1 (3), other in situ TEM studies failed to detect a MM surrounding the individual magnetite crystals in this organism and Mbav, which are only distantly related to the prototypical magnetospirilla. This led to speculations that bullet-shaped magnetosomes are generally not formed within a MM, and that these MTB may have evolved a divergent molecular mechanism of magnetite biomineralization (13, 14).

However, our discovery of similar structures and genes in this study is strongly indicative of homologous mechanisms of biomineralization also in distantly related MTB outside the *Proteobacteria*. By using several advanced electron-microscopic techniques including focus ion beam sectioning of cryofixed cells, which to our knowledge has been successfully applied for the first time for the 3D reconstruction of a bacterial cell, an unprecedented insight into the subcellular organization of Mbav was obtained. The complex structure of its cell envelope and its intricate magnetosome architecture represent one of the highest structural levels found in a bacterial cell. In particular, we were able to demonstrate that, contrary to previous observations (13), magnetite crystals of Mbav are surrounded by a MM, which strongly resembles the well-analyzed structure in α -proteobacterial MTB, such as *M. gryphiswaldense* (4, 33). However, the relatively large distance (20–50 nm) of the magnetosome bundles from the CM in Mbav makes it unlikely that the MM remains permanently contiguous with the CM, but may become detached from it during magnetosome assembly.

The presence of a MM is consistent with the identification of genes that encode homologs of magnetosome proteins MamI, -P, -A, -M, -B, -Q, and -E, which are all known to be associated with the MM and are implicated in its biogenesis as well as magnetosomal transport of iron in *Magnetospirillum* species (8, 10, 33). *mamI*, -P, -A, -M, -B, -Q, and -E belong to the group-specific “signature genes” of magnetotaxis, which has recently been identified by comparative genomics (41), i.e., they are conserved and located within the MAI of all MTB, but exhibit no (MTB-specific, *mamI*), or only remote (MTB-related, *mamPAMQE*) similarity to any genes from nonmagnetotactic organisms. Despite general conservation, homologous genes within the Mbav *mam* cluster are less conserved with respect to sequences and synteny than among the proteobacterial MTB. For example, a peculiarity not found in other magnetobacterial genomes is the presence of two divergent *mamQ* copies (Fig. 3), which might be related to a somewhat distinct mechanism of MM formation in this organism. However, a number of the previously identified magnetosome genes, such as *mamHRSTNOLKJ*, which are conserved in most or all proteobacterial MTB, is missing. One possible reason might be a slightly distinct genetic control of biomineralization in Mbav. On the other hand, however, the cluster is bound by a *mamP*-like gene at one end of the assembled contig sequence, but on the basis of the usual central position of *mamP* within the MAI of other MTB, it can be expected that a significant portion of the operon containing additional magnetosome genes extends further upstream beyond the boundary of the contig and might be part of an even larger MAI.

One example for such a “missing” gene is *mamK*, which is conserved in all MTB and encodes an actin-like protein that in magnetospirilla forms the cytoskeletal MF and is involved in intracellular assembling, aligning, and positioning of the linear magnetosome chains (4–7). We have demonstrated by cryo-SEM and -TEM the presence of a similar filamentous structure in Mbav, which is aligned along the magnetosome chains in close vicinity. Unlike the MF in magnetospirilla, which form a network of filament bundles, filaments found in Mbav appear to form an ordered tubular structure with a hollow interior, around which the individual magnetosome strands are arranged. However, its general resemblance suggests that this structure might be homologous to the MF of magnetospirilla and is possibly also formed by a MamK-like protein encoded elsewhere in the genome.

On the other hand, the intricate 3D tubular organization of magnetosome chains in multiple discrete bundles is significantly more complicated than the single or double linear chains found

in magnetospirilla. Therefore, it is very likely to be governed by a much more elaborate mechanism of assembly, which, in addition to constituents of the magnetosome pathway that are generally conserved among all MTB, involves further specific genetic determinants. These might be encoded elsewhere in the genome, or for example, by the genes that follow the identified *mam* genes immediately downstream. Although the function of these gene is not known, their colocalization with known *mam* genes within a single putative operon and their partial conservation in other MTB suggests that they might be involved in magnetosome formation and biomineralization as well.

Our discovery of structures and genes in MTB from the deep-branching *Nitrospira* phylum similar to those in distantly related proteo-MTB also raises another important question, which is the phylogenetic origin and evolution of magnetotaxis. In contrast to previous postulations (13, 14), our results provide further evidence that the mechanism of magnetite biomineralization (apart from some species-specific variations) might be universal. Recently, we have demonstrated that horizontal gene transfer rather than independent evolution is likely to account for the emergence of magnetotaxis among diverse lines of proteobacterial MTB (16), which has been confirmed by the detection of homologous genes in RS-1 (19). Similar studies on greigite-forming uncultivated MTB can be expected to reveal the genetic basis and evolution of greigite-based magnetotaxis in the future.

As revealed by phylogenetic trees, putative magnetosome proteins of Mbav, such as the CDF transporters MamB and MamM, branch together with their proteo-MTB relatives, whereas homologs from non-MTB form a distinct phylogenetic group (Fig. S11), suggesting that proteins within MTB-specific branches have distinct functions and are universally conserved in all MTB. Because Mbav and the proteobacterial MTB are not closely related and phylogenetically separated by numerous bacterial species lacking the magnetotactic trait (8), there are two possible scenarios to explain the presence of homologous magnetosome genes. One would be the assumption of a common magnetotactic ancestor of the *Nitrospira* and *Proteobacteria*. However, this scenario would require multiple events of loss of magnetosome genes in all other nonmagnetotactic proteobacterial descendants. Although spontaneous loss of MAI genes at rather high frequency has been demonstrated in cultivated MTB (15), and therefore cannot be entirely dismissed, secondary loss in almost all other proteobacteria seems rather unlikely. In contrast, a second scenario, in which horizontal gene transfer of magnetosome genes between proteobacterial MTB and the *Nitrospira* phylum provides a more likely explanation for the occurrence of highly conserved magnetotactic signature genes in Mbav. Similar examples of horizontal gene transfer between the *Nitrospira* phylum and other bacterial phyla have been already demonstrated for genes encoding other metabolic pathways, such for instance as sulfite reductase genes (42), or genes involved in nitrite oxidation (43). The observed compositional differences, such as the percentage of G+C content of the MAI (Mbav 49.7%, *M. gryphiswaldense* 61.1%) argue against recent HGT, but indicate a rather ancient event of transfer. However, whether or not magnetotaxis has originated from the deep branching *Nitrospira* phylum and thus, formation of magnetosomes is an evolutionary ancient trait, requires more sequencing efforts that have to include further distantly related MTB from other groups.

Materials and Methods

Electron Microscopy. TEM and SEM of samples prepared by chemical fixation and high-pressure freezing was performed with an EM 912 transmission microscope (Zeiss) and a Zeiss Auriga SEM equipped with a focused ion beam consisting of Ga⁺ ions for “sectioning.” See *SI Materials and Methods* for details.

Environmental Sampling, Magnetic Enrichments, DNA Extraction, Fosmid-Library Construction, and Screening. Sediment sample collection, magnetic Mbav enrichment, DNA extraction and fosmid library construction was performed as previously described (18, 21). Six fosmid libraries were screened via endsequencing and PCR as previously described (18, 21). See *SI Materials and Methods* for details.

Single Cell Sorting and WGA. Single cell sorting was achieved via micromanipulation and subsequent phi29-mediated whole genome amplification as explained in detail in *SI Materials and Methods*.

Sequence Analysis. WGA DNA was analyzed by the Genome Sequencer FLX system (GS FLX Titanium chemistry) and reads were assembled via MIRA as previously described (44). Sequence determination of entire fosmids as well as phylogenetic analysis were performed as previously described (21).

- Jogler C, Schüler D (2007) Genetic and biochemical analysis of magnetosomes in *Magnetospirillum gryphiswaldense*. *Handbook of Biomineralization*, Vol Biological aspects and structure formation, ed Bauerlein E (Wiley-VCH, Weinheim, Germany), pp 145–162.
- Schüler D (2004) Biochemical and genetic analysis of the magnetosome membrane in *Magnetospirillum gryphiswaldense*. *Biomineralization*, ed Bauerlein E (Wiley-VCH, Weinheim), 2nd Ed, pp 61–74.
- Matsunaga T, Nemoto M, Arakaki A, Tanaka M (2009) Proteomic analysis of irregular, bullet-shaped magnetosomes in the sulphate-reducing magnetotactic bacterium *Desulfovibrio magneticus RS-1*. *Proteomics* 9:3341–3352.
- Scheffel A, et al. (2006) An acidic protein aligns magnetosomes along a filamentous structure in magnetotactic bacteria. *Nature* 440:110–114.
- Katzmann E, Scheffel A, Gruska M, Plietzko JM, Schüler D (2010) Loss of the actin-like protein MamK has pleiotropic effects on magnetosome formation and chain assembly in *Magnetospirillum gryphiswaldense*. *Mol Microbiol* 77:208–224.
- Komeili A, Li Z, Newman DK, Jensen GJ (2006) Magnetosomes are cell membrane invaginations organized by the actin-like protein MamK. *Science* 311:242–245.
- Pradel N, Santini CL, Bernadac A, Fukumori Y, Wu LF (2006) Biogenesis of actin-like bacterial cytoskeletal filaments destined for positioning prokaryotic magnetic organelles. *Proc Natl Acad Sci USA* 103:17485–17489.
- Jogler C, Schüler D (2009) Genomics, genetics, and cell biology of magnetosome formation. *Annu Rev Microbiol* 63:501–521.
- Faivre D, Schüler D (2008) Magnetotactic bacteria and magnetosomes. *Chem Rev* 108:4875–4898.
- Murat D, Quinlan A, Vali H, Komeili A (2010) Comprehensive genetic dissection of the magnetosome gene island reveals the step-wise assembly of a prokaryotic organelle. *Proc Natl Acad Sci USA* 107:5593–5598.
- Komeili A (2007) Molecular mechanisms of magnetosome formation. *Annu Rev Biochem* 76:351–366.
- DeLong EF, Frankel RB, Bazylinski DA (1993) Multiple evolutionary origins of magnetotaxis in bacteria. *Science* 259:803–806.
- Hanzlik M, Winklhofer M, Petersen N (2002) Pulsed-field-remnance measurements on individual magnetotactic bacteria. *J Magn Magn Mater* 248:258–267.
- Byrne ME, et al. (2010) *Desulfovibrio magneticus RS-1* contains an iron- and phosphorus-rich organelle distinct from its bullet-shaped magnetosomes. *Proc Natl Acad Sci USA* 107:12263–12268.
- Ullrich S, Kube M, Schübbe S, Reinhardt R, Schüler D (2005) A hypervariable 130-kilobase genomic region of *Magnetospirillum gryphiswaldense* comprises a magnetosome island which undergoes frequent rearrangements during stationary growth. *J Bacteriol* 187:7176–7184.
- Jogler C, et al. (2009) Comparative analysis of magnetosome gene clusters in magnetotactic bacteria provides further evidence for horizontal gene transfer. *Environ Microbiol* 11:1267–1277.
- Schübbe S, et al. (2009) Complete genome sequence of the chemolithoautotrophic marine magnetotactic coccus strain MC-1. *Appl Environ Microbiol* 75:4835–4852.
- Jogler C, et al. (2009) Toward cloning of the magnetotactic metagenome: Identification of magnetosome island gene clusters in uncultivated magnetotactic bacteria from different aquatic sediments. *Appl Environ Microbiol* 75:3972–3979.
- Nakazawa H, et al. (2009) Whole genome sequence of *Desulfovibrio magneticus* strain RS-1 revealed common gene clusters in magnetotactic bacteria. *Genome Res* 19:1801–1808.
- Spring S, et al. (1993) Dominating role of an unusual magnetotactic bacterium in the microaerobic zone of a freshwater sediment. *Appl Environ Microbiol* 59:2397–2403.
- Jogler C, et al. (2010) Cultivation-independent characterization of ‘*Candidatus Magnetobacterium bavaricum*’ via ultrastructural, geochemical, ecological and metagenomic methods. *Environ Microbiol* 12:2466–2478.
- Flies CB, Peplies J, Schüler D (2005) Combined approach for characterization of uncultivated magnetotactic bacteria from various aquatic environments. *Appl Environ Microbiol* 71:2723–2731.
- Lin W, Li J, Schüler D, Jogler C, Pan Y (2009) Diversity analysis of magnetotactic bacteria in Lake Miyun, northern China, by restriction fragment length polymorphism. *Syst Appl Microbiol* 32:342–350.
- Lefèvre CT, et al. (2010) Moderately thermophilic magnetotactic bacteria from hot springs in Nevada. *Appl Environ Microbiol* 76:3740–3743.
- Hanzlik M, Winklhofer M, Petersen N (1996) Spatial arrangement of chains of magnetosomes in magnetotactic bacteria. *Earth Planet Sci Lett* 145:125–134.
- Watson SW, Bock E, Valois FW, Waterbury JB, Schlosser U (1986) *Nitrospira marina* gen. nov., sp. nov.: A chemolithotrophic nitrite-oxidizing bacterium. *Arch Microbiol* 144:1–7.
- Ehrich S, Behrens D, Lebedeva E, Ludwig W, Bock E (1995) A new obligately chemolithoautotrophic, nitrite-oxidizing bacterium, *Nitrospira moscoviensis* sp. nov. and its phylogenetic relationship. *Arch Microbiol* 164:16–23.
- Off S, Alawi M, Spieck E (2010) Enrichment and physiological characterization of a novel *Nitrospira*-like bacterium obtained from a marine sponge. *Appl Environ Microbiol* 76:4640–4646.
- Scheffel A, Gärdes A, Grünberg K, Wanner G, Schüler D (2008) The major magnetosome proteins MamGFDC are not essential for magnetite biomineralization in *Magnetospirillum gryphiswaldense* but regulate the size of magnetosome crystals. *J Bacteriol* 190:377–386.
- Lin W, Jogler C, Schüler D, Pan Y (2010) Metagenomic analysis reveals unexpected subgenomic diversity of magnetotactic bacteria within the *Nitrospira* phylum. *Appl Environ Microbiol* 10.1128/AEM.01476-10.
- Jogler C, Schüler D (2006) Genetic analysis of magnetosome biomineralization. *Magnetoreception and Magnetosomes in Bacteria*, Microbiology Monographs, ed Schüler D (Springer, Heidelberg), Vol 3, pp 133–162.
- Komeili A, Vali H, Beveridge TJ, Newman DK (2004) Magnetosome vesicles are present before magnetite formation, and MamA is required for their activation. *Proc Natl Acad Sci USA* 101:3839–3844.
- Grünberg K, et al. (2004) Biochemical and proteomic analysis of the magnetosome membrane in *Magnetospirillum gryphiswaldense*. *Appl Environ Microbiol* 70:1040–1050.
- Montanini B, Blaudez D, Jeandroz S, Sanders D, Chalot M (2007) Phylogenetic and functional analysis of the Cation Diffusion Facilitator (CDF) family: Improved signature and prediction of substrate specificity. *BMC Genomics* 8:107.
- Grass G, et al. (2005) FieF (YiP) from *Escherichia coli* mediates decreased cellular accumulation of iron and relieves iron stress. *Arch Microbiol* 183:9–18.
- Arakaki A, Shibusawa M, Hosokawa M, Matsunaga T (2010) Preparation of genomic DNA from a single species of uncultured magnetotactic bacterium by multiple-displacement amplification. *Appl Environ Microbiol* 76:1480–1485.
- Woyke T, et al. (2009) Assembling the marine metagenome, one cell at a time. *PLoS ONE* 4:e5299.
- Podar M, et al. (2007) Targeted access to the genomes of low-abundance organisms in complex microbial communities. *Appl Environ Microbiol* 73:3205–3214.
- Rodrigue S, et al. (2009) Whole genome amplification and de novo assembly of single bacterial cells. *PLoS ONE* 4:e6864.
- Woyke T, et al. (2010) One bacterial cell, one complete genome. *PLoS ONE* 5:e10314.
- Richter M, et al. (2007) Comparative genome analysis of four magnetotactic bacteria reveals a complex set of group-specific genes implicated in magnetosome biomineralization and function. *J Bacteriol* 189:4899–4910.
- Klein M, et al. (2001) Multiple lateral transfers of dissimilatory sulfite reductase genes between major lineages of sulfate-reducing prokaryotes. *J Bacteriol* 183:6028–6035.
- Lücker S, et al. (2010) A *Nitrospira* metagenome illuminates the physiology and evolution of globally important nitrite-oxidizing bacteria. *Proc Natl Acad Sci USA* 107:13479–13484.
- Chevreur B, Wetter T, Suhai S (1999) Genome sequence assembly using trace signals and additional sequence information. *Computer Science and Biology: Proceedings of the German Conference on Bioinformatics* (German Conference on Bioinformatics, Hannover, Germany), Vol 99, pp 45–56.

Supporting Information

Jogler et al. 10.1073/pnas.1012694108

SI Materials and Methods.

Electron Microscopy. For chemical fixation, cells were incubated in 2.5% glutardialdehyde containing fixative buffer (75 mM sodium cacodylate, 2 mM MgCl₂, pH 7.0), for 1 h at room temperature. Afterward, samples were rinsed several times in fixative buffer and postfixed at room temperature for 1 h with 1% osmium tetroxide in fixative buffer. After two washing steps in water, the cells were stained *en bloc* for 30 min with 1% uranyl acetate in 20% acetone. Dehydration was performed with a graded acetone series. Samples were then infiltrated and embedded in Spurr's low-viscosity resin.

For high-pressure freezing, aluminum platlets were filled with concentrated cell suspensions and the cells immobilized by high-pressure freezing (Leica; HPM100). Freeze substitution was performed in acetone with 2% osmium tetroxide and 0.2% uranyl acetate, including 5% water. After embedding the samples in Epon, ultrathin sections were cut with a diamond knife and mounted onto uncoated copper grids. The sections were post-stained with aqueous lead citrate (100 mM, pH 13.0).

Transmission electron micrographs were taken with an EM 912 electron microscope (Zeiss) equipped with an integrated OMEGA energy filter operated at 80 kV in the zero loss mode. The FIB serial sectioning was performed by a Zeiss-Auriga workstation. The focused ion beam consisted of Ga⁺ ions accelerated by a voltage of 30 kV. In the cut-and-view mode, sections ranging in thickness between 5 nm and 10 nm (dependent on the magnification) were produced with the FIB and FESEM images, which were recorded at 1.5 kV using the in-lens energy selective backscattered (EsB) detector. Specimens were tilted to an angle of 54°; images were tilt corrected for undistorted surface view.

For SEM, drops of the sample were placed onto a glass slide, covered with a coverslip, and rapidly frozen with liquid nitrogen. The coverslip was removed with a razor blade and the glass slide was immediately fixed with 2.5% glutaraldehyde in 75 mM cacodylate buffer (pH 7.0), postfixed with 1% osmium tetroxide in fixative buffer, dehydrated in a graded series of acetone solutions, and critical-point dried after transfer to liquid CO₂. Specimens were mounted on stubs, coated with 3 nm platinum using a magnetron sputter coater, and examined with a Zeiss Auriga scanning electron microscope operated at 1–2 kV. For cryo-scanning electron microscopy high-pressure frozen samples were fractured with a Leica EM MED020, sublimated for 1–2 min at

–95 °C and coated with 3 nm of tungsten, transferred to the scanning electron microscope and examined at 1 kV.

Single Cell Sorting and Whole Genome Amplification (WGA). Single cell sorting was achieved via an Eppendorf TransferMan NK2 micromanipulator and the Eppendorf CellTram Oil manual hydraulic pressure-control system mounted to an Olympus BX61 microscope equipped with a 40× LD objective and a double slide holder. Samples were kept on microscopic slides attached to a custom-build plastic frame, while an Advalytix AmpliGrid AG480F was placed next to it in the double slide holder (Fig. S6C). Five to 15 individual Mbav cells were transferred via micromanipulation from the 5-μL sample droplet (containing variable amounts of MTB) into two different washing droplets (5 μL) and finally into 0.75 μL sample buffer (Illustra GenomiPhi V2 DNA amplification kit; GE Healthcare) covered with 5 μL of sealing solution (Advalytix). Together, this washing procedure resulted in a 10¹⁸-fold dilution of sample liquid, which is likely to have outdiluted any contaminating DNA to extinction (Fig. S10). Loaded AmpliGrid was transferred into a customized Ampli-Speed slide cyler (Advalytix) calibrated to operate at 4 °C. Samples were heated to 95 °C for 3 min and incubated at 4 °C for 10 min. A total of 0.75 μL of reaction buffer containing enzyme mix (Illustra GenomiPhi V2 DNA amplification kit; GE Healthcare) was added by pipetting on top of the sealing solution (Advalytix) and reactions were incubated for 4 h at 30 °C. The phi29 enzyme was inactivated by incubating the sample at 65 °C for 10 min. After amplification, seven independent reactions—based on a total number of 158 individually sorted Mbav cells—were pooled to overcome phi29 bias and a 16S rRNA gene library was constructed as described previously (1). Sequence analysis of 25 clones revealed identical Mbav sequences (cutoff 99%).

Screening of Fosmid Libraries. Six fosmid libraries that were constructed before were screened via endsequencing as previously described (2, 3). Based on sequence analysis of individually sorted cells after WGA, the primers CJ272 (cactacgccaccctgaagt) and CJ273 (tgaggaatcgcatcaaca) targeting a 130-bp region of *mamE*, as well as the primers CJ280 (ttgatattacatgatctg) and CJ281 (cgaggcaacggagaagatac) targeting a 555-bp region of *mamP* were deduced. The PCR-based fosmid library screening was performed as previously described (3).

1. Lin W, Pan Y (2009) Uncultivated magnetotactic cocci from yuandadu park in beijing, china. *Appl Environ Microbiol* 75:4046–4052.
2. Jogler C, et al. (2009) Toward cloning of the magnetotactic metagenome: Identification of magnetosome island gene clusters in uncultivated magnetotactic bacteria from different aquatic sediments. *Appl Environ Microbiol* 75:3972–3979.
3. Jogler C, et al. (2010) Cultivation-independent characterization of 'Candidatus Magnetobacterium bavaricum' via ultrastructural, geochemical, ecological and metagenomic methods. *Environ Microbiol* 12:2466–2478.

4. Preusting H, Kingma J, Huisman G, Steinbüchel A, Witholt B (1993) Formation of polyester blends by a recombinant strain of *Pseudomonas oleovorans*: Different poly (3-hydroxyalkanoates) are stored in separate granules. *J Environ Polym Degrad* 1: 11–21.

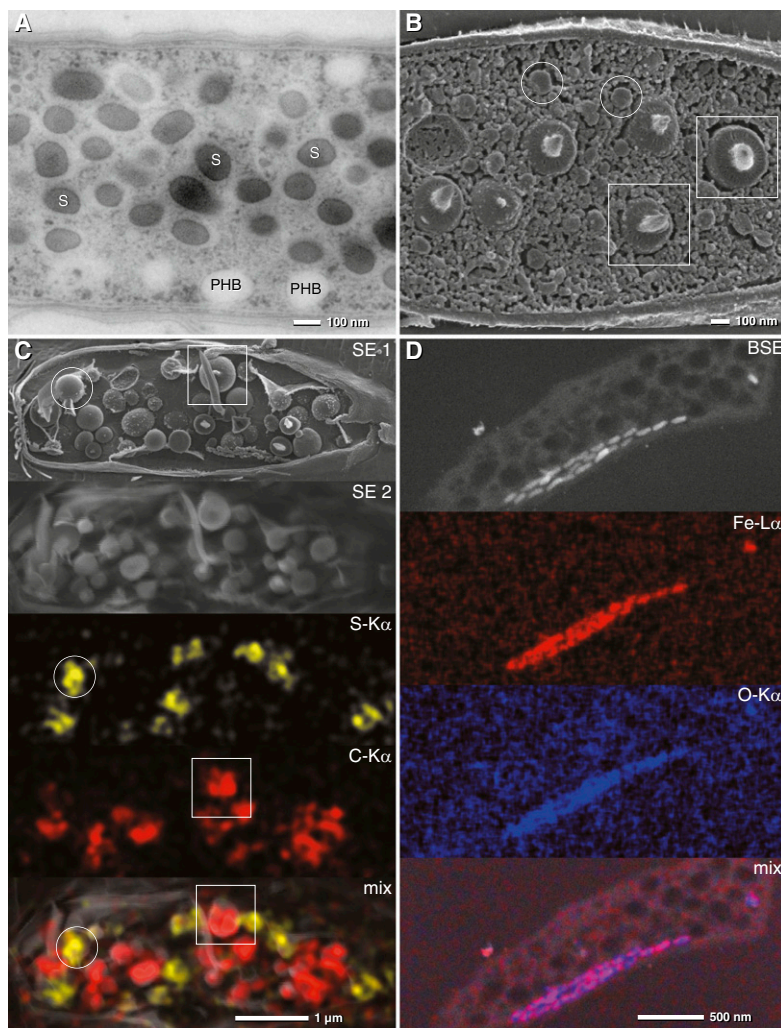


Fig. S2. TEM, SEM, and X-ray analysis of the different intracellular inclusions. (A) TEM of a section from high-pressure frozen and freeze-substituted *Candidatus Magnetobacterium bavaricum* (Mbav) cell. Two types of roughly globular inclusions are visible: electron dense sulfur globules (50–150 nm) and electron translucent polyhydroxybutyrate (PHB) granules (300–500 nm). The PHB granules can be recognized by their characteristic freeze-fracturing behavior resulting in the formation of “mushroom”-like protrusions (squares) (4) as seen in cryo-SEM (B). Frozen hydrated cell (C) before element mapping (SE1) and after mapping (SE2) revealing some distortion by beam damage at the rather high voltage of 4 kV necessary for elemental analysis. Sulfur globules (circles) and PHB granules (squares) can be discerned by their different signals ($S-K_{\alpha}$) and higher carbon content of PHB as shown in the Lower panels. (D) SEM of ultrathin sections of Mbav. Detection of backscattered electron gives a bright signal of the magnetosome crystals (D, BSE). X-ray mapping of oxygen and iron generated by the particles is consistent with magnetite (Fe_3O_4).

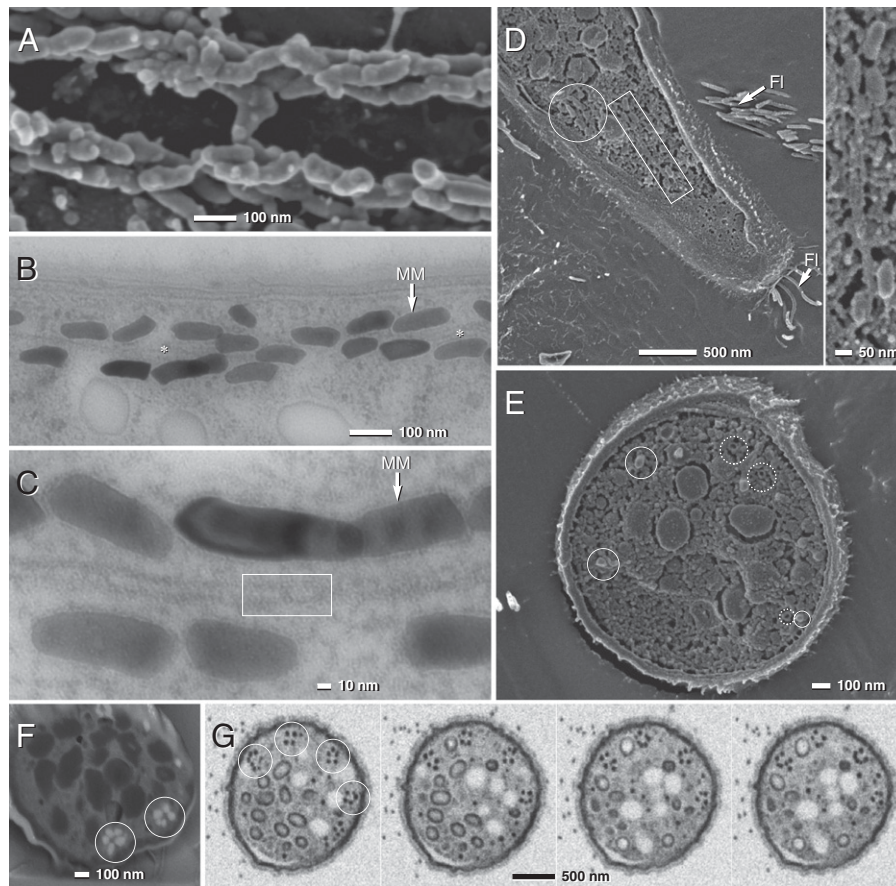


Fig. S3. TEM and SEM micrographs of Mbav magnetosome chains. (A) SEM micrograph of a cryofractured cell (after chemical fixation) showing two bundles of magnetosome strands. (B and C) TEM ultrathin sections of high-pressure frozen and freeze-substituted cells showing strands of magnetosomes aligned parallel to a tubular filamentous structure (asterisk, framed area; MM, magnetosome membrane). (D and E) Cryo-SEM (frozen hydrated) of tangential (D) and cross-fractured (E) cells of Mbav (rectangular frame, magnetosomes aligned along MF; solid circles, magnetosomes crystals; dotted circle, empty MM vesicles). (F and G) SEM of focused ion beam (FIB) sections (F), and high-pressure frozen and freeze-substituted (G) Mbav cells. Circles indicate several rosette-like magnetosome bundles. Different micrographs in G represent selected sections from FIB-milling series (every 10th section is shown from left to right). Each section has a thickness of 8 nm.

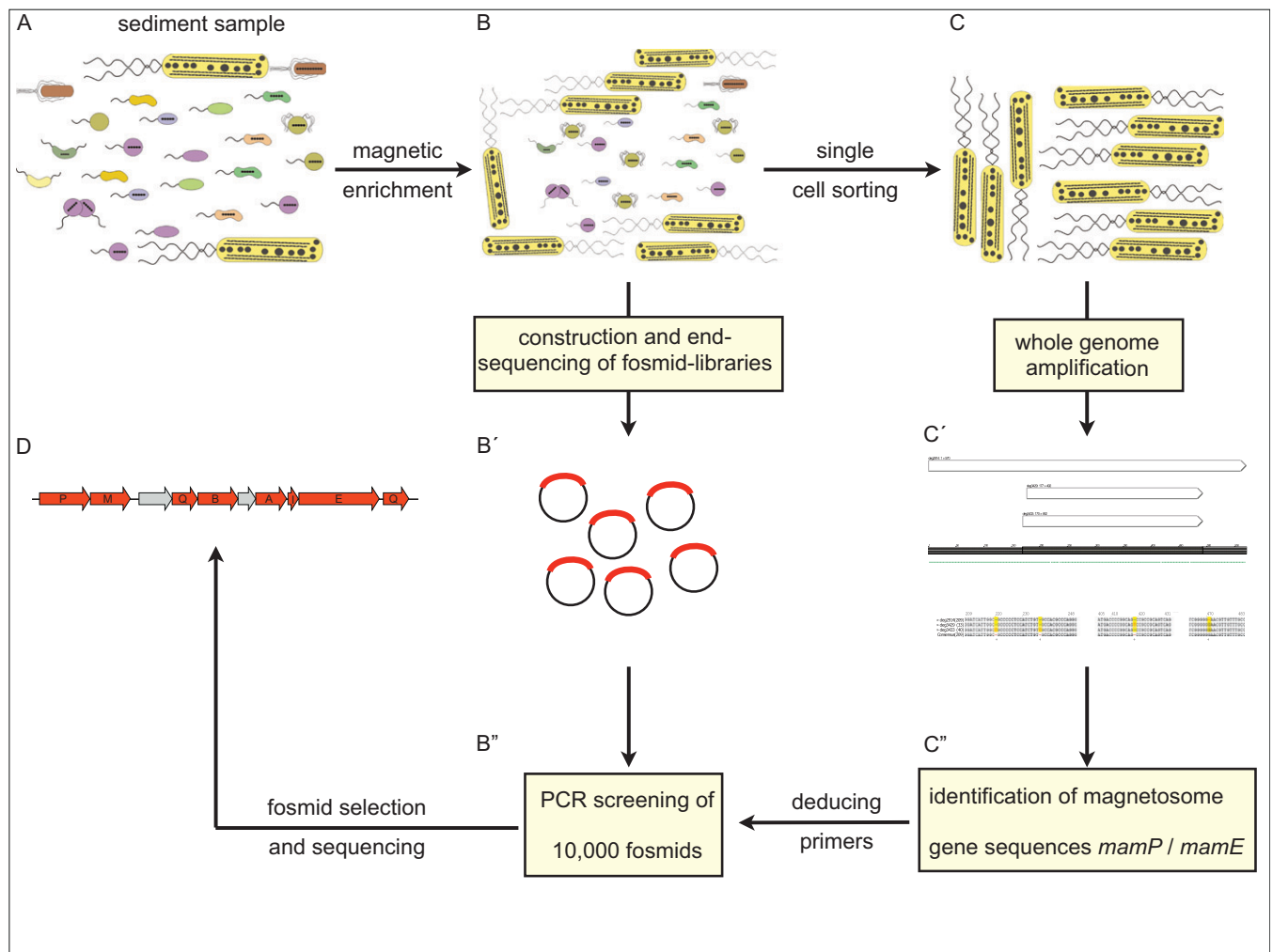


Fig. 54. Schematic representation of the strategy that led to the identification of a 37-kb genomic fragment of *Candidatus Magnetobacterium bavaricum* (Mbav) containing a part of a putative magnetosome island (MAI). (A) Starting point were environmental sediment samples. (B) A two-step magnetic separation process resulted in selective collection of MTB highly enriched in Mbav content. (B') This enrichment was used for the construction of metagenomic fosmid libraries and for single cell sorting. (C) Single cell sorting via micromanipulation. (C') The manually sorted Mbav cells were subject to phi29 mediated whole genome amplification and subsequent sequence determination via pyrosequencing. (C'') Two putative magnetosome gene fragments (*mamE* and *mamP*) were identified. These fragments were used to deduce specific PCR primers. (B'') Subsequent screening of fosmid libraries led to the identification of five fosmids. (D) Sequence analysis of these five fosmids resulted in a 37-kb contig containing several magnetosome genes. (B') Conventional endsequencing of the fosmid libraries done in parallel failed to identify any magnetosome gene containing fosmid.

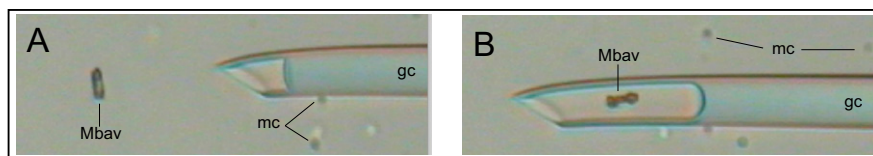


Fig. 55. Micromanipulation of individual Mbav cells from a magnetically enriched mixture of different MTB. Micrographs (400 \times magnification) show a glass capillary (gc) before A and after B aspiration of an individual target cell. Contaminating magnetic cocci (mc) can be clearly discriminated.

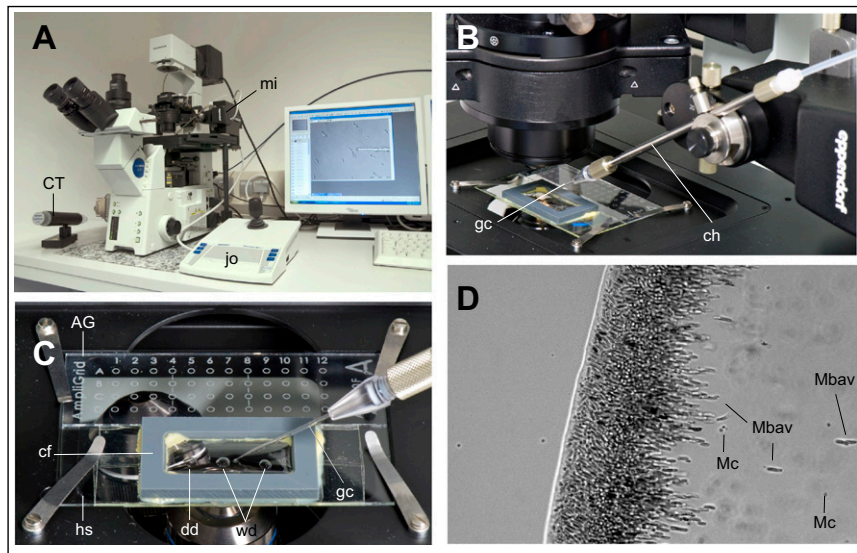


Fig. 56. Experimental setup for single cell sorting for whole genome amplification. (A) Eppendorf TransferMan NK2 micromanipulator (mi) attached to an Olympus BX61 microscope equipped with a long distance 40× lens. The micromanipulator is operated by a joystick control unit (jo), whereas aspiration and dispensing of individual cells is achieved by the Eppendorf manual CellTram (CT) hydraulic pressure-control system. (B) Capillary holder (ch) equipped with a glass capillary (gc). (C) Harvesting slide (hs) and AmpliGrip slide (AG). A custom-made frame (cf) filled with mineral oil prevents evaporation of the donor droplet (dd) and the wash droplets (wd). The glass capillary (gc) is first inserted into the donor droplet (dd), which contains a mixture of magnetically collected MTB from environmental sediment samples. (D) Micrograph of a section from a “hanging drop” containing diverse MTB from such an enrichment. *Candidatus Magnetobacterium bavaricum* (Mbav) cells and contaminating magnetotactic cocci (Mc) can be easily distinguished.

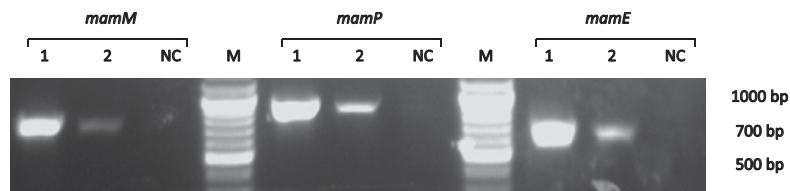
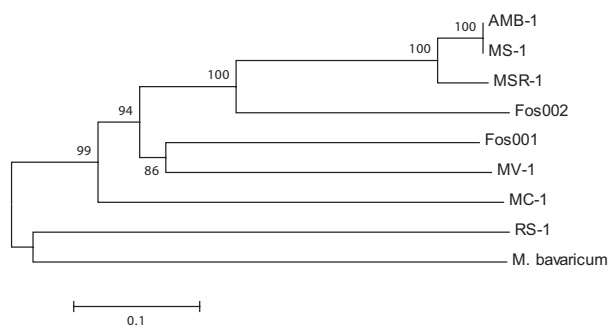
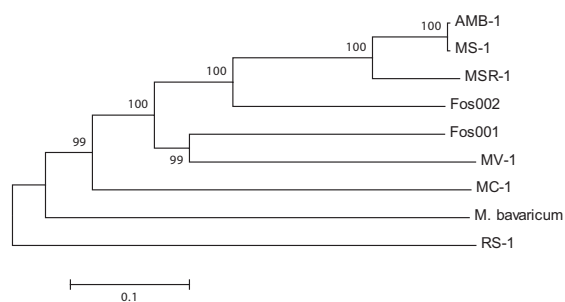


Fig. 57. Results of a control PCR to verify the Mbav origin of representative genes from the 37-kb contig. DNA generated from two independent WGA reactions on one and four individually sorted Mbav cells, respectively, were used as template in two independent PCR experiments (no.1 and no. 2) with primers targeting the *mamM*, *mamP*, and *mamE* genes of Mbav. Bands with a size of 693 bp, 809 bp, and 565 bp, respectively, were amplified as expected (NC, negative control with filter sterilized sample water). As a further control, a 1,068-bp fragment of the Mbav16S rRNA gene was amplified from the same templates using universal primers. Sequence analysis revealed a 100% match to the known 16S rRNA gene sequence of Mbav.

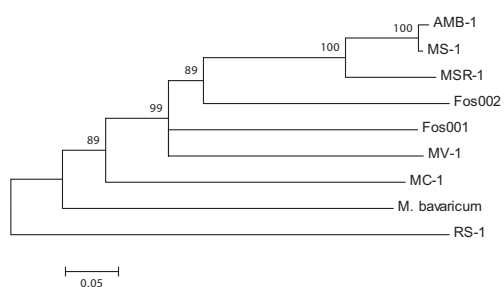
MamA



MamE



MamP



MamQ

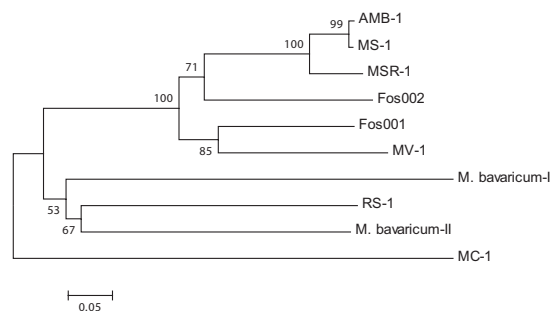


Fig. S8. Phylogenetic trees of further putative magnetosome proteins MamA, -E, -P, -Q, which display branching patterns congruent to those obtained for MamB and MamM. AMB-1, *Magnetospirillum magneticum*; MS-1, *Magnetospirillum magnetotacticum*; MSR-1, *Magnetospirillum gryphiswaldense*; Fos, Metagenomic clone; MV-1, magnetotactic vibrio strain MV-1; MC-1, magnetotactic coccus strain MC-1; and RS-1, *Desulfovibrio magneticus*.

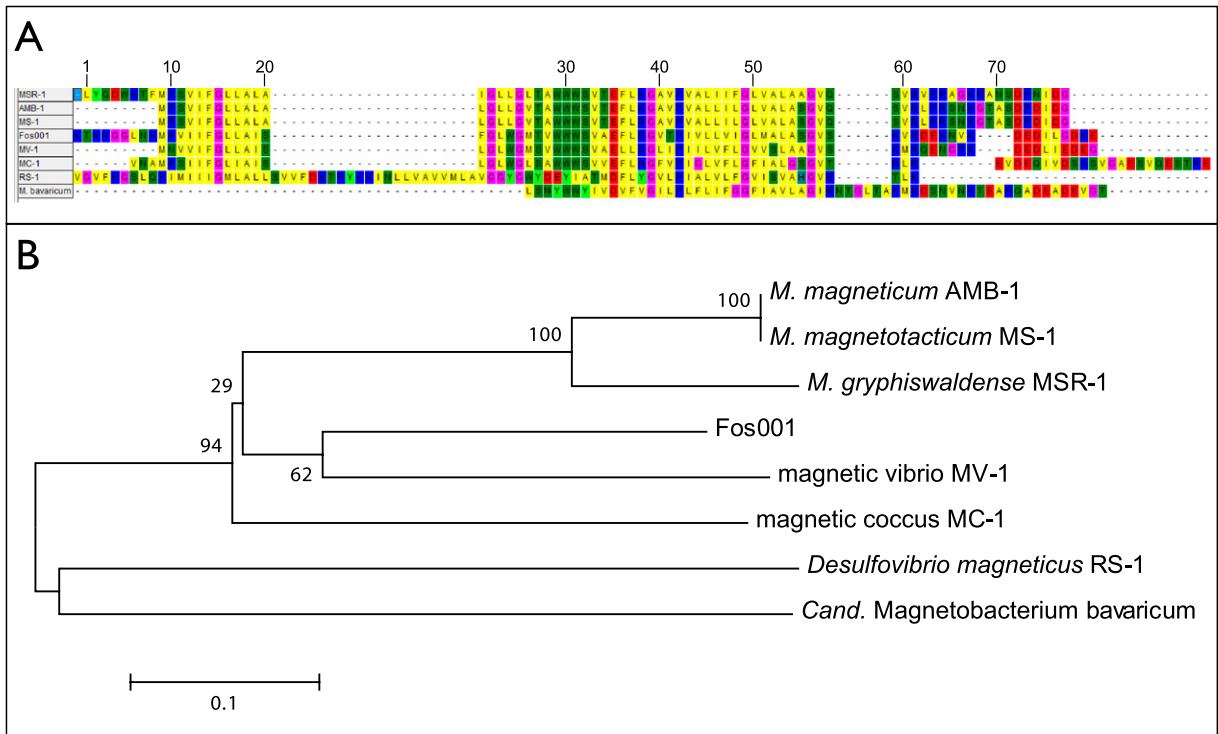


Fig. 59. (A) Multiple sequence alignment of Maml homologs from *Candidatus Magnetobacterium bavaricum* (Mbav), selected cultivated MTB, and a metagenomic clone (Fos001). Amino acid positions correspond to the Maml protein of *M. gryphiswaldense* MSR-1. The putative Mbav Maml protein is shorter than all other Maml proteins. (B) Phylogenetic tree calculated from the alignment shown in A. Maml homologs from *Desulfovibriomagneticus* RS-1 and Mbav cluster together, but are separated from other MTB. Bootstrap values and the bootstrap consensus tree are shown.

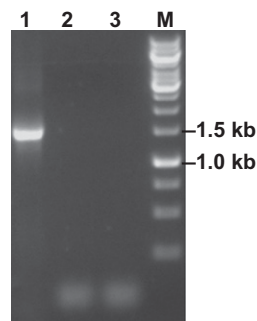


Fig. 510. Results of a nontemplate control experiment for whole genome amplification (WGA). The control experiment was performed as the previously described sorting experiment and the preparation of WGA DNA for pyrosequencing (Fig. 55 and *Materials and Methods*), except one modification: About 15 *Candidatus Magnetobacterium bavaricum* (Mbav) cells were transferred from a 5- μ L sample droplet into a 5- μ L sorting droplet, which consists of 5 μ L of filter-sterilized (0.45 μ m pore size) sample water (identical to the 5- μ L sample droplet, but without cells). As previously described, sorted cells were subsequently transferred into a 5- μ L H₂O droplet for further washing before transfer onto the Ampligridd was performed. After processing 82 cells in total, the capillary was used to harvest nontemplate control samples from sorting- and washing droplet. Together with the sorted cells, these samples were subjected to WGA and subsequent PCR experiments to check for extracellular DNA contaminations. PCR amplification of the 16S rRNA gene from the MTB sample (line 1), the filter-sterilized sample water (line 2), and the H₂O washing droplet (line 3) was performed as previously described (2), (lane M, Fermentas 1-kb DNA ladder). Only lane 1 shows the expected band corresponding to the full-length 16S rRNA gene, whereas lanes 2 and 3 do not show any band. Therefore, it can be confidently concluded from the nontemplate WGA control that the washing procedure was sufficiently stringent to remove any extracellular DNA contaminations.

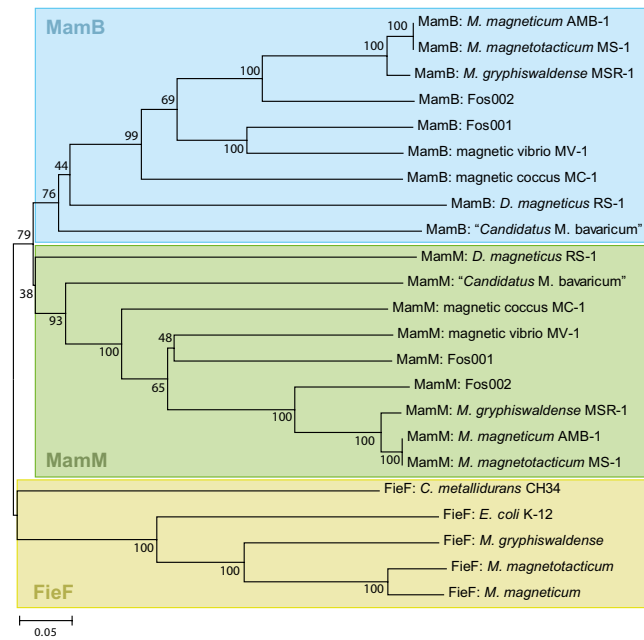


Fig. S11. Phylogenetic tree of cation diffusion facilitator (CDF) proteins of MTB. Two different types of FieF proteins from *Escherichia coli* K12 and *Wautersia metallidurans* served as outgroup and cluster together with FieF proteins from *Magnetospirillum* species (yellow). In contrast, the magnetosome proteins MamB and MamM form separate clusters (blue and green). The predicted MamB and MamM proteins of Mbav branching within these two clusters point toward horizontal gene transfer of *mamM* and *mamB* genes.

Table S1. Blast analysis of proteins encoded by predicted genes against the NCBI database

Locus tag	Annotation	Best hit	Identity, %	e-value	aa
emg00001	Hypothetical protein	<i>Gloeobacter violaceus</i>	38	1–32	516
emg00002	XRE family transcriptional regulator	<i>Yersinia pseudotuberculosis</i>	33	7–17	206
emg00003	Aspartate 1-decarboxylase	<i>Thermodesulfovibrio yellowstonii</i>	52	4–32	117
emg00004	4-hydroxy-3-methylbut-2-en-1-yl diphosphate synthase	<i>Thermodesulfovibrio yellowstonii</i>	60	3–120	348
emg00005	Hypothetical protein	<i>Thermodesulfovibrio yellowstonii</i>	45	3–72	319
emg00006	Hypothetical protein	<i>Thermodesulfovibrio yellowstonii</i>	61	1–51	180
emg00007	Transcriptional regulator, MerR family	<i>Sphaerobacter thermophilus</i>	33	4–16	128
emg00008	IS1 transposase B	<i>Escherichia coli</i>	100	1–94	167
emg00009	Hypothetical protein	<i>Syntrophomonas wolfei</i>	30	4–57	791
emg00010	Transposase	Plasmid R100	100	0.0	402
emg00011	Hypothetical protein	<i>Syntrophobacter fumaroxidans</i>	41	1–67	1,038
emg00012	Hypothetical protein	<i>Chloroflexus aggregans</i>	32	5–64	1,135
emg00013	Polysaccharide biosynthesis protein	<i>Methanococcus aeolicus</i>	23	2–20	489
emg00014	Hypothetical protein	<i>Sulfurihydrogenibium azorense</i>	51	0.032	63
emg00015	Conserved hypothetical protein	<i>Aspergillus flavus</i>	47	5–04	229
emg00016	Hypothetical protein	<i>Desulfovibrio magneticus</i>	39	1–15	237
emg00017	Pyruvate phosphate dikinase	<i>Anaplasma marginale</i>	23	0.003	196
emg00018	Hypothetical protein	<i>Desulfovibrio magneticus</i>	39	1–73	543
emg00019	Putative membrane protein	<i>Carboxydotherrmus hydrogenoformans</i>	43	5–46	358
emg00020	Hypothetical protein	<i>Bacteroides coprocola</i>	35	0.16	383
emg00021	NA	NA	NA	N.A.	69
emg00022	Condensin subunit Smc	<i>Methanohalophilus mahii</i>	27	1.9	252
emg00023	NA	NA	NA	N.A.	46
emg00024	Similar to GA14224-PA	<i>Tribolium castaneum</i>	22	0.14	146
emg00025	LemA protein (<i>mamQ-I</i>)	<i>Mitsuokella multacida</i>	36	5–25	186
emg00026	Magnetosome protein MamE	Uncultured bacterium	31	2–57	603
emg00027	Magnetosome protein MamI	Magnetic vibrio MV-1	29	0.78	62
emg00028	TPR Domain containing protein (<i>mamA</i>)	<i>Tetrahymina thermophila</i>	32	8–23	216
emg00029	Hypothetical membrane protein	<i>Desulfovibrio magneticus</i>	28	1–07	127
emg00030	Magnetosome protein MamB	Uncultured bacterium	32	3–41	297
emg00031	LemA protein (<i>mamQ-II</i>)	<i>Campylobacter showae</i>	32	2–17	182
emg00032	Hypothetical protein	<i>Desulfotobacterium hafniense</i>	27	7–08	227
emg00033	Magnetosome protein MamM	<i>Magnetospirillum gryphiswaldense</i>	35	2–44	307
emg00034	Magnetosome protein MamP	Magnetic vibrio MV-1	37	2–23	375

Results of BlastP analysis of proteins encoded by predicted genes of the 37,160-bp genomic fragment from *Candidatus Magnetobacterium bavaricum* against the NCBI database. Best BlastP hits are shown. Genes of a magnetosome cluster are in boldface type. The genes *emg00025* and *emg00031* encode proteins that were found to contain a LemA motive and were annotated as *mamQ*-like. Gene *emg00028* encodes a protein containing a TPR domain and was annotated as *mamA*-like (see text for details). All other genes were annotated according their best BlastP hits. NCBI, National Center for Biotechnology Information.

Table S2. BlastP similarities of putative magnetosome proteins from *Candidatus Magnetobacterium bavaricum* with their homologs from all MTB sequenced thus far

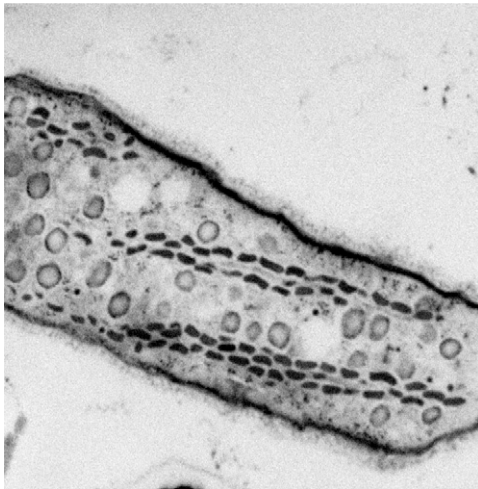
Protein	MSR-1, %	AMB-1, %	MS-1, %	MV-1, %	MC-1, %	RS-1, %
MamP	38	38	39	37	43	40
MamM	35	35	36	32	36	27
MamQ-II	24	21	21	23	22	26
MamB	31	30	30	30	32	34
MamA	24	23	23	26	NA	25
MamI	25	23	23	29	35	35
MamE	40	26	26	36	30	30
MamQ-I	28	27	28	26	NA	36

Local identity values are shown. See Figs. 4 and 5 and Figs. S7 and S8 for analysis involving ClustalW alignments of entire protein sequences. MTB, magnetotactic bacteria.



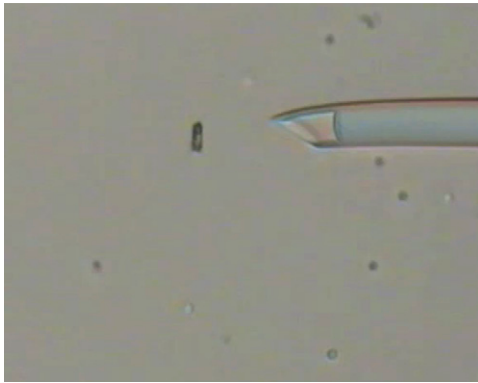
Movie S1. Three-dimensional reconstruction by SEM and focused ion beam (FIB) cross-sectioning (anterior toward posterior) of high-pressure frozen and freeze-substituted *Candidatus Magnetobacterium bavaricum* cell.

[Movie S1](#)



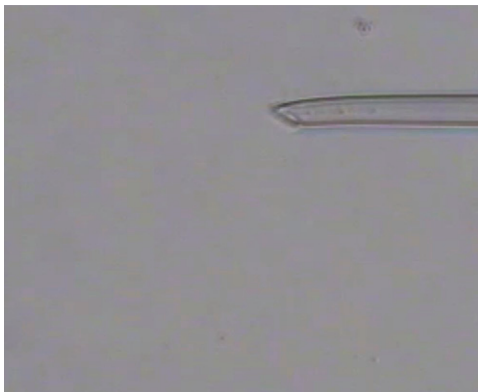
Movie S2. Three-dimensional reconstruction by SEM and FIB tangential sectioning of high-pressure frozen and freeze-substituted *Candidatus Magnetobacterium bavaricum* cell.

[Movie S2](#)



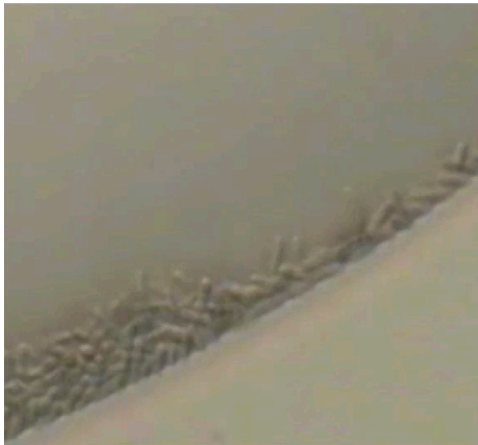
Movie S3. Micromanipulation of *Candidatus Magnetobacterium bavaricum* cells: Selection and aspiration of a single target cell from a mixture of MTB into a microcapillary.

[Movie S3](#)



Movie S4. Ejection of >1,000 collected *Candidatus Magnetobacterium bavaricum* cells from a microcapillary into a droplet of pure H₂O. Cells, which had been trapped within the microcapillary for a prolonged time, remained intact and viable in H₂O as indicated by their active swimming motility after release.

[Movie S4](#)



Movie S5. "*Candidatus Magnetobacterium bavaricum*" survives the cell sorting procedure. After being washed and transferred into a droplet of water ([Movie S4](#)), cells swim actively toward magnetic north to the edge of the water droplet.

[Movie S5](#)

6. Manuskript:

Monophyletic origin of magnetotaxis and the first magnetosomes.

Monophyletic origin of magnetotaxis and the first magnetosomes

Christopher T. Lefèvre,^{1**} Denis Trubitsyn,²
Fernanda Abreu,³ Sebastian Kolinko,⁴
Luiz Gonzaga Paula de Almeida,⁵
Ana Tereza R. de Vasconcelos,⁵ Ulysses Lins,³
Dirk Schüller,⁴ Nicolas Ginet,¹ David Pignol¹ and
Dennis A. Bazylinski^{2*}

¹CEA Cadarache/CNRS/Aix-Marseille Université, UMR7265 Service de Biologie Végétale et de Microbiologie Environnementale, Laboratoire de Bioénergétique Cellulaire, 13108, Saint Paul lez Durance, France.

²University of Nevada at Las Vegas, School of Life Sciences, Las Vegas, NV 89154-4004, USA.

³Instituto de Microbiologia Professor Paulo de Góes, Universidade Federal do Rio de Janeiro, 21941-590 Rio de Janeiro, RJ, Brazil.

⁴Ludwig Maximilians Universität München, Biozentrum, Großhaderner Str. 2, D-82152 Planegg Martinsried, Germany.

⁵Laboratório de Bioinformática, Laboratório Nacional de Computação Científica, Rio de Janeiro, Brazil.

Summary

Horizontal gene transfer (HGT), the transfer of genetic material other than by descent, is thought to have played significant roles in the evolution and distribution of genes in prokaryotes. These include those responsible for the ability of motile, aquatic magnetotactic bacteria (MTB) to align and swim along magnetic field lines and the biomineralization of magnetosomes that are responsible for this behaviour. There is some genomic evidence that HGT might be responsible for the distribution of magnetosome genes in different phylogenetic groups of bacteria. For example, in the genomes of a number of MTB, magnetosome genes are present as clusters within a larger structure known as the magnetosome genomic island surrounded by mobile elements such as insertion sequences and transposases as well as tRNA genes. Despite this, there is no strong direct proof of

HGT between these organisms. Here we show that a phylogenetic tree based on magnetosome protein amino acid sequences from a number of MTB was congruent with the tree based on the organisms' 16S rRNA gene sequences. This shows that evolution and divergence of these proteins and the 16S rRNA gene occurred similarly. This suggests that magnetotaxis originated monophyletically in the *Proteobacteria* phylum and implies that the common ancestor of all *Proteobacteria* was magnetotactic.

Introduction

The *Proteobacteria* represent the largest and most diverse phylogenetic lineage of Bacteria (Kerstens *et al.*, 2006). Widespread in this group are magnetotactic bacteria (MTB), motile, Gram-negative, aquatic prokaryotes that swim along magnetic field lines (Bazylinski and Frankel, 2004). MTB contain intracellular magnetosomes which are nano-sized, single-magnetic-domain iron-mineral crystals of either magnetite (Fe₃O₄) or greigite (Fe₃S₄), each enveloped by a lipid-bilayer membrane (Bazylinski and Frankel, 2004). Magnetosomes are usually arranged in chains within the cell, providing it with a permanent magnetic dipole moment that facilitates the cell's ability to locate and maintain an optimal position in vertical chemical and redox gradients (e.g. the oxic/anoxic interface) (Bazylinski and Frankel, 2004). Phylogenetically, known MTB are associated with the *Alpha*-, *Gamma*- and *Deltaproteobacteria* classes of the *Proteobacteria* phylum, the *Nitrospirae* phylum and the candidate division OP3, part of the *Planctomycetes–Verrucomicrobia–Chlamydiae* (PVC) bacterial superphylum (Bazylinski and Frankel, 2004; Kolinko *et al.*, 2012; Lefèvre *et al.*, 2012a).

Genetic determinants for magnetosome synthesis, the *mam*, *mtx* and *mms* genes, are organized as clusters in the genomes of all MTB examined thus far (Komeili, 2012). These clusters are in close proximity to each other and are flanked and sometimes interrupted by specific genomic features (e.g. insertion sequences, transposases) in some species that suggest that magnetosome genes are organized as a genomic island presumably transmitted to different bacteria through horizontal gene transfer (HGT) (Komeili, 2012). Such is the case, for example, for *Magnetospirillum magneticum* strain AMB-1 (Matsunaga *et al.*, 2005), *M. gryphiswal-*

Received 9 December, 2012; accepted 14 January, 2013. For correspondence. *E-mail dennis.bazylinski@unlv.edu; Tel. (+1) (702) 895 2053; Fax (+1) (702) 895 3956 or **E-mail lefevrechristopher@hotmail.com; Tel. (+33) 6 34 55 36 39; Fax (+33) 4 42 25 47 01.

dense strain MSR-1 (Lohsse *et al.*, 2011) and *Desulfovibrio magneticus* strain RS-1 (Nakazawa *et al.*, 2009) but not for the region harbouring the magnetosome genes of *Magnetococcus marinus* strain MC-1 which does not have a typical island organization (Schübbe *et al.*, 2009) and has an apparent genetic stability regarding magnetosome genes (spontaneous non-magnetotactic mutants have never been observed) indicating an earlier acquisition of magnetotaxis.

Results from some recent studies do not support a scenario where the magnetotaxis developed polyphyletically and had multiple evolutionary origins based on iron oxide and iron sulfide biomineralization (DeLong *et al.*, 1993), and instead are consistent with a model where magnetotaxis originated monophyletically regardless of the mineral formed (Abreu *et al.*, 2011; Jogler *et al.*, 2011; Lefèvre *et al.*, 2012b). In these studies, however, the number of magnetosome gene sequences available from cultured and uncultured MTB was seriously limited and probably not sufficient to build robust phylogenies to be used in elucidating the evolution of magnetotaxis and understanding how the magnetotactic trait was acquired by the different clades of MTB known to date. Thus, the evolution of magnetotaxis and how genes involved in magnetosome formation are distributed among and/or transferred between many different groups of prokaryotes is not clear.

In this study, we determined a large number of magnetosome gene sequences of cultured MTB, some of which have been only recently isolated, and many uncultured MTB characterized using culture-independent techniques. These sequences were used to determine phylogenies based on Mam protein amino acid sequences with the goal of understanding how magnetotaxis and magnetosome biomineralization originated and evolved.

Results and discussion

Magnetotactic bacteria are widely distributed in the Bacteria

The phylogeny based on 16S rRNA gene sequences of all known MTB and their closest relatives shows that they are relatively widely distributed in the Bacteria (Fig. 1). They are present in: two orders of the *Alphaproteobacteria* class, the Rhodospirillales (e.g. *Magnetospirillum*, *Magnetovibrio* and *Magnetospira*) (Schleifer *et al.*, 1991; Bazylnski *et al.*, 2012a; Williams *et al.*, 2012) and the Magnetococcales (e.g. *Magnetococcus*) (Bazylnski *et al.*, 2012b); in two orders of the *Gammaproteobacteria* class, the Thiotrichales (strain SS-5) and the Chromatiales (strain BW-2) (Lefèvre *et al.*, 2012a); in two orders of the *Deltaproteobacteria* class, the Desulfovibrionales (e.g. *Desulfovibrio*) (Sakaguchi *et al.*, 1993) and the Desulfobacterales (e.g. *Candidatus Magnetoglobus*, *Ca. Desul-*

famplus) (Abreu *et al.*, 2007; Lefèvre *et al.*, 2011a); in the *Nitrospirae* phylum (e.g. *Ca. Magnetobacterium*, *Ca. Magnetooovum*) (Jogler *et al.*, 2010; Lefèvre *et al.*, 2011b); and in the candidate OP3 division (strain SKK-01) (Kolinko *et al.*, 2012) (Fig. 1).

Thus far, there is only indirect evidence that HGT is responsible for the distribution of magnetotaxis and magnetosome biomineralization. One major line of evidence is the fact that magnetosome genes are present as clusters within a larger structure known as the magnetosome genomic island (MAI) that is surrounded by mobile elements such as insertion sequences and transposases in the genomes of a number of MTB (e.g. *M. gryphiswaldense*) (Ullrich *et al.*, 2005). Moreover, in some MTB, the trait of magnetosome biomineralization appears to be easily lost (Komeili, 2012) and in *M. gryphiswaldense*, this is due, in some cases, to the loss of the MAI (Schübbe *et al.*, 2003). Magnetosome genes have been shown to be organized as operons in *M. gryphiswaldense* (Schübbe *et al.*, 2006). This might explain why these genes continue to be present as clusters as genes organized as operons have selective pressure to keep these genes together as clusters during evolution. Thus, conservation of gene clusters is not necessarily evidence for HGT (Tamames, 2001; Fang *et al.*, 2008).

An additional line of indirect evidence is the discovery and identification of strains of non-MTB very closely related to MTB that are not magnetotactic and apparently do not possess magnetosome genes. For example, non-magnetotactic *Phaeospirillum* species and *Magnetospirillum bellicus* (Thrash *et al.*, 2010) phylogenetically lie within the *Magnetospirillum* group and thus likely share a common ancestor (Lefèvre *et al.*, 2012b) (Fig. 1). Several newly isolated, alkaliphilic, sulfate reducing MTB are so closely related to *Desulfonatronum thiodismutans* strain MLF-1, that they appear to be different strains of the same species, although the latter is not magnetotactic and does not produce magnetosomes even when grown under conditions where the former do (Lefèvre *et al.*, 2011c) (Fig. 1). Finally, non-magnetotactic forms of the magnetotactic multicellular prokaryotes (MMPs) that do not biomineralize magnetosomes have been discovered to belong to the same phylogenetic group formed by the MMPs (Lefèvre *et al.*, 2010).

16S rRNA genes and magnetosome proteins of MTB appear to have evolved similarly

Genome sequences of a number of MTB are now complete or nearly so. Genomic information from MTB has recently been used to argue against a polyphyletic origin of magnetotaxis (Abreu *et al.*, 2011; Jogler *et al.*, 2011), an idea originally suggested prior to the discovery and identification of magnetosome genes and based on the

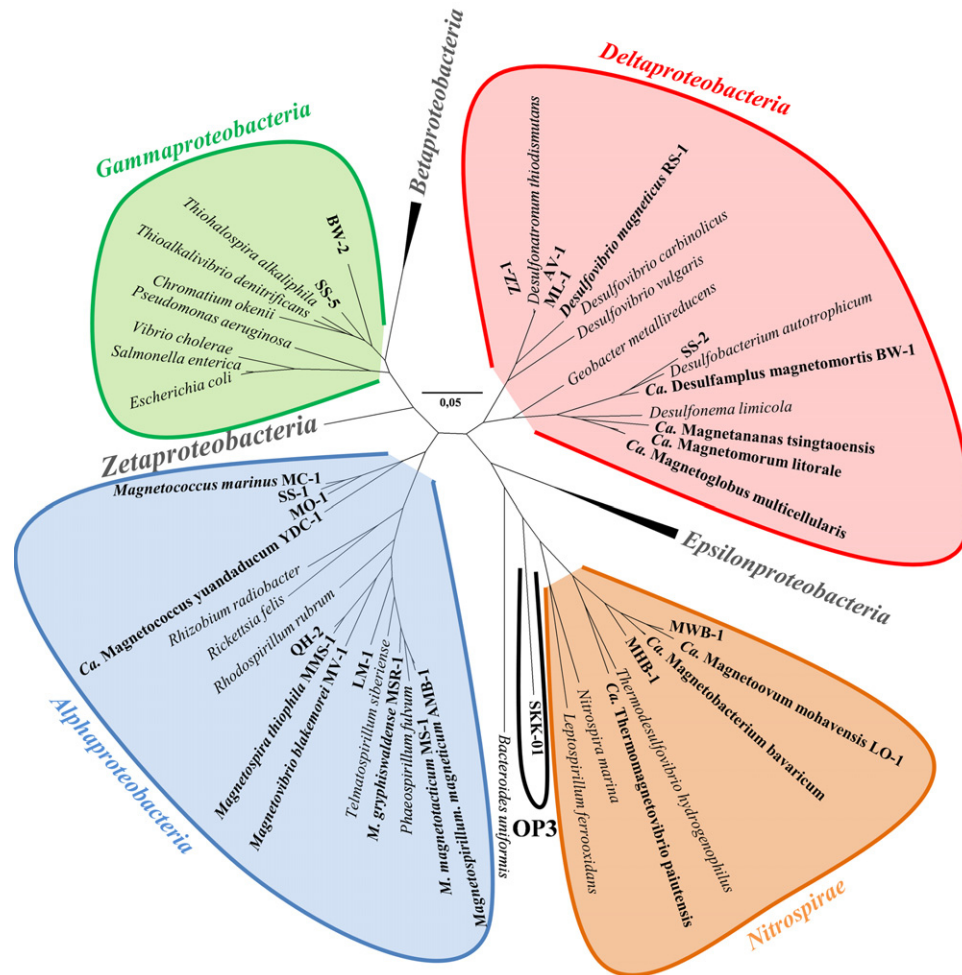


Fig. 1. Phylogenetic tree based on 16S rRNA gene sequences showing the phylogenetic position of all known MTB in the *Proteobacteria* and *Nitrospirae* phyla and in the candidate OP3 division (part of the PVC bacterial superphylum). The 16S rRNA gene sequence of *Bacteroides uniformis* was used to root the tree. Bar represents 5% sequence divergence. Note the basal position of the clade formed by the magnetotactic cocci in the *Alphaproteobacteria* class (e.g. *Magnetococcus marinus*). Depending on the number of species used to generate the tree, the magnetotactic cocci group can also emerge basal to the *Alpha*- and *Gammaproteobacteria* (e.g. Fig. 2A). *Ca.*, *Candidatus*, meaning organism has only been provisionally named.

finding that magnetotaxis based on iron-sulfide and iron-oxide magnetosomes occurred in two separate evolutionary lines of descent (DeLong *et al.*, 1993).

Our comparative genomic analyses reveal that all MTB examined from three classes of the *Proteobacteria* phylum and one strain of the *Nitrospirae* phylum have in common nine genes involved in magnetosome formation (Table 1). Phylogenies based on 16S rRNA gene sequences and some amino acid sequences of house-keeping proteins of the 11 MTB studied are congruent, that is, the pattern of divergence is similar to that of the nine magnetosome protein sequences (Figs 2 and S1). This indicates that the evolution and divergence of these proteins and the organisms' 16S rRNA genes occurred similarly and strongly suggests that magnetotaxis/magnetosome biomineralization evolved monophyleti-

cally. If the trait of magnetotaxis was distributed to the many different MTB through recent HGT, one would not expect this congruence and instead would result in a phylogenetic tree of the Mam proteins where the MTB in the *Proteobacteria* formed a clade that is clearly not observed in the 16S rRNA gene tree. It is important to note that these results do not preclude the possibility of ancient HGT of magnetosome genes or even some occurrences of recent HGT of magnetosome genes as has been recently suggested for some species of *Magnetospirillum* (Rioux *et al.*, 2010; Lefèvre *et al.*, 2012b).

Our genomic data also suggest that the common ancestor of all *Proteobacteria* was magnetotactic. If true, this is an important finding because known MTB represent only a minority of organisms in the *Proteobacteria*. This might be explained by the fact that some cultivated MTB

Table 1. Accession numbers of the nine proteins involved in magnetosome formation found in all MTB with their genome or part of it sequenced.

Magnetotactic bacterium	mamA	mamB	mamE	mamI	mamK	mamM	mamP	mamQ	feoB
AMB-1	YP_420334	YP_420337	YP_420326	YP_420325	YP_420328	YP_420330	YP_420333	YP_420335	YP_420387
MS-1	ZP_00054410	ZP_00054413	ZP_00054403	ZP_00208239	ZP_00054405	ZP_00054406	ZP_00054409	ZP_00053530	ZP_00054713
MSR-1	CAM78031	CAM78034	CAM78023	CAM78022	CAM78025	CAM78027	CAM78030	CAM78032	ABL14106
MV-1	CAV30810	CAV30807	CAV30818	CAV30819	CAV30816	CAV30814	CAV30811	CAV30809	CAV30756
SS-5	AFX88984	AFX88985	AFX88986	AFX88987	AFX88988	AFX88990	AFX88991	AFX88992	AFX88983
MC-1	ABK44754	ABK44751	ABK44768	ABK44769	ABK44760	ABK44757	ABK44755	ABK44752	ABK44237
RS-1	YP_002955493	YP_002955479	YP_002955485	NC_012796	YP_002955471	YP_002955479	YP_002955486	YP_002955490	YP_002955474
ML-1	AFX88975	AFX88976	AFX88977	AFX88978	AFX88979	AFX88980	AFX88981	AFX88982	AFX88974
BW-1 cluster 1	AET24905	AET24907	AET24911	CCO06668	AET24913	AET24908	AET24921	JN830638	JN830642
BW-1 cluster 2	AET24906	AET24910	AET24912	AFX88993	AET24913	AET24909	AET24922	AET24917	AET24920
Ca. M. magnetoglobus	ADV17394	ADV17395	ADV17396	HQ336746	ADV17375	ADV17392	ADV17391	ADV17393	ADV17385
Ca. M. bavaricum	FQ377626	FQ377626	FQ377626	FQ377626	AFX60119	FQ377626	FQ377626	FQ377626	AFX60118

The protein FeoB was considered as magnetosome protein since it has been shown to be involved in iron transport in the magnetosome (Rong *et al.*, 2012), its corresponding gene is in close proximity to the *mam* genes for most MTB and specific to MTB.

appear to lose the magnetotactic trait relatively easily in culture through loss of the magnetosome island (Komeili, 2012). Presumably these organisms were the ancestors that gave rise to the *Beta*-, *Epsilon*-, and *Zetaproteobacteria* groups that do not appear to contain MTB. Alternatively, there could be magnetotactic members of these groups that have not yet been discovered. Our data also support the possibility that the common ancestor of all *Proteobacteria*, *Nitrospirae* and the candidate division OP3 was magnetotactic. However, to make such hypothesis we would require additional magnetosome gene, (i.e. *mam* gene) sequences from more MTB from the *Nitrospirae* and the OP3. In addition, the phylogenetic status of bacteria of the candidate division OP3 should be better resolved.

The *Proteobacteria* emerged 2.5–3.0 billion years ago (Battistuzzi *et al.*, 2004) when levels of atmospheric oxygen were low (Anbar *et al.*, 2007) and anaerobic-to-microaerobic environments dominated. About this time magnetosomes may have been important to MTB in scavenging reactive oxygen species (Guo *et al.*, 2012) and later, when atmospheric oxygen levels increased, served to aid MTB in navigation.

The mineral phase of the magnetosomes appears to correlate with the phylogeny and therefore the evolution of MTB: the first magnetosomes

There is a strong correlation between phylogeny of MTB and composition and morphology of the magnetosome mineral they produce (Abreu *et al.*, 2011; Lefèvre *et al.*, 2011d; 2012a). Known MTB of the candidate division OP3 and the *Nitrospirae*, the more deeply branching phylogenetic groups (Jogler *et al.*, 2011; Kolinko *et al.*, 2012), biomineralize bullet-shaped magnetite crystals (Fig. 2B). MTB of the *Deltaproteobacteria*, the most deeply diverging group of the *Proteobacteria*, also only biomineralize bullet-shaped magnetite crystals (some produce greigite as well as magnetite) (Lefèvre *et al.*, 2011d). MTB of the later diverging *Alpha*- and *Gammaproteobacteria* only biomineralize well-defined crystals of cuboctahedral and elongated prismatic magnetite. Thus it seems likely that the highly variable, bullet-shaped magnetite crystals were the mineral present in the first magnetosomes.

An interesting question is how the biomineralization of iron-sulfide (greigite) magnetosomes developed. It is clear that this process must have originated in the *Deltaproteobacteria*, the only group known to contain greigite-producing MTB (Abreu *et al.*, 2011; Lefèvre *et al.*, 2011a) but not the most deeply branching of the groups that contain MTB. Both magnetite- and greigite-producing MTB possess a similar suite of magnetosome genes although those for greigite biomineralization are slightly different than those for magnetite biomineralization in

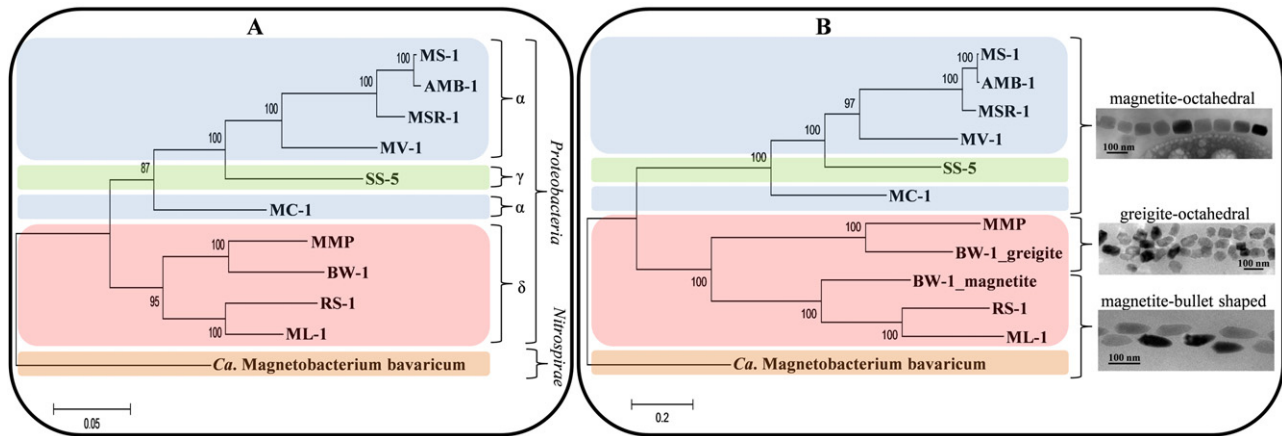


Fig. 2. Phylogenetic trees based on 16S rRNA gene sequences reflecting the evolution of MTB (A) and on concatenated magnetosome protein sequences (MamABEIKMPQ and FeoB) reflecting the evolution of magnetotaxis (B).

MTB. Based on this and the discovery of an MTB that biomineralizes both minerals and has a separate suite of enzymes for the synthesis of each mineral, it seems plausible that the genes for greigite biomineralization originated from gene duplication and/or subsequent mutation or other genetic changes that appears to have only occurred in the *Desulfobacterales* order of the *Deltaproteobacteria*. This adaptation appears to have resulted in the replacement of oxygen with sulfur in magnetosome crystals of some anaerobic MTB in highly reduced environments (Lefèvre *et al.*, 2011a).

Organisms from lineages in the Eukaryota (e.g. trout, pigeon) also biomineralize magnetite possibly for navigation in the geomagnetic field (Kirschvink *et al.*, 2001). For example, a magnetotactic euglenoid algae contains numerous chains of bullet-shaped magnetite crystals and a number of animals appear to contain magnetosome-like structures (Torres de Araujo *et al.*, 1986). Although there is no evidence of the existence of *mam*-like genes in these higher organisms, if present, they likely originated from MTB and might indicate that magnetoreception in the Eukaryota emerged from a magnetotactic bacterium.

Conclusions

Results from our phylogenetic analyses of magnetosome-related genes and proteins presented here provide new insight into the evolutionary origin of magnetotaxis and magnetosome biomineralization in MTB. The analyses show that the divergence of nine magnetosome-related proteins, based on amino acid sequences, in a large number of MTB, is congruent with the divergence of the organisms' 16S rRNA gene sequences and a number of housekeeping protein amino

acid sequences. This unambiguously indicates that magnetotaxis originated monophyletically in the *Proteobacteria* phylum and provides evidence that the common ancestor of all *Proteobacteria* was magnetotactic. This is in contradiction with the multiple evolutionary origins model previously described (DeLong *et al.*, 1993). Lastly, the strong correlation between the overall phylogeny of MTB and specific magnetosome crystal types of different groups of MTB suggests that the first magnetosome crystals biomineralized by MTB were bullet-shaped crystals of magnetite.

Experimental procedures

Genome sequencing and annotation

Genomes of *Candidatus Desulfamplus magnetomortis* strain BW-1 (Lefèvre *et al.*, 2011a) and the *Gammaproteobacteria* strain SS-5 (Lefèvre *et al.*, 2012a) were sequenced using a 454 GS FLX System sequencer (Roche Diagnostics GmbH/454 Life Sciences Corporation, Branford, CT, USA). While the genome of the alkaliphilic magnetotactic strain ML-1 (Lefèvre *et al.*, 2011c) was sequenced using Ion Torrent technology (DeWalch Technologies, Houston, TX, USA). Sequences of *Ca. Magnetobacterium bavaricum* (Jogler *et al.*, 2011) were obtained from an incomplete genome assembly derived from a Phi29 polymerase-amplified DNA of few microsorted cells (Jogler *et al.*, 2011).

Manual annotation of genomes was conducted using MaGe comparative genomic software (Vallenet *et al.*, 2006) for strains SS-5 and BW-1 while strain ML-1 genome was analysed with Rapid Annotation using Subsystem Technology (RAST) (Meyer *et al.*, 2008). The *mam* genes of *Magnetospirillum magneticum* strain AMB-1 (GenBank Accession Number AP007255) (Matsunaga *et al.*, 2005), *M. gryphiswaldense* strain MSR-1 (AM085146) (Lohsse *et al.*, 2011), *M. magnetotacticum* strain MS-1 (NZ_AAAP01003731) (Bertani *et al.*, 2001), *Magnetococcus marinus* strain MC-1 (NC_008576) (Schübbe *et al.*, 2009), *Magnetovibrio*

blakemorei strain MV-1 (FP102531) (Jogler *et al.*, 2009), *Ca. Magnetoglobus multicellularis* (HQ336745 and HQ336746) (Abreu *et al.*, 2011) and *Desulfovibrio magneticus* strain RS-1 (AP010904) (Nakazawa *et al.*, 2009) were compared with the genomes of strains BW-1, SS-5 and ML-1 genome sequences using tblastx (Altschul *et al.*, 1997).

Phylogenetic analysis

Alignment of sequences were performed using CLUSTAL W multiple alignment accessory application in the BioEdit sequence alignment editor (Hall, 1999). Phylogenetic trees were constructed using MEGA version 5 (Tamura *et al.*, 2011) applying the maximum likelihood algorithm (Guindon and Gascuel, 2003). Bootstrap values were calculated with 100 replicates.

Electron microscopy

Transmission electron microscopy (TEM) of magnetosome chains was done with a Tecnai (FEI Company, Hillsboro, OR, USA) model G2 F30 Super-Twin transmission electron microscope.

Acknowledgements

We thank Joseph L. Kirschvink, Nicolas Menguy and Pascal Arnoux for helpful comments, suggestions and discussions. D. A. B. is supported by US National Science Foundation (NSF) Grant EAR-0920718. N. G., D. P. and C. T. L. are funded by the French national research agency ANR-P2N entitled MEFISTO. C. T. L. is the recipient of an award from the Fondation pour la Recherche Médicale (FRM: SPF20101220993). U. L., F. A. and A. T. V. are supported by Brazilian CNPq/FAPERJ/CAPES. D. S. and S. K. are supported by Deutsche Forschungsgemeinschaft (Grant DFG Schu1080/11-1).

References

Abreu, F., Martins, J.L., Silveira, T.S., Keim, C.N., de Barros, H.G., Filho, F.J., *et al.* (2007) 'Candidatus Magnetoglobus multicellularis', a multicellular, magnetotactic prokaryote from a hypersaline environment. *Int J Syst Evol Microbiol* **57**: 1318–1322.

Abreu, F., Cantão, M.E., Nicolás, M.F., Barcellos, F.G., Morillo, V., Almeida, L.G., *et al.* (2011) Common ancestry of iron oxide- and iron-sulfide-based biomineralization in magnetotactic bacteria. *ISME J* **5**: 1634–1640.

Altschul, S.F., Madden, T.L., Schäffer, A.A., Zhang, J., Zhang, Z., Miller, W., *et al.* (1997) Gapped BLAST and PSI-BLAST: a new generation of protein database search programs. *Nucleic Acids Res* **25**: 3389–3402.

Anbar, A.D., Duan, Y., Lyons, T.W., Arnold, G.L., Kendall, B., Creaser, R.A., *et al.* (2007) A whiff of oxygen before the Great Oxidation Event? *Science* **317**: 1903–1906.

Battistuzzi, F.U., Feijao, A., and Hedges, S.B. (2004) A genomic timescale of prokaryote evolution: insights into the origin of methanogenesis, phototrophy, and the colonization of land. *BMC Evol Biol* **4**: 44.

Bazylinski, D.A., and Frankel, R.B. (2004) Magnetosome formation in prokaryotes. *Nat Rev Microbiol* **2**: 217–230.

Bazylinski, D.A., Williams, T.J., Lefèvre, C.T., Trubitsyn, D., Fang, J., Beveridge, T.J., *et al.* (2012a) *Magnetovibrio blakemorei*, gen. nov. sp. nov., a new magnetotactic bacterium (*Alphaproteobacteria: Rhodospirillaceae*) isolated from a salt marsh. *Int J Syst Evol Microbiol*. doi: 10.1099/ijs.0.044453-0.

Bazylinski, D.A., Williams, T.J., Lefèvre, C.T., Berg, R.J., Zhang, C.L., Bowser, S.S., *et al.* (2012b) *Magnetococcus marinus* gen. nov., sp. nov., a marine, magnetotactic bacterium that represents a novel lineage (*Magnetococcaceae* fam. nov.; *Magnetococcales* ord. nov.) at the base of the *Alphaproteobacteria*. *Int J Syst Evol Microbiol* **63**. doi: 10.1099/ijs.0.038927-0.

Bertani, L.E., Weko, J., Phillips, K.V., Gray, R.F., and Kirschvink, J.L. (2001) Physical and genetic characterization of the genome of *Magnetospirillum magnetotacticum*, strain MS-1. *Gene* **264**: 257–263.

DeLong, E.F., Frankel, R.B., and Bazylinski, D.A. (1993) Multiple evolutionary origins of magnetotaxis in bacteria. *Science* **259**: 803–806.

Fang, G., Rocha, E.P., and Danchin, A. (2008) Persistence drives gene clustering in bacterial genomes. *BMC Genomics* **9**: 4.

Guindon, S., and Gascuel, O. (2003) A simple, fast, and accurate algorithm to estimate large phylogenies by maximum likelihood. *Syst Biol* **52**: 696–704.

Guo, F.F., Yang, W., Jiang, W., Geng, S., Peng, T., and Li, J.L. (2012) Magnetosomes eliminate intracellular reactive oxygen species in *Magnetospirillum gryphiswaldense* MSR-1. *Environ Microbiol* **14**: 1722–1729.

Hall, T. (1999) BioEdit: a user-friendly biological sequence alignment editor and analysis program for Windows 95/98/NT. *Nucleic Acids Symp Ser* **41**: 95–98.

Jogler, C., Kube, M., Schübbe, S., Ullrich, S., Teeling, H., Bazylinski, D.A., *et al.* (2009) Comparative analysis of magnetosome gene clusters in magnetotactic bacteria provides further evidence for horizontal gene transfer. *Environ Microbiol* **11**: 1267–1277.

Jogler, C., Niebler, M., Lin, W., Kube, M., Wanner, G., Kolinko, S., *et al.* (2010) Cultivation-independent characterization of 'Candidatus Magnetobacterium bavaricum' via ultrastructural, geochemical, ecological and metagenomic methods. *Environ Microbiol* **12**: 2466–2478.

Jogler, C., Wanner, G., Kolinko, S., Niebler, M., Amann, R., Petersen, N., *et al.* (2011) Conservation of proteobacterial magnetosome genes and structures in an uncultivated member of the deep-branching *Nitrospira* phylum. *Proc Natl Acad Sci USA* **108**: 1134–1139.

Kerstens, K., De Vos, P., Gillis, M., Swings, J., Vandamme, P., and Stackebrandt, E. (2006) Introduction to the *Proteobacteria*. In *The Prokaryotes: a Handbook on the Biology of Bacteria*, Vol. 5. Dworkin, M., Falkow, S., Rosenberg, E., Schleifer, K.H., and Stackebrandt, E., (eds). New York, USA: Springer, pp. 3–37.

Kirschvink, J.L., Walker, M.M., and Diebel, C.E. (2001) Magnetite-based magnetoreception. *Curr Opin Neurobiol* **11**: 462–467.

Kolinko, S., Jogler, C., Katzmann, E., Wanner, G., Peplies, J., and Schüler, D. (2012) Single-cell analysis reveals a novel

- uncultivated magnetotactic bacterium within the candidate division OP3. *Environ Microbiol* **14**: 1709–1721.
- Komeili, A. (2012) Molecular mechanisms of compartmentalization and biomineralization in magnetotactic bacteria. *FEMS Microbiol Rev* **36**: 232–255.
- Lefèvre, C.T., Abreu, F., Lins, U., and Bazylinski, D.A. (2010) Nonmagnetotactic multicellular prokaryotes from low-saline, nonmarine aquatic environments and their unusual negative phototactic behavior. *Appl Environ Microbiol* **76**: 3220–3227.
- Lefèvre, C.T., Menguy, N., Abreu, F., Lins, U., Pósfai, M., Prozorov, T., *et al.* (2011a) A cultured greigite-producing magnetotactic bacterium in a novel group of sulfate-reducing bacteria. *Science* **334**: 1720–1723.
- Lefèvre, C.T., Frankel, R.B., Abreu, F., Lins, U., and Bazylinski, D.A. (2011b) Culture-independent characterization of a novel, uncultivated magnetotactic member of the *Nitrospirae* phylum. *Environ Microbiol* **13**: 538–549.
- Lefèvre, C.T., Frankel, R.B., Pósfai, M., Prozorov, T., and Bazylinski, D.A. (2011c) Isolation of obligately alkaliphilic magnetotactic bacteria from extremely alkaline environments. *Environ Microbiol* **13**: 2342–2350.
- Lefèvre, C.T., Pósfai, M., Abreu, F., Lins, U., Frankel, R.B., and Bazylinski, D.A. (2011d) Morphological features of elongated-anisotropic magnetosome crystals in magnetotactic bacteria of the *Nitrospirae* phylum and the *Deltaproteobacteria* class. *Earth Planet Sci Lett* **312**: 194–200.
- Lefèvre, C.T., Vioria, N., Schmidt, M.L., Pósfai, M., Frankel, R.B., and Bazylinski, D.A. (2012a) Novel magnetite-producing magnetotactic bacteria belonging to the *Gammaproteobacteria*. *ISME J* **6**: 440–450.
- Lefèvre, C.T., Schmidt, M.L., Vioria, N., Trubitsyn, D., Schüller, D., and Bazylinski, D.A. (2012b) Insight into the evolution of magnetotaxis in *Magnetospirillum* spp., based on *mam* gene phylogeny. *Appl Environ Microbiol* **78**: 7238–7248.
- Lohsse, A., Ullrich, S., Katzmann, E., Borg, S., Wanner, G., Richter, M., *et al.* (2011) Functional analysis of the magnetosome island in *Magnetospirillum gryphiswaldense*: the *mamAB* operon is sufficient for magnetite biomineralization. *PLoS ONE* **6**: e25561.
- Matsunaga, T., Okamura, Y., Fukuda, Y., Wahyudi, A.T., Murase, Y., and Takeyama, H. (2005) Complete genome sequence of the facultative anaerobic magnetotactic bacterium *Magnetospirillum* sp. strain AMB-1. *DNA Res* **12**: 157–166.
- Meyer, F., Paarmann, D., D'Souza, M., Olson, R., Glass, E.M., Kubal, M., *et al.* (2008) The metagenomics RAST server – a public resource for the automatic phylogenetic and functional analysis of metagenomes. *BMC Bioinformatics* **9**: 386.
- Nakazawa, H., Arakaki, A., Narita-Yamada, S., Yashiro, I., Jinno, K., Aoki, N., *et al.* (2009) Whole genome sequence of *Desulfovibrio magneticus* strain RS-1 revealed common gene clusters in magnetotactic bacteria. *Genome Res* **19**: 1801–1808.
- Rioux, J.-B., Philippe, N., Pereira, S., Pignol, D., Wu, L.F., and Ginet, N. (2010) A second actin-like MamK protein in *Magnetospirillum magneticum* AMB-1 encoded outside the genomic magnetosome island. *PLoS ONE* **5**: e9151.
- Rong, C., Zhang, C., Zhang, Y., Qi, L., Yang, J., Guan, G., *et al.* (2012) FeoB2 functions in magnetosome formation and oxidative stress protection in *Magnetospirillum gryphiswaldense* strain MSR-1. *J Bacteriol* **194**: 3972–3976.
- Sakaguchi, T., Burgess, J.G., and Matsunaga, T. (1993) Magnetite formation by a sulfate-reducing bacterium. *Nature* **365**: 47–49.
- Schleifer, K.H., Schüller, D., Spring, S., Weizenegger, M., Amann, R., Ludwig, W., *et al.* (1991) The genus *Magnetospirillum* gen. nov. description of *Magnetospirillum gryphiswaldense* sp. nov. and transfer of *Aquaspirillum magnetotacticum* to *Magnetospirillum magnetotacticum* comb. nov. *Syst Appl Microbiol* **14**: 379–385.
- Schübbe, S., Kube, M., Scheffel, A., Wawer, C., Heyen, U., Meyerdierks, A., *et al.* (2003) Characterization of a spontaneous nonmagnetic mutant of *Magnetospirillum gryphiswaldense* reveals a large deletion comprising a putative magnetosome island. *J Bacteriol* **185**: 5779–5790.
- Schübbe, S., Würdemann, C., Peplies, J., Heyen, U., Wawer, C., Glöckner, F.O., *et al.* (2006) Transcriptional organization and regulation of magnetosome operons in *Magnetospirillum gryphiswaldense*. *Appl Environ Microbiol* **72**: 5757–5765.
- Schübbe, S., Williams, T.J., Xie, G., Kiss, H.E., Brettin, T.S., Martinez, D., *et al.* (2009) Complete genome sequence of the chemolithoautotrophic marine magnetotactic coccus strain MC-1. *Appl Environ Microbiol* **75**: 4835–4852.
- Tamames, J. (2001) Evolution of gene order conservation in prokaryotes. *Genome Biol* **2**: 0020.1.
- Tamura, K., Peterson, D., Peterson, N., Stecher, G., Nei, M., and Kumar, S. (2011) MEGA5: molecular evolutionary genetics analysis using maximum likelihood, evolutionary distance, and maximum parsimony methods. *Mol Biol Evol* **28**: 2731–2739.
- Thrash, J.C., Ahmadi, S., Torok, T., and Coates, J.D. (2010) *Magnetospirillum bellicus* sp. nov., a novel dissimilatory perchlorate-reducing alphaproteobacterium isolated from a bioelectrical reactor. *Appl Environ Microbiol* **76**: 4730–4737.
- Torres de Araujo, F.F., Pires, M.A., Frankel, R.B., and Bicudo, C.E. (1986) Magnetite and magnetotaxis in algae. *Biophys J* **50**: 375–378.
- Ullrich, S., Kube, M., Schübbe, S., Reinhardt, R., and Schüller, D. (2005) A hypervariable 130-kilobase genomic region of *Magnetospirillum gryphiswaldense* comprises a magnetosome island which undergoes frequent rearrangements during stationary growth. *J Bacteriol* **187**: 7176–7184.
- Vallenet, D., Labarre, L., Rouy, Z., Barbe, V., Bocs, S., Cruveiller, S., *et al.* (2006) MaGe: a microbial genome annotation system supported by synteny results. *Nucleic Acids Res* **34**: 53–65.
- Williams, T.J., Lefèvre, C.T., Zhao, W., Beveridge, T.J., and Bazylinski, D.A. (2012) *Magnetospira thiophila* gen. nov., sp. nov., a marine magnetotactic bacterium that represents a novel lineage within the *Rhodospirillaceae*

(*Alphaproteobacteria*). *Int J Syst Evol Microbiol* **62**: 2443–2450.

Supporting information

Additional Supporting Information may be found in the online version of this article at the publisher's web-site:

Fig. S1. Phylogenetic tree based on concatenated amino acid sequences of housekeeping genes *rpoD* and *ftsZ* of the 11 MTB under study. MMP, Magnetotactic multicellular prokaryotes *Ca. Magnetoglobus multicellularis*, M.bav, *Ca. Magnetobacterium bavaricum*.

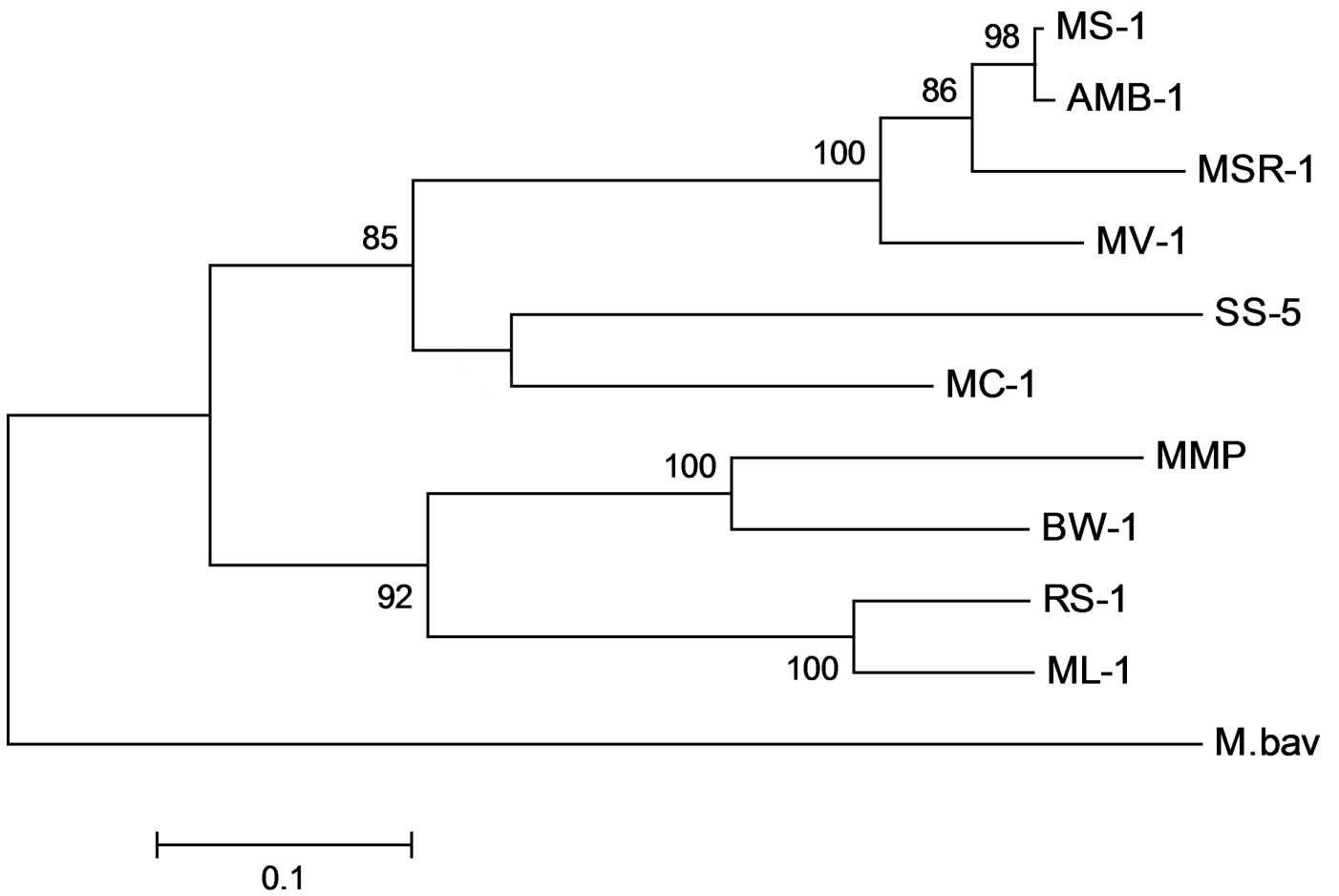


Fig. S1. Phylogenetic tree based on concatenated amino acid sequences of housekeeping genes *rpoD* and *ftsZ* of the 11 MTB under study. MMP, Magnetotactic multicellular prokaryotes *Ca. Magnetoglobus multicellularis*, *M.bav*, *Ca. Magnetobacterium bavaricum*.

7. Manuskript:

Comparative genomic analysis of magnetotactic bacteria from the *Deltaproteobacteria* provides new insights into magnetite and greigite magnetosome genes required for magnetotaxis.

Comparative genomic analysis of magnetotactic bacteria from the *Deltaproteobacteria* provides new insights into magnetite and greigite magnetosome genes required for magnetotaxis

Christopher T. Lefèvre,^{1*} Denis Trubitsyn,² Fernanda Abreu,³ Sebastian Kolinko,⁴ Christian Jogler,⁵ Luiz Gonzaga Paula de Almeida,⁶ Ana Tereza R. de Vasconcelos,⁶ Michael Kube,^{7,8} Richard Reinhardt,⁹ Ulysses Lins,³ David Pignol,¹ Dirk Schüller,⁴ Dennis A. Bazylinski² and Nicolas Ginet¹

¹CEA Cadarache/CNRS/Aix-Marseille Université, UMR7265 Service de Biologie Végétale et de Microbiologie Environnementale, Laboratoire de Bioénergétique Cellulaire, 13108, Saint Paul lez Durance, France.

²University of Nevada at Las Vegas, School of Life Sciences, Las Vegas, Nevada 89154-4004, USA.

³Instituto de Microbiologia Paulo de Góes, Universidade Federal do Rio de Janeiro, 21941-590 Rio de Janeiro, RJ, Brazil.

⁴Ludwig Maximilians Universität München, Biozentrum, Großhaderner Str. 2, D-82152 Planegg Martinsried, Germany.

⁵Leibniz-Institut DSMZ, Inhoffenstraße 7B, 38124, Braunschweig, Germany.

⁶Laboratório de Bioinformática, Laboratório Nacional de Computação Científica, Rio de Janeiro, Brazil.

⁷Max-Planck Institute for Molecular Genetics, Ihnestr. 63-73, D-14195 Berlin, Germany.

⁸Humboldt-Universität zu Berlin, Faculty of Agriculture and Horticulture, Lentzeallee 55/57, D-14195 Berlin, Germany.

⁹Max-Planck Genome centre Cologne, Carl-von-Linné-Weg 10, D-50829 Cologne, Germany.

Summary

Magnetotactic bacteria (MTB) represent a group of diverse motile prokaryotes that biomineralize magnetosomes, the organelles responsible for magnetotaxis. Magnetosomes consist of intracellular, membrane-bounded, tens-of-nanometre-sized crys-

tals of the magnetic minerals magnetite (Fe₃O₄) or greigite (Fe₃S₄) and are usually organized as a chain within the cell acting like a compass needle. Most information regarding the biomineralization processes involved in magnetosome formation comes from studies involving *Alphaproteobacteria* species which biomineralize cuboctahedral and elongated prismatic crystals of magnetite. Many magnetosome genes, the *mam* genes, identified in these organisms are conserved in all known MTB. Here we present a comparative genomic analysis of magnetotactic *Deltaproteobacteria* that synthesize bullet-shaped crystals of magnetite and/or greigite. We show that in addition to *mam* genes, there is a conserved set of genes, designated *mad* genes, specific to the magnetotactic *Deltaproteobacteria*, some also being present in *Candidatus Magnetobacterium bavaricum* of the *Nitrospirae* phylum, but absent in the magnetotactic *Alphaproteobacteria*. Our results suggest that the number of genes associated with magnetotaxis in magnetotactic *Deltaproteobacteria* is larger than previously thought. We also demonstrate that the minimum set of *mam* genes necessary for magnetosome formation in *Magnetospirillum* is also conserved in magnetite-producing, magnetotactic *Deltaproteobacteria*. Some putative novel functions of *mad* genes are discussed.

Introduction

Magnetotactic bacteria (MTB) comprise a metabolically, morphologically and phylogenetically heterogeneous group of aquatic, motile prokaryotes that passively align and actively swim along magnetic field lines (Bazylinski and Frankel, 2004). This behaviour, termed magnetotaxis, is due to the presence of intracellular single-magnetic-domain crystals of magnetite (Fe₃O₄) and/or greigite (Fe₃S₄) surrounded by a lipid bilayer membrane. These unique organelles, called magnetosomes, are generally organized in chain(s) within the cell and impart a permanent magnetic dipole to the cell resulting in the magnetotactic behaviour (Bazylinski and Frankel, 2004). MTB are

Received 3 February, 2013; accepted 20 March, 2013. *For correspondence. E-mail lefevrechristopher@hotmail.com; Tel. (+33) 6 34 55 36 39; Fax (+33) 4 42 25 47 01.

ubiquitous in aquatic habitats with vertical oxygen and redox gradients in the water column or sediments and magnetotaxis is thought to aid MTB in locating and maintaining an optimal position within these gradients (Bazylinski and Frankel, 2004).

It was first shown in the genome of magnetite-producing *Magnetospirillum gryphiswaldense* and later in other *Magnetospirillum* species that the genes necessary for magnetite magnetosome biomineralization, termed *mam* (magnetosome membrane) and *mms* (magnetosome membrane specific), are present as clusters that are in close proximity and organized within a genomic island termed the 'magnetosome island' (MAI) (Grünberg *et al.*, 2001; Schübbe *et al.*, 2003; Ullrich *et al.*, 2005). Homologous genes have subsequently been found to be organized similarly within the genomes of all MTB examined with some variations. In most, but not all MTB, the genomic region that contains the magnetosome genes also contains mobile elements including transposases of the insertion sequence type and integrases, as well as tRNA genes that act as insertion sites for integrases (Matsunaga *et al.*, 2005; Ullrich *et al.*, 2005; Jogler *et al.*, 2009; Nakazawa *et al.*, 2009), features typical of genomic islands (Dobrindt *et al.*, 2004). All identified *mam* and *mms* genes are located on a genomic segment of about 45 kb in length in *M. gryphiswaldense*, which are flanked and interspersed with genes and pseudogenes with unknown functions as well as mobile elements. The operon-like, collinear organization of the *mam* and *mms* clusters suggests that they are transcribed as single long mRNAs and experimental evidences provide support for these polycistronic transcriptional units (Schübbe *et al.*, 2006).

Although the first comparative genomic studies on MTB (Richter *et al.*, 2007; Murat *et al.*, 2010; Lohße *et al.*, 2011) led to a greater understanding of the type and number of genetic determinants required for magnetosome biogenesis, these approaches were biased towards the magnetotactic *Alphaproteobacteria*, which constituted five of the six MTB genomes available, including: three species of *Magnetospirillum*, *M. magneticum* (Matsunaga *et al.*, 2005), *M. gryphiswaldense* (Lohße *et al.*, 2011) and *M. magnetotacticum* (Bertani *et al.*, 2001); *Magnetococcus marinus* (Schübbe *et al.*, 2009) and *Magnetovibrio blakemorei* (Jogler *et al.*, 2009). Like all known magnetotactic *Alphaproteobacteria*, these strains biomineralize cuboctahedral or prismatic magnetite nanocrystals of more or less elongated shapes (Devouard *et al.*, 1998).

Recently, several new partial or complete genome sequences of distantly related MTB have recently become available. These include that of *Desulfovibrio magneticus* strain RS-1, an anaerobic, dissimilatory sulfate-reducing bacterium isolated from a freshwater river in Japan that biomineralizes bullet-shaped crystals of magnetite

(Sakaguchi *et al.*, 1993; 2002; Nakazawa *et al.*, 2009). Additional genomic information from this group was recently obtained from: the uncultured *Candidatus Magnetoglobus multicellularis*, a greigite-producing, magnetotactic multicellular prokaryote (MMP) collected from a marine lagoon in Brazil (Abreu *et al.*, 2007) and the cultured *Candidatus Desulfamplus magnetomortis* strain BW-1, another anaerobic, dissimilatory sulfate-reducing MTB that biomineralizes both greigite and magnetite magnetosomes, recently isolated from a brackish spring in California (Lefèvre *et al.*, 2011a). Using culture independent techniques, *mam* genes were identified in two genomic contigs in *Ca. Magnetoglobus multicellularis* (Abreu *et al.*, 2011), while a preliminary genomic analysis of *Ca. Desulfamplus magnetomortis* revealed the presence of two different magnetosome gene clusters with potentially distinct functions, suggesting that one is responsible for greigite biomineralization and the other for magnetite synthesis (Lefèvre *et al.*, 2011a).

In addition to MTB of the *Proteobacteria* phylum, a recent study on the uncultivated *Candidatus Magnetobacterium bavaricum*, phylogenetically affiliated with the deeper branching *Nitrospirae* phylum, revealed the presence of a genomic cluster containing several magnetosome genes homologous to those found in magnetotactic *Proteobacteria* (Jogler *et al.*, 2011). However, despite this accumulating genomic data, these genomic information still does not match the ever-expanding, newly acquired information on the phylogenetic diversity of MTB, as MTB of the *Gammaproteobacteria* class and the candidate division OP3 have recently been described (Kolinko *et al.*, 2012; Lefèvre *et al.*, 2012a).

A comparative genomic approach can predict novel candidate genes for subsequent experiments, such as targeted mutagenesis, which have the potential to determine the minimal genetic inventory essential for the biomineralization of magnetite or greigite magnetosomes in MTB. Results from two independent studies of this type, conducted in *Magnetospirillum* species, suggest that from the suite of magnetosome genes present in the MAI, only the *mamAB* operon which is about 16–17 kb in length, is essential and sufficient for the biomineralization of magnetite, albeit the crystals produced by mutants lacking this operon are smaller and aberrantly-shaped compared with those of wild-type cells of *Magnetospirillum magneticum* and *M. gryphiswaldense* (Murat *et al.*, 2010; Lohße *et al.*, 2011). In *M. magneticum* and *M. gryphiswaldense* (Murat *et al.*, 2010; Lohße *et al.*, 2011; Uebe *et al.*, 2011), there is evidence that MamI, L and Q participate in magnetosome membrane synthesis, MamE, P and O are involved in magnetite biomineralization, MamM and B are involved in magnetite biomineralization and magnetosome membrane assembly, and MamA activates magnetosome vesicles and is involved in magnetite crystal maturation

(Komeili *et al.*, 2004; Murat *et al.*, 2010; Zeytuni *et al.*, 2011). However, whether each of these proteins encoded by the *mamAB* operon is absolutely necessary for magnetite magnetosome formation in *Magnetospirillum* is unclear. For instance, *mamJ* is only present in *Magnetospirillum* species and its deletion appears to have no effect on magnetite biomineralization although it results in a dramatic defect in magnetosome chain assembly in *M. gryphiswaldense* (Scheffel *et al.*, 2006). Another gene from the *mamAB* operon, *mamN*, is absent in the genomes of *Magnetococcus marinus* and *Desulfovibrio magneticus* (Nakazawa *et al.*, 2009; Schübbe *et al.*, 2009). Other genes, for example *mamK* that encodes an actin-like cytoskeletal protein filaments involved in the linear assembly and segregation of magnetosomes (Komeili *et al.*, 2006; Katzmann *et al.*, 2010; Komeili, 2012), is present in the *mamAB* gene clusters of all MTB examined, although its deletion in *M. magneticum* and *M. gryphiswaldense* has little to no effect on the biomineralization of magnetite crystals (Katzmann *et al.*, 2010).

It has been shown recently that genes encoding other metabolic functions, such as nitrate reduction, participate in redox control required for magnetite biomineralization (Li *et al.*, 2012), and the possibility that further genes located outside the MAI participate in magnetosome formation cannot be excluded, by either acting in synergy with or by having functions redundant to other magnetosome genes (Rioux *et al.*, 2010). In *Magnetospirillum* species, other operons in the MAI have important accessory functions in controlling the synthesis of regularly shaped and sized crystals that are functional for magnetic orientation (Murat *et al.*, 2010; Ullrich and Schüller, 2010; Lohße *et al.*, 2011). One of such accessory operons, the *mamGFDC* cluster, is about 2.1 kb in length located about 15 kb upstream of the *mamAB* operon and is composed of four genes which encode a group of abundant magnetosome membrane proteins involved in size control of magnetite crystals (Scheffel *et al.*, 2008). The 3.6 kb *mms* cluster is located 368 bp upstream of the *mamGFDC* operon and contains five genes (Schübbe *et al.*, 2003) that encode proteins including *mms6* that has been shown to be involved in the nucleation and the size control of magnetite crystals (Tanaka *et al.*, 2011; Wang *et al.*, 2012). Another gene encoding a magnetosome membrane protein, the monocistronic gene *mamW*, is localized outside these operons, about 10 kb upstream of the *mms* operon (Ullrich *et al.*, 2005).

The *Deltaproteobacteria* class contains both magnetite- and greigite-producing MTB that currently can be divided into four different subcategories: (i) various forms of uncultured MMPs which biomineralize either or both minerals (DeLong *et al.*, 1993; Abreu *et al.*, 2007; Simmons and Edwards, 2007); (ii) a group of large, rod-shaped bacteria, including uncultured strains (Heywood *et al.*,

1990; Bazylinski *et al.*, 1993) and two cultured members (*Ca. Desulfamplus magnetomortis* and strain SS-2) (Lefèvre *et al.*, 2011a), that biomineralize either or both minerals; (iii) the magnetite-producing, rod-shaped, sulfate-reducer *Desulfovibrio magneticus* (Sakaguchi *et al.*, 1993; 2002); and (iv) several similar strains of obligately alkaliphilic, sulfate-reducing, magnetite-producing rods isolated from extremely alkaline habitats in California (USA) that likely represent new strains of *Desulfonatronum thiodismutans*, a known non-magnetotactic deltaproteobacterium (Lefèvre *et al.*, 2011b).

Here we present a comparative analysis of all available magnetite and greigite gene clusters from MTB belonging to the *Deltaproteobacteria* class including those of: *Ca. Desulfamplus magnetomortis* (Lefèvre *et al.*, 2011a); *Desulfovibrio magneticus* (Nakazawa *et al.*, 2009); *Ca. Magnetoglobus multicellularis* (Abreu *et al.*, 2011); and two newly isolated magnetotactic *Deltaproteobacteria* strains ML-1 (Lefèvre *et al.*, 2011b) and FH-1. We also compare these DNA regions with the MAI of MTB from other classes of the *Proteobacteria* and other phyla and show the existence of a subset of genes likely involved in magnetosome formation specific to the magnetotactic *Deltaproteobacteria*. Finally, by comparing sequences from magnetite- and greigite-producing magnetotactic *Deltaproteobacteria*, we attempted to identify the genetic determinants shared between those responsible for magnetite and greigite biomineralization and those specific for the synthesis of each mineral.

Results

Heterogeneity of the region harbouring magnetosome genes in magnetotactic Deltaproteobacteria

Genomic data of three newly isolated MTB belonging to the *Deltaproteobacteria* class were examined including: *Ca. Desulfamplus magnetomortis* (Lefèvre *et al.*, 2011a), the alkaliphilic strain ML-1 (Lefèvre *et al.*, 2011b) and strain FH-1, a sulfate-reducing bacterium closely related to *Desulfovibrio magneticus* (Nakazawa *et al.*, 2009) (Table 1).

Candidatus *Desulfamplus magnetomortis* strain BW-1. Gap closure by PCR in this study revealed that the two clusters containing *mam* genes in the genome of *Ca. Desulfamplus magnetomortis* are in close proximity to each other within a single genomic region of about 40 kb (Fig. 1). This region begins with a cluster of *mam* genes similar to those of magnetite producing MTB, with a similar gene order (synteny) to that of the magnetite-producing *Desulfovibrio magneticus* (Fig. 1). It is followed by a second *mam* cluster more likely related to greigite production as suggested by the high similarities of a

Table 1. General genomic features of the regions harbouring genes involved in magnetosome formation of all magnetotactic bacteria whose genomes have been sequenced or nearly so.

Magnetotactic species	Magnetosome type	Genome GC% (length bp)	Genes delimiting the magnetosome gene cluster	mam cluster GC% (length bp)
<i>Magnetospirillum magneticum</i> AMB-1	Cubooctahedral magnetite	65.1 (4 967 148)	<i>mamC_mamF</i>	61.4 (73 014)
<i>Magnetospirillum gryphiswaldense</i> MSR-1	Cubooctahedral magnetite	62.8 (4 264 908)	<i>mamW_mamY</i>	61.1 (74 615)
<i>Magnetospirillum magnetotacticum</i> MS-1	Cubooctahedral magnetite	66.4 (4 503 280)	<i>mamC_mamW</i>	ND**
<i>Magnetococcus marinus</i> MC-1	Pseudo-hexagonal prismatic magnetite	54.2 (4 719 581)	<i>mms6_mamA-like</i>	52.3 (55 827)
<i>Magnetovibrio blakemorei</i> MV-1	Truncated hexa-octahedral magnetite	52.9–53.5 (3 700 000)	<i>mamI_mamR-like</i>	53.5 (66 034)
<i>Desulfovibrio magneticus</i> RS-1	Bullet-shaped magnetite	62.8 (5 248 049)	<i>mamI-1_mad27</i>	62.8 (42 137)
FH-1	Bullet-shaped magnetite	ND	<i>mamI-1_mad25</i>	ND**
Alkaliphilic magnetotactic strain ML-1	Bullet-shaped magnetite	ND	<i>mamI-1_mad25</i>	62.3 (23 818)**
Ca. <i>Desulfamplus magnetomortis</i> BW-1	Bullet-shaped magnetite	40.7 (6 670 319)	<i>mamI-1_mad12-like*</i>	41.2 (70 026)
Ca. <i>Magnetoglobus multicellularis</i>	Greigite	ND	<i>mad13_mad30</i>	42.2 (15 707)**
Ca. <i>Magnetobacterium bavaricum</i>	Bullet-shaped magnetite	ND	<i>mad12_mamK</i>	38.9 (8 673)**
			<i>mamP_mad26</i>	50.3 (16 067)**

*Strain BW-1 has two copies of *mad12* (Accession Number: CCO06700), one upstream the greigite gene cluster and another, named *mad12-like* (Accession Number: CCO06747), situated downstream the *mad17-30* cluster; **based on the draft of the genome. ND, Not determined.

number of *mam* genes and the conserved synteny with homologous regions from *Ca. Magnetoglobus multicellularis* (Fig. 1). Unlike most of the magnetosome genes in *Ca. Desulfamplus magnetomortis*, *mamK* is present as a single copy that is situated between the two distinct *mam* clusters. Downstream of the *mam* clusters, there is an additional region that contains genes that we identified as specific to the magnetotactic *Deltaproteobacteria* and thus could be involved in magnetosome biomineralization (discussed below). The total size of the gene cluster containing genes potentially involved in magnetosome formation is approximately 70 kb. The G + C content of this region is 41.2% while the draft of the whole genome has a G + C content of 40.7%. Flanking 50 kb gene regions at both ends of the 70 kb region have G + C content of 39.6% and 41.3%. In contrast to the MAI of many MTB of the *Alphaproteobacteria* class, no insertion elements (IS) were identified in the 70 kb region, and the closest transposase gene (DEMABW1_80145) is present about 14 kb downstream of this region. The absence of such elements and other features suggests that the region harbouring *mam* genes in *Ca. Desulfamplus magnetomortis* does not represent a clearly delineated genomic island such as that found in *Magnetospirillum* species and *Desulfovibrio magneticus* (Schübbe *et al.*, 2003; Nakazawa *et al.*, 2009) and indicates that the island may have been acquired by an ancient horizontal gene transfer event and is now stably inserted into the chromosome of *Ca. Desulfamplus magnetomortis*.

Alkaliphilic magnetotactic strain ML-1. A draft of the genome of strain ML-1 reveals the presence of clustered *mam* genes, each gene sharing maximum similarity with those of *Desulfovibrio magneticus*. Synteny of the magnetosome genes with those of *D. magneticus* is also reasonably conserved (Fig. 1). This genomic cluster of approximately 18 kb starts with *mamI-1* (the first copy of the gene *mamI*) and ends with *mamK*. Downstream of *mamK*, there are genes specific to magnetotactic *Deltaproteobacteria*. Adding these latter genes, the total size of the cluster containing potential magnetosome-related genes becomes about 24 kb. In contrast to the MAI in *D. magneticus*, no transposase genes or IS are present at least within 10 kb upstream of the first gene of the magnetite gene cluster (*mamI-1*) in strain ML-1. Transposase genes similar to those present in the MAI of *D. magneticus* were found in the genome of ML-1 although we presently do not know if these genes are in close proximity to the magnetosome gene cluster, and thus we do not have enough information to determine whether the region harbouring *mam* genes in strain ML-1 represents a genomic island or not.

Strain FH-1. Strain FH-1 was isolated in axenic culture from water and mud collected from a fish hatchery in

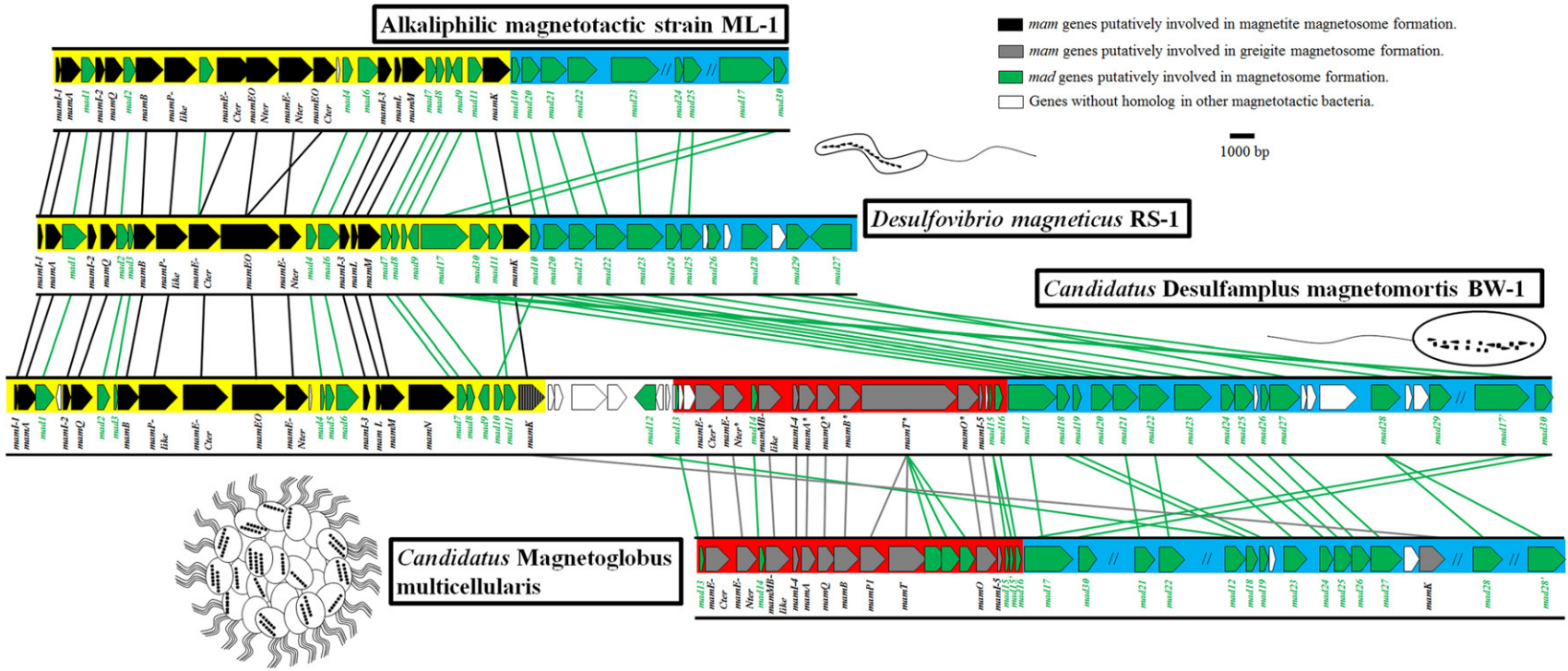


Fig. 1. Comparison of chromosomal sections of magnetotactic *Deltaproteobacteria* containing magnetosome genes. Magnetosome gene order (synteny) of chromosome sections containing genes involved in magnetosome formation of the magnetite-producing alkaliphilic strain ML-1 and *Desulfovibrio magneticus* strain RS-1, the magnetite- and greigite-producing *Candidatus Desulfamplus magnetomortis* and the greigite-producing *Ca. Magnetoglobus multicellularis*. Bars between clusters indicate homologous genes. The *mamAB-like* operon putatively involved in magnetite production is surrounded of yellow and the *mamAB-like** operon putatively involved in greigite production is surrounded of red. The third cluster of genes putatively involved in magnetosome formation, specific to the magnetotactic *Deltaproteobacteria*, is surrounded of blue.

Montana, USA. Cells are magnetotactic curved rods (vibrios) that possess a single polar flagellum. It is an obligate anaerobe that grows and respire with sulfate and fumarate. Organic molecules such as succinate and lactate support heterotrophic growth in this organism. Several contigs harbouring *mam* genes of strain FH-1 present features very similar to the magnetite magnetosome gene cluster of *D. magneticus*. Amino acid sequences of the Mam proteins are identical (e.g. MamA and MamK) or very close to those of *D. magneticus*. In the region flanking the *mam* gene cluster of strain FH-1, transposases and ISs are present in the same locations as in the magnetite magnetosome gene cluster of *D. magneticus* (data not shown). Thus, the magnetosome gene cluster in strain FH-1 appears to represent a *bonafide* genomic island. On the basis of 16S rRNA gene sequence similarity (99.5%), this strain appears to represent a new strain of the closely related *Desulfovibrio magneticus* that was isolated from a geographically remote location (Fig. S1) (Sakaguchi *et al.*, 1993). However, phylogenetically, *D. magneticus* is more closely related to *D. burkinensis* (Ouattara *et al.*, 1999) and *D. carbinolicus* (Nanninga and Gottschal, 1987) than FH-1. This might indicate that the latter species were magnetotactic in the past and lost the ability to form magnetosomes, as it has been previously discussed for *Desulfonatronum thiodismutans* and *Phaeospirillum* species (Lefèvre *et al.*, 2011b; 2012b). Based on 16S rRNA gene sequence, another non-magnetotactic bacterium, strain Maddinglay MBC34, is closely related to strain FH-1 and *Desulfovibrio magneticus* (100% similarity of its partial 16S rRNA gene sequence). Strain Maddinglay MBC34 is an uncharacterized bacterium, its draft genome sequence was obtained from a metagenomic sequence of a methanogenic enrichment isolated from coal-seam formation water in Victoria, Australia and is available on GenBank (Accession Number NZ_A-LAO0000000). Interestingly, the genome of strain Maddinglay MBC34 does not contain genes involved in magnetosome formation. When the region harbouring *mam* genes of *Desulfovibrio magneticus* is compared with the genome of strain Maddinglay MBC34, the region between the genes DMR_40250 and DMR_42030 of *Desulfovibrio magneticus* has no area of homology in the genome of strain Maddinglay, while the region surrounding the cluster DMR_40250-DMR_42030 shows high sequence homology with a genomic area of strain Maddinglay (e.g. DMR_40250 and DMR_42030 have 95.6% and 97.4% homology with MMBC34v1_3950005 and MMBC34v1_2150010 respectively). It seems likely that the MAI was either acquired by *Desulfovibrio magneticus* with its insertion between the genes DMR_40250 and DMR_42030 or lost by strain Maddinglay MBC34.

The minimum set of genes required for magnetite magnetosome formation is conserved in the Alpha- and Deltaproteobacteria

A careful examination of the genome of *Desulfovibrio magneticus* (Nakazawa *et al.*, 2009) revealed some mis-annotations or missing genes as reported by Jogler and colleagues (2011) regarding, for example, the existence of a previously overlooked *maml* homologue in this species. For these reasons and in order to establish a careful comparison with the newly sequenced genomes of *Deltaproteobacteria* presented in this paper, we re-annotated the region harbouring the magnetosome-related genes in *D. magneticus* using MaGe software. This revealed another previously overlooked open reading frame (ORF), positioned between nt 4652590 and 4652784 (reverse strand on the chromosome), which immediately precedes the *mamQ* gene. The gene product of this ORF named *maml-1* is homologous to Maml proteins as shown by the protein sequence alignment in Fig. 1. We found two additional genes encoding for Maml proteins: DMR_41140 (*maml-2*) and DMR_41040 (*maml-3*) (Fig. 1; Table 2). DMR_41030, originally annotated as 'hypothetical membrane protein' clearly displays homology to the *mamL* protein family (Fig. S2). Thus, *mamL* should now be added to the list of genes involved in magnetite biomineralization found to be conserved in all magnetite-producing MTB with the possible exception of *Ca. Magnetobacterium bavaricum* whose genome has not yet been completed.

Among the *mam* genes previously described in *Desulfovibrio magneticus*, four needed to be re-annotated after careful examination. The genes DMR_41100, DMR_41090, DMR_41080, DMR_41070 were originally annotated as *mamT*, *mamP*, *mamE* and *mamO* respectively. However, based on the length of their encoded proteins, the identity of sequence with their corresponding proteins in the magnetotactic *Alphaproteobacteria* and their predicted domains, these genes were re-annotated *mamP-like*, *mamE-Cter*, *mamEO* and *mamE-Nter* respectively (Fig. 1; Table 2; see Supplemental information for a more complete bioinformatic analysis).

In *Ca. Desulfamplus magnetomortis* and strains FH-1 and ML-1, the proteins encoded by the genes homologous to DMR_41100, DMR_41090, DMR_41080 and DMR_41070 present the same domain organization of the corresponding proteins and were thus named MamP-like, MamE-Cter, MamEO and MamE-Nter, respectively, for consistency (Fig. 1; Table 2). However, in strain ML-1, *mamEO* seems to be split into 2 genes, *mamEO-Nter* that presents higher similarity with the N-terminal section of *mamEO* (trypsin-like protease domain followed by a magnetochrome domain) and *mamEO-Cter* that is more similar with the C-terminal section of *mamEO*.

Table 2. Comparison of known Mam proteins identified from the genome of *Candidatus Desulfamplus magnetomorphus* with those of all MTB.

Putative protein (Accession Number) (previous name)	Putative function	Magnetotactic bacterium with protein with highest sequence identity ^a	Accession Number	e-value	Coverage (%)	Identity (%)	Magnetotactic bacterium with protein with second highest sequence identity ^a	Accession Number	e-value	Coverage (%)	Identity (%)	Magnetotactic bacterium with protein with third highest sequence identity ^a	Accession Number	e-value	Coverage (%)	Identity (%)
Mami-1 (CCO06668)	magnetosome membrane synthesis	RS-1	NC_012796	5e-23	95	57	FH-1	KC332883	5e-23	95	57	ML-1	AFZ77009	3e-18	82	50
Mama (CCO06669)	Activation of magnetosome vesicles and biomineralization	ML-1	AFX88975	4e-74	90	45	RS-1	YP_002955493	1e-61	79	48	FH-1	KC196864	1e-61	79	48
Mami-2 (CCO06672)	magnetosome membrane synthesis	RS-1	YP_002955491	9e-34	96	48	FH-1	KC196865	9e-34	96	48	ML-1	AFZ77012	4e-28	95	44
MamQ (CCO06673)	magnetosome membrane synthesis	ML-1	AFX88982	6e-56	97	42	RS-1	YP_002955490	6e-60	91	48	FH-1	KC196866	2e-58	100	43
MamiB (CCO06676)	magnetite biomineralization and magnetosome membrane assembly	ML-1	AFZ77014	5e-116	98	53	FH-1	KC196868	4e-117	98	53	RS-1	YP_002955488	8e-117	98	53
MamP-like (CCO06677) (MamT)	redox control and Fe ²⁺ /Fe ³⁺ stoichiometry	ML-1	AFZ77015	8e-70	65	43	FH-1	KC196869	5e-67	68	48	RS-1	YP_002955487	6e-66	63	49
MamiE-Cter (CCO06678) (MamP)	magnetite biomineralization	ML-1	AFZ77017	1e-112	88	38	RS-1	YP_002955486	3e-104	99	38	FH-1	KC196870	6e-104	99	38
MamiO (CCO06679) (MamE)	magnetite biomineralization	RS-1	YP_002955485	4e-70	71	48	FH-1	KC196871	1e-74	40	57	ML-1	AFZ77018 (MamEO-Nter)	2e-76	34	49
MamiE-Nter (CCO06680) (MamO)	magnetite biomineralization	RS-1	YP_002955484	8e-88	98	45	FH-1	KC196872	8e-88	98	45	ML-1	AFZ77019	6e-83	99	45
Mami-3 (CCO06685)	magnetosome membrane synthesis	RS-1	YP_002955481	3e-21	95	49	FH-1	KC196875	4e-20	95	48	ML-1	AFZ77024	1e-12	87	39
MamiL (CCO06686)	magnetosome membrane synthesis	RS-1	YP_002955480	5e-26	88	52	ML-1	AFZ77025	6e-25	87	49	FH-1	KC196876	1e-24	88	52
MamiM (CCO06687)	magnetite biomineralization and magnetosome membrane assembly	RS-1	YP_002955479	3e-79	91	39	FH-1	KC196877	1e-76	89	40	ML-1	AFZ77026	7e-76	90	35
MamiN (CCO06688)	unknown	Fos001	CAX83794	5e-72	75	42	MV-1	CAV30813	2e-71	74	35	Fos002	CAX84222	4e-68	68	32
MamiK (CCO06694)	magnetosome chain alignment	MMP	ADV17375	1e-170	98	63	ML-1	AFZ77032	6e-159	98	71	RS-1	YP_002955471	7e-154	98	56

MamE Cter* (CCO06705) (MamP*)	magnetite biomineralization	MMP	ADV17397	7e-93	93	45	MMP (MamP1)	ADV17391	1e-32	63	32	ML-1	AFZ77017	4e-23	62	29
MamE Nter* (CCO06706) (MamE*)	magnetite biomineralization	MMP	ADV17396	7e-106	98	56	BW-1 (MamO*)	CCO06714	4e-61	81	47	MMP (MamO*)	ADV17386	4e-61	77	47
MamMB-like (CCO06708) (MamB*)	magnetite biomineralization and magnetosome membrane assembly	MMP	ADV17395	7e-84	98	41	MMP (MamB)	ADV17392	6e-30	84	25	Fos001	CAX83800	2e-29	86	50
MamI-4 (CCO06709)	magnetosome membrane synthesis	MMP	HQ336746	6e-32	94	55	M.bav	FQ377626	9e-14	96	36	MV-1	CAV30819	7e-13	89	34
MamA* (CCO06710)	Activation of magnetosome vesicles and biomineralization	MMP	ADV17394	2e-75	85	49	Fos001	CAX83797	1e-30	89	28	ML-1	AFX88975	6e-27	94	27
MamQ* (CCO06711)	magnetosome membrane synthesis	MMP	ADV17393	4e-80	86	52	BW-1 (mamQ)	CCO06673	2e-26	74	30	M. bav.	FQ377626	1e-24	67	33
MamB* (CCO06712) (MamM*)	magnetite biomineralization and magnetosome membrane assembly	MMP	ADV17392	2e-141	96	62	Fos002	CAX84216	3e-62	88	36	MC-1	YP_866157	6e-61	89	38
MamT* (CCO06713)	redox control and Fe ²⁺ /Fe ³⁺ stoichiometry	MMP	ADV17390	9e-72	55	88	BW-1 (MamP-like)	CCO06677	3e-20	39	47	ML-1 (MamP-like)	AFZ77015	8e-20	51	55
MamO* (CCO06714)	magnetite biomineralization	MMP	ADV17386	7e-106	95	57	MMP (MamE-Nter*)	ADV17396	2e-61	81	45	BW-1 (MamE-Nter*)	CCO06706	5e-56	88	36
MamI-5 (CCO06715)	magnetosome membrane synthesis	MV-1	CAV30819	1e-13	86	36	MMP	HQ336746	1e-12	60	51	MMP (MamI-4)	HQ336746	1e-12	91	38

a. MMP = *Ca. Magnetoglobus multicellularis*. RS-1 = *Desulfovibrio magneticus*. MC-1 = *Magnetococcus marinus*. MV-1 = *Magnetovibrio blakemorei*. M. bav. = *Ca. Magnetobacterium bavaricum*. Fos001 and Fos002 are fosmids carrying a metagenomic *mam* gene cluster from unidentified, uncultivated, magnetotactic bacteria from the environment (Jogler *et al.*, 2009). Proteins are classified in the order they appear in the genome of *Ca. D. magnetotomtis*. The same colour is used to highlight the organisms that predominantly have homologous *mam* genes with *Ca. Desulfamplus magnetotomtis*.

The gene order or synteny of the *mam* genes in this region is remarkably conserved among the *Deltaproteobacteria*, and has the following order: *maml-1*, *mamA*, *maml-2*, *mamQ*, *mamB*, *mamP-like*, *mamE-Cter*, *mamEO*, *mamE-Nter*, *maml-3*, *mamL*, *mamM* and *mamK* (Table 2). A noticeable exception is the presence of a gene homologous to *mamN* in *Ca. Desulfamplus magnetomortis* found downstream of *mamM*. In analogy to the *mamAB* operon in the *Magnetospirillum* species, we designated this cluster of genes the *mamAB-like* operon, although we have no evidence whether the genes in this putative operon are transcribed under the control of a single promoter in the magnetotactic *Deltaproteobacteria*.

Orthologous genes easily identified in both the *mamAB-like* operon of magnetotactic *Deltaproteobacteria* and *Magnetospirillum* species include *maml*, *mamA*, *mamQ*, *mamB*, *mamL*, *mamM* and *mamK*. The genes *mamP* and *mamO* can be included as the *mamAB-like* operon encompasses genes with similar functional modules (*mamEO*, *mamP-like*). Finally, *mamE* can be added to the list: in *mamAB-like* it is split into two separate proteins (MamE-Nter and MamE-Cter). Although the magnetochrome domains generally found in MamE proteins between the protease and the double PDZ domains are absent from either MamE-Nter or MamE-Cter, it has been shown in *M. magneticum* that the deletion of the magnetochrome domain in MamE has no effect on magnetite biomineralization (Quinlan *et al.*, 2011). Alternatively MamE-Nter and MamE-Cter could interact with MamEO that comprises two magnetochrome domains. As a consequence, the core *mam* gene set common to magnetite-producing MTB of both the *Alpha-* and *Deltaproteobacteria* comprises *mamA*, *B*, *I*, *E* (or *E-Nter* and *E-Cter*), *K*, *L*, *M*, *O* (or *EO*), *P* (or *P-like*) and *Q*. Genes clustered in the *mamAB-like* operon of the *Deltaproteobacteria* likely encode proteins with similar functions as those described for Mam proteins of the *Alphaproteobacteria*.

Despite a rather extensive set of genes shared by both *Alpha-* and *Deltaproteobacteria* magnetite producers, a number of *mam* genes present in the *Alphaproteobacteria* are missing and include those of the *mamGFDC* operon and some genes of the *mamAB* operon (*mamH*, *J*, *R*, *S*, *U*, *V*, *W*, *X*, *Y*, *Z*). However, it has been shown that the entire *mamGFDC* operon and a number of genes in the *mamAB* operon (*mamA*, *H*, *U*, *V*, *P*, *T*, *R*, *S*, *X*, *Y*, *Z*) are not essential for magnetosome synthesis in *Magnetospirillum magneticum* and *M. gryphiswaldense* (Murat *et al.*, 2010; Lohße *et al.*, 2011). The *mamN* gene, which encodes for a protein that is thought to be involved in iron uptake and initiation of magnetite crystal formation (Murat *et al.*, 2010), is only present in *Ca. Desulfamplus magnetomortis* (DEMABW1_80077); in this organism, this gene is found downstream of *mamL* and *mamM* as in other MTB genomes when present. The *mamN* gene is notably

absent from the genome of the magnetite-producing *Magnetococcus marinus* (Schübbe *et al.*, 2009), indicating that MamN is either not essential for magnetosome formation, or that its function is redundant with, or can be replaced by, other genes. Some genes that have been described to be important for magnetosome formation, in controlling the shape of the magnetite crystal, such as *mms6* (Scheffel *et al.*, 2008) and *mmsF* (Murat *et al.*, 2012) in *Magnetospirillum* species, are missing from the genomes of the magnetotactic *Deltaproteobacteria*.

The minimum set of genes required for magnetite magnetosome formation is conserved in the greigite gene cluster

A comparison of the *mam* genes identified in *Ca. Desulfamplus magnetomortis* and *Ca. Magnetoglobus multicellularis* indicates that the second set of *mam* genes found in the former organism is most likely involved in greigite rather than magnetite magnetosome formation (Lefèvre *et al.*, 2011a) (Fig. 1; Table 2). In *Ca. M. multicellularis*, *mam* genes are scattered on two separate contigs (Accession Numbers: HQ336746 and HQ336745) (Abreu *et al.*, 2011). As the genome of *Ca. M. multicellularis* is only a draft sequence, the actual position of *mamK* with respect to the 10 other *mam* genes is uncertain. If we exclude *mamK*, synteny of the *mam* genes is well conserved between these MTB.

In the course of this study, we reassessed the annotation of the greigite gene clusters of *Ca. Magnetoglobus multicellularis* and *Ca. Desulfamplus magnetomortis*, which revealed several previously undisclosed features. As a consequence, we propose new functional annotations for some genes of these greigite-producing MTB when previous annotations by Abreu and colleagues (2011) and Lefèvre and colleagues (2011a) were not well supported. In *Ca. D. magnetomortis*, we identified 10 *mam* and *mam-like* genes within the putative greigite gene cluster. In both of these greigite-producing MTB, we unambiguously identified *maml* (*maml-4* and *maml-5*), *mamA*, *mamQ*, *mamB* and *mamO* (Fig. 1). The genes *maml-4*, *mamA*, *mamQ* and *mamB* are contiguous and in the same order than in the magnetite gene cluster (Fig. 1) (Jogler and Schüler, 2009).

Based on the length of their encoded proteins, the identity of sequence with their corresponding proteins in the magnetotactic *Alphaproteobacteria* and their predicted domains, OMM_23 (*mamP2*) from *Ca. Magnetoglobus multicellularis* and the gene DEMABW1_80097 (*mamP**) from *Ca. Desulfamplus magnetomortis* were re-annotated *mamE-Cter** (Fig. 1; Table 2; see Supplemental information for a more complete bioinformatic analysis). For similar reasons, DEMABW1_80098 and OMM_22 that were annotated MamE, were re-annotated

as *mamE-Nter* and DEMABW1_80100 as *mamMB-like* (Fig. 1; Table 2; see Supplemental information for a more complete bioinformatic analysis).

In the genome of *Ca. Desulfamplus magnetomortis*, DEMABW1_80105 was previously annotated as *mamT* based on the best hit retrieved by BLASTp, i.e. OMM_16 (*mamT*) in *Ca. Magnetoglobus multicellularis*, overlooking the fact that the latter gene covers only a small, central portion of DEMABW1_80105. Furthermore, *mamT* proteins include two magnetochrome domains which is not the case for these *Ca. D. magnetomortis* and *Ca. M. multicellularis* proteins. DEMABW1_80105 represents a relatively long gene (3978 bases) that seems to be a composite of five genes conserved in *Ca. M. multicellularis* (*mamP1* = OMM_17, *mamT* = OMM_16, OMM_15, OMM_14 and OMM_13) (Fig. S4). It comprises two PDZ domains followed by 3 NifX/NifB predicted domains, reminiscent of the domain structure predicted for a protein found in the magnetite gene clusters of *Desulfovibrio magneticus* (DMR_41100), strains FH-1, ML-1 and *Ca. D. magnetomortis* (DEMABW1_80066). These proteins from these latter organisms comprise two PDZ domains and two NifX/NifB and N-terminus magnetochrome domains: we annotated these proteins *mamP-like* because of their predicted functions, as explained in the previous section dealing with the re-annotation of the magnetite gene cluster of *D. magneticus*. In DEMABW1_80105 there is an additional NifX/NifB domain but no magnetochrome domain. It is thus difficult to draw any comparison with *mam* genes but it can be expected that novel protein functions are required to biomineralize greigite and DEMABW1_80105 might represent one of these types of proteins. This hypothesis is strengthened by the fact that all functional modules are conserved in the greigite gene cluster of *Ca. M. multicellularis* but appear to be divided between separate proteins. We lack genomic data pertaining to other representatives of greigite-producing MTB, but this protein might be central in the electron transfer chain required for greigite biomineralization. Although this protein does not have the same structure as MamT, we retained for conventional purposes the names *mamT** and *mamT* for the genes DEMABW1_80105 and OMM_16, respectively (Fig. 1; Table 2), until experimental studies provide clues to the molecular function of this protein. The first module present in MamT* (Fig. S4) is homologous to the protein MamP1 of *Ca. M. multicellularis*, thus *mamP* can be added to the set of *mam* genes in the greigite gene cluster conserved in *Ca. D. magnetomortis*.

To summarize, in the greigite gene clusters of *Ca. Desulfamplus magnetomortis* and *Ca. Magnetoglobus multicellularis*, we unambiguously identified *mamI* (in two copies), *mamA*, *mamQ*, *mamB* and *mamO*, a possible *mamE* (via the likely interaction of *mamE-Nter* and *mamE-Cter* gene products), *mamM* (with *mamMB-like*), *mamP*

(*mamP1* in *Ca. M. multicellularis* and included as *mamT** in *Ca. D. magnetomortis*) and *mamK* (situated between the magnetite and greigite gene clusters in *Ca. D. magnetomortis*) (Fig. 1; Table 2). Except for *mamL*, which is not present in these organisms, this gene set is identical to those found in the *mamAB* and *mamAB-like* operons previously described in the magnetotactic, magnetite-producing *Alphaproteobacteria* and the magnetite gene cluster of the magnetotactic *Deltaproteobacteria*. The *mamT** gene represents a major exception with its multiple PDZ and NifX/NifB predicted domains, hinting towards a novel route of electron transfer. For convenience we chose to name this cluster of genes the *mamAB-like** operon.

Comparative genomics reveals novel genes likely involved in magnetosome formation in the magnetotactic Deltaproteobacteria

In addition to *mam* genes, the region harbouring magnetite and greigite genes in *Ca. Desulfamplus magnetomortis* also contains 30 ORFs whose synteny is strongly conserved in its magnetite or greigite gene clusters, or in the magnetosome gene clusters in all the magnetotactic *Deltaproteobacteria* examined in this study (Fig. 1). These genes do not share homology with other magnetosome-related genes found in the magnetotactic *Alphaproteobacteria*, and most of the predicted gene products have been classified as 'protein with unknown function' without clear homologies in the protein databanks (Table 2). Thus, these ORFs appear to be specific to the magnetotactic *Deltaproteobacteria*, as were the *mam* genes at the time of their discovery in the *Alphaproteobacteria*. For this reason we chose to refer to these magnetotactic *Deltaproteobacteria*-specific ORFs as the *mad* genes (for 'magnetosome associated deltaproteobacteria'). They were annotated in the order they appear in the genome of *Ca. D. magnetomortis*. From the genes map presented in Fig. 1, it is clear that the *mad* genes form three different clusters with (i) a first group of *mad* genes interspersing *mam* genes of the magnetite gene cluster; (ii) a second group of *mad* genes interspersing *mam* genes of the greigite gene cluster; (iii) a third group of *mad* genes common to all magnetotactic *Deltaproteobacteria* found downstream of the region of the chromosome harbouring magnetosome (either magnetite or greigite) genes.

There is a remarkably conserved synteny for the *mad* genes that interspace the *mam* genes, both in the magnetite and greigite gene clusters (Fig. 1). There are 11 *mad* genes, designated *mad1* to *mad11*, within the magnetite gene cluster and likely included in the *mamAB-like* operon (Fig. 1). The others, designated *mad12-16*, are specific to the cluster of genes putatively involved in greigite formation in *Ca. Desulfamplus magnetomortis*

and *Ca. Magnetoglobus multicellularis* and are likely included in the *mamAB-like** operon (Fig. 1). The *mad3* and *mad5* genes appear to be missing from the genome of strain ML-1. Although *mad5* gene is present in the genome of *Desulfovibrio magneticus*, it is not shown in Fig. 1 because this gene, noted as DMR_41230, is present upstream of the region diagrammed in this figure. We found no homologies between the *mad* genes of the magnetite gene cluster and those of the greigite gene cluster. The genes *mad10* and *mad11*, homologous to *mad19* and *mad18* (found in the third group of *mad* genes), respectively, encode proteins with unknown functions and do not share homology with any protein from other bacteria. Thus in *Ca. D. magnetomortis*, the greigite gene cluster is flanked by two homologous regions.

While the genes *mad1-11* are likely required for magnetite biomineralization in *Deltaproteobacteria* and *mad12-16* necessary for greigite magnetosome formation in this class of MTB, the genes *mad17-30* of the third group of *mad* genes, appear to be a signature of the entire family of magnetotactic *Deltaproteobacteria*, regardless of the mineral they biomineralize. Interestingly, *Ca. Magnetobacterium bavaricum*, an uncultured MTB of the *Nitrospirae* phylum, contains homologous *mad* genes within its magnetite gene cluster in addition to *mam* genes (Fig. 2; Table S1) (Jogler *et al.*, 2011). Although the protein similarity scores were not very high in most cases, the best hit retrieved by a BLAST search against all the magnetotactic *Deltaproteobacteria* presented in this study was always a Mad protein. The synteny of the *mam* genes is not conserved between *Ca. M. bavaricum* and the magnetotactic *Deltaproteobacteria*, but that of the *mad* genes is well preserved. This homologous *mad* gene set includes *mad2*, 20, 22–26 and 28 (Table S1). A partial sequence of *mad17* was also found in the incomplete genome of *Ca. M. bavaricum* (73 aa; Accession Number AFX60118; e.g. *mad17* of *Ca. Desulfamplus magnetomortis* is 650 aa long) (Table S1). It is possible that additional *mad* genes are present in the genome of *Ca. M. bavaricum* but escaped detection due to sequencing bias. Some of these genes were previously identified by their homologies to genes of *Desulfovibrio magneticus* (Jogler *et al.*, 2011). In sum and importantly, *mad* genes found in the genomes of the magnetotactic *Deltaproteobacteria* and *Nitrospirae* are not present in the genomes of the magnetotactic *Alphaproteobacteria*.

As previously pointed out, most of the Mad proteins (Mad1–5, 7, 8, 10, 11, 13, 15, 16, 18–22, 24–26) are automatically annotated as putative proteins with unknown function (Table 3), and present neither homologues nor known domains when compared with GenBank or Pfam databases. Nevertheless, a deeper bioinformatic analysis suggests some possible functions to some of the Mad proteins. Here we will focus on the

most salient features (see Supplemental information for a more complete bioinformatic analysis).

Strong functional predictions can be made for two Mad proteins, Mad17 and Mad30. Both display high similarity with FeoB [34% (*e*-value 5e-113) similarity of Mad17 of *Ca. Desulfamplus magnetomortis* with FeoB of *Anaerolinea thermophila*], a membrane protein (Velayudhan *et al.*, 2000), and FeoA [37% (*e*-value 3e-37) similarity of Mad30 of *Ca. D. magnetomortis* with FeoA of *Anaeromyxobacter dehalogenans*], a small soluble protein (Kim *et al.*, 2012), both of which are involved in iron transport in microorganisms. Below, we refer to the gene cluster formed by *mad17* and *mad30* as *feoBA-like*. In most bacteria, the *feo* transport system appears to be the main route for ferrous iron uptake (Cartron *et al.*, 2006). The genes *feoB* and *feoA* are often contiguous genes in bacterial genomes and belong to an operon (Cartron *et al.*, 2006). A *feoAB-like* or *feoBA-like* gene cluster is present in every MTB genome known to date, usually in two copies. Such is the case for the *Alphaproteobacteria Magnetospirillum magneticum*, *M. gryphiswaldense* and *M. magnetotacticum*. In *M. magneticum*, one of the *feoAB-like* gene clusters is located within its MAI (*amb1023* and *amb1024*, respectively for *feoA-like* and *feoB-like*). In the magnetotactic *Deltaproteobacteria*, a *feoBA-like* gene cluster encoded by *mad17* and *mad30* is situated downstream of the magnetite or the greigite gene clusters. At present, strain ML-1 might represent an exception; its *feoBA-like* is on a separated contig, but as the genome is only a draft sequence, it is impossible to know whether *feoBA-like* is within the vicinity of the magnetite gene cluster. It is noteworthy that the order of *mad* genes encoding for FeoA-like and FeoB-like in magnetotactic *Deltaproteobacteria* is reversed (*feoBA-like*) when compared with other MTB (*feoAB-like*). Three *feoBA* gene clusters are present in the genome of *Desulfovibrio magneticus*: the *feoBA-like* cluster in its magnetite gene cluster [DMR_40970 and DMR_40960, respectively for *feoB-like* (i.e. *mad17*) and *feoA-like* (i.e. *mad30*)]; the *feoAB1* cluster (DMR_16640 and DMR_16650 for *feoA1* and *feoB1* respectively); and the *feoAB2* cluster (DMR_11980 and DMR_11990 for *feoA2* and *feoB2* respectively). In *Ca. D. magnetomortis* the situation is a bit more complex: *mad17* (*feoB-like*) in the greigite gene cluster is not followed by *mad30* (*feoA-like*) on the chromosome but by *mad18* whose size is comparable to *mad30*, but its gene product bears no homology with any FeoA-type protein. Nevertheless, there is a bonafide *feoBA-like* gene cluster (*mad17'-mad30*), but found elsewhere in the genome [Accession Numbers: KC196854 and KC196855 for *feoB-like* (i.e. *mad17'*) and *feoA-like* (i.e. *mad30*) respectively]. And finally, there is also a conventional *feoAB* cluster in the genome of *Ca. D. magnetomortis* (KC196852 and KC196853 for *feoB* and *feoA*

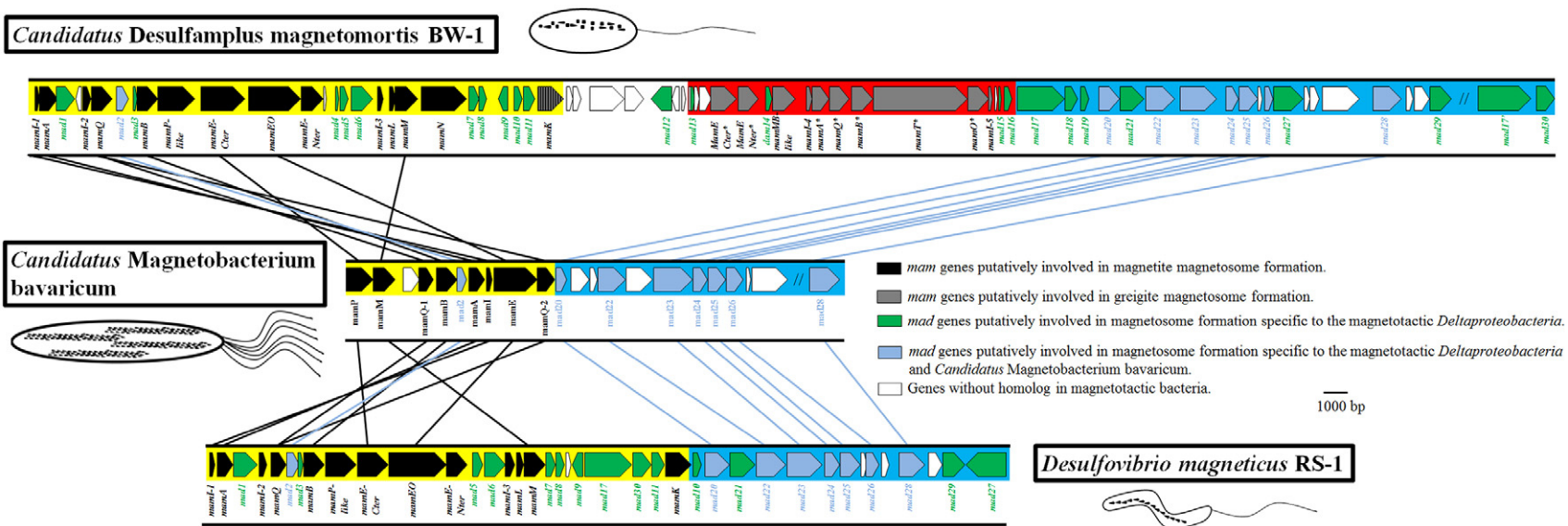


Fig. 2. Comparison of chromosomal sections containing magnetosome genes of magnetotactic *Deltaproteobacteria* and *Nitrospirae*. Synteny of magnetosome genes of chromosomal sections containing genes involved in magnetosome formation of the magnetite- and greigite-producing *Candidatus Desulfamplus magnetomortis* strain BW-1 and the magnetite-producing *Desulfovibrio magneticus* strain RS-1 of the *Deltaproteobacteria* class and the magnetite-producing *Ca. Magnetobacterium bavaricum* of the *Nitrospirae* phylum. Bars between clusters indicate homologous genes. The *mamAB-like* operon putatively involved in magnetite production is surrounded of yellow and the *mamAB-like** operon putatively involved in greigite production is surrounded of red. The third cluster of genes putatively involved in magnetosome formation, specific to the magnetotactic *Deltaproteobacteria* and *Nitrospirae*, is surrounded of blue.

Table 3. Comparison of Mad proteins putatively involved in magnetosome formation of *Candidatus Desulfamplus magnetomortis* with those of *Desulfovibrio magneticus*, strains FH-1, ML-1 and the multicellular magnetotactic prokaryote (MMP) *Ca. Magnetoglobus multicellularis* (coverage, *e*-value, maximum identity).

Protein's name (Accession Number)	Size (aa)	Putative function	Homologue in RS-1	Homologue in FH-1	Homologue in ML-1	Homologue in MMP
Mad1 (CCO06670)	261	Unknown	YP_002955492 (91, 1e-62, 45) YP_002955502 (59, 2e-37, 67)	KC332884 (91, 1e-63, 47)	AFZ77011 (77, 9e-48, 41)	–
Mad2 (CCO06674)	166	Unknown	YP_002955489 (95, 1e-71, 63)	KC196867 (95, 1e-71, 63)	AFZ77013 (95, 1e-72, 63)	–
Mad3 (CCO06675)	48	Unknown	NC_012796 (89, < 1e-5, 33)	–	–	–
Mad4 (CCO06682)	58	Unknown	YP_002955483 (86, 3e-09, 40)	KC196873 (86, 3e-09, 40)	AFZ77022 (94, 3e-15, 38)	–
Mad5 (CCO06683)	112	Unknown	YP_002955500 (35, 1e-16, 60)	–	–	–
Mad6 (CCO06684)	292	Putative 4Fe-4S ferredoxin	YP_002955482 (93, 9e-135, 57)	KC196874 (93, 6e-135, 57)	AFZ77023 (92, 2e-122, 55)	–
Mad7 (CCO06689)	137	Unknown	YP_002955478 (95, 1e-18, 36)	KC196878 (95, 1e-18, 36)	AFZ77027 (94, 9e-15, 33)	–
Mad8 (CCO06690)	132	Unknown	YP_002955477 (70, 5e-29, 48)	KC196879 (69, 3e-29, 48)	AFZ77028 (66, 6e-17, 50)	–
Mad9 (CCO06691)	138	Putative 4Fe-4S ferredoxin	YP_002955475 (98, 3e-51, 55)	KC196881 (98, 7e-53, 56)	AFZ77030 (99, 4e-54, 53)	–
Mad10 homologue to Mad19 (CCO06692)	113	Unknown	YP_002955470 (91, 3e-21, 37)	KC196886 (91, 3e-21, 37)	AFZ77033 (85, 2e-22, 36)	–
Mad11 homologue to Mad18 (CCO06693)	153	Unknown	YP_002955472 (84, 1e-08, 28)	KC196884 (84, 1e-08, 28)	AFZ77031 (87, 6e-17, 35)	–
Mad12 (CCO06700)	293	Unknown	–	–	–	ADV17383 (92, 5e-81, 41)
Mad13	48	Unknown	–	–	–	HQ336746 (95, 6e-07, 48)
Mad14 (CCO06707)	86	Putative membrane protein	–	–	–	HQ336746 (82, 5e-19, 42)
Mad15	41	Unknown	–	–	–	HQ336746 (95, 1e-15, 59) HQ336746 (90, 4e-14, 57) HQ336746 (43, 1e-12, 58)
Mad16 (CCO06716)	98	Unknown	–	–	–	HQ336746 (43, 1e-12, 58)
Mad17 (CCO06717)	650	Iron transport protein	YP_002955474 (98, 0, 47)	KC196882 (98, 0, 47)	AFX88974 (96, 2e-78, 27)	ADV17385 (100, 0, 60)
Mad17' (KC196854)	733		(75, 2e-146, 56)	(75, 2e-146, 56)	(85, 3e-53, 46)	(85, 0, 63)

Mad18 homologue to Mad11 (CCO06718)	173	Unknown	–	–	–	HQ336745 (91, 4e-09, 38)
Mad19 homologue to Mad10 (CCO06719)	113	Unknown	–	–	–	ADV17382 (94, 2e-21, 37)
Mad20 (CCO06720)	287	Unknown	YP_002955469 (24, < 1e-5, 29)	KC196887 (24, < 1e-5, 29)	AFZ77034 (28, < 1e-5, 31)	–
Mad21 (CCO06721)	335	Unknown	YP_002955468 (71, < 1e-5, 23)	KC196888 (97, < 1e-5, 23)	AFZ77035 (57, < 1e-5, 50)	AFX88996 (73, 5e-07, 22)
Mad22 (CCO06722)	398	Unknown	YP_002955467 (55, 2e-07, 38)	KC196889 (55, 2e-07, 38)	AFZ77036 (49, < 1e-5, 23)	AFX88997 (33, 4e-06, 43)
Mad23 (CCO06723)	502	Protein interaction	YP_002955466 (88, 2e-83, 35)	KC196890 (88, 2e-83, 35)	AFZ77038 (88, 2e-81, 50)	ADV17381 (47, 3e-80, 48)
Mad24 (CCO06724)	175	Unknown	YP_002955465 (80, 5e-10, 22)	KC196891 (80, 5e-10, 22)	KC196857 (56, 3e-07, 29)	ADV17380 (94, 8e-22, 31)
Mad25 (CCO06725)	265	Unknown	YP_002955464 (67, 5e-35, 37)	KC196892 (67, 3e-36, 37)	KC196858 (82, 4e-26, 36)	ADV17379 (76, 3e-44, 37)
Mad26 (CCO06727)	112	Unknown	YP_002955463 (–) ^a	KC196893 (–) ^a	–	ADV17378 (84, 4e-21, 41)
Mad27 (CCO06728)	415	ATPase	YP_002955458 (97, 2e-126, 44)	KC196898 (97, 2e-126, 44)	–	ADV17377 (98, 5e-162, 55)
Mad28 (CCO06732)	403	Actin-like	YP_002955461 (88, 3e-166, 59)	KC196895 (88, 3e-166, 59)	–	AFX88998 (100, 4e-121, 47)
Mad29 (CCO06735)	304	ATPase	YP_002955459 (96, 7e-88, 45)	KC196897 (96, 3e-87, 45)	–	AFX88999 (84, 5e-101, 46)
Mad30 (KC196855)	246	Iron transport protein	YP_002955473 (84, 2e-65, 45)	KC196883 (84, 2e-65, 45)	KC196859 (84, 2e-41, 34)	ADV17384 (91, 4e-87, 54)

a. Note that proteins with e -values < 10^{-5} were considered homologues when the proteins were the closest relative in their entire genome. For example, the protein Mad26 of *Candidatus Desulfamplus magnetomortis* has a weak homology (e -value < $1e-5$) with Mad26 of strains RS-1 and FH-1; however, it is homologous to Mad26 of *Ca. Magnetoglobus multicellularis*. Moreover, Mad26 of *Ca. M. multicellularis* is homologous (e -value > $1e-5$) with Mad26 of strain RS-1 and FH-1.

respectively). We generated phylogenetic trees from the protein sequences alignment of all homologues of FeoB or FeoA identified in MTB together with their closest non-magnetotactic relatives. Interestingly in MTB, most of the FeoA-like or FeoB-like proteins form two separate clades (Fig. 3). The latter are convergent with their 16S rRNA affiliation, forming an *Alpha*- and a *Deltaproteobacteria* leaf into the FeoA and FeoB phylogenetic trees. When found in the genome (as in *M. magneticum*, *M. magnetotacticum*, *M. gryphiswaldense*, *D. magneticus* and *Ca. D. magnetomortis*), additional copies of FeoA and FeoB do not fit into the two phylogenetic clades described above, but are related to homologous proteins found in their closest non-magnetotactic relatives on the 16S rRNA-based phylogenetic tree (Fig. S1). The amino acid sequences of FeoA-like proteins of the magnetotactic *Deltaproteobacteria* are longer than those of the magnetotactic *Alphaproteobacteria* (~240 aa vs ~100 aa respectively). In addition to the classical FeoA domain, there is an N-terminus domain similar to that in the iron-activated diphtheria *tox* repressor DtxR (Schiering *et al.*, 1995). In *Corynebacterium diphtheriae*, expression of the *tox* genes, involved in diphtheria toxin production, is repressed by the binding of iron-activated DtxR to DNA (Schiering *et al.*, 1995). Thus, FeoA-like could act as an iron-dependent regulator for gene expression in magnetotactic *Deltaproteobacteria*. In contrast, FeoA-like would likely not play such a role in the magnetotactic *Alphaproteobacteria* as it does not contain the DtxR domain. Moreover, it has been shown that in *M. gryphiswaldense* of the *Alphaproteobacteria*, expression of the core set of *mam* genes is not iron regulated (Murat *et al.*, 2010; Lohße *et al.*, 2011).

Lastly, the Mad28 protein contains a conserved actin-like domain and is also found in the magnetotactic *Nitrospirae* *Ca. Magnetobacterium bavaricum*. In the genome of strain ML-1, Mad28 appears to be only 58 aa long (e.g. Mad 28 of *Ca. Desulfamplus magnetomortis* is 403 aa long), which might be due to sequencing issues as it is found at a border of a contig. Phylogeny of actin-like proteins found in all MTB (MreB, MamK and Mad28) and their closest relatives indicates that Mad28 is not orthologous with MamK, but forms a separate clade from MreB and MamK (Fig. 4). However, since *mad28* encodes an actin-like protein and is found in close proximity to magnetosome genes, Mad28 might also be involved in the positioning and segregation of the magnetosome chain(s) in cells of magnetotactic *Deltaproteobacteria* and in *Ca. M. bavaricum* as does MamK in *Magnetospirillum* (Katzmann *et al.*, 2011). The magnetotactic multicellular *Ca. Magnetoglobus multicellularis* is known to biomineralize numerous chains of greigite magnetosomes within a single cell, which might be associated with the presence of multiple copies of divergent *mad28* genes (Fig. 1; Table 2).

Discussion

The first genome sequence information from MTB regarding magnetosome synthesis was published at the turn of the 21st century (Grünberg *et al.*, 2001). This pioneering work subsequently enhanced genetic studies and thus set the foundation for gene and protein functional studies focused on magnetosome membrane formation, magnetite biomineralization and the cellular organization of magnetosome chains (Murat *et al.*, 2010; Lohße *et al.*, 2011).

Based on genomic data mostly acquired from *Alphaproteobacteria*, a core set of magnetosome genes was identified that is shared by all currently known magnetite-biomineralizing MTB (Murat *et al.*, 2010; Lohße *et al.*, 2011). In this study, we confirm the presence of additional signature genes also present in the genomes of magnetotactic *Deltaproteobacteria*, including *mamI* and *mamL*. In *Desulfovibrio magneticus*, a homologue of *mamI* (DMR_41140) escaped detection in an initial genome analysis (Nakazawa *et al.*, 2009) but was later identified by Jogler and colleagues (2011) and here we report the presence of two new *mamI* homologues (DESMR_4697 and DMR_41040). Upstream of *mamM* (DMR_41020) in *D. magneticus* we also identified a previously unreported *mamL* gene (DMR_41030). Taking these new findings into account, we suggest an updated *mam* core genes set shared by all magnetite-biomineralizing MTB that comprises *mamABEIKLMOPQ*. Recently, Abreu and colleagues (2011) and Lefèvre and colleagues (2011a) demonstrated that greigite biomineralization is likely to involve at least a subset of this minimum *mam* gene set, namely *mamABEKOPQ*. Here, after a thorough reannotation of genome sequences of *Ca. Magnetoglobus multicellularis* and *Ca. Desulfamplus magnetomortis*, we show that a subset of *mam* genes, namely *mamABEIKMOPQ*, is also shared by greigite-biomineralizing MTB, which is the same as those for magnetite-biomineralizing MTB *minus mamL*.

Until the present study, genome information from MTB outside the *Alphaproteobacteria* was limited to a single *deltaproteobacterium*, *Desulfovibrio magneticus*. The work presented herein represents the first comprehensive and most complete comparative genomic study that includes a number of different cultured and uncultured magnetotactic *Deltaproteobacteria*, including (in addition to *D. magneticus*) *Ca. Desulfamplus magnetomortis*, strains FH-1 and ML-1, and *Ca. Magnetoglobus multicellularis*. We also provide a reassessment of the previous annotation of genes within the magnetite gene cluster of *Desulfovibrio magneticus* (Nakazawa *et al.*, 2009). Initial annotations were based on partial protein sequence homologies without taking into account the presence of functional domains predicted in some Mam proteins first discovered in *Magnetospirillum gryphiswaldense*

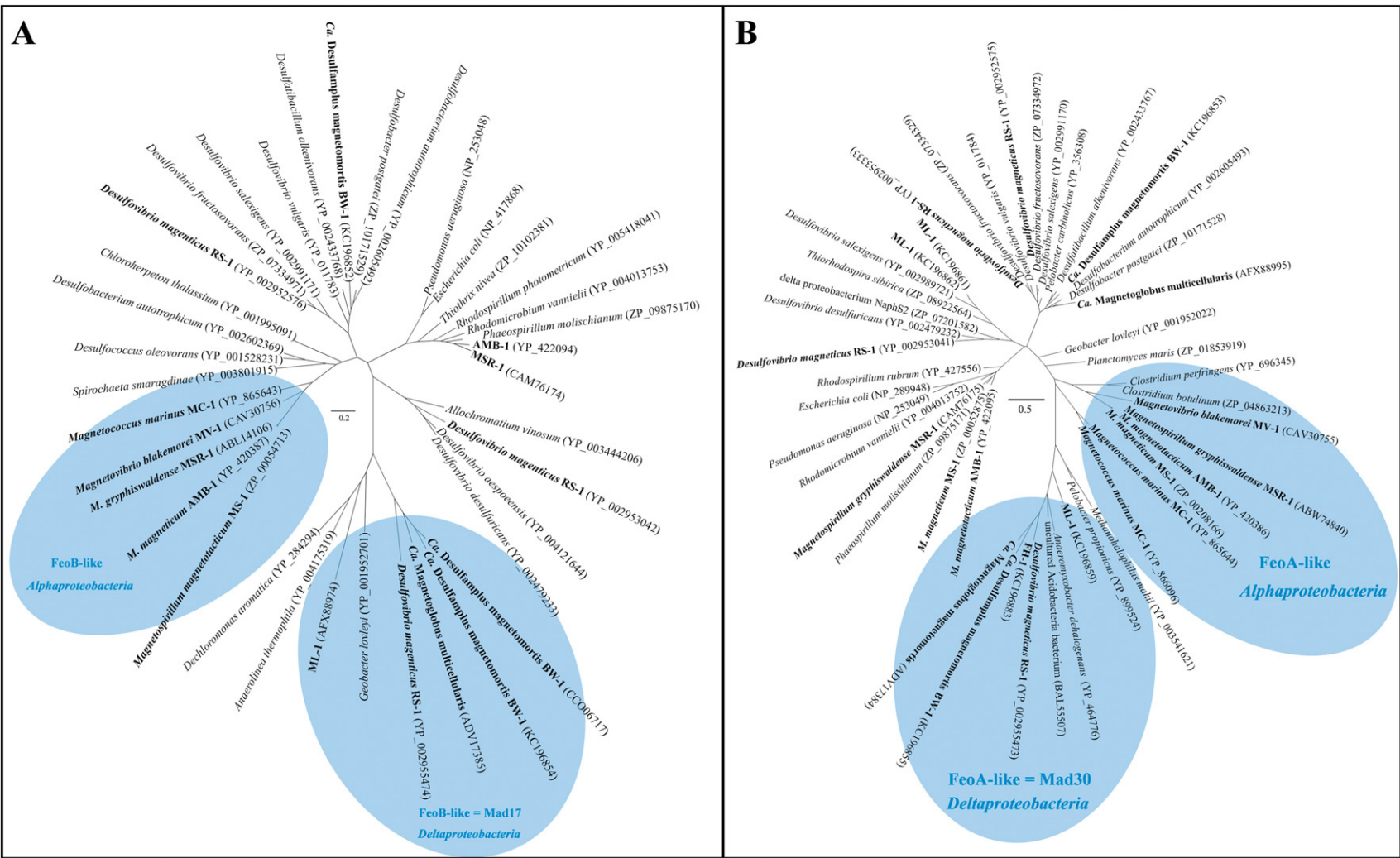


Fig. 3. Phylogenetic trees based on amino acid sequences of all iron transport proteins found in magnetotactic bacteria. Phylogenetic trees based on amino acid sequences of FeoB (A) and FeoA (B) proteins found in all magnetotactic bacteria and proteins closely related to them. The tree suggests that *feoAB*-like cluster, putatively involved in magnetosome formation, have different origins in the magnetotactic *Alpha*- and *Deltaproteobacteria* as well as it has different origins than the *feoAB* cluster present in all bacteria. Accession numbers are given in parentheses. Phylogenetic reconstructions were based on maximum likelihood algorithm. Bars represent the percentage of sequence divergence.

(Grünberg *et al.*, 2001; Nakazawa *et al.*, 2009). Most of the time, the presence of functional domains was predicted only by bioinformatic analysis but some were also supported by experimental evidence, for instance, the MamK protein known to form *in vivo* cytoskeletal filaments contains an actin-like domain (Komeili *et al.*, 2006; Pradel *et al.*, 2006), or MamP that contains two magnetochrome domains (Siponen *et al.*, 2012). Previous comparative genomic studies of the magnetotactic *Alphaproteobacteria* allowed for the design of a blueprint for most of the Mam protein families with: specific sequence features (e.g. acidic amino acid residue repeats in MamJ); predicted domain structures (e.g. a magnetochrome and two PDZ domains in MamE); and/or predicted functions (e.g. MamH belongs to a family of permeases of the major facilitator superfamily). Our data represent a collection of genes that encode proteins with molecular functions or domain structures that define an entire gene set required for magnetosomes and magnetosome chain biogenesis. It is reasonable to assume that such functions are well conserved among all MTB: invagination of the cytoplasmic membrane to form the magnetosome vesicle, iron import into the vesicle, management of redox equilibrium to ensure the required Fe²⁺/Fe³⁺ stoichiometry during magnetite and greigite biomineralization and crystal nucleation. While one might expect some subtle differences in the functions of these proteins depending on the chemical composition of the magnetic crystal (i.e. magnetite or greigite) and the size and shape of magnetosome nanoparticles, it seems likely that there is an additional, more variable set of genes that accounts for the differences in magnetosome crystal composition, morphology, number and alignment observed between different phylogenetic groups of MTB (e.g. *mam* or *mad* genes in MTB of the *Alpha*- or *Deltaproteobacteria* respectively). This variability may have been caused by genetic rearrangements (e.g. disrupted gene synteny of the MAI of *Magnetococcus marinus* compared with that of *Magnetospirillum* species), gene duplication (e.g. *mamK-I* and *mamK-II* in the MAI of *Magnetovibrio blakemorei*), gene splitting (e.g. *mamT** of the greigite gene cluster in *Ca. Desulfamplus magnetomortis* appears to have split into five separate genes in *Ca. Magnetoglobus multicellularis*) or gene fusion (*mamEO* in magnetotactic *Deltaproteobacteria* that encompasses functional modules belonging to both *mamE* and *mamO* gene products).

With the inclusion of genomic data from magnetotactic *Deltaproteobacteria* in this comparative genomic study of magnetotaxis-related genes, we propose a core set of genes involved in magnetosome formation, regardless of the composition, size or shape of the crystal or the phylogenetic position of the MTB. All MTB appear to have a common cluster of genes that include nine *mam* genes (A, E, I, K, M, O, P, Q and B) that are organized within a single

operon in some MTB (Murat *et al.*, 2010; Lohße *et al.*, 2011). As mentioned previously, presence of the *mamAB* operon is sufficient for magnetite magnetosome synthesis in *Magnetospirillum gryphiswaldense*, although magnetite crystals produced by mutants in which all other *mam* and *mms* genes were deleted are smaller in size and irregularly shaped; this phenotype indicates that the essential molecular functions leading to the magnetosome membrane formation, iron import and nucleation of magnetite are likely encoded within this operon. As the core set of nine *mam* genes above-defined belongs to this operon in *Magnetospirillum gryphiswaldense* (Scheffel *et al.*, 2008), it is likely that these genes encode proteins that are responsible for the minimal set of universal functions required for magnetosome formation in all MTB. The gene *mamI* encodes a protein that is MTB-specific with no known homologue in other non-magnetotactic bacteria (Richter *et al.*, 2007) and does not contain known domains or recognizable sequence patterns. Experimental evidence, however, suggests that MamI might be involved in the invagination of the magnetosome membrane, the first step in magnetosome formation (Murat *et al.*, 2010). Additional functional domains have been identified in this core set of proteins through *in silico* and/or experimental evidence including: (i) one tetratricopeptide repeat (TPR) (e.g. MamA) that participates in assembly of the magnetosome membrane through protein–protein interaction (Komeili *et al.*, 2004; Zeytuni *et al.*, 2011); (ii) at least one cation diffusion facilitator (CDF) necessary for iron transport and magnetosome membrane assembly (e.g. MamB and MamM) (Uebe *et al.*, 2011); (iii) PDZ domains that mediate protein–protein interactions (e.g. two in MamE and one in MamP) (Murat *et al.*, 2010; Lohße *et al.*, 2011; Quinlan *et al.*, 2011); (iv) a LemA domain (MamQ) whose function is uncertain (Murat *et al.*, 2010; Lohße *et al.*, 2011), (v) at least four magnetochrome domains (two in MamP, two in MamE and/or MamT) that putatively ensure redox control and Fe²⁺/Fe³⁺ stoichiometry (Siponen *et al.*, 2012); (vi) one or two actin-like domains (MamK) involved in the magnetosome chain assembly and its positioning inside the cell (Komeili *et al.*, 2006; Katzmann *et al.*, 2010). There are also proteins with different multiple domains such as the proteases MamE which contains trypsin, magnetochrome and PDZ domains or MamO which contains one trypsin and one TauE domain (Murat *et al.*, 2010; Lohße *et al.*, 2011). Any putative magnetosome gene should be analysed for predicted functions beyond the mere protein sequences homologies; this is particularly well illustrated by our reassessment of *Desulfovibrio magneticus*, *Ca. Desulfamplus magnetomortis* and *Ca. Magnetoglobus multicellularis* genomes.

Bullet-shaped magnetosome magnetite crystals show much more variability than other morphological types and

their crystal structure is less defined than octahedral or elongated prismatic magnetite particles (Lefèvre *et al.*, 2011c). Because of this, the biomineralization of bullet-shaped particles is thought to be less controlled through genetic means than that of cuboctahedral (e.g. produced by *Magnetospirillum* species) or elongated prismatic (e.g. produced by *Magnetovibrio blakemorei*) magnetite crystals (Nakazawa *et al.*, 2009; Abreu *et al.*, 2011; Lefèvre *et al.*, 2011c). In addition, this type of crystal is only found in MTB of the more deeply branching phylogenetic groups, the OP3 candidate division, the *Nitrospirae* and the *Deltaproteobacteria*, that contain MTB leading to the suggestion that the first magnetosomes contained bullet-shaped magnetite crystals (Lefèvre *et al.*, 2013). However, our data suggest that the number of genes responsible for the biomineralization of bullet-shaped magnetite magnetosomes is even higher than in the *Alphaproteobacteria* which biomineralize cuboctahedral and elongated prismatic magnetite magnetosomes, indicating a greater genetic complexity, although in itself a higher number of genes does not necessarily argue for tighter genetic control. Taking into consideration the genomes of the three described *Magnetospirillum* species and that of *Magnetococcus marinus*, the MAI of these *Alphaproteobacteria* have in common 29 putative magnetosome genes (Table S2). In the genomes of MTB of the *Deltaproteobacteria* class, the set of magnetosome-related genes contains 12 *mam* and 18 *mad* genes the latter specific to the magnetotactic *Deltaproteobacteria* that biomineralize bullet-shaped magnetosomes, leading to a total of 30 magnetosome-related genes found in these MTB (Table S3). As discussed above, the minimal functions required for magnetite magnetosome synthesis are mediated by fewer genes. Thus, it is possible that some genes specific to the magnetotactic *Deltaproteobacteria* (*mad* genes) or *Alphaproteobacteria* (*mamGFDC*, those in the *mms* operons and others such as *mamW*) have accessory or redundant functions such as control of the size, morphology and organization of magnetosomes or are not directly involved in magnetosome formation and have physiological functions related to magnetotaxis (e.g. magneto-aerotaxis) (Schübbe *et al.*, 2003; Ullrich *et al.*, 2005; Scheffel *et al.*, 2008; Philippe and Wu, 2010).

Our comparative genomic analysis on magnetotactic *Deltaproteobacteria* reveals new genes, called *mad* genes, likely involved in magnetosome formation. These genes are present either in the magnetite or greigite gene clusters or downstream of the region containing the *mam* genes. Among the 30 *mad* genes, 20 do not have homologues in the databases and can thus be considered magnetotactic *Deltaproteobacteria*-specific. The presence of the *mad* genes raises important questions regarding the functions of their protein products in magnetosome synthesis. Some predictions can be made, however. For

example, Mad17 and Mad30 are likely involved in ferrous iron uptake for magnetite and/or greigite biomineralization in magnetosome vesicles. These proteins are homologous to FeoB and FeoA respectively. In magnetotactic *Alphaproteobacteria*, an FeoAB cluster is present, but not always in close proximity to the MAI. In *Magnetospirillum gryphiswaldense*, FeoB1 (the product of *feoB*-like gene in the MAI of this strain) and FeoB2 (the product of an *feoB* gene found elsewhere in the genome) in the absence of FeoB1, are both involved in magnetosome formation and appear to have a complementary function (Rong *et al.*, 2008; 2012). However, Mad17 and Mad30 are not orthologous to the cluster FeoAB specific to the magnetotactic *Alphaproteobacteria* (Fig. 3). This suggests that Mad17 and Mad30, representing the FeoBA-like cluster of the magnetotactic *Deltaproteobacteria*, might have a different origin and different functions than the FeoAB-like cluster of the magnetotactic *Alphaproteobacteria*. For instance FeoA-like in *Deltaproteobacteria* may be involved in an iron-dependant regulation of gene expression due to the inclusion of a DtxR domain, an iron-dependant repressor; this domain is not present in the FeoA-like found in *Alphaproteobacteria* where iron does not regulate *mam* gene expression (Murat *et al.*, 2010; Lohße *et al.*, 2011). Interestingly, we also identified a gene encoding a protein, Mad28, that is a member of the actin-like family (that also includes MamK proteins). Thus, it is possible that the positioning and assembly of magnetosome chains in the magnetotactic *Deltaproteobacteria* might be under the control of additional genes such as *mad28* in addition to *mamK*. The situation might be similar in the case of the *Nitrospirae* in that the genome of *Ca. Magnetobacterium bavaricum* contains both *mamK* and *mad28*.

The *mad* genes, only found in the genomes of the magnetotactic *Deltaproteobacteria*, which biomineralize greigite and/or bullet-shaped crystals of magnetite and the *Nitrospirae*, which only biomineralize bullet-shaped crystals of magnetite, are absent from the genomes of the magnetotactic members of the latter diverging *Alphaproteobacteria* that produce only cuboctahedral and elongated prismatic magnetite particles (Devouard *et al.*, 1998). These genes, which might have important roles in magnetosome formation, might have been lost by the latter diverging, more recent phylogenetic groups of MTB that biomineralize octahedral and elongated prismatic magnetite magnetosomes such as the *Alphaproteobacteria* and perhaps the *Gammaproteobacteria*. Alternatively, it is also possible that the acquisition of the *mam* genes occurred through a magnetotactic ancestor of the magnetotactic *Alpha*- and *Deltaproteobacteria* and that the *mad* genes were recruited later by the *Deltaproteobacteria* and the *Nitrospirae*. The organization of the *mad* genes between the *Deltaproteobacteria* and the *Nitrospirae* is

more conserved than that of the *mam* genes indicating that there was a selective pressure during evolution to keep these genes in close proximity indicating again that the *mad* genes play an important role in magnetosome synthesis (Fang *et al.*, 2008).

The ability of *Ca. Desulfamplus magnetomortis* to biomineralize both magnetite and greigite could provide important clues in the differentiation between genes involved in magnetite and greigite biomineralization (Lefèvre *et al.*, 2011a). Based on experimental observations, it appears that magnetite and greigite magnetosomes are formed independently in this bacterium depending on culture conditions. Thus the composition of the magnetosome membrane surrounding each type of crystals is likely to be different, i.e. they contain a different subset of magnetosome proteins, encoded by genes in either the magnetite or greigite gene cluster. Indeed, the putative minimal set of genes necessary for magnetite formation (*mamAB-like*) and for greigite formation (*mamAB-like**) are in close proximity in the genome of *Ca. D. magnetomortis*. The cluster of genes *mad17-30* situated downstream of the magnetite and greigite gene cluster, is only in one copy in *Ca. D. magnetomortis* and is also present in the greigite-producer *Ca. Magnetoglobus multicellularis*.

How the greigite cluster in *Ca. Desulfamplus magnetomortis* evolved remains an open question; however, it seems likely that the *mamAB-like** cluster with its associated *mad* genes was inserted between the magnetite and *mad17-30* cluster. This hypothesis is supported by the existence of two homologous regions flanking the greigite gene cluster, *mad10-11* situated upstream and *mad18-19* found downstream, suggesting a possible site for recombination or transposition. However, the absence of integrase and/or transposase genes in close proximity suggests that this region is relatively stable and that the greigite cluster was acquired either from an ancient horizontal gene transfer or an ancient gene duplication of the magnetite gene cluster that evolved separately (Lefèvre *et al.*, 2013).

It is interesting to note that genes encoding several proteins with high similarity to proteins putatively involved in magnetosome formation are present in the genomes of non-magnetotactic bacteria. For example, the genomes of the *Deltaproteobacteria* *Desulfurivibrio alkaliphilus* (Sorokin *et al.*, 2008) and strain MLMS-1 (Hoefft *et al.*, 2004) each contain two copies of the *mamK* gene (YP_003691852, YP_003691854, ZP_01287033 and ZP_01287035) and one copy of *mad28* (YP_003690051 and ZP_01287136) that are orthologous to those found in the magnetotactic *Deltaproteobacteria* (Fig. 4). In addition, the genomes of strain NaphS2 (DiDonato *et al.*, 2010), *Thiothrix nivea* (Lapidus *et al.*, 2011) and *Phycisphaera mikurensis* (Fukunaga *et al.*, 2009) contain a gene that encodes for a protein homologous to MamK

(ZP_07200422, ZP_10105633 and YP_005444893) (Fig. 4). We hypothesize that these non-magnetotactic species acquired these genes through HGT from an MTB, or that they were once magnetotactic and lost most of the genes involved in magnetosome formation except the genes for actin-like proteins retained either as a remnant or for a function other than magnetosome synthesis.

Interestingly, at least some of the *mad* genes are also found in the *Nitrospirae*, specifically *Ca. Magnetobacterium bavaricum* (Jogler *et al.*, 2011), suggesting that the *mad* genes are only present in the genomes of MTB that biomineralize bullet-shaped crystals of magnetite and/or greigite as their magnetosome phase (magnetotactic members of the more deeply diverging phylogenetic groups, OP3 candidate division, the *Nitrospirae* and the *Deltaproteobacteria*) and not in the other, later diverging groups that contain MTB and produce cuboctahedral and elongated prismatic crystals of magnetite (the *Alpha-* and *Gammaproteobacteria*). This has important implications regarding the evolution of magnetotaxis, magnetosome synthesis and MTB themselves. Additional genomic information, particularly from MTB of the OP3 candidate division and the *Gammaproteobacteria* as well as additional *Deltaproteobacteria*, is clearly required to answer this important question.

Experimental procedures

Growth conditions, medium composition and isolation of magnetotactic strains

Cells of MTB sampled from a fish hatchery in Montana, USA, were concentrated using the magnetic 'capillary racetrack' technique (Wolfe *et al.*, 1987) and used as inocula in a modified semi-solid oxygen-gradient enrichment medium similar to that described by Bazylinski and colleagues (2004). We brought the following modifications to the basal medium (per litre): 5 ml modified Wolfe's mineral elixir (Wolin *et al.*, 1963; Bazylinski *et al.*, 2000); 0.2 ml 1% aqueous resazurin; 0.25 g NH₄Cl; 0.1 g MgSO₄•7H₂O. The medium was then to pH 7. Before autoclaving, 2.0 g of Bacto-Agar (Difco Laboratories, Detroit, MI) was added. The sterilized medium then was supplemented from sterile stock solutions (per litre): 0.5 ml of vitamin solution (Frankel *et al.*, 1997); 1.8 ml of 0.5 M KHPO₄ buffer pH 6.9; 2.67 ml freshly made 0.8 M NaHCO₃ (the NaHCO₃ is autoclaved dry); 2.5 ml of 10 mM ferric quinate (Blakemore *et al.*, 1979) and 0.4 g of freshly made neutralized filtered sterilized cysteine•HCl•2H₂O. Screw-capped glass culture tubes were filled to ~60% of their volume with medium. The medium was allowed to sit at room temperature for several hours to solidify and allow the O₂ concentration gradient to form as evidenced by the presence of a pink (oxidized) zone near the surface and a colourless (reduced) zone in the low part of the tubes. After inoculation at the surface of the gradient, cultures were incubated at 25°C. Axenic cultures of strain FH-1 was obtained by shake tubes technique. Purity of the cultures was determined using light microscopy. *Ca. Desulfamplus magnetomortis* and the alka-

lipophilic strain ML-1 were grown using the same conditions described by Lefèvre and colleagues (2011a,b).

Genome sequencing and bioinformatic analyses

The genomes of *Ca. Desulfamplus magnetomortis* and strain FH-1 were sequenced on 454 GS FLX System sequencer (Roche Diagnostics GmbH/454 Life Sciences Corporation, Branford, CT, USA) at the Laboratório Nacional de Computação Científica, Rio de Janeiro, Brazil and at Max Planck Institute for Molecular Genetics, Berlin, Germany respectively. The genome of the alkaliphilic magnetotactic strain ML-1 was sequenced using Ion Torrent technology (DeWalch Technologies, Houston, TX, USA). The sequence of *mad28* and the partial sequences of *mamK* and *mad17* in *Ca. Magnetobacterium bavaricum* were obtained from an incomplete genome assembly derived from a Phi29 polymerase-amplified DNA of few microsorted cells (Jogler *et al.*, 2011).

In order to close the gaps in the region harbouring *mam* genes of *Ca. Desulfamplus magnetomortis*, whole cell polymerase chain reaction (PCR) were performed using fresh cell lysates obtained by boiling cell suspensions for 5 min with either JumpStart Red Taq ReadyMix PCR Reaction Mix (Sigma Aldrich Co. LLC, St Louis MO) and/or GoTaq Green Master Mix (Promega Corporation, Madison WI) and the protocol as follows: initial denaturation at 94°C for 2 min; and then 35 cycles of 30 s denaturation at 94°C, annealing for 30 s (temperature varied depending on GC% of primer sets), extension at 72°C (time varied depending on sequence length to amplify), a final extension at 72°C for 7 min and then reactions held at 4°C.

Manual annotation of genomes was conducted using MicroScope (Vallenet *et al.*, 2009) in the MaGe comparative genomic software (Vallenet *et al.*, 2006). The *mam* genes of *Magnetospirillum magneticum* strain AMB-1 (GenBank Accession Number AP007255) (Matsunaga *et al.*, 2005), *M. gryphiswaldense* strain MSR-1 (AM085146) (Lohße *et al.*, 2011), *M. magnetotacticum* strain MS-1 (NZ_AAAP01003731) (Bertani *et al.*, 2001), *Magnetococcus marinus* strain MC-1 (NC_008576) (Schübbe *et al.*, 2009), *Magnetovibrio blakemorei* strain MV-1 (FP102531) (Jogler *et al.*, 2009), *Ca. Magnetoglobus multicellularis* (HQ336745 and HQ336746) (Abreu *et al.*, 2011) and *Desulfovibrio magneticus* (AP010904) (Nakazawa *et al.*, 2009) were compared with *Ca. Desulfamplus magnetomortis*, and strains FH-1 and ML-1 genome sequences using blastx (Altschul *et al.*, 1997).

Alignment of sequences were performed using CLUSTAL W multiple alignment accessory application in the BioEdit sequence alignment editor (Hall, 1999). Phylogenetic trees were constructed using MEGA version 5 (Tamura *et al.*, 2011) applying the maximum likelihood algorithm (Guindon and Gascuel, 2003). Bootstrap values were calculated with 100 replicates.

Accession numbers

The region harbouring magnetosome genes of *Ca. Desulfamplus magnetomortis* and strain ML-1 were deposited into database and carry Accession Numbers HF547348, JX869936-JX869937 respectively. Accession numbers of the *mam* genes of strain FH-1 are KC196864-KC196902. Acces-

sion numbers of the partial sequences of *Mad17*, and *MamK* of *Ca. Magnetobacterium bavaricum* described are AFX60118 and AFX60119 respectively. Accession numbers of *FeoB*, *FeoA*, *Mad21*, *Mad22*, *Mad28* and *Mad28'* of *Ca. Magnetoglobus multicellularis* are JX628775, JX628776, JX628777, JX628778, JX628779, JX628780 respectively.

Acknowledgements

We thank Pascal Arnoux for helpful comments, suggestions, and discussions. N. G., D. P. and C. T. L. are funded by the French national research agency ANR-P2N entitled MEFISTO. C. T. L. is the recipient of an award from the Fondation pour la Recherche Médicale (FRM: SPF20101220993). D. A. B. is supported by US National Science Foundation (NSF) Grant EAR-0920718. U. L., F. A. and A. T. V. are supported by Brazilian CNPq/FAPERJ/CAPES. D. S. and S. K. are supported by Deutsche Forschungsgemeinschaft (Grant DFG Schu1080/11-1). M. K. is supported by DFG projects KU 2679/2-1 and BU 890/21-1. M. K. and R. R. like to thanks the Max-Planck society for financial support.

References

- Abreu, F., Martins, J.L., Silveira, T.S., Keim, C.N., de Barros, H.G.P.L., Filho, F.J.G., and Lins, U. (2007) '*Candidatus Magnetoglobus multicellularis*', a multicellular, magnetotactic prokaryote from a hypersaline environment. *Int J Syst Evol Microbiol* **57**: 1318–1322.
- Abreu, F., Cantão, M.E., Nicolás, M.F., Barcellos, F.G., Morillo, V., Almeida, L.G., *et al.* (2011) Common ancestry of iron oxide- and iron-sulfide-based biomineralization in magnetotactic bacteria. *ISME J* **5**: 1634–1640.
- Altschul, S.F., Madden, T.L., Schaffer, A.A., Zhang, J.H., Zhang, Z., Miller, W., and Lipman, D.J. (1997) Gapped BLAST and PSI-BLAST: a new generation of protein database search programs. *Nucleic Acids Res* **25**: 3389–3402.
- Bazylnski, D.A., and Frankel, R.B. (2004) Magnetosome formation in prokaryotes. *Nat Rev Microbiol* **2**: 217–230.
- Bazylnski, D.A., Heywood, B.R., Mann, S., and Frankel, R.B. (1993) Fe₃O₄ and Fe₃S₄ in a bacterium. *Nature* **366**: 218.
- Bazylnski, D.A., Dean, A.J., Schüller, D., Phillips, E.J., and Lovley, D.R. (2000) N₂-dependent growth and nitrogenase activity in the metal-metabolizing bacteria, *Geobacter* and *Magnetospirillum* species. *Environ Microbiol* **2**: 266–273.
- Bazylnski, D.A., Dean, A.J., Williams, T.J., Long, L.K., Middleton, S.L., and Dubbels, B.L. (2004) Chemolithoautotrophy in the marine, magnetotactic bacterial strains MV-1 and MV-2. *Arch Microbiol* **182**: 373–387.
- Bertani, L.E., Weko, J., Phillips, K.V., Gray, R.F., and Kirschvink, J.L. (2001) Physical and genetic characterization of the genome of *Magnetospirillum magnetotacticum*, strain MS-1. *Gene* **264**: 257–263.
- Blakemore, R.P., Maratea, D., and Wolfe, R.S. (1979) Isolation and pure culture of a freshwater magnetic spirillum in chemically defined medium. *J Bacteriol* **140**: 720–729.
- Cartron, M.L., Maddocks, S., Gillingham, P., Craven, C.J., and Andrews, S.C. (2006) Feo – transport of ferrous iron into bacteria. *Biometals* **19**: 143–157.

- DeLong, E.F., Frankel, R.B., and Bazylinski, D.A. (1993) Multiple evolutionary origins of magnetotaxis in bacteria. *Science* **259**: 803–806.
- Devouard, B., Posfai, M., Hua, X., Bazylinski, D.A., Frankel, R.B., and Buseck, P.R. (1998) Magnetite from magnetotactic bacteria: size distributions and twinning. *Am Mineral* **83**: 1387–1398.
- DiDonato, R.J., Young, N.D., Butler, J.E., Chin, K.-J., Hixson, K.K., Mouser, P., *et al.* (2010) Genome sequence of the deltaproteobacterial strain NaphS2 and analysis of differential gene expression during anaerobic growth on naphthalene. *PLoS ONE* **5**: e14072.
- Dobrindt, U., Hochhut, B., Hentschel, U., and Hacker, J. (2004) Genomic islands in pathogenic and environmental microorganisms. *Nat Rev Microbiol* **2**: 414–424.
- Fang, G., Rocha, E.P.C., and Danchin, A. (2008) Persistence drives gene clustering in bacterial genomes. *BMC Genomics* **9**: 4.
- Frankel, R.B., Bazylinski, D.A., Johnson, M.S., and Taylor, B.L. (1997) Magneto-aerotaxis in marine coccoid bacteria. *Biophys J* **73**: 994–1000.
- Fukunaga, Y., Kurahashi, M., Sakiyama, Y., Ohuchi, M., Yokota, A., and Harayama, S. (2009) *Phycisphaera mikurensis* gen. nov., sp. nov., isolated from a marine alga, and proposal of *Phycisphaeraceae* fam. nov., *Phycisphaerales* ord. nov. and *Phycisphaerae* classis nov. in the phylum *Planctomycetes*. *J Gen Appl Microbiol* **55**: 267–275.
- Grünberg, K., Wawer, C., Tebo, B.M., and Schüler, D. (2001) A large gene cluster encoding several magnetosome proteins is conserved in different species of magnetotactic bacteria. *Appl Environ Microbiol* **67**: 4573–4582.
- Guindon, S., and Gascuel, O. (2003) A simple, fast, and accurate algorithm to estimate large phylogenies by maximum likelihood. *Syst Biol* **52**: 696–704.
- Hall, T. (1999) BioEdit: a user-friendly biological sequence alignment editor and analysis program for Windows 95/98/NT. *Nucleic Acids Symp Ser* **41**: 95–98.
- Heywood, B.R., Bazylinski, D.A., Garrattreed, A., Mann, S., and Frankel, R.B. (1990) Controlled biosynthesis of greigite (Fe₃S₄) in magnetotactic bacteria. *Naturwissenschaften* **77**: 536–538.
- Hoefl, S.E., Kulp, T.R., Stolz, J.F., Hollibaugh, J.T., and Oremland, R.S. (2004) Dissimilatory arsenate reduction with sulfide as electron donor: experiments with mono lake water and Isolation of strain MLMS-1, a chemoautotrophic arsenate respirer. *Appl Environ Microbiol* **70**: 2741–2747.
- Jogler, C., and Schüler, D. (2009) Genomics, genetics, and cell biology of magnetosome formation. *Annu Rev Microbiol* **63**: 501–521.
- Jogler, C., Kube, M., Schübbe, S., Ullrich, S., Teeling, H., Bazylinski, D.A., *et al.* (2009) Comparative analysis of magnetosome gene clusters in magnetotactic bacteria provides further evidence for horizontal gene transfer. *Environ Microbiol* **11**: 1267–1277.
- Jogler, C., Wanner, G., Kolinko, S., Niebler, M., Amann, R., Petersen, N., *et al.* (2011) Conservation of proteobacterial magnetosome genes and structures in an uncultivated member of the deep-branching *Nitrospira* phylum. *Proc Natl Acad Sci USA* **108**: 1134–1139.
- Katzmann, E., Scheffel, A., Gruska, M., Plitzko, J.M., and Schüler, D. (2010) Loss of the actin-like protein MamK has pleiotropic effects on magnetosome formation and chain assembly in *Magnetospirillum gryphiswaldense*. *Mol Microbiol* **77**: 208–224.
- Katzmann, E., Müller, F.D., Lang, C., Messerer, M., Winkhofer, M., Plitzko, J.M., and Schüler, D. (2011) Magnetosome chains are recruited to cellular division sites and split by asymmetric septation. *Mol Microbiol* **82**: 1316–1329.
- Kim, H., Lee, H., and Shin, D. (2012) The FeoA protein is necessary for the FeoB transporter to import ferrous iron. *Biochem Biophys Res Commun* **423**: 733–738.
- Kolinko, S., Jogler, C., Katzmann, E., Wanner, G., Peplies, J., and Schüler, D. (2012) Single-cell analysis reveals a novel uncultivated magnetotactic bacterium within the candidate division OP3. *Environ Microbiol* **14**: 1709–1721.
- Komeili, A. (2012) Molecular mechanisms of compartmentalization and biomineralization in magnetotactic bacteria. *FEMS Microbiol Rev* **36**: 232–255.
- Komeili, A., Vali, H., Beveridge, T.J., and Newman, D.K. (2004) Magnetosome vesicles are present before magnetite formation, and MamA is required for their activation. *Proc Natl Acad Sci USA* **101**: 3839–3844.
- Komeili, A., Li, Z., Newman, D.K., and Jensen, G.J. (2006) Magnetosomes are cell membrane invaginations organized by the actin-like protein MamK. *Science* **311**: 242–245.
- Lapidus, A., Nolan, M., Lucas, S., Glavina Del Rio, T., Tice, H., Cheng, J.-F., *et al.* (2011) Genome sequence of the filamentous, gliding *Thiothrix nivea* neotype strain (JP2(T)). *Stand Genomic Sci* **5**: 398–406.
- Lefèvre, C.T., Menguy, N., Abreu, F., Lins, U., Pósfai, M., Prozorov, T., *et al.* (2011a) A cultured greigite-producing magnetotactic bacterium in a novel group of sulfate-reducing bacteria. *Science* **334**: 1720–1723.
- Lefèvre, C.T., Frankel, R.B., Pósfai, M., Prozorov, T., and Bazylinski, D.A. (2011b) Isolation of obligately alkaliphilic magnetotactic bacteria from extremely alkaline environments. *Environ Microbiol* **13**: 2342–2350.
- Lefèvre, C.T., Posfai, M., Abreu, F., Lins, U., Frankel, R.B., and Bazylinski, D.A. (2011c) Morphological features of elongated-anisotropic magnetosome crystals in magnetotactic bacteria of the *Nitrospirae* phylum and the *Deltaproteobacteria* class. *Earth Planet Sci Lett* **312**: 194–200.
- Lefèvre, C.T., Vioria, N., Schmidt, M.L., Pósfai, M., Frankel, R.B., and Bazylinski, D.A. (2012a) Novel magnetite-producing magnetotactic bacteria belonging to the *Gammaproteobacteria*. *ISME J* **6**: 440–450.
- Lefèvre, C.T., Schmidt, M.L., Vioria, N., Trubitsyn, D., Schüler, D., and Bazylinski, D.A. (2012b) Insight into the evolution of magnetotaxis in *Magnetospirillum* spp., based on *mam* gene phylogeny. *Appl Environ Microbiol* **78**: 7238–7248.
- Lefèvre, C.T., Trubitsyn, D., Abreu, F., Kolinko, S., Almeida, L.G.P., Vasconcelos, A.T., *et al.* (2013) Monophyletic origin of magnetotaxis and the first magnetosomes. *Environ Microbiol*. DOI: 10.1111/1462-2920.12097.
- Li, Y., Katzmann, E., Borg, S., and Schüler, D. (2012) The periplasmic nitrate reductase Nap is required for anaerobic growth and involved in redox control of magnetite biomineralization in *Magnetospirillum gryphiswaldense*. *J Bacteriol* **194**: 4847–4856.
- Lohße, A., Ullrich, S., Katzmann, E., Borg, S., Wanner, G., Richter, M., *et al.* (2011) Functional analysis of the magne-

- osome island in *Magnetospirillum gryphiswaldense*: the *mamAB* operon is sufficient for magnetite biomineralization. *PLoS ONE* **6**: e25561.
- Matsunaga, T., Okamura, Y., Fukuda, Y., Wahyudi, A.T., Murase, Y., and Takeyama, H. (2005) Complete genome sequence of the facultative anaerobic magnetotactic bacterium *Magnetospirillum* sp. strain AMB-1. *DNA Res* **12**: 157–166.
- Murat, D., Quinlan, A., Vali, H., and Komeili, A. (2010) Comprehensive genetic dissection of the magnetosome gene island reveals the step-wise assembly of a prokaryotic organelle. *Proc Natl Acad Sci USA* **107**: 5593–5598.
- Murat, D., Falahati, V., Bertinetti, L., Csencsits, R., Körnig, A., Downing, K., et al. (2012) The magnetosome membrane protein, MmsF, is a major regulator of magnetite biomineralization in *Magnetospirillum magneticum* AMB-1. *Mol Microbiol* **85**: 684–699.
- Nakazawa, H., Arakaki, A., Narita-Yamada, S., Yashiro, I., Jinno, K., Aoki, N., et al. (2009) Whole genome sequence of *Desulfovibrio magneticus* strain RS-1 revealed common gene clusters in magnetotactic bacteria. *Genome Res* **19**: 1801–1808.
- Nanninga, H.J., and Gottschal, J.C. (1987) Properties of *Desulfovibrio carbinolicus* sp. nov. and other sulfate reducing bacteria isolated from an anaerobic purification plant. *Appl Environ Microbiol* **53**: 802–809.
- Ouattara, A.S., Patel, B.K.C., Cayol, J.L., Cuzin, N., Traore, A.S., and Garcia, J.L. (1999) Isolation and characterization of *Desulfovibrio burkinensis* sp. nov. from an African rice-field, and phylogeny of *Desulfovibrio alcoholivorans*. *Int J Syst Bacteriol* **49**: 639–643.
- Philippe, N., and Wu, L.-F. (2010) An MCP-like protein interacts with the MamK cytoskeleton and is involved in magnetotaxis in *Magnetospirillum magneticum* AMB-1. *J Mol Biol* **400**: 309–322.
- Pradel, N., Santini, C.-L., Bernadac, A., Fukumori, Y., and Wu, L.-F. (2006) Biogenesis of actin-like bacterial cytoskeletal filaments destined for positioning prokaryotic magnetic organelles. *Proc Natl Acad Sci USA* **103**: 17485–17489.
- Quinlan, A., Murat, D., Vali, H., and Komeili, A. (2011) The HtrA/DegP family protease MamE is a bifunctional protein with roles in magnetosome protein localization and magnetite biomineralization. *Mol Microbiol* **80**: 1075–1087.
- Richter, M., Kube, M., Bazylnski, D.A., Lombardot, T., Glöckner, F.O., Reinhardt, R., and Schüler, D. (2007) Comparative genome analysis of four magnetotactic bacteria reveals a complex set of group-specific genes implicated in magnetosome biomineralization and function. *J Bacteriol* **189**: 4899–4910.
- Rioux, J.-B., Philippe, N., Pereira, S., Pignol, D., Wu, L.-F., and Ginet, N. (2010) A second actin-like MamK protein in *Magnetospirillum magneticum* AMB-1 encoded outside the genomic magnetosome island. *PLoS ONE* **5**: e9151.
- Rong, C., Huang, Y., Zhang, W., Jiang, W., Li, Y., and Li, J. (2008) Ferrous iron transport protein B gene (*feoB1*) plays an accessory role in magnetosome formation in *Magnetospirillum gryphiswaldense* strain MSR-1. *Res Microbiol* **159**: 530–536.
- Rong, C., Zhang, C., Zhang, Y., Qi, L., Yang, J., Guan, G., et al. (2012) FeoB2 functions in magnetosome formation and oxidative stress protection in *Magnetospirillum gryphiswaldense* strain MSR-1. *J Bacteriol* **194**: 3972–3976.
- Sakaguchi, T., Burgess, J.G., and Matsunaga, T. (1993) Magnetite formation by a sulfate-reducing bacterium. *Nature* **365**: 47–49.
- Sakaguchi, T., Arakaki, A., and Matsunaga, T. (2002) *Desulfovibrio magneticus* sp. nov., a novel sulfate-reducing bacterium that produces intracellular single-domain-sized magnetite particles. *Int J Syst Evol Microbiol* **52**: 215–221.
- Scheffel, A., Gruska, M., Faivre, D., Linaroudis, A., Plitzko, J.M., and Schüler, D. (2006) An acidic protein aligns magnetosomes along a filamentous structure in magnetotactic bacteria. *Nature* **440**: 110–114.
- Scheffel, A., Gärdes, A., Grünberg, K., Wanner, G., and Schüler, D. (2008) The major magnetosome proteins MamGFDC are not essential for magnetite biomineralization in *Magnetospirillum gryphiswaldense* but regulate the size of magnetosome crystals. *J Bacteriol* **190**: 377–386.
- Schiering, N., Tao, X., Zeng, H.Y., Murphy, J.R., Petsko, G.A., and Ringe, D. (1995) Structures of the apo-activated and the metal ion-activated forms of the diphtheria toxin repressor from *Corynebacterium diphtheriae*. *Proc Natl Acad Sci USA* **92**: 9843–9850.
- Schübbe, S., Kube, M., Scheffel, A., Wawer, C., Heyen, U., Meyerdierks, A., et al. (2003) Characterization of a spontaneous nonmagnetic mutant of *Magnetospirillum gryphiswaldense* reveals a large deletion comprising a putative magnetosome island. *J Bacteriol* **185**: 5779–5790.
- Schübbe, S., Würdemann, C., Peplies, J., Heyen, U., Wawer, C., Glöckner, F.O., and Schüler, D. (2006) Transcriptional organization and regulation of magnetosome operons in *Magnetospirillum gryphiswaldense*. *Appl Environ Microbiol* **72**: 5757–5765.
- Schübbe, S., Williams, T.J., Xie, G., Kiss, H.E., Brettin, T.S., Martinez, D., et al. (2009) Complete genome sequence of the chemolithoautotrophic marine magnetotactic coccus strain MC-1. *Appl Environ Microbiol* **75**: 4835–4852.
- Simmons, S.L., and Edwards, K.J. (2007) Unexpected diversity in populations of the many-celled magnetotactic prokaryote. *Environ Microbiol* **9**: 206–215.
- Siponen, M.I., Adryanczyk, G., Ginet, N., Arnoux, P., and Pignol, D. (2012) Magnetochrome: a c-type cytochrome domain specific to magnetotactic bacteria. *Biochem Soc Trans* **40**: 1319–1323.
- Sorokin, D.Y., Tourova, T.P., Musmann, M., and Muyzer, G. (2008) *Dethiobacter alkaliphilus* gen. nov. sp. nov., and *Desulfurivibrio alkaliphilus* gen. nov. sp. nov.: two novel representatives of reductive sulfur cycle from soda lakes. *Extremophiles* **12**: 431–439.
- Tamura, K., Peterson, D., Peterson, N., Stecher, G., Nei, M., and Kumar, S. (2011) MEGA5: molecular evolutionary genetics analysis using maximum likelihood, evolutionary distance, and maximum parsimony methods. *Mol Biol Evol* **28**: 2731–2739.
- Tanaka, M., Mazuyama, E., Arakaki, A., and Matsunaga, T. (2011) MMS6 protein regulates crystal morphology during nano-sized magnetite biomineralization in vivo. *J Biol Chem* **286**: 6386–6392.
- Uebe, R., Junge, K., Henn, V., Poxleitner, G., Katzmann, E., Plitzko, J.M., et al. (2011) The cation diffusion facilitator

- proteins MamB and MamM of *Magnetospirillum gryphiswaldense* have distinct and complex functions, and are involved in magnetite biomineralization and magnetosome membrane assembly. *Mol Microbiol* **82**: 818–835.
- Ullrich, S., and Schüler, D. (2010) Cre-lox-based method for generation of large deletions within the genomic magnetosome island of *Magnetospirillum gryphiswaldense*. *Appl Environ Microbiol* **76**: 2439–2444.
- Ullrich, S., Kube, M., Schübbe, S., Reinhardt, R., and Schüler, D. (2005) A hypervariable 130-kilobase genomic region of *Magnetospirillum gryphiswaldense* comprises a magnetosome island which undergoes frequent rearrangements during stationary growth. *J Bacteriol* **187**: 7176–7184.
- Vallenet, D., Labarre, L., Rouy, Z., Barbe, V., Bocs, S., Cruveiller, S., *et al.* (2006) MaGe: a microbial genome annotation system supported by synteny results. *Nucleic Acids Res* **34**: 53–65.
- Vallenet, D., Engelen, S., Mornico, D., Cruveiller, S., Fleury, L., Lajus, A., *et al.* (2009) MicroScope: a platform for microbial genome annotation and comparative genomics. *Data-base* **2009**: bap021.
- Velayudhan, J., Hughes, N.J., McColm, A.A., Bagshaw, J., Clayton, C.L., Andrews, S.C., and Kelly, D.J. (2000) Iron acquisition and virulence in *Helicobacter pylori*: a major role for FeoB, a high-affinity ferrous iron transporter. *Mol Microbiol* **37**: 274–286.
- Wang, L., Prozorov, T., Palo, P.E., Liu, X., Vaknin, D., Prozorov, R., *et al.* (2012) Self-assembly and biphasic iron-binding characteristics of Mms6, a bacterial protein that promotes the formation of superparamagnetic magnetite nanoparticles of uniform size and shape. *Biomacromolecules* **13**: 98–105.
- Wolfe, R.S., Thauer, R.K., and Pfennig, N. (1987) A 'capillary racetrack' method for isolation of magnetotactic bacteria. *FEMS Microbiol Lett* **45**: 31–35.
- Wolin, E.A., Wolin, M.J., and Wolfe, R.S. (1963) Formation of methane by bacterial extracts. *J Biol Chem* **238**: 2882–2886.
- Zeytuni, N., Ozyamak, E., Ben-Harush, K., Davidov, G., Levin, M., Gat, Y., *et al.* (2011) Self-recognition mechanism of MamA, a magnetosome-associated TPR-containing protein, promotes complex assembly. *Proc Natl Acad Sci USA* **108**: E480–E487.

Supporting information

Additional Supporting Information may be found in the online version of this article at the publisher's web-site:

Supplementary information

Fig. S1. Phylogenetic positions of magnetotactic *Deltaproteobacteria*. Phylogenetic tree, based on 16S rRNA gene sequences, showing the positions of the magnetotactic *Deltaproteobacteria* under study (bold) including *Desulfovibrio magneticus*, strain FH-1, strain ML-1, *Candidatus Desulfamplus magnetomortis* and *Ca. Magnetoglobus multicellularis* compared with magnetotactic bacteria from other classes or phylum (grey). Bootstrap values (higher than 50) at nodes are percentages of 100 replicates. Accession numbers are given in parentheses. Bar represents 5% sequence divergence.

Fig. S2. Multiple sequence alignment of MamL homologues found in magnetotactic *Alpha*- and *Deltaproteobacteria*.

Fig. S3. Phylogenetic tree based on amino acid sequences of the CDF proteins MamM and MamB, involved in magnetosome formation. The FieF protein from *Escherichia coli* K12 was used as an out-group. Phylogenetic reconstruction was based on maximum likelihood algorithm. Bar represents the percentage of sequence divergence.

Fig. S4. Representation of the MamT* protein found in *Candidatus Desulfamplus magnetomortis*. MamT* appears to be a composite of 5 proteins (MamP1, MamT, OMM_15, OMM_14 and OMM_13) present in the greigite gene cluster of *Ca. Magnetoglobus multicellularis*.

Table S1. Homologues of the Mad proteins of the magnetotactic *Nitrospirae Candidatus Magnetobacterium bavaricum* from *Ca. Desulfamplus magnetomortis* strain BW-1, *Desulfovibrio magneticus* strain RS-1, strains FH-1, ML-1 and *Ca. Magnetoglobus multicellularis*. Proteins are classified in the order they appear in the genome of *Ca. M. bavaricum* (% coverage, *e*-value, maximum identity).

Table S2. Magnetosome genes present in the putative magnetosome gene islands of different cultured magnetotactic bacteria of the *Alphaproteobacteria* class that biomineralize cuboctahedral or elongated prismatic magnetite magnetosomes.

Table S3. Magnetosome genes present in the putative magnetite gene cluster of different cultured magnetotactic bacteria of the *Deltaproteobacteria* class that biomineralize bullet-shaped magnetite magnetosomes.

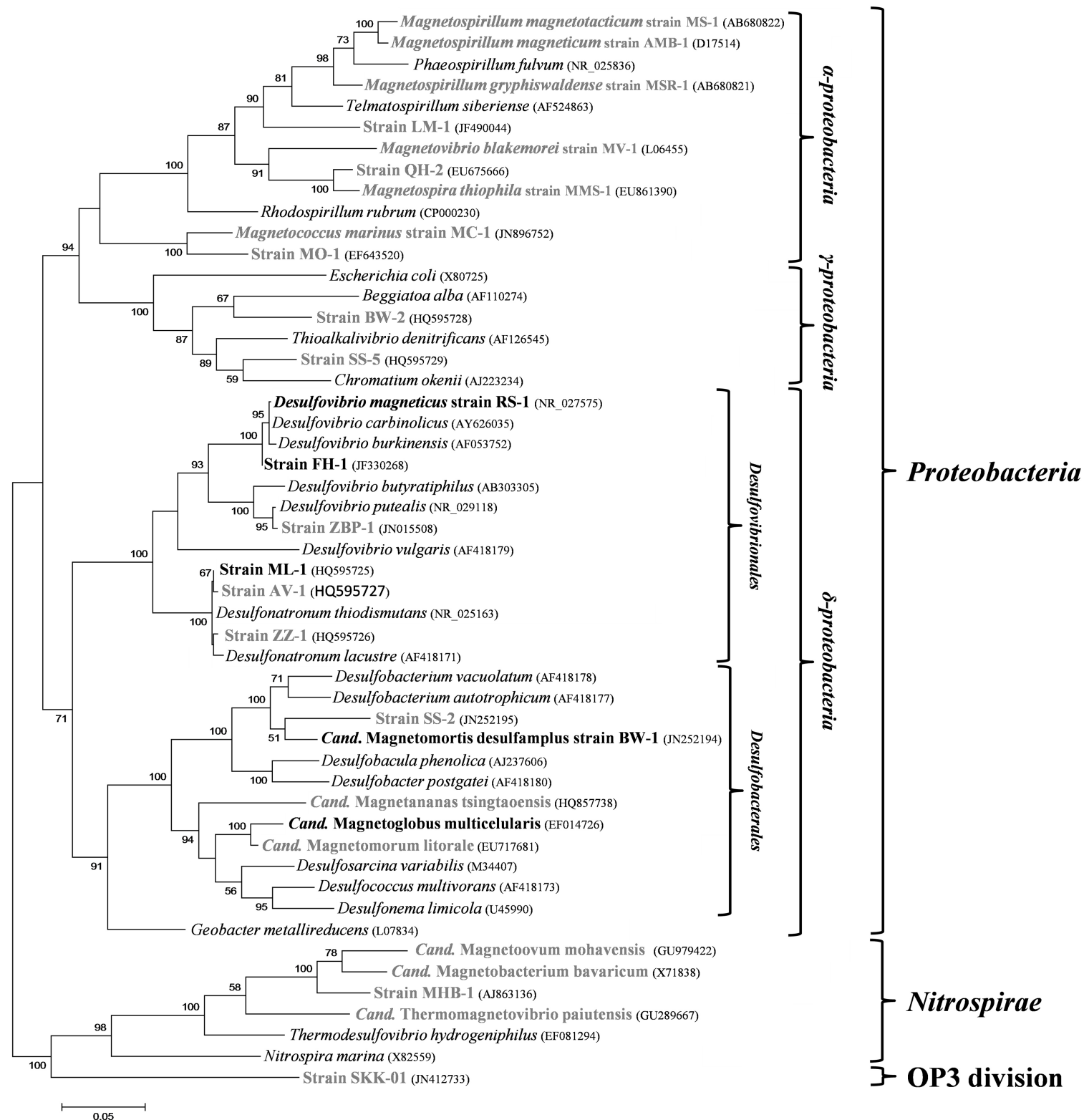


Fig. S1. Phylogenetic positions of magnetotactic Deltaproteobacteria. Phylogenetic tree, based on 16S rRNA gene sequences, showing the positions of the magnetotactic Deltaproteobacteria under study (bold) including *Desulfovibrio magneticus*, strain FH-1, strain ML-1, *Candidatus Desulfamplus magnetomortis* and *Ca. Magnetoglobus multicellularis* compared with magnetotactic bacteria from other classes or phylum (grey). Bootstrap values (higher than 50) at nodes are percentages of 100 replicates. Accession numbers are given in parentheses. Bar represents 5% sequence divergence.

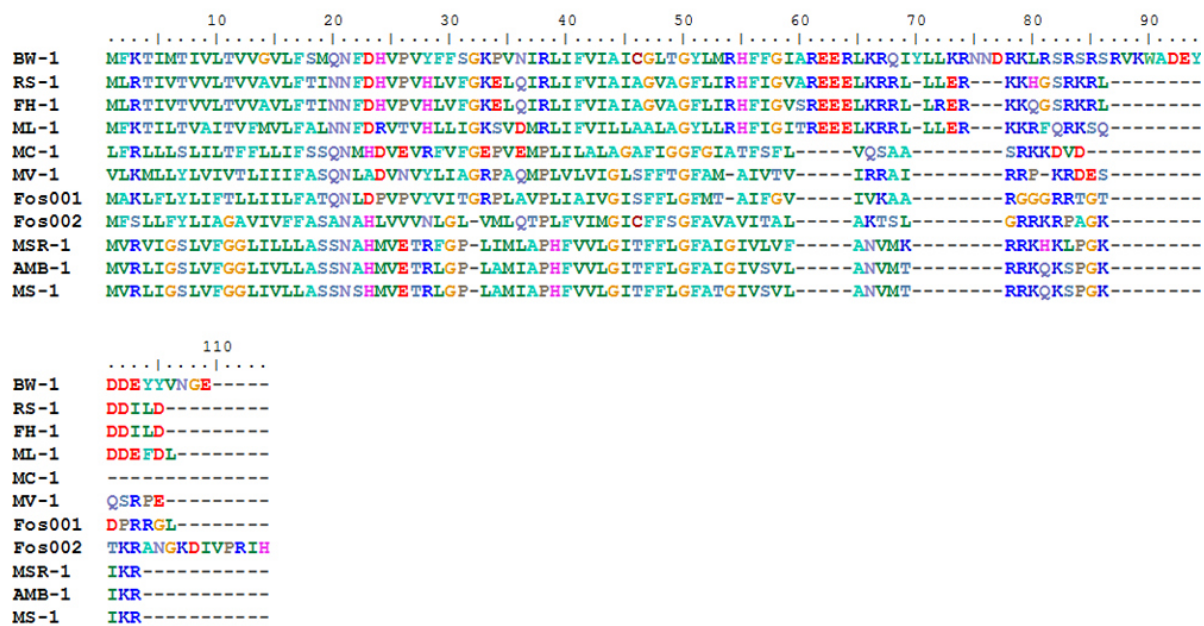


Fig. S2. Multiple sequence alignment of MamL homologues found in magnetotactic *Alpha*- and *Deltaproteobacteria*.

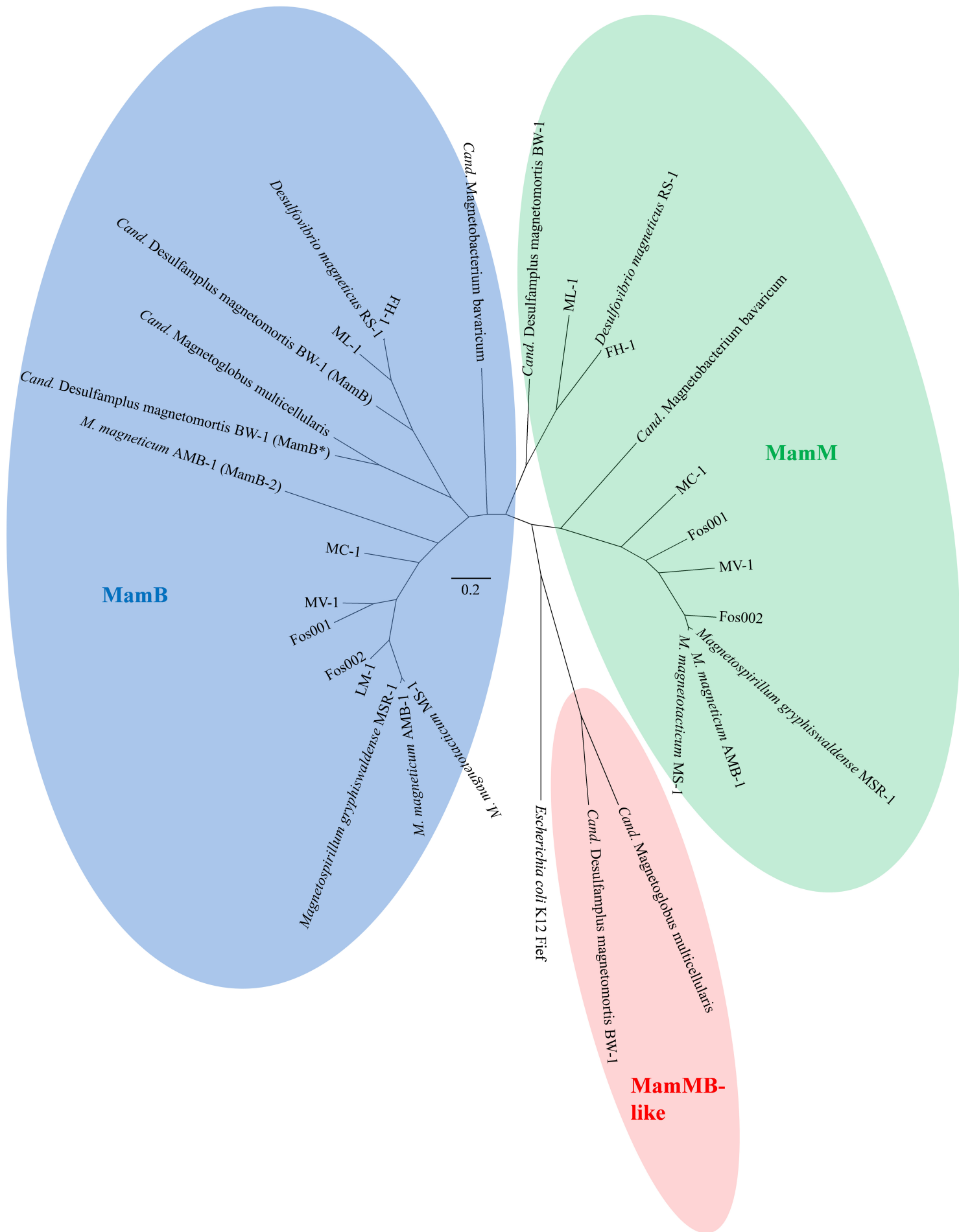


Fig. S3. Phylogenetic tree based on amino acid sequences of the CDF proteins MamM and MamB, involved in magnetosome formation. The FieF protein from *Escherichia coli* K12 was used as an out-group. Phylogenetic reconstruction was based on maximum likelihood algorithm. Bar represents the percentage of sequence divergence.

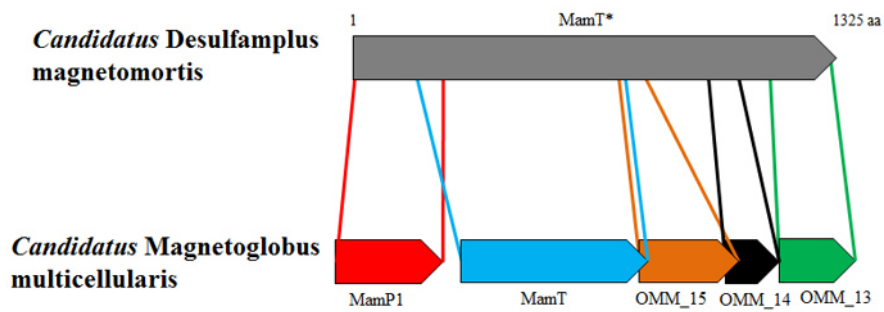


Fig. S4. Representation of the MamT* protein found in *Candidatus Desulfamplus magnetomortis*. MamT* appears to be a composite of 5 proteins (MamP1, MamT, OMM_15, OMM_14 and OMM_13) present in the greigite gene cluster of *Ca. Magnetoglobus multicellularis*.

Table S1. Homologues of the Mad proteins of the magnetotactic *Nitrospirae Candidatus Magnetobacterium bavaricum* from *Ca. Desulfamplus magnetomortis* strain BW-1, *Desulfovibrio magneticus* strain RS-1, strains FH-1, ML-1 and *Ca. Magnetoglobus multicellularis*. Proteins are classified in the order they appear in the genome of *Ca. M. bavaricum* (% coverage, e-value, maximum identity).

Gene	Homolog in BW-1	Homolog in RS-1	Homolog in FH-1	Homolog in ML-1	Homolog in MMP
Mad2 FQ377626	CCO06674 (90, 2e-16, 28)	YP_002955492 (90, 1e-16, 28)	KC196867 (90, 1e-16, 28)	AFZ77011 (90, 5e-16, 37)	-
Mad20 FQ377626	CCO06720 (39, 1e-08, 48)	YP_002955469 (27, <1e-5, 57)	KC196887 (27, <1e-5, 57)	AFZ77034 (93, <1e-5, 60)	-
Mad22 FQ377626	CCO06722 (41, 6e-07, 26)	YP_002955467 (15, <1e-5, 30)	KC196889 (15, <1e-5, 30)	AFZ77036 (19, <1e-5, 46)	AFX88997 (62, 7e-08, 24)
Mad23 FQ377626	CCO06723 (87, 3e-90, 37)	YP_002955466 (79, 5e-92, 39)	KC196890 (79, 5e-92, 38)	AFZ77038 (81, 6e-79, 52)	ADV17381 (47, 7e-83, 75)
Mad24 FQ377626	CCO06724 (54, 6e-13, 26)	YP_002955465 (59, 2e-06, 39)	KC196891 (59, 2e-06, 39)	KC196857 (51, 6e-14, 27)	ADV17380 (90, 4e-18, 27)
Mad25 FQ377626	CCO06725 (76, 3e-33, 38)	YP_002955464 (57, 7e-25, 39)	KC196892 (57, 8e-25, 40)	KC196858 (94, 3e-20, 28)	ADV17379 (75, 6e-32, 37)
Mad26 FQ377626	CCO06727 (41, 6e-18, 30)	YP_002955463 (65, 7e-12, 71)	KC196893 (65, 9e-12, 71)	-	ADV17378 (65, 2e-16, 23)
Mad17 AFX60118	CCO06717 (13, 3e-30, 60)	YP_002955474 (11, 2e-20, 49)	KC196882 (14, 2e-20, 49)	AFX88974 (10, 9e-10, 60)	ADV17385 (16, 5e-26, 58)
Mad28	CCO06732 (99, 1e-137, 51)	YP_002955461 (79, 2e-146, 58)	KC196895 (79, 2e-146, 58)	- (15, 1e-15, 55)	AFX88998 (79, 2e-116, 53) AFX88999 (81, 4e-104, 48)

Table S2. Magnetosome genes present in the putative magnetosome gene islands of different cultured magnetotactic bacteria of the *Alphaproteobacteria* class that biomineralize cuboctahedral or elongated prismatic magnetite magnetosomes.

Gene	MSR-1 ^a	MS-1	AMB-1	MC-1
<i>mamA</i>	+ ^b	+	+	+
<i>mamB</i>	+	+	+	+
<i>mamC</i>	+	+	+	+
<i>mamD</i>	+	+	+	+
<i>mamE</i>	+	+	+	+
<i>mamF</i>	+	+	+	+
<i>mamG</i>	+	+	+	-
<i>mamH</i>	+	+	+	+
<i>mamI</i>	+	+	+	+
<i>mamJ</i>	+	+	+	-
<i>mamK</i>	+	+	+	+
<i>mamL</i>	+	+	+	-
<i>mamM</i>	+	+	+	+
<i>mamN</i>	+	+	+	-
<i>mamO</i>	+	+	+	+
<i>mamP</i>	+	+	+	+
<i>mamQ</i>	+	+	+	+
<i>mamR</i>	+	+	+	-
<i>mamS</i>	+	+	+	+
<i>mamT</i>	+	+	+	+
<i>mamU</i>	+	+	+	-
<i>mamV</i>	-	+	+	-
<i>mamW</i>	+	-	+	-
<i>mamX</i>	+	+	+	+
<i>mamY</i>	+	+	+	-
<i>mamZ</i>	+	+	+	+
<i>feoA-like</i>	+	+	+	+
<i>feoB-like</i>	+	+	+	+
<i>mgI462</i>	+	+	+	-
<i>mms6</i>	+	+	+	+
<i>mgI459</i>	+	+	+	+
<i>mgI458</i>	+	+	+	-
<i>mgI457</i>	+	+	+	-
<i>mamE/S-like</i>	+	+	+	+
<i>mamF-like</i>	+	+	+	+
<i>mamH-like</i>	+	+	+	+
<i>mamA-like</i>	-	-	-	+
<i>mamP-like</i>	-	-	-	-
<i>mgr4150</i>	+	+	+	-
<i>mgr0208</i>	+	+	+	+
<i>mgr0207</i>	+	+	+	+
<i>mgr0206</i>	+	+	+	+
<i>mgr3500</i>	+	+	+	+
<i>mgr3499</i>	+	+	+	-
<i>mgr3497</i>	+	+	+	+
<i>mgr3495</i>	+	-	+	-

^aOrganisms: MSR-1, *Magnetospirillum gryphiswaldense*; MS-1, *M. magnetotacticum*; AMB-1, *M. magneticum*; MC-1, *Magnetococcus marinus*.

^bSymbols: +, homologue present in genome; -, homologue absent from genome.

Table S3. Magnetosome genes present in the putative magnetite gene cluster of different cultured magnetotactic bacteria of the *Deltaproteobacteria* class that biomineralize bullet-shaped magnetite magnetosomes.

Gene	BW-1 ^a	RS-1	FH-1	ML-1
<i>mamI-1</i>	+ ^b	+	+	+
<i>mamA</i>	+	+	+	+
<i>mamI-2</i>	+	+	+	+
<i>mamQ</i>	+	+	+	+
<i>mamB</i>	+	+	+	+
<i>mamP-like</i>	+	+	+	+
<i>mamE-Cter</i>	+	+	+	+
<i>mamEO</i>	+	+	+	+
<i>mamE-Nter</i>	+	+	+	+
<i>mamI-3</i>	+	+	+	-
<i>mamL</i>	+	+	+	+
<i>mamM</i>	+	+	+	+
<i>mamN</i>	+	-	-	-
<i>mamK</i>	+	+	+	+
<i>mad1</i>	+	+	+	+
<i>mad2</i>	+	+	+	+
<i>mad3</i>	+	-	-	-
<i>mad4</i>	+	+	+	+
<i>mad5</i>	+	+	+	-
<i>mad6</i>	+	+	+	+
<i>mad7</i>	+	+	+	+
<i>mad8</i>	+	+	+	+
<i>mad9</i>	+	+	+	+
<i>mad10</i>	+	+	+	+
<i>mad11</i>	+	+	+	+
<i>mad17</i>	+	+	+	+
<i>mad20</i>	+	+	+	+
<i>mad21</i>	+	+	+	+
<i>mad22</i>	+	+	+	+
<i>mad23</i>	+	+	+	+
<i>mad24</i>	+	+	+	+
<i>mad25</i>	+	+	+	+
<i>mad26</i>	+	+	+	-
<i>mad27</i>	+	+	+	-
<i>mad28</i>	+	+	+	+
<i>mad29</i>	+	+	+	-
<i>mad30</i>	+	+	+	+

^aOrganisms: BW-1, *Candidatus Desulfamplus magnetomortis*, RS-1, *Desulfovibrio magneticus*.

^bSymbols: +, homologue present in genome; -, homologue absent from genome.

1 **Supplementary information**

2 We present here the detailed bioinformatic analysis that supported the re-annotation of 4 *mam*
3 genes in *Desulfovibrio magneticus* involved in magnetite biomineralization as well as 3 *mam*
4 genes putatively involved in greigite biomineralization in *Ca. Magnetoglobus multicellularis* and
5 *Ca. D. magnetomortis* BW-1. Among the *mad* genes family specific to the magnetotactic
6 *Deltaproteobacteria*, we could provide strong functional predictions for 3 *mad* genes (*mad17*,
7 *mad30* and *mad28*) that were detailed in the main manuscript. Here we also propose some
8 putative functions for some other *mad* genes.

9 **Re-annotation of *mam* genes putatively involved in magnetite biomineralization in** 10 **magnetotactic *Deltaproteobacteria***

11 The gene DMR_41100 was originally annotated as *mamT* although the match with *mamT* from
12 other MTB is only partial. Indeed, DMR_41100 encodes for a large 423 aa long multidomain
13 protein, whereas the average length reported for MamT orthologs in the *Magnetospirillum* genus
14 is only ca. 170 aa. Only the N-terminus region of DMR_41100 (71-130 aa) bears homology with
15 MamT from *Magnetospirillum magneticum* (amb0976). This region in both proteins contains a
16 double CXXCH, a signature characteristic of a newly discovered magnetochrome domain. This
17 magnetochrome domain so far has only been found in proteins (MamP, MamT, MamE and
18 MamX) from MTB (Siponen *et al.*, 2012). This domain binds one *c*-type hemes and is usually
19 found in tandem; the magnetochrome domain forms a redox-active cytochrome module that is
20 proposed to participate in electron transfer chain reactions involved in magnetite
21 biomineralization (Siponen *et al.*, 2012). In *Magnetospirillum*, a typical MamT contains two
22 magnetochrome domains and MamP differs from MamT by the presence of a PDZ domain at the

1 N-terminus (a domain that binds to a short region of the C-terminus of other specific proteins
2 (Ponting *et al.*, 1997)). Interestingly, in DMR_41100 the magnetochrome domain is associated
3 with a PDZ module as in MamP from *Magnetospirillum* species, but with two major
4 discrepancies: (i) the PDZ module follows the N-terminal magnetochrome domain (the order is
5 reversed in typical MamP proteins); (ii) there is a predicted NifX/NifB domain added to the C-
6 terminus of the protein. The NifB and NifX domains belong to a family of iron-molybdenum
7 cluster-binding proteins that includes NifB, NifX, and NifY, all of which are involved in the
8 maturation of the iron-molybdenum cofactor (FeMo-co) that binds the active site of
9 dinitrogenase enzymes in other bacteria (Shah and Brill, 1977). In particular, NifB and NifX
10 serve as scaffolds for the synthesis of iron-sulfur clusters prior to their insertion into the
11 dinitrogenase enzyme (Curatti *et al.*, 2006). Thus DMR_41100 might also contain redox active
12 iron-sulfur clusters involving the shuttling of electrons to or from the magnetochrome domain.
13 These functional considerations prompted us to re-annotate DMR_41100 as *mamP-like* (Fig. 1;
14 Table 2).

15 DMR_41090 was previously annotated as *mamP* despite its poor low similarity to other
16 MamP proteins found in magnetotactic *Alphaproteobacteria* (e.g., comparison with MamP of
17 *Magnetospirillum magneticum*: coverage 58%, e-value 1e-10, identity 30%). DMR_41090 is 542
18 aa long whereas the average length for MamP is ca. 270 aa in the *Alphaproteobacteria*. The
19 predicted domains comprise 3 concatenated PDZ domains but lack a magnetochrome domain,
20 although the latter is an unambiguous signature of the MamP family as mentioned above. This
21 domain organization is reminiscent of the C-terminus of MamE that is composed of two
22 concatenated PDZ domains. We thus annotated DMR_41090, the gene downstream of *mamP-*
23 *like*, as *mamE-Cter* (Fig. 1; Table 2).

1 DMR_41080 is annotated as *mamE* and comprises a trypsin-like protease domain
2 followed by two magnetochrome domains. However, DMR_41080 lacks the double PDZ domain
3 situated at the C-terminus of other known MamE proteins such as amb0963 in *Magnetospirillum*
4 *magneticum* or mgI487 in *M. gryphiswaldense*. In DMR_41080 it is replaced by a permease
5 domain with 5 predicted transmembrane (TM) helices similar to those found in the MamO
6 protein family. Thus, the overall domain organization of DMR_41080 product is more
7 reminiscent of MamO proteins than MamE if the magnetochrome domain is omitted. For this
8 reason we choose to annotate DMR_41080, the gene downstream of *mamE-Cter*, as *mamEO*
9 (Fig. 1; Table 2).

10 DMR_41070 is annotated as *mamO* whereas the gene product contains only 285 aa vs.
11 c.a. 640 aa for MamO in other MTB. As previously discussed, MamO proteins comprise a C-
12 terminus permease domain made up of five TM helices. In DMR_41070, the domain prediction
13 only identifies the protease domain (no permease domain as in MamO proteins). When a BLAST
14 analysis is performed in MaGe against all the MTB included in the database, the first hits are
15 MamE, more precisely its N-terminus domains (the trypsin-like protease). Thus, we assigned
16 DMR_41070, the gene downstream of *mamEO*, as *mamE-Nter* (Fig. 1; Table 2).

17

18 **Re-annotation of *mam* genes putatively involved in greigite biomineralization in** 19 **magnetotactic *Deltaproteobacteria***

20 Due to its high similarity (45% sequence identity) with OMM_23 (*mamP2*) from *Ca.*
21 *Magnetoglobus multicellularis*, the gene DEMABW1_80097 from *Ca. Desulfamplus*
22 *magnetomortis* was previously annotated as *mamP** in GenBank (JN830644). However, we

1 revised this annotation according to a functional prediction of this gene product and because of
2 significant differences between this gene and *mamP*; the DEMABW1_80097 gene product
3 comprises two PDZ domains but is devoid of the two magnetochrome domains as expected for
4 an archetypical MamP protein (Siponen *et al.*, 2012). The greatest similarity between
5 DEMABW1_80097 and other Mam proteins is the C-terminus domain of MamE which is made
6 up of two PDZ domains (the C-terminus part comprised a protease followed by a
7 magnetochrome domain). Our analysis suggests that OMM_23 was misannotated as a gene
8 belonging to the *mamP* family and as a consequence that DEMABW1_80097 should not be
9 annotated as *mamP* but rather as *mamE-Cter** (Fig. 1; Table 2): this situation is similar for
10 DMR_41090 which we annotated as *mamE-Cter* in *Desulfovibrio magneticus* (and thus
11 DEMABW1_80067 in the magnetite gene cluster of *Ca. D. magnetomortis*).

12 The protein DEMABW1_80098 contains a trypsin-like protease domain reminiscent of a
13 MamE protein, but is devoid of the magnetochrome and the double PDZ domains at its C-
14 terminus end. When a BLAST analysis is performed in the MaGe database, DEMABW1_80098
15 matches with the trypsin-like domain of most MTB included in MaGe. This situation is
16 essentially the same as the re-annotation (as *mamE-Nter*) that we proposed in the previous
17 section for the DMR_41070 gene in *Desulfovibrio magneticus* and its homolog
18 DEMABW1_80069 in the magnetite gene cluster of *Ca. Desulfamplus magnetomortis*.
19 Therefore we annotate DEMABW1_80098 in the greigite gene cluster of *Ca. D. magnetomortis*
20 and OMM_22 of *Ca. Magnetoglobus multicellularis* as *mamE-Nter* (Fig. 1; Table 2). As
21 postulated for *D. magneticus*, a functional MamE-like protein could be encoded in the greigite
22 gene cluster of *Ca. D. magnetomortis* through possible protein interactions of MamE-Nter* and

1 MamE-Cter*, despite the absence of the magnetochrome domains (whose deletion results in no
2 obvious phenotype in MamE from *Magnetospirillum magneticum* (Quinlan *et al.*, 2011)).

3 The annotation of DEMABW1_80100 is ambiguous as it is equally similar to both
4 MamM and MamB [22% (e-value 3e-12) and 24% (e-value 4e-23), respectively], as illustrated
5 by its branching position within the similarity tree of the cation diffusion facilitator (CDF) family
6 (Fig. S3). For this reason we chose to name this gene *mamMB-like* (Fig. 1; Table 2).

7 **Putative function of some *mad* genes**

8 Bioinformatic analysis suggests some possible functions to Mad proteins, for example, Mad6 and
9 Mad9 are paralogous proteins and are predicted as putative membrane 4Fe-4S ferredoxins which
10 are iron-sulfur binding proteins (Bruschi and Guerlesquin, 1988). These metalloproteins might
11 be involved in electron transfer reactions in the magnetosome membrane for magnetite
12 crystallization. The gene DEMABW1_80087 in *Ca. Desulfamplus magnetomortis* also encodes
13 for a putative ferredoxin but it is not orthologous to Mad6 and Mad9. The synteny of *mad6* is
14 well conserved between *Ca. D. magnetomortis*, *Desulfovibrio magneticus*, and strains FH-1 and
15 ML-1 and lies upstream of *mamI-3*, *mamL* and *mamM*. The synteny of *mad9* is also well
16 conserved in these strains and transcribed in the opposite direction of most of the *mam* and *mad*
17 genes.

18 Mad12 is a protein found in *Ca. Desulfamplus magnetomortis* and *Ca. Magnetoglobus*
19 *multicellularis* that contains an EcsC domain originally described in *Bacillus subtilis* as a
20 component of an ABC transporter (Leskelä *et al.*, 1996). The function of Mad12 is unknown. *Ca.*
21 *D. magnetomortis* has two copies of *mad12*, one in its magnetosome gene cluster and another
22 one downstream of this region (DEMABW1_80141). Mad23 contains one HEAT repeat domain

1 which is found in a number of cytoplasmic proteins including the four that give rise to the
2 acronym HEAT (Huntingtin, elongation factor 3, protein phosphatase 2A, and the yeast kinase
3 TOR1) (Groves *et al.*, 1999). HEAT repeats form rod-like helical structures involved in
4 intracellular transport. Based on phylogenetic analyses, Mad23 is a protein specific to MTB (data
5 not shown). Mad27 is found in the genome of *Ca. Desulfamplus magnetomortis*, *Desulfovibrio*
6 *magneticus*, strain FH-1 and *Ca. M. multicellularis*. This protein contains a AAA+ domain which
7 is an abbreviation for ATPases associated with diverse cellular activities (Neuwald *et al.*, 1999).
8 Proteins with such domain are involved in a range of processes, including DNA replication,
9 protein degradation, membrane fusion, microtubule severing, peroxisome biogenesis, signal
10 transduction and the regulation of gene expression (Neuwald *et al.*, 1999). Based on
11 phylogenetic analyses, Mad27 is a protein specific to the magnetotactic *Deltaproteobacteria*
12 (data not shown). Mad29 is a putative ATPase found in *Ca. D. magnetomortis*, *D. magneticus*
13 and strain FH-1. Based on phylogenetic analyses, Mad29 is also a protein specific to the
14 magnetotactic *Deltaproteobacteria* (data not shown).

15

16 **Supplementary references**

17 Bruschi, M., and Guerlesquin, F. (1988) Structure, function and evolution of bacterial
18 ferredoxins. *FEMS Microbiol Rev* **4**: 155–175.

19 Curatti, L., Ludden, P.W., and Rubio, L.M. (2006) NifB-dependent in vitro synthesis of the iron-
20 molybdenum cofactor of nitrogenase. *Proc Natl Acad Sci U S A* **103**: 5297–5301.

21 Groves, M.R., Hanlon, N., Turowski, P., Hemmings, B.A., and Barford, D. (1999) The structure
22 of the protein phosphatase 2A PR65/A subunit reveals the conformation of its 15
23 tandemly repeated HEAT motifs. *Cell* **96**: 99–110.

- 1 Leskelä, S., Kontinen, V.P., and Sarvas, M. (1996) Molecular analysis of an operon in *Bacillus*
2 *subtilis* encoding a novel ABC transporter with a role in exoprotein production,
3 sporulation and competence. *Microbiology* **142** (Pt 1): 71–77.
- 4 Neuwald, A.F., Aravind, L., Spouge, J.L., and Koonin, E.V. (1999) AAA+: A class of
5 chaperone-like ATPases associated with the assembly, operation, and disassembly of
6 protein complexes. *Genome Res* **9**: 27–43.
- 7 Ponting, C.P., Phillips, C., Davies, K.E., and Blake, D.J. (1997) PDZ domains: targeting
8 signalling molecules to sub-membranous sites. *Bioessays* **19**: 469–479.
- 9 Quinlan, A., Murat, D., Vali, H., and Komeili, A. (2011) The HtrA/DegP family protease MamE
10 is a bifunctional protein with roles in magnetosome protein localization and magnetite
11 biomineralization. *Mol Microbiol* **80**: 1075–1087.
- 12 Shah, V.K., and Brill, W.J. (1977) Isolation of an iron-molybdenum cofactor from nitrogenase.
13 *Proc Natl Acad Sci U S A* **74**: 3249–3253.
- 14 Siponen, M.I., Adryanczyk, G., Ginet, N., Arnoux, P., and Pignol, D. (2012) Magnetochrome: a
15 *c*-type cytochrome domain specific to magnetotactic bacteria. *Biochem Soc Trans* **40**:
16 1319–1323.
- 17

Curriculum vitae

Persönliche Daten

Name: Kolinko Sebastian
Geburtstag: 07.11.1983
Geburtsort: München
Staatsangehörigkeit: Deutsch

Ausbildung

04/2010 – 09/2014 Doktorand
Department Biologie I, Ludwig-Maximilians-Universität, München
Betreuer: Prof. Dr. Dirk Schüler
Titel: Einzelzell-Analyse unkultivierter magnetotaktischer Bakterien

07/2009 – 03/2010 Diplomarbeit
Department Biologie I, Ludwig-Maximilians-Universität, München
Betreuer: Prof. Dr. Dirk Schüler
Titel: Charakterisierung unkultivierter magnetotaktischer Bakterien
mittels metagenomischer- und auf Einzelzellen basierender
Methoden

10/2008 – 03/2009 Studentische Hilfskraft
Department für Molekularbiologie, Ludwig-Maximilians-Universität,
München
Betreuer: Prof. Dr. Gunnar Schotta
Titel: Enzymatische Charakterisierung von
Histonmethyltransferasen im Maus-Model

03/2008 – 04/2008 Studentische Hilfskraft
Department für Molekularbiologie, Ludwig-Maximilians-Universität,
München
Betreuer: Prof. Dr. Kirsten Jung
Titel: Charakterisierung des Zwei-Komponenten-Systems CadA

Danksagung

Die vorliegende Arbeit wurde vom März 2010 bis September 2014 in der Abteilung von Herrn Prof. Dr. Dirk Schüler im Biozentrum der Ludwig-Maximilians-Universität in München durchgeführt.

An dieser Stelle möchte ich gerne einigen Menschen danken, die mich während der Promotion unterstützt und zum Gelingen dieser Arbeit beigetragen haben.

Mein besonderer Dank gilt Herrn Prof. Dr. Dirk Schüler für die Möglichkeit meine Doktorarbeit zu diesem interessanten Thema zu verfassen und der durch seine gute und kompetente Betreuung, seine hilfreichen Gespräche und Anregungen viel zum Erfolg dieser Arbeit beigetragen hat.

Ich bin Herrn Prof. Dr. Anton Hartmann für sein Interesse an meiner Arbeit dankbar. Zudem danke ich ihm für die Übernahme des Zweitgutachtens.

Ich möchte Prof. Dr. G. Wanner, Dr. A. Brachmann und Dr. M. Richter für die enge und produktive Zusammenarbeit danken, ohne die Teile dieser Arbeit nicht möglich gewesen wären. Allen ehemaligen und derzeitigen Mitarbeitern der Arbeitsgruppe „Magnetotaktische Bakterien“ für die freundschaftliche, inspirierende und kollegiale Arbeitsatmosphäre. Insbesondere bedanken möchte ich mich bei Dr. C. Jogler, Dr. E. Katzmann, S. Borg und O. Raschdorf für die gemeinsame Zeit, angefertigte TEMs und legendäre Tischfußballschlachten. Besonderer Dank gilt meiner ehemaligen Bachelor-Studentin F. Kiemer für die gute Zusammenarbeit.

Spezieller Dank gilt meinen Eltern die unsere kleine Familie während dieser turbulenten Zeit unermüdlich unterstützt haben.

Meine tiefste Dankbarkeit gebührt meiner Frau Isabel für ihre Unterstützung, Anmerkungen und den ein oder anderen Motivationsschub während den letzten Jahren.

Eidesstattliche Erklärung

Ich erkläre hiermit an Eides statt, dass die vorgelegte Dissertation von mir selbständig und ohne unerlaubte Hilfe angefertigt ist. Des Weiteren erkläre ich, dass ich nicht anderweitig ohne Erfolg versucht habe, eine Dissertation einzureichen oder mich der Doktorprüfung zu unterziehen. Die vorliegende Dissertation liegt weder ganz, noch in wesentlichen Teilen einer anderen Prüfungskommission vor.

Sebastian Kolinko, München